



**TECHNICAL REPORT 0-6831-1**  
TxDOT PROJECT NUMBER 0-6831

# **End-Region Behavior and Shear Strength of Pretensioned Concrete Girders Employing 0.7-in. Diameter Strands**

Hossein Yousefpour  
Hyun su Kim  
Rodolfo Bonetti  
Roya Alirezaei Abyaneh  
Alex Katz  
Alistair Longshaw  
Jessica Salazar  
Trevor Hrynyk  
Oguzhan Bayrak

August 2017; Published August 2018

<http://library.ctr.utexas.edu/ctr-publications/0-6831-1.pdf>



Technical Report Documentation Page

1. Report No. FHWA/TX-17/0-6831-1		2. Government Accession No.	3. Recipient's Catalog No.	
4. Title and Subtitle End-Region Behavior and Shear Strength of Pretensioned Concrete Girders Employing 0.7-in. Diameter Strands		5. Report Date August 2017; Published August 2018		
7. Author(s) Hossein Yousefpour, Hyun su Kim, Rodolfo Bonetti, Roya Alirezaei Abyaneh, Alex Katz, Alistair Longshaw, Jessica Salazar, Trevor Hrynyk, and Oguzhan Bayrak		6. Performing Organization Code		
9. Performing Organization Name and Address Center for Transportation Research The University of Texas at Austin 1616 Guadalupe St., Suite 4.202 Austin, TX 78701		8. Performing Organization Report No. 0-6831-1		
12. Sponsoring Agency Name and Address Texas Department of Transportation Research and Technology Implementation Office P.O. Box 5080 Austin, TX 78763-5080		10. Work Unit No. (TRAIS)		
		11. Contract or Grant No. 0-6831		
13. Type of Report and Period Covered Technical Report August 2014–August 2017		14. Sponsoring Agency Code		
15. Supplementary Notes Project performed in cooperation with the Texas Department of Transportation and the Federal Highway Administration.				
16. Abstract This report provides an overview of a comprehensive research project at The University of Texas at Austin on the end-region serviceability and shear strength of Texas pretensioned bulb-tee girders (Tx-girders) that employ 0.7-in. diameter strands on a 2- by 2-in. grid. Seven full-scale specimens were fabricated and tested at Ferguson Structural Engineering Laboratory. The detailing for mild-steel reinforcement in four specimens was identical to that currently used in Tx-girders with smaller-diameter strands whereas three girders were fabricated with modified end-region detailing. The specimens were extensively instrumented and monitored for transfer length as well as stresses and cracking within their end-regions at the time of prestress transfer. Greater end-region stresses and greater crack widths were detected in the specimens compared to girders with smaller-diameter strands. However, the greatest crack widths within the girder end-regions were generally less than 0.007 in. Moreover, the specimens did not show unusual cracking patterns that trigger new concerns regarding the end-region serviceability of Tx-girders that employ 0.7-in. diameter strands. To investigate their load-carrying capacity and failure mechanisms, the specimens were later subjected to shear-critical loading until failure. Significant strand slip indicating anchorage-zone distress was detected in all specimens prior to reaching the peak applied load. However, widespread yielding of the shear reinforcement was also confirmed in all specimens, and the capacities of all specimens were conservatively estimated using the general method in AASHTO LRFD Bridge Design Specifications. It was also found that adding a cap bar to the bottom flange confinement reinforcement can significantly reduce the strand slip and increase the ultimate strength of the girder. The experimental program was supplemented by an extensive parametric investigation that provided insights into benefits and limitations of using 0.7-in. diameter strands and a series of computational simulations that aimed to shed light into mechanics of prestress transfer, failure modes, and effects of potential changes to end-region reinforcement in Tx-girders with 0.7-in. diameter strands.				
17. Key Words Prestressed, Pretensioned, 0.7 in. Strands, Transfer Length, Development Length, Cracking, Horizontal Shear, Anchorage-Induced Shear Failure		18. Distribution Statement No restrictions. This document is available to the public through the National Technical Information Service, Springfield, Virginia 22161; www.ntis.gov.		
19. Security Classif. (of report) Unclassified	20. Security Classif. (of this page) Unclassified	21. No. of pages 194	22. Price	



THE UNIVERSITY OF TEXAS AT AUSTIN  
**CENTER FOR TRANSPORTATION RESEARCH**

## **End-Region Behavior and Shear Strength of Pretensioned Concrete Girders Employing 0.7-in. Diameter Strands**

Hossein Yousefpour  
Hyun su Kim  
Rodolfo Bonetti  
Roya Alirezaei Abyaneh  
Alex Katz  
Alistair Longshaw  
Jessica Salazar  
Trevor Hrynyk  
Oguzhan Bayrak

---

CTR Technical Report:	0-6831-1
Report Date:	August 2017; Published August 2018
Project:	0-6831
Project Title:	End-Region Behavior of Pretensioned Concrete Beams with 0.7-in. Prestressing Strands
Sponsoring Agency:	Texas Department of Transportation
Performing Agency:	Center for Transportation Research at The University of Texas at Austin

Project performed in cooperation with the Texas Department of Transportation and the Federal Highway Administration.

Center for Transportation Research  
The University of Texas at Austin  
3925 W. Braker Lane, 4<sup>th</sup> floor  
Austin, TX 78759

<http://ctr.utexas.edu/>

## **Disclaimers**

**Author's Disclaimer:** The contents of this report reflect the views of the authors, who are responsible for the facts and the accuracy of the data presented herein. The contents do not necessarily reflect the official view or policies of the Federal Highway Administration or the Texas Department of Transportation (TxDOT). This report does not constitute a standard, specification, or regulation.

**Patent Disclaimer:** There was no invention or discovery conceived or first actually reduced to practice in the course of or under this contract, including any art, method, process, machine manufacture, design or composition of matter, or any new useful improvement thereof, or any variety of plant, which is or may be patentable under the patent laws of the United States of America or any foreign country.

**Notice:** The United States Government and the State of Texas do not endorse products or manufacturers. If trade or manufacturers' names appear herein, it is solely because they are considered essential to the object of this report.

### **Engineering Disclaimer**

NOT INTENDED FOR CONSTRUCTION, BIDDING, OR PERMIT PURPOSES.

Project Engineer: Oguzhan Bayrak  
Professional Engineer License State and Number: Texas No. 106598  
P. E. Designation: Research Supervisor

## **Acknowledgments**

The authors gratefully acknowledge the Texas Department of Transportation (TxDOT) for providing financial support for this research project. In particular, the authors would like to thank Gregg Freeby, Wade Odell, and the members of Project Monitoring Committee, David Fish, Jason Tucker, Todd Speck, Taya Retterer, Geetha Chandar, and Hector Garcia, for their valuable feedback. The authors are also thankful to the staff members and graduate and undergraduate research assistants at Ferguson Structural Engineering Laboratory who made this research possible through their remarkable support. Many thanks are also due to Coreslab Structures, Inc. in Cedar Park, Texas, for donating the concrete that was used for the majority of the specimens in the experimental program.

## **Products**

This report contains Product 1 (0-6831-P1), Design Recommendations and Fabrication Specifications, provided as Appendix B.

# TABLE OF CONTENTS

<b>CHAPTER 1 Introduction .....</b>	<b>1</b>
1.1 Overview.....	1
1.2 Background.....	1
1.3 Research Plan.....	3
1.3.1 Task 1: Literature Review.....	3
1.3.2 Task 2: Manufacturer Survey.....	4
1.3.3 Task 3: Analytical Program .....	4
1.3.4 Tasks 4: Experimental Program – End-Region Serviceability .....	5
1.3.5 Task 5: Review Potential End-Region Modifications.....	5
1.3.6 Task 6: Experimental Program – Ultimate Shear Strength.....	5
1.3.7 Task 7: Development of Design Recommendations.....	6
1.3.8 Task 8: Presentation of Preliminary Design Recommendations.....	6
1.4 Report Organization.....	6
<b>CHAPTER 2 Background.....</b>	<b>7</b>
2.1 Overview.....	7
2.2 Prestress Transfer and Development Length.....	7
2.3 Review of Literature on Transfer and Development Lengths for 0.5- and 0.6-in. Strands .....	9
2.3.1 Janney (1954).....	10
2.3.2 Hanson and Kaar (1959).....	10
2.3.3 Cousins, Johnston, and Zia (1990).....	10
2.3.4 Lane (1992).....	10
2.3.5 Russell and Burns (1993, 1996).....	10
2.3.6 Mitchell, Cook, Khan, and Tham (1993).....	11
2.3.7 Deatherage, Burdette, and Chew (1994).....	11
2.3.8 Barnes, Burns, and Kreger (1999) .....	11
2.3.9 Braun (2002) .....	12
2.3.10 Marti-Vargas et al. (2007).....	12
2.3.11 Summary of Previous Results and Equations of Transfer and Development Length .....	13
2.4 End-Region Stresses and Cracking.....	14
2.5 Shear Strength.....	15
2.5.1 Horizontal Shear Failure .....	16
2.5.1 Anchorage-Induced Shear Failure .....	17
2.6 Previous Research Specific to the Application of 0.7-in. Strands .....	19
2.6.1 University of Tennessee, Knoxville.....	19
2.6.2 University of Nebraska-Lincoln.....	19
2.6.3 University of Arkansas.....	22
2.7 Summary and Conclusions .....	22
<b>CHAPTER 3 Manufacturer Survey.....</b>	<b>25</b>
3.1 Overview.....	25
3.2 Background.....	25
3.2.1 Texas Precast Fabricators Survey .....	25

3.2.2 State Transportation Departments Survey .....	26
3.3 Survey Results .....	26
3.3.1 Texas Precast Fabricator Survey .....	26
3.3.2 State Transportation Departments Survey .....	27
3.4 Analysis of Survey Results .....	29
3.4.1 Texas Precast Fabricator Survey .....	29
3.4.2 State Transportation Department Survey .....	29
3.5 Summary .....	29
<b>CHAPTER 4 Parametric Investigation .....</b>	<b>31</b>
4.1 Overview .....	31
4.2 Background .....	31
4.3 Methodology of Investigation .....	32
4.3.1 The Parametric Study Tool .....	33
4.3.2 Parametric Investigation .....	36
4.4 Results and Discussion .....	38
4.4.1 Steel Quantity .....	38
4.4.2 Maximum Span Capability .....	44
4.4.3 Slenderness of the Superstructure .....	47
4.4.4 Girder Spacing .....	50
4.5 Summary and Conclusions .....	51
<b>CHAPTER 5 Experimental Program .....</b>	<b>53</b>
5.1 Overview .....	53
5.2 Specimen Design .....	53
5.3 Specimen Fabrication .....	58
5.4 Shear Testing .....	69
5.5 Summary .....	73
<b>CHAPTER 6 Experimental Results and Discussion .....</b>	<b>75</b>
6.1 Overview .....	75
6.2 Measured Mechanical Properties .....	75
6.3 End-Region Behavior .....	76
6.3.1 Transfer Length .....	76
6.3.2 End-Region Cracking .....	80
6.3.3 End-Region Stresses .....	89
6.4 Shear-Resisting Performance .....	93
6.4.1 Conditions of Specimens Prior to Shear Tests .....	94
6.4.2 Load-Deflection and Load-Strand Slip Behavior .....	94
6.4.3 Stirrup Stresses at Peak Load .....	96
6.4.4 Cracking Patterns .....	97
6.4.5 Post-Failure Conditions .....	100
6.4.6 Discussion of Shear Test Results .....	108
6.5 Summary and Conclusions .....	118
<b>CHAPTER 7 Finite Element Studies .....</b>	<b>121</b>
7.1 Overview .....	121
7.2 Background .....	121
7.3 Methodology of Investigation .....	122

7.3.1 Experimental Data Used for the First Stage of Validation .....	122
7.3.2 Finite Element Model .....	124
7.3.3 Loading Conditions.....	126
7.3.4 Behavioral Models and Analysis Parameters .....	126
7.4 Results and Discussion .....	127
7.4.1 Prestress Transfer.....	127
7.4.2 End-Region Modification .....	132
7.4.3 Shear-Resisting Performance.....	134
7.5 Summary and Conclusions .....	144
<b>CHAPTER 8 Summary and Conclusions.....</b>	<b>147</b>
8.1 Summary.....	147
8.2 Conclusions.....	148
8.2.1 Benefits of Using 0.7-in. Strands.....	148
8.2.2 Transfer Length.....	149
8.2.3 End-Region Cracking.....	149
8.2.4 End-Region Stresses .....	149
8.2.5 Shear Strength.....	150
8.2.6 Modifications to End-Region Detailing.....	151
<b>REFERENCES.....</b>	<b>153</b>
<b>APPENDIX A .....</b>	<b>157</b>
<b>APPENDIX B .....</b>	<b>175</b>



## LIST OF TABLES

Table 2-1- Factors affecting bond. Adapted from [7].....	9
Table 2-2- Summary of transfer and development length equations.....	13
Table 4-1- Input variables used within the parametric study tool .....	34
Table 4-2- Properties used in the parametric study .....	37
Table 5-1- Specimen design parameters .....	55
Table 5-2- Concrete mixture properties.....	67
Table 6-1- Measured mechanical properties of concrete.....	75
Table 6-2- Measured mechanical properties of the mild steel used for the fabrication of the specimens.....	76
Table 6-3- Transfer lengths determined for the specimens based on strain gauge data .....	78
Table 6-4- Splitting resistance in the specimens according to AASHTO LRFD (2016) compared to initial prestressing force.....	92
Table 6-5- Summary of test results.....	93
Table 6-6- Shear strength calculations according to the general procedure in AASHTO LRFD .....	112
Table 6-7- Shear strength calculations according to the longitudinal reinforcement requirement in AASHTO LRFD.....	113
Table 6-8- Nominal shear strength calculations .....	114
Table 7-1- Prestress transfer results for 6-Tx and 7-Tx series specimens .....	128
Table 7-2- Summary of measured and computed ultimate capacities .....	144



## LIST OF FIGURES

Figure 1-1- Cross sections of different strand sizes.....	2
Figure 2-1- Steel stresses vs. distance from the free end of the strand (Vadivelu, 2009).....	7
Figure 2-2- Stresses induced in the flange due to Hoyer’s effect (Garber et al., 2016) .....	8
Figure 2-3- Determination of transfer length in the method used by Marti-Vargas et al (2007)......	12
Figure 2-4- End-region stresses and potential cracks formed after prestress transfer (CEB, 1987).....	14
Figure 2-5- Atypical failure modes observed in previous experimental studies on Tx-girders .....	15
Figure 2-6- Horizontal shear failure (Hovell et al., 2011) .....	16
Figure 2-7- Definition of <i>lcrit</i> (Hovell et al., 2011).....	17
Figure 2-8- Anchorage free-body diagram (AASHTO, 2016) .....	17
Figure 2-9- Idealized relationship between stress and distance from the free end of strand. Adapted from AASHTO LRFD (2016). .....	18
Figure 3-1- Responses to the nationwide survey of state transportation departments.....	28
Figure 4-1- Cross sections evaluated in the parametric investigation .....	33
Figure 4-2- Design procedure for the parametric study tool.....	35
Figure 4-3- Number of strands vs. span length for I- and bulb-tee girders with different strand diameters .....	39
Figure 4-4- Number of strands vs. span length for U- and X-girders with different strand diameters.....	40
Figure 4-5- Percent reduction in steel weight and number of strands for 0.6- and 0.7-in. diameter strands compared to 0.5-in. diameter strands within I- and bulb-tee girders .....	42
Figure 4-6- Percent reduction in steel weight and number of strands for 0.6- and 0.7-in. diameter strands compared to 0.5-in. diameter strands within U- and X-girders.....	43
Figure 4-7- Maximum span lengths achieved for I- and bulb-tee girders with different strand diameters. Note: H= strands harped as needed; S= Straight strands only.....	45
Figure 4-8- Maximum span lengths achieved for U- and X-girders with different strand diameters.....	46
Figure 4-9- Maximum attainable slenderness ratio (MASR) for 0.5-, 0.6-, and 0.7-in. diameter strands in Tx-girders .....	49
Figure 4-10- Allowable girder spacing at maximum practical spans for I- and bulb-tee girders employing 0.5-, 0.6-, and 0.7-in. diameter strands.....	50
Figure 5-1- Cross-sectional properties of Tx46 ad Tx70 girders.....	54
Figure 5-2- End-region and shear reinforcement in the first four specimens .....	57
Figure 5-3- Additional bars added to the end-region reinforcement in Tx46-V.....	58
Figure 5-4- Prestressing facility at FSEL.....	59

Figure 5-5- Strand installation .....	60
Figure 5-6- Specimen fabrication steps .....	61
Figure 5-7- Modified end-region reinforcement in Tx46-IV .....	62
Figure 5-8- Strain gauge locations for monitoring transfer length and transverse reinforcement stresses .....	63
Figure 5-9- Instrumentation embedded in the specimens .....	64
Figure 5-10- Additional embedded instrumentation .....	65
Figure 5-11- Concrete placement .....	65
Figure 5-12- Match-curing system .....	67
Figure 5-13- Testing of match-cured cylinders .....	68
Figure 5-14- Determining the time of release for a typical specimen based on match-cured specimens .....	68
Figure 5-15- Construction of the cast-in-place deck .....	69
Figure 5-16- Testing configuration .....	70
Figure 5-17- Supports for the shear test .....	71
Figure 5-18- Photos of the shear test setup .....	71
Figure 5-19- Displacement transducers used for measuring strand slip .....	72
Figure 6-1- Determining the transfer length based on strain gauge data .....	77
Figure 6-2- Transfer lengths from individual strands in comparison with the value estimated by AASHTO LRFD .....	79
Figure 6-3- Crack-measurement tools .....	80
Figure 6-4- Observed cracking patterns in Tx46-I .....	81
Figure 6-5- Observed cracking patterns in Tx46-II .....	82
Figure 6-6- Observed cracking patterns in Tx70-I .....	83
Figure 6-7- Observed cracking patterns in Tx70-II .....	84
Figure 6-8- Maximum crack widths in specimens with standard detailing for end-region reinforcement .....	85
Figure 6-9- Observed cracking patterns in Tx46-IV .....	87
Figure 6-10- Observed cracking patterns in Tx46-V .....	88
Figure 6-11- End-region stresses in the first four specimens .....	90
Figure 6-12- End-region stresses in specimens with modified end-region detailing .....	91
Figure 6-13- Comparison between transverse forces determined in this study and those in the database of bursting and spalling stresses developed by Dunkman (2009). Note: D= Dead end; L=Live end. ....	93
Figure 6-14- Plots of shear force versus deflection and shear force versus strand slip (first four specimens) .....	95
Figure 6-15- Plots of shear force versus deflection and shear force versus strand slip for Tx46-IV and Tx46-V .....	96
Figure 6-16- Stresses in the transverse reinforcement at peak shear force .....	97
Figure 6-17- Cracking conditions in the specimens immediately prior to failure .....	99

Figure 6-18- Post-failure conditions of Tx46-I (Dead end).....	101
Figure 6-19- Post-failure conditions of Tx46-II (Dead end) .....	102
Figure 6-20- Post-failure conditions of Tx70-I (Dead end).....	103
Figure 6-21- Post-failure conditions of Tx70-II (Live end).....	104
Figure 6-22- Post-failure conditions of Tx46-IV (Dead end).....	105
Figure 6-23- Post-failure conditions of Tx46-V (Dead end) .....	106
Figure 6-24- Details of the damage observed in Tx46-V after failure .....	107
Figure 6-25- Comparison between load-deflection and load-slip behavior of Tx46-IV and Tx46-V .....	116
Figure 6-26- Comparison of results from the current test program with the database of shear tests on prestressed concrete members .....	117
Figure 7-1- Cross-section and reinforcement details in the 6-Tx series .....	123
Figure 7-2- Shear test setup used for the 6-Tx series.....	123
Figure 7-3- Cross section and reinforcement details for the 7-NU series.....	124
Figure 7-4- FE mesh created for a typical Tx46 girder .....	125
Figure 7-5- Boundary conditions for different stages of analysis.....	125
Figure 7-6- Comparison of computed and measured strand forces after transfer of prestress for 6-Tx28-I .....	127
Figure 7-7- Comparison of live-end cracking in 6-Tx series specimens. Notations (a) and (b) refer to measured and computed results for each specimen, respectively. Photos from O’Callaghan (2007).....	129
Figure 7-8-7-Tx46-I release cracks (live end) .....	130
Figure 7-9-7-Tx46-II release cracks (live end).....	130
Figure 7-10-7-Tx70-I release cracks (live end) .....	130
Figure 7-11-7-Tx70-II release cracks (live end).....	131
Figure 7-12-7-Tx46-IV release cracks (live end) .....	131
Figure 7-13-7-Tx46-V release cracks (live end).....	131
Figure 7-14- Alternative details to control end-region cracking in Tx-girders fabricated with 0.7-in. diameter strands. (Note: E.E.= Each end) .....	132
Figure 7-15- Efficiency of recommended end-region detailing .....	133
Figure 7-16- Load-deflection response of the 6-Tx series specimens .....	135
Figure 7-17- Comparison of load test results for the 7-NU series specimens .....	136
Figure 7-18- Comparison of load test results in for 7-Tx series .....	137
Figure 7-19- Shear test damage in 7-Tx46-I (a) measured (b) computed.....	138
Figure 7-20- Shear test damage in 7-Tx46-II (a) measured (b) computed .....	139
Figure 7-21- Shear test damage in 7-Tx70-I (a) measured (b) computed.....	140
Figure 7-22- Shear test damage in 7-Tx70-II (a) measured (b) computed .....	141
Figure 7-23- Shear test damage in 7-Tx46-IV (a) measured (b) computed.....	142
Figure 7-24- Shear test damage in 7-Tx46-V (a) measured (b) computed .....	143



# CHAPTER 1

## Introduction

### 1.1 Overview

In the majority of pretensioned concrete elements currently fabricated in the United States, 0.5- or 0.6-in. diameter strands are used as the prestressing steel. However, in recent years, there has been interest in using 0.7-in. strands in pretensioning applications. The use of these larger-diameter strands is believed to improve the efficiency of pretensioned concrete elements by reducing the number of required strands and making it possible to concentrate a greater steel area near the bottom of the cross section. However, the effects of using 0.7-in. strands on the serviceability and strength of pretensioned girders need to be identified and addressed before potential implementation of girders that employ these larger-diameter strands in bridge applications. Greater transverse tensile stresses are expected to develop within the end-regions of such girders, which may lead to excessive cracking and diminished serviceability of girders. Moreover, potential damage to the interface between web and bottom flange and increased transfer and development lengths result in an increase in the likelihood of atypical shear failure modes in girders that employ 0.7-in. diameter strands.

This report provides a summary of Project 0-6831, a comprehensive research project initiated by the Texas Department of Transportation (TxDOT) at The University of Texas at Austin (UT) on the end-region serviceability and shear strength of Texas pretensioned bulb-tee girders (Tx-girders) that employ 0.7-in. diameter strands on a 2- by 2-in. grid. The primary activities performed as part of this research project consisted of an experimental program on full-scale specimens at Ferguson Structural Engineering Laboratory (FSEL), computational studies using nonlinear finite element (FE) models, and parametric investigations on the design of bridge girders to evaluate the potential benefits and limitations of using 0.7-in. diameter strands. It should be noted that prior to the publication of this report, some of the findings of this project has been published in journal articles and conference papers (Salazar et al., 2017; Salazar et al., 2017; Katz et al., 2017; Alirezai Abyaneh et al., 2017; Kim et al., 2017), the submission of which have been coordinated with TxDOT.

### 1.2 Background

Figure 1-1 shows the cross sections of seven-wire 0.5-, 0.6- and 0.7-in. diameter prestressing strands. As can be seen in this figure, the cross-sectional area of a 0.7-in. strand is approximately twice that of a 0.5-in. strand and is about 35 percent greater than that of a 0.6-in. strand. As a result, considerably fewer 0.7-in. strands would be needed to provide the same steel area of prestressing steel compared to 0.5- or 0.6-in. strands. Therefore, the time and cost of the fabrication process for the pretensioned girders could be reduced.

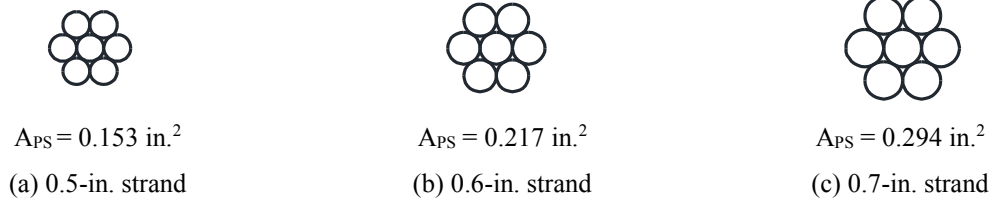


**Figure 1-1- Cross sections of different strand sizes**

With the use of 0.7-in. strands, it is also possible to concentrate a greater steel area near the bottom of the precast cross sections, leading to a potential increase in the internal lever arm and therefore the nominal flexural and shear capacities of the cross sections. Depending on the design objectives, such an increase in the capacity of girders can be used to increase the span capability of existing precast cross sections, increase the transverse spacing between the girders, or reduce the depth of bridge superstructures. These benefits could improve the capabilities of pretensioned bridge girders in terms of fabrication time and cost, competitiveness with steel bridge girders, and aesthetics.

Despite the benefits associated with 0.7-in. diameter strands, the only real-world applications of pretensioned girders with these larger-diameter strands in the United States have been limited to two bridges in Nebraska, which were opened to traffic in 2008 and 2013, as reported by Morcoux et al. (2011) and Morcoux et al. (2014), respectively. In fact, there has been a general apprehension toward the use of these larger-diameter strands because of the potential need for upgrading the prestressing facilities, concerns related to the availability of materials and accessories, and concerns regarding the structural behavior of girders that employ 0.7-in. strands.

To minimize the potential impacts of using 0.7-in. strands on the fabrication plants, it is critical to use these larger-diameter strands within the same precast cross sections and on the standard 2- by 2-in. grid that is commonly used for smaller-diameter strands. The most crucial concerns regarding the structural behavior of girders that employ 0.7-in. strands on a 2- by 2-in. grid include: (1) possibility of undesirable cracking within the girder end regions, which might negatively affect the serviceability of girders, and (2) possibility of diminished shear strength due to atypical failure modes.

At prestress transfer, the end regions of pretensioned girders are subjected to transverse tensile stresses that might result in cracking near the end-faces of the girders after the prestressing strands are released. To ensure the serviceability and safety of precast pretensioned girders, it is essential to use appropriate detailing within the end regions of girders so that the width of aforementioned cracks is controlled. However, current reinforcement detailing used for precast, pretensioned girders has been developed based on the use of 0.5- and 0.6-in. strands, and its suitability for 0.7-in. strands has yet to be verified.

Atypical shear failure modes are another important concern regarding the use of 0.7-in. strands. The web-flange interface regions of pretensioned concrete girders are prone to high stress concentrations. This situation can lead to horizontal shear failure, especially in pretensioned sections with relatively thin webs (Hovell et al., 2011 and Nakamura et al., 2013). A horizontal shear failure occurs when there is a loss of strain compatibility along a horizontal plane within the beam. Current design specifications for shear strength are not developed to take this atypical failure mode into account and therefore, there is a potential for unconservative shear strength estimates when this mode controls. Increased web-flange interface stresses, which could potentially develop

in girders employing large-diameter strands, increase the likelihood of this failure mode and therefore need to be considered in different pretensioned cross sections.

End regions of prestressed concrete girders constructed with larger-diameter strands are also more likely to experience anchorage-induced shear failures. When a shear crack first initiates near the edge of the bearing pad, it is prevented from opening further by the restraining force provided by the prestressing strand. If the steel crossing the crack does not provide an adequate amount of restraining force (e.g., when proper development of the strands is impeded by anchorage zone distress) further progression of the diagonal shear cracking or total loss of anchorage for the strand will occur. The use of 0.7-in. diameter strands is expected to result in a reduction in the restraining force available near the supports of pretensioned girders. Unless proper end-region reinforcement detailing is provided in girders employing 0.7-in. diameter strands, end-region stress development attributed to the large-diameter strands could potentially result in anchorage-zone distress and lead to shear strengths that fall below code estimates.

The behavior of pretensioned members fabricated using 0.7-in. diameter prestressing strands has been the subject of a number of previous studies, which are discussed in detail in Chapter 2. While these past efforts represent valuable contributions toward improving the current understanding of the behavior of precast pretensioned girders with 0.7-in. diameter strands, significant gaps remain in the knowledge regarding the performance of such members. Some of these studies have been conducted on small-scale test specimens, which possess unrealistic strand spacing and boundary conditions. As a result, the applicability of results from such specimens to pretensioned girders is questionable. The majority of full-scale girders that have been investigated experimentally were not sufficiently instrumented and were subjected to prestress transfer at concrete release strengths considerably greater than what is used in common practice. Due to these discrepancies, the behavior of the specimens and the observed parameters of interest in these studies may not be indicative of the performance of actual pretensioned girders to be used in the field. Additionally, the atypical failure modes described above are sensitive to the geometry of the pretensioned concrete element, reinforcement detailing, and interaction between stresses and damage due to prestress transfer and those due to subsequent applied load. Therefore, the results obtained from a certain precast member may not be applicable to a different family of precast cross sections with different reinforcement detailing. To address the concerns related to the use of 0.7-in. diameter strands in Tx-girders, TxDOT Project 0-6831 was initiated.

## **1.3 Research Plan**

The primary objectives of Project 0-6831 were to evaluate the potential serviceability and strength implications of using 0.7-in. diameter prestressing strands on a standard 2- by 2-in. grid in Tx-girders and develop design recommendations for potential implementation of Tx-girders with these larger-diameter strands. These objectives were accomplished through a series of tasks that included reviewing the literature, conducting an industry survey, and performing extensive experimental and computational studies. A brief introduction to these tasks is provided in this section.

### **1.3.1 Task 1: Literature Review**

A literature review was conducted to enhance the research team's understanding of prestress force transfer mechanisms and effects of using larger-diameter strands on the serviceability and strength of the end-region in pretensioned concrete girders. Existing knowledge

and insights obtained from previous implementation of 0.7-in. prestressing strands were also extracted from the literature. Synthesis of these topics provided the basis for the development of the Manufacturer Survey (Task 2), Analytical Program (Task 3) and Experimental Program (Tasks 4 and 6).

### **1.3.2 Task 2: Manufacturer Survey**

The research team conducted a survey of precast manufacturers in Texas to collect information on their current capabilities, necessary upgrades to their equipment to accommodate 0.7-in. diameter strands, and the manufacturers' perception of value for these larger-diameter strands. The primary objective of this survey was to recognize issues that could potentially affect the constructability of Tx-girders that employ 0.7-in. strands.

In addition to this statewide survey of precast manufacturers, the team conducted a nationwide survey of state transportation departments to recognize any previous experience with 0.7-in. strands outside Texas and the potential interest in using these larger-diameter strands. The information collected from this second survey was valuable in identifying any previous projects in which 0.7-in. diameter strands had been used without being reported in the literature, as well as potential challenges related to the implementation of 0.7-in. strands.

### **1.3.3 Task 3: Analytical Program**

The experimental studies outlined in Sections 1.3.4 and 1.3.6 were the primary tool for investigation and as such, formed the basis for the conclusions of this research program. However, extensive computational studies were also conducted to complement the experimental investigation. These computational studies included a series of finite element analyses and parametric studies.

#### *1.3.3.1 Finite Element Analysis*

To shed light on the force transfer mechanisms and distribution of end-region stresses and damage in pretensioned girders that employ 0.7-in. strands on a 2- by 2-in. grid, a series of FE models were developed in ATENA 3D (2015). These models were also used to understand the load-carrying mechanisms and the failure mode in the girders under shear-critical loading. The FE models were carefully validated based on experimental results from this research projects as well as previous experimental studies on pretensioned girders. The validated FE models were employed to evaluate the potential modifications to end-region detailing before specimens with modified details were fabricated as part of the experimental program.

#### *1.3.3.2 Parametric Study*

The parametric studies were performed to quantify the benefits and limitations of using 0.7-in. diameter strands in pretensioned girders. Thousands of design cases were investigated using a parametric study tool that was developed originally by Garber et al. (2013 and 2016) and was modified for the purposes of this research project. A wide set of parameters, including strand diameter, girder cross-section type, concrete release strength, span length, and spacing between the girders was considered in developing the design cases. The results were used to examine important design parameters such as steel quantity, span capability, slenderness of the superstructure, and maximum allowable spacing between girders and assess the benefits of using 0.7-in. diameter prestressing strands in different bridge configurations.

#### **1.3.4 Tasks 4: Experimental Program – End-Region Serviceability**

An experimental program consisting of 14 end-region tests on seven full-scale Tx-girder specimens (five Tx46 and two Tx70 girders) was completed to identify and address serviceability concerns associated with using 0.7-in. strands in Tx-girders. The specimens were fabricated in the controlled laboratory environment at FSEL using the common industry practices. Fabrication of the specimens at FSEL made it possible to gain unlimited access to the specimens for instrumentation as well as firsthand insights into potential constructability issues.

Key parameters considered in designing the specimens for the experimental program included the concrete release strength, strand patterns, and girder cross-section type. All specimens were fabricated using 0.7-in. diameter strands on the standard 2-by-2-in. grid. The design process was completed according to the 7<sup>th</sup> edition of AASHTO LRFD Bridge Design Specifications, considering the 2015 and 2016 interim revisions (AASHTO, 2016). To examine the most critical conditions with regards to prestress transfer, all specimens were designed to reach the maximum allowable tensile stresses, compressive stresses, or both at the time of release. The mild-steel reinforcement used within the end-regions of the first four specimens was detailed according to the current TxDOT standard drawings for Tx-girders with 0.6-in. diameter strands (Texas Department of Transportation, 2015). However, modified end-region detailing was used within the last three specimens.

Note that the concrete release strength for one of the specimens in the testing program was undesirably low. As a result, this specimen was not deemed representative of the conditions of pretensioned girders in the field. The results obtained from this specimen were not used in drawing the conclusions of this research project, and the research team repeated the specimen to meet the objectives of the project.

Each end-region test involved detailed studies of the prestress force transfer and corresponding end-region response, which were obtained during the fabrication process and over time. The specimens were extensively monitored for strains in the strands and stirrups within the end-region, as well as patterns and widths of end-region cracks. The measurements obtained from the specimens were employed to estimate the transfer length for 0.7-in. strands, evaluate the distribution of bursting and spalling stresses, and efficacy of different end-region details. Monitoring of crack widths and patterns continued for a minimum of four weeks after specimen fabrication to study the potential changes in end-region cracks over time.

#### **1.3.5 Task 5: Review Potential End-Region Modifications**

Following the completion of the first three specimens with standard TxDOT detailing, a meeting was held with the Project Monitoring Committee (PMC) to discuss the results from end-region testing, assess the necessity of modifying the end-region detailing in Tx-girders with 0.7-in. diameter strands, and review efficient and constructible modifications to the reinforcement within the end-region. The feedback obtained from PMC guided the research team in selecting the end-region detailing for later specimens in the experimental program.

#### **1.3.6 Task 6: Experimental Program – Ultimate Shear Strength**

All specimens fabricated during the course of the end-region serviceability program (Task 4) were loaded in a shear-critical loading configuration until failure, during which the applied loads, deflections, strains in the shear reinforcement, slip of the strand ends relative to the end face of the specimens, and patterns of cracking and damage were monitored. The parameters that were varied in this testing program included girder cross-section, concrete strength, and the shear span-

depth ratio. The results obtained from this testing program made it possible to assess the impacts of using 0.7-in. diameter strands and corresponding end-region modifications on the failure mechanisms and ultimate strength of Tx-girders.

### **1.3.7 Task 7: Development of Design Recommendations**

Based on the experimental data obtained from Tasks 4 and 6, the research team developed a set of design recommendations for the implementation of 0.7-in. diameter prestressing strands in Tx-girders.

### **1.3.8 Task 8: Presentation of Preliminary Design Recommendations**

Prior to final submission of the project deliverables, a meeting was held with the TxDOT PMC to present the findings of the research project and obtain the committee's feedback on the findings of the investigation and the preliminary design recommendations and fabrication specifications. The guidance provided by the committee facilitated the development of final project deliverables, including the design recommendations.

## **1.4 Report Organization**

This report is divided into nine chapters, including this introduction. Chapter 2 provides the background information and summarizes the existing knowledge on the use of 0.7-in. diameter prestressing strands in pretensioned girders. Chapter 3 introduces the industry surveys conducted as part of Task 2 and presents the findings from the surveys. An overview of the parametric investigation on the benefits and limitations of using 0.7-in. strands in pretensioned bridge girders is provided in Chapter 4. Chapter 5 introduces the experimental program that was performed to evaluate the end-region serviceability (Task 4) and shear strength (Task 6) of Tx-girders with 0.7-in. diameter strands. The findings of the experimental program are presented and discussed in Chapter 6, whereas Chapter 7 presents the FE analyses conducted to supplement the experimental studies. Finally, Chapter 8 provides a summary of this research project and its overall findings.

This report also includes two appendices: Appendix A includes the surveys that were distributed to the precast manufacturers in Texas and to state transportation departments. Appendix B contains a summary of the design recommendations for the use of 0.7-in. diameter strands in Tx-girders based on the findings of this research project.

# CHAPTER 2

## Background

### 2.1 Overview

The background information related to the use of 0.7-in. diameter strands in pretensioned concrete girders is presented in this chapter. This information includes review of the knowledge regarding the prestress transfer mechanisms, end-region behavior in pretensioned concrete elements, and atypical failure mechanisms that might occur in girders with larger-diameter prestressing strands. Following this background information, a review of previous studies investigating the use of 0.7-in. diameter strands in pretensioned concrete elements is presented. The existing knowledge reviewed in this chapter sheds light on the necessity of the experimental and computational investigations described within the remainder of this report.

### 2.2 Prestress Transfer and Development Length

In pretensioned concrete elements, the effective stress in prestressing strands develops with distance from the end face of the member. Figure 2-1 shows the variation of strand stresses along the length of a pretensioned concrete beam. As shown in the figure, the effective stress in the prestressing steel is increased from zero at the end of the member to the full prestress level over a distance known as the “*transfer length*” or  $l_t$ . An increase in the transfer length corresponds to a more gradual development of prestress with distance from the end face, which results in reduced end-region damage at the time of prestress transfer. On the other hand, a longer transfer length means reduced prestress levels within the regions that might be critical in resisting shear. As a result, the transfer length is a critical design parameter that should be estimated with reasonable accuracy.

When an external load is applied to the pretensioned element, an additional length is needed for developing the increase in strand stresses from the prestress level to the stress at the nominal flexural strength of the cross section. This additional length is known as the “*flexural bond length*”. The sum of the transfer length and flexural bond length is known as the “*development length*” or  $l_d$ , which is the total distance from the free end of the member required to develop the ultimate stress in the strand.

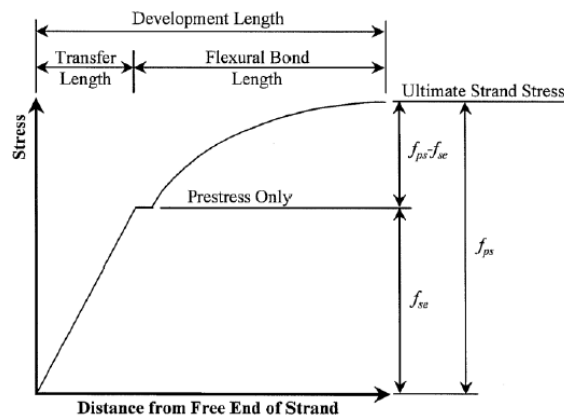
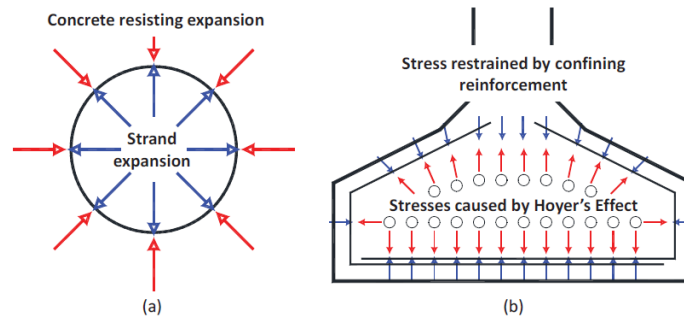


Figure 2-1- Steel stresses vs. distance from the free end of the strand (Vadivelu, 2009)

The quality of the bond between the strands and the concrete plays a crucial role in the stress transfer and development of prestressing strands. The bond between the strand and concrete is provided through adhesion, mechanical interlock, and the phenomenon known as “Hoyer’s effect” (Hoyer & Friedrich, 1939; Hanson & Kaar, 1959; Janney, 1954). Adhesion is the “glue” effect between the strand and the concrete while mechanical interlock is a result of the cement paste filling the voids around the seven wire strands. When the prestressing strand is tensioned longitudinally, its radial dimension decreases due to Poisson’s effect. However, as the stress in the strand is reduced during release, the strand tends to return to its original diameter, thereby inducing stresses in the surrounding concrete as shown in Figure 2-2(a). The surrounding concrete restricts this lateral strand expansion and causes a wedging of the strand, which is referred to as the Hoyer’s effect (Hoyer & Friedrich, 1939). Over the transfer length, adhesion provides no contribution to the bond due to the slipping of the strand along the concrete interface (Braun, 2002; Janney, 1954; Russell & Burns, 1993; Zia & Mostafa, 1977). Therefore, the Hoyer’s effect and mechanical interlock serve as the primary mechanisms of bond in this region.



**Figure 2-2- Stresses induced in the flange due to Hoyer’s effect (Garber et al., 2016)**

Stresses around the strand caused by Hoyer’s effect will be resisted by the surrounding concrete and confining reinforcement, as shown in Figure 2-2(b). These stresses must be kept beneath a certain level by way of adequate strand spacing and controlled using confining reinforcement to minimize concrete cracking. If the combination of confining reinforcement and strand spacing is inadequate, excessive cracking around the strand can lead to reduced bond performance or bond failure.

Physical characteristics of a prestressing strand including size, type, and surface conditions have a significant effect on the stress transfer and development length. A summary of the primary contributing factors, provided by Zia and Mostafa (1977), is presented in Table 2-1. Coating, presence of rust, oil, grit, or indentation can affect the surface conditions of the strands and hence the bond between the strands and the concrete. The influence of strand surface condition on transfer and development length has been noted in several studies (Braun, 2002; Cousins, Johnston, & Zia, 1990; Detherage, Burdette, & Chew, 1994; Gross & Burns, 1995; Hanson & Kaar, 1959; Janney, 1954; Lane, 1992; Russell & Burns, 1993). While it is difficult to quantify the effects of the strand conditions, the results conclude that both stress transfer and flexural bond behavior improve with surface roughness.

**Table 2-1- Factors affecting bond. Adapted from [7]**

<b>Steel</b>	- Size of prestressing strand
	- Type of prestressing strand
	- Effective prestress Force
	- Release method
	- Surface condition of steel
	- Strand spacing
	- Amount of confining reinforcement
<b>Concrete</b>	- Compressive release strength
	- Amount of cover around steel
<b>Other</b>	- Time-dependent effects
	- Type of loading applied

At prestress transfer, the method of release has also been shown to contribute to the bond performance of prestressing strands. In a gradual release system, hydraulic jacks are retracted slowly to introduce the prestress forces to the system in a highly-controlled manner. In contrast, flame cutting or sawing of strands can be used to provide immediate release. Compared to gradually releasing strands, immediate strand release can lead to longer transfer lengths (Gross & Burns, 1995).

### **2.3 Review of Literature on Transfer and Development Lengths for 0.5- and 0.6-in. Strands**

The work that took place in the 1950s through the late 1980s serves as the foundation for research on the use of pretensioning strands. Through years, economic benefits associated with using fewer, more concentrated prestressing strands resulted in an interest in employing larger-diameter strands in pretensioning applications. However, in 1988, the Federal Highway Administration (FHWA) issued a moratorium on the use of 0.6-in. diameter strands on the 2-in. grid. The reason for this decision was experimental evidence suggesting that transfer and development lengths might be unconservatively estimated for 0.6-in. strands using the existing design equations. Extensive research was conducted in the following years, the results of which indicated that transfer length provisions did not differ between 0.6- and 0.5-in. strands (Burkett & Kose, 1999; Russel & Burns, 1996). As a result, the moratorium was lifted in 1996, paving the way for increasing the diameter of prestressing strands. In Texas, the majority of pretensioned girders currently fabricated employ 0.6-in. strands.

Previous studies on the prestress transfer mechanisms and transfer and development lengths have been performed on members that were reinforced with 0.6 in. or smaller-diameter strands. The applicability of results from such studies to girders with larger-diameter strands needs to be verified. However, knowledge of these previous studies is essential in understanding the mechanisms that govern the transfer and development of pretensioned strands, and identifying the set of parameters that need to be assessed for the newly introduced 0.7-in. strands.

The following sections provide a review of some of the major research efforts on transfer and development lengths of prestressing strands, with a focus on studies that might be relevant to the purpose of this report.

### **2.3.1 Janney (1954)**

Janney (1954) conducted a series of tests on small prisms and beam specimens to evaluate the bond stresses near the ends of prestressed members after release. Changes in prestress transfer and bond stresses due to different steel diameters, different surface conditions of steel, and different concrete strengths were evaluated. By conducting an elastic analysis on the deformations that occurred at prestress release, it was found the influence of circumferential tensile stresses lead to inelastic response along the transfer length. In addition, Janney concluded that bond stresses were largely due to friction between concrete and steel. Due to high bond stresses developed after cracking and reported limited interaction between the transfer bond stresses and the flexural bond stresses, the reliability of the expressions available at that time for calculating bond stresses was questioned.

### **2.3.2 Hanson and Kaar (1959)**

Hanson and Kaar (1959) tested 47 small rectangular beams for flexural bond. The specimens were prestressed with 0.25-, 0.375-, and 0.5-in. diameter strands. The focus of the investigation was on the influence of strand size and embedment length on the bond behavior of pretensioned beams. Test results showed a linear correlation between the strand diameter and transfer and development lengths. This work emphasized the previous work performed by Janney (1954) and became a basis for ACI and AASHTO equations.

### **2.3.3 Cousins, Johnston, and Zia (1990)**

Cousins et al. (Cousins, Johnston, & Zia, 1990) studied the effects of strand surface conditions on transfer and development lengths. Flexural tests were performed on two types of rectangular prisms consisting of a single prestressing strand, placed either concentrically for transfer length tests or eccentrically for development length. Strand diameters included 0.375, 0.5, and 0.6 in., and some of the strands were coated with epoxy and grit. The transfer lengths measured in these tests for uncoated strands were found to be two to three times greater than the predictions by the ACI 318 and AASHTO code equations of the time, indicating a lack of conservatism in code equations. The work by Cousins et al. was a major factor leading to the FHWA's moratorium on the use of 0.6-in. diameter strands.

### **2.3.4 Lane (1992)**

Lane (1992) looked into the effects of strand surface conditions and epoxy coating on transfer length, using small-scale prisms. The number of strands used within the specimens ranged from one to four. It was found that the transfer length increased as the number and size of strands increased. The average transfer length, considering all diameters of epoxy-coated strands, was found to be 50 times the strand diameter while a transfer length of 43 times the strand diameter was reported for 0.6-in. diameter strand. It was also reported that the transfer length for uncoated strands was 60 percent greater compared to epoxy-coated strands.

### **2.3.5 Russell and Burns (1993, 1996)**

To study the transfer and development length, Russell and Burns (1993) tested nineteen AASHTO girders and nine rectangular beams, which included 0.5- and 0.6-in. diameter strands. It was noted that shear may play a significant role in the bond between the concrete and prestressed strands. During this investigation, Russell and Burns proposed a method commonly referred to as the *95 percent of Average Maximum Stress (AMS) method* to determine the transfer length of

strands after obtaining a strain profile along the length of the member using a Demountable Mechanical (DEMEC) strain gauge. This method is extensively used today to find the transfer length in small and full-scale specimens.

Additional work was conducted by Russell and Burns (1996). Thirty-two rectangular prisms and 12 scaled AASHTO-type beams were constructed with 0.5- and 0.6-in. diameter strands. The specimens were tested to identify the relationship between transfer lengths and strand spacing, debonding effects, confining reinforcement, number of strands, and cross-sectional shape. The researchers primarily determined transfer length using a DEMEC gauge. Alternative transfer length measurement methods included the use of electrical resistance strain gauges attached to the strands, physical slip measurements, and visual inspection.

The primary conclusion from this study was that 0.6-in. diameter strands could successfully transfer prestressing stresses to surrounding concrete on a 2-in. by 2-in. grid without evidence of cracking. The results were the major evidence that prompted FHWA to lift the moratorium on the use of 0.6-in. strands (Burkett & Kose, 1999; Russel & Burns, 1996). The team also reported that on average, the transfer length for 0.6-in. strands was 36 percent longer than that of 0.5-in. strands. Confinement was found to have no appreciable effect on transfer length, and on average, larger beams with more strands were found to have shorter transfer lengths than small-scale beams.

### **2.3.6 Mitchell, Cook, Khan, and Tham (1993)**

Mitchell et al. (1993) performed flexural tests on 22 precast, pretensioned small rectangular beams that were constructed using high-strength concrete and were reinforced with a single strand. Three strand diameters, 0.375, 0.5, and 0.62 in. were used. The strength of concrete at transfer ranged from 3,000 to 7,250 psi and the compressive strength varied from 4,500 to almost 13,000 psi. Transfer lengths were determined based on a slope-intercept method. Mitchell et al. reported that higher concrete strengths resulted in smaller transfer lengths and flexural bond lengths. As a result of these tests, an equation, which is presented in Table 2-2, was developed to account for the effect of concrete strength on transfer length.

### **2.3.7 Deatherage, Burdette, and Chew (1994)**

Deatherage et al. (1994) performed tests to evaluate the effects of strand size and surface conditions and investigate minimum strand spacing. Twenty full-scale tests were conducted on AASHTO Type I beams with lengths of 31 feet and strand sizes up to 0.6-in. diameter. The transfer length was obtained through slope-intercept method. Results showed an inconsistent and shorter transfer length for 0.6-in. diameter strands. The team also tested center-to-center strand spacing of 3.5 times and 4 times the strand diameter and found that the smaller strand spacing was adequate. In addition, Deatherage et al. compared their findings with ACI 318 and AASHTO LRFD equations and found those equations to slightly underestimate the development length.

### **2.3.8 Barnes, Burns, and Kreger (1999)**

Barnes et al. (1999) studied the influence of compressive strength of concrete, strand surface condition, prestress release method, and time-dependent effects on transfer and development length were investigated. The research involved 36 high strength concrete AASHTO Type I beams, which incorporated 0.6-in. strands arranged on 2-in. grids. To determine the transfer length, the team used the 95 percent AMS method proposed by Russell and Burns (1993). The transfer length was found to be indirectly proportional to the square root of the strength of concrete at release. It was also reported that the transfer length increased by 10-20 percent over time, with

most of the change happening in the first 28 days. The results also indicated that the transfer length in beams constructed using high-strength concretes were less affected by prestress release method.

### 2.3.9 Braun (2002)

Braun (2002) investigated the transfer and development length of 0.6-in. strands on a 2-in. grid in Texas I-beams. The test program involved four beams that were fabricated in 1995. Two beams were made of normal strength concrete and the other two were constructed using high-performance concrete. Two methods were used to determine transfer length: DEMEC measurements and strand end-slip measurements. The only parameter that varied between the specimens was the concrete strength. The transfer length was found to be 26 percent greater in the normal strength concrete beams compared to the high-performance concrete beams. However, Braun noted that other factors, such as strand surface condition and the release method may be of greater significance than concrete strength. The transfer lengths from all of the beams were found to be less than 50 times the strand diameter.

### 2.3.10 Marti-Vargas et al. (2007)

Marti-Vargas et al. (2007) conducted an experimental investigation to evaluate the transfer length of a seven-wire prestressing strand using a series of 4- by 4-in. prisms. The specimens were fabricated using 12 concrete mixes with different strengths, water-to-cement ratios, and cement contents. The prisms were prestressed using a concentric 0.5-in. strand. To determine the transfer length, the loss in strand force after transfer was measured for specimens with different embedment lengths. The force loss data were then plotted versus embedment length, which resulted in a bilinear trend, as shown in Figure 2-3. The transfer length was determined by finding the embedment length corresponding to the beginning of the horizontal branch.

Based on the results of this study, the reliability of methods for estimating the transfer length from strand end slip was evaluated. The results were also used to develop expressions for average bond stress along transfer and the flexural bond length as functions of concrete strength at the time of prestress transfer and at the time of loading, respectively. Based on these expressions, a model was developed for transfer and development length (2007). This model, which is presented in Table 2-2, is believed by some researchers (Pozolo & Andrawes, 2011) to be one of the most accurate models currently available for determining transfer and development length.

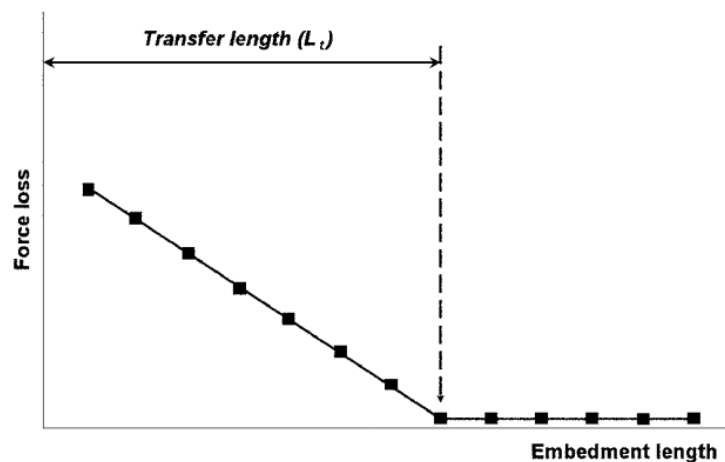


Figure 2-3- Determination of transfer length in the method used by Marti-Vargas et al (2007).

### 2.3.11 Summary of Previous Results and Equations of Transfer and Development Length

Table 2-2 provides a non-exhaustive summary of some of the most important equations that have been suggested to estimate transfer and development lengths (Braun, 2002; Gross & Burns, 1995; Kose & Burkett, 2005). Note that the studies supporting these equations were done on specimens reinforced with strands that had diameters less than or equal to 0.6 in., and the applicability of such provisions to larger-diameter 0.7 in. strands needs to be verified.

**Table 2-2- Summary of transfer and development length equations**

Year	Transfer Length ( $L_t$ )	Development Length( $L_d$ )	Reference
2014	$L_t = 60d_b$	$L_d = \left(f_{ps} - \frac{2}{3}f_{se}\right)d_b$	AASHTO LRFD (2016)
2014	$L_t = \frac{f_{se}}{3}d_b$	$L_d = L_t + (f_{ps} - f_{se})d_b$	ACI 318 (2014)
2007	$L_t = \frac{2.5A_p\sigma_{pi}}{\Sigma_p f' c i^{\frac{2}{3}}}$	$L_A = \frac{2.5A_p}{\Sigma_p f' c i^{\frac{2}{3}}}(\sigma_{pi} + 1.6(\sigma_{pa} - \sigma_{pa}^*))$	Marti-Vargas et al. <sup>(1)</sup> (2007)
1998	$L_t = \frac{4f_{pt}}{f'_c}d_b - 5$	$L_d = L_t + \frac{6.4(f_{ps} - f_{se})d_b}{f'_c} + 15$	Lane (1992)
1994	$L_t = \frac{f_{si}}{3}d_b$	$L_d = L_t + (f_{ps} - f_{se})d_b$	Deatherage et al. (1994)
1993	$L_t = \frac{f_{si}d_b}{3} \sqrt{\frac{3}{f'_c i}}$	$L_d = L_t + 1.5(f_{ps} - f_{se})d_b \sqrt{\frac{4.5}{f'_c i}}$	Mitchell et al. (1993)
1993	$L_t = \frac{f_{se}}{2}d_b$	$M_{cr} > L_t V_u$ Fully Bonded $\frac{L_b + L_t}{span} \leq 0.5 \left(1 - \sqrt{1 - \frac{M_{cr}}{M_u}}\right)$ Debonded	Russell and Burns (1993)
1990	$L_t = \frac{U'_t}{2B} \sqrt{f'_c i} + \frac{f_{si} + A_{ps}}{\pi d_b U'_t \sqrt{f'_c i}}$	$L_d = L_t + (f_{ps} - f_{se}) \left(\frac{A_{ps}}{\pi d_b U'_d \sqrt{f'_c i}}\right)$	Cousins et al. (1990)

B- Bond stress

$d_b$ - Diameter of the prestressing strand (in.)

$E_C$ - Modulus of elasticity of concrete (ksi)

$f'_c$ - Concrete compressive strength (ksi)

$f'_{ci}$ - Concrete compressive strength at transfer(ksi)

$f_{pi}$ - Stress in strand prior to release (ksi)

$f_{ps}$ - Stress in strand at nominal flexural strength(ksi)

$f_{se}$ - Effective prestress after all losses (ksi)

$f_{si}$ - Initial prestress after release (ksi)

$M_{cr}$ - Cracking moment of cross section

$M_u$ - Nominal Flexural strength

$U'_d$ - Strand surface coefficient development length

$U'_t$ - Strand surface coefficient transfer length

**Note:** (1) Work performed in SI units:

$\Sigma_p$ -perimeter of prestressing reinforcement (mm)

$L_t$ - transmission/transfer length (mm)

$L_d$ - anchorage/development length (mm)

$\sigma_{pi}$ - effective prestress (MPa)

$\sigma_{pa}$ -maximum stress in strand at loading (MPa)

## 2.4 End-Region Stresses and Cracking

Due to the increased magnitude and eccentricity of the prestressing force, pretensioned concrete girders with 0.7-in. strands might be prone to increased cracking within their end-region. At prestress transfer, the end-regions of pretensioned girders are subjected to transverse stresses that are generally categorized as bursting, spalling, and splitting stresses. These stresses might result in cracking near the end-faces of the girders after the prestressing strands are released. Figure 2-4 shows the primary locations of end-region stresses and the potential cracking that might happen as a result of each type of stress.

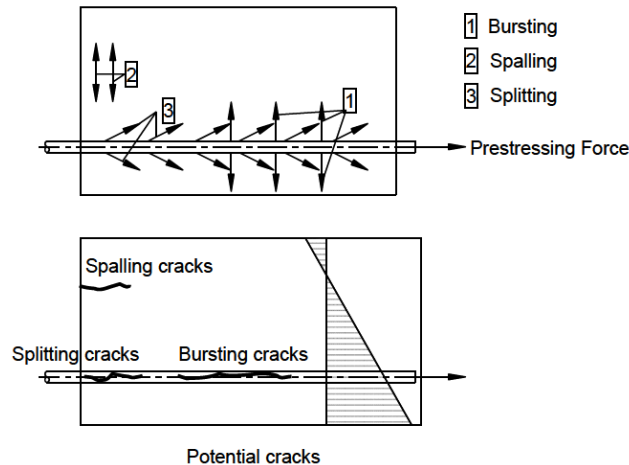


**Figure 2-4- End-region stresses and potential cracks formed after prestress transfer (CEB, 1987)**

Bursting cracks are primarily related to the magnitude of force in the bottom flange, and as shown in Figure 2-4, form along the strands. Spalling cracks are associated with the compatibility of strains near the end face and depend on the eccentricity of the strands or the distance between the centroid of the strands and the geometric centroid of the cross section. These cracks are usually localized near the end face of the beam at some distance from the strands within the cross section. Splitting cracks form near the end face and are a result of the radial compressive stresses that are generated as a result of Hoyer's effect (Hoyer & Friedrich, 1939).

To ensure the serviceability and safety of precast pretensioned girders, it is essential to use appropriate detailing within the end-regions of girders so that the width of aforementioned cracks is controlled. Due to variety of parameters that govern the conditions of bursting, spalling, and splitting cracks, such detailing needs to be independently developed for each family of precast cross sections.

The current detailing used in Tx-girders is primarily developed based on an experimental study by O'Callaghan and Bayrak (2007). In this study, a series of full-scale specimens was fabricated to determine an end-region reinforcement scheme for girders that are fabricated using 0.6-in. diameter strands. The specimens consisted of four Tx-girders: two Tx28, one Tx46, and one Tx70. The layout of 0.6-in. strands used in the construction of the girders was developed to yield a bottom fiber compressive stress equal to  $0.65f'_{ci}$ . The strands in most of the specimens were concentrated near the centroid of the cross section to maximize the prestressing force and hence, bursting stresses. Per relevant AASHTO LRFD requirements, end-region reinforcement was provided within a distance equal to one quarter of the girder height ( $h/4$ ) from the end face of the

girder. The vertical reinforcement was instrumented within the first 46 in. of each end to monitor the spalling and bursting stresses that developed in the end-regions.

Bursting stresses appeared to be directly related to the amount of prestressing force applied and the transfer length. A maximum transverse reinforcement stress of 32 ksi was documented, which was coupled with measured crack widths of 0.009 in. at the end of the transfer length. Shear reinforcement placed within the transfer length (and outside  $h/4$ ) was generally overstressed (above the 20 ksi limit stipulated by AASHTO LRFD); additional reinforcement was recommended to counteract the bursting stresses and limit unintended shear strength consequences.

## 2.5 Shear Strength

Due to the potential for increased end-region stresses, Tx-girders with 0.7-in. diameter strands may be more susceptible to two non-traditional failure mechanisms: horizontal shear failure and anchorage-induced shear failure. Both non-traditional shear failure mechanisms are brittle, explosive mechanisms that may initiate below code-estimated shear capacities. Examples of these failure modes observed in previously tested Tx-girders are provided in Figure 2-5.



(a) Horizontal shear failure (Hovell et al., 2011)



(b) Anchorage-induced shear failure (Garber et al., 2016)

**Figure 2-5- Atypical failure modes observed in previous experimental studies on Tx-girders**

Note that these atypical failure modes are not exclusive to Tx-girders. Nakamura (Nakamura, Avendano, & Bayrak, 2013) compiled a database of shear tests performed on prestressed concrete members in North America, Japan, and Europe from 1954 to 2010. The resulting database includes 1,696 tests and was utilized to evaluate the accuracy of various methods used to predict the shear strength of prestressed concrete members. Horizontal shear or anchorage-zone distress were specifically identified in 52 tests among those included in the database, out of which only four tests had been conducted on Tx-girders. Based on the findings of this study, the sectional design expressions based on MCFT were found to be the most accurate in estimating the shear strength of members with sufficient shear reinforcement. However, members that failed in shear but showed signs of horizontal shear damage, anchorage zone distress, or had insufficient shear reinforcement demonstrated shear capacities lower than those predicted by the sectional MCFT-based procedure.

### 2.5.1 Horizontal Shear Failure

A horizontal shear failure occurs when there is a breakdown along a horizontal plane within the girder, as shown in Figure 2-6. Shear slip along the plane leads to the development of horizontal sliding, and the beam no longer acts compositely but as two shallower beams, as shown in Figure 2-6 (b). Commonly used bulb-tee cross-sections have been optimized for economic efficiency, which has led to relatively small web geometries in comparison to the bottom flange sizes. This small web-large flange intersection results in the development of large horizontal shear stresses and makes the beam susceptible to horizontal shear failure.

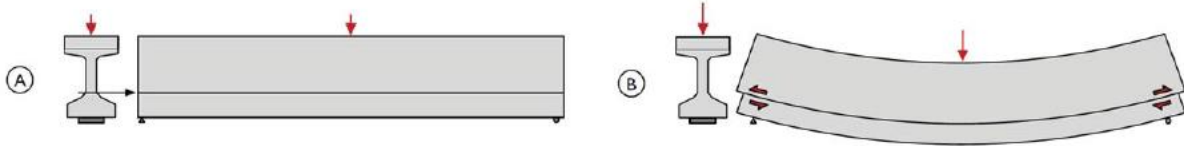


Figure 2-6- Horizontal shear failure (Hovell et al., 2011)

Avendaño (2008) performed shear tests on two Tx28 girders constructed by O’Callaghan (2007). A horizontal shear failure was observed in all four of the shear tests performed. However, Avendaño concluded that for Tx28 girders, the ACI 318-08 and AASHTO LRFD general shear design specifications were conservative, although they did not explicitly consider horizontal shear failure modes. While the effect of increasing strand diameter on the horizontal shear capacity was not within the scope of this study, it can be predicted that with the increased congestion of strands in the bottom flange, the stress at the web-flange interface increases; hence the interface weakens, resulting in a reduced shear capacity.

Horizontal shear failure in Texas U-beams was investigated in detail by Hovell et al. (2011). Eight full-scale Texas U54 prestressed concrete girders were fabricated to investigate their behavior at the time of prestress transfer and under applied loads. Horizontal shear failure occurred in four specimens at a load below the calculated capacity of the specimen. As a result of this study, a systematic procedure was developed for evaluating the horizontal shear demand on the web-flange interface in any precast concrete cross section as well as the capacity of this interface in resisting the horizontal shear demand. The calculations in this method are based on the theories of beam bending and shear friction, and are shown to provide conservative estimates compared with data from the U54 tests and other data from the literature.

In the method proposed by Hovell et al., the horizontal shear crack is assumed to start at the point where a 45-degree shear crack originating from the applied load point intersects the web-flange interface (Figure 2-7). Horizontal shear failure is assumed to happen when the horizontal shear demand,  $V_{uhs}$ , reaches the nominal capacity of the interface plane,  $V_{ni}$ . Values of  $V_{uhs}$  and  $V_{ni}$  are determined using Equations 2-1 and 2-2, respectively.

$$V_{uhs} = V_u \frac{l_{crit}}{d} \quad \text{Equation 2-1}$$

$$V_{ni} = k_d [cA_{cv} + \mu(A_{vf}f_y - 0.04P_{PS})] \quad \text{Equation 2-2}$$

$$l_{crit} = a - \frac{l_{LP}}{2} - h + y_{crit} \quad \text{Equation 2-3}$$

In these equations,  $V_u$  is the applied shear force;  $l_{crit}$  is the length of demand determined from Equation 2-2;  $d$  is the distance from extreme compression fiber to the centroid of tensile

reinforcement;  $k_d$  is a shape factor taken as 1 for I-shaped beams;  $A_{cv}$  is the area of concrete engaged in interface shear transfer;  $A_{vf}$  and  $f_y$  are the area and yield strength of shear reinforcement crossing the horizontal shear plane;  $P_{PS}$  is the prestressing force transferred to the beam within the region of interest; and  $c$  and  $\mu$  are the cohesion and friction constants equal to 0.4 ksi and 1.4, respectively. The geometrical parameters used in Equation 3 are shown in Figure 2-7. Hovell et al. recommended that the horizontal shear capacity in this method not be taken greater than the minimum of  $K_1 f'_c A_{cv}$  and  $K_2 A_{cv}$ , where  $f'_c$  is the compressive strength of concrete;  $K_1$  is equal to 0.25; and  $K_2$  is equal to 1.5 ksi for monolithic, normal-weight concrete.

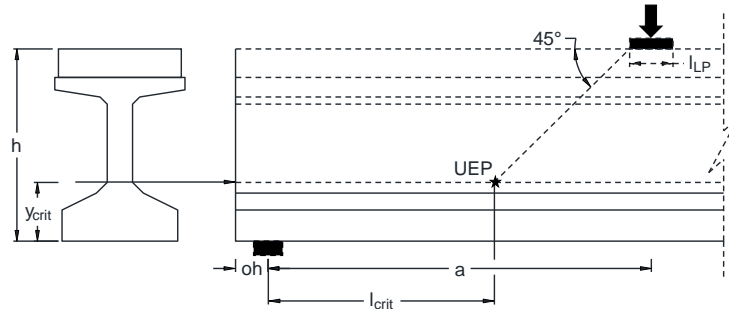


Figure 2-7- Definition of  $l_{crit}$  (Hovell et al., 2011)

### 2.5.1 Anchorage-Induced Shear Failure

A shear failure can be induced by distress in the anchorage zone or failure of the bond between the strand and surrounding concrete. When a shear crack first initiates near the edge of the bearing pad, it is restrained from opening further by the tension provided by the prestressing strand ( $T_{max}$ ), as shown in Figure 2-8. If there is an inadequate amount of restraining force provided by the steel crossing the crack (e.g., when proper development of the strands is impeded by anchorage zone distress), progression of the diagonal shear crack crossing the longitudinal steel or total slippage and loss of bond in the strands will occur, leading to anchorage-induced shear failure. This failure mode is generally more likely at the inside edge of the bearing area of pretensioned girders, where the available capacity of the strands will be smaller because the bearing region is usually located within the transfer length.

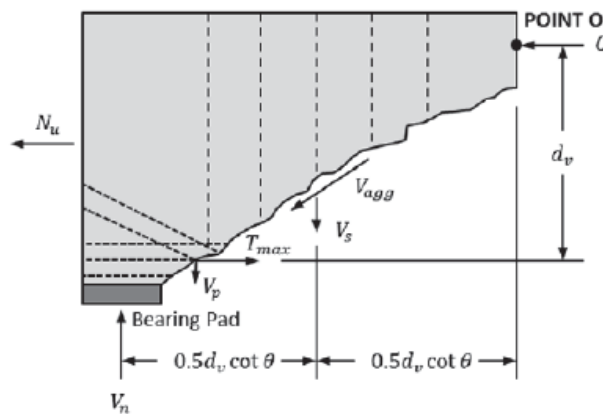


Figure 2-8- Anchorage free-body diagram (AASHTO, 2016)

The anchorage-induced shear failure mode is taken into account in the calculations of load-carrying capacity according to AASHTO LRFD Bridge Design Specifications (AASHTO, 2016). According to these specifications, Equation 2-4 is used to determine the total demand on the longitudinal reinforcement as a result of combined bending moment, axial force, and shear.

$$T = \frac{|M_u|}{\phi_f d_v} + 0.5 \frac{N_u}{\phi_c} + \left( \left| \frac{V_u}{\phi_v} - V_p \right| - 0.5 V_s \right) \cot \theta \quad \text{Equation 2-4}$$

In this equation,  $T$  is the longitudinal demand;  $M_u$ ,  $N_u$ , and  $V_u$  are ultimate bending moment, axial force, and shear force at the section;  $\phi_f$ ,  $\phi_c$ , and  $\phi_v$  are resistance factors;  $V_p$  is the vertical component of the effective prestressing force;  $V_s$  is shear resistance provided by the transverse reinforcement; and  $\theta$  is the angle of inclination of diagonal compressive stresses.

On the other hand, the capacity of longitudinal steel in resisting this longitudinal demand is dependent on the distance from the end face of the girder, and is calculated using the idealized bi-linear relationship shown in Figure 2-9.

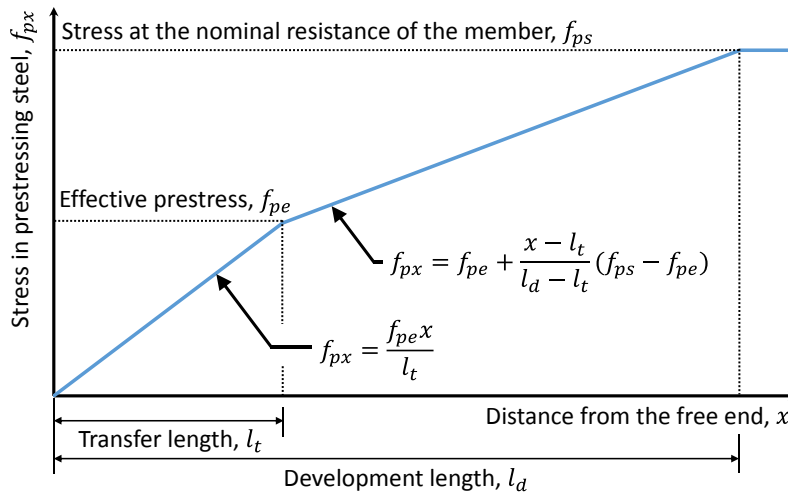


Figure 2-9- Idealized relationship between stress and distance from the free end of strand. Adapted from AASHTO LRFD (2016).

Langefeld (2012) carried out a research program focused on the influence of strand debonding on anchorage-controlled shear failure in prestressed concrete bridge girders. Results from the testing program were subsequently used to evaluate the accuracy of existing anchorage design methodologies. Two full-scale Tx-46 girders, one with 0.6-in. and the other with 0.5-in. diameter strands, were fabricated and tested. In both cases, the girders were designed to fail in anchorage through the use of debonded strands in the end-regions. The experimental shear strengths of the specimens exceeded the values computed in accordance with the AASHTO LRFD 2010 provisions. Results indicated that if a ‘reasonable’ percentage of strands are debonded in Tx-girders, the shear capacity of the girder will not be significantly impacted. However, Langefeld suggested that a broader range of Tx-girders be tested to verify the applicability of the conclusions to other girders. As part of the analytical study phase, a subset of the shear database assembled by Nakamura et al. (2013) was analyzed to investigate anchorage-induced shear failures. The database

analysis revealed that shear failures induced by anchorage zone distress were unconservatively estimated by the AASHTO LRFD provisions in nearly half of the cases.

Garber et al. (2016) conducted a series of shear tests on five identical, full-scale Tx46 girders that were reinforced with 0.5-in. strands. The shear span was the same among the specimens; however, the overhang length varied among the specimens to change the location of the critical section relative to the transfer length. Atypical failure modes were observed in two specimens with the smallest overhang length. It was concluded that atypical failure modes become more likely when the critical section for shear falls within the transfer length. The load-carrying capacity of the specimen failing in anchorage-induced shear failure was less than that associated with other failure modes. However, the horizontal shear failure occurred at a load corresponding to traditional failure modes.

## **2.6 Previous Research Specific to the Application of 0.7-in. Strands**

As previously noted, the studies consisting the main body of literature on prestress transfer, development length, and atypical failure modes have been conducted on specimens reinforced with 0.6-in. or smaller-diameter strands. However, in recent years, a number of studies have been conducted on pretensioned elements that contained 0.7-in. strands.

The following subsections present some of the major studies identified in the literature regarding the use of 0.7-in. prestressing strands. This section is not intended to review all previous studies on the use of 0.7-in. strands. However, it has been tried to introduce the studies that are most relevant to the purposes of this report. The studies are categorized based on the location (university or research center) at which the research has been performed.

### **2.6.1 University of Tennessee, Knoxville**

Vadivelu (2009) investigated the feasibility of using a standard 2-in. grid spacing for AASHTO girders constructed using 0.7-in. diameter strands. A three-dimensional finite element model was developed to evaluate the effects of the prestressing force at transfer. Results from the analyses showed that girders constructed with 0.7-in. diameter strands demonstrated greater potential for cracking at the flange-web interface regions (i.e., greater potential for developing damage related to horizontal shear) than girders constructed with 0.6-in. diameter strands. In addition to the analytical study, one full-scale AASHTO Type I-girder with 0.7-in. strand was fabricated. The transfer length was determined using DEMEC measurements and the 95 percent AMS method proposed by Russel and Burns (1993). The transfer length was found to be between 21 and 22 in., which is shorter than that predicted by the AASHTO LRFD 2008 provisions and ACI 318-08. It was also reported that end-regions designed in accordance with the AASHTO provisions for confinement experienced more cracking than end-regions designed using strut-and-tie modeling procedures according to ACI 318-08. To aid in minimizing end-region cracking, it was suggested that large ratios of confining steel be placed close to the ends of the girder.

### **2.6.2 University of Nebraska-Lincoln**

Prior to the current research at UT, perhaps the most extensive research studies on the behavior of pretensioned concrete elements with 0.7-in. diameter strands were conducted at the University of Nebraska-Lincoln, among which, the following are deemed most relevant to the purposes of this report.

### 2.6.2.1 *Tadros and Morcouc (2011)*

Tadros and Morcouc (2011) reported the results of a number of experimental investigations on specimens reinforced with 0.7-in. strands, as follows:

#### 2.6.2.1.1 Small-Scale Prisms

Four small-scale prisms with cross-sectional dimensions of 7- by 7 in. and a length of 96 in. were fabricated to measure the transfer length. The specimens were reinforced with only one concentric 0.7-in. strand. The strand was stressed to 75 percent of its ultimate strength, and was released at a concrete strength of 6 ksi through gradual retraction of hydraulic rams. The transfer length was estimated using surface strains that were measured using a DEMEC gauge. Based on the 95 percent AMS method proposed by Russel and Burns, the transfer length was determined to be between 26 and 28 in.

#### 2.6.2.1.2 UHPC NU900

A single NU900 girder was fabricated at a precasting facility using Ultra High-Performance Concrete (UHPC) that had a release strength of 12 ksi. The specimen contained thirty 0.7-in. Grade 270 strands on a 2- by 2-in. spacing. However, the strands were stressed only to 66 percent of their ultimate strength. The strands were released through flame cutting, after which no visible cracks were reported within the end-regions of the girder. DEMEC measurements were used to determine the transfer length. Based on the 95 percent AMS method proposed by Russel and Burns (1993), a value of 26 in. was found for transfer length, which is less than estimates by AASHTO LRFD (2010) and ACI 318-14.

An 8.5-in. thick reinforced concrete slab was constructed on the specimen, after which the specimen tested twice, first at a shear span of 15 ft and then, at a shear span of 10 ft at the other end. Due to the limitations of the testing equipment, the specimen was loaded only up to 800 kips without failure. However, reaching the 800-kip load in the second test was accompanied by a notable reduction in stiffness, suggesting imminent failure. The same specimen was reported as part of a separate publication by Morcouc, Hanna, and Tadros (2011).

#### 2.6.2.1.3 UHPC Bridge Double Tee

A bridge double tee girder was fabricated at a precast plant as two separate tee specimens. Each tee contained ten 0.7-in. strands on the 2-in. grid, which were stressed to 60 percent of their ultimate strength. To control the end-region stresses, the strands were harped using a fanned pattern. The strands were released at a concrete strength of 12 ksi through flame cutting. DEMEC measurements were made on the top flange of the specimens 30 minutes and 14 days after release, from which values of 16.5 in. and 18.5 in. were reported, respectively. While the presence of splitting cracks was reported, no detailed information on the crack widths was provided.

A 7.5 in. thick reinforced concrete slab was constructed on each tee specimen, after which each specimens was tested in three configurations: 1) with a shear span equal to the nominal development length according to AASHTO LRFD, the specimen was loaded up to nominal flexural capacity and then unloaded; 2) the specimen was loaded at midspan until flexural failure; and 3) the failed specimen was again tested in shear, with a shear span of 66 in. The specimens could reach their nominal flexural capacities in first and second tests without significant strand slip. Despite significant damage due to flexural tests, each specimen could also reach its nominal shear strengths in the third test.

#### 2.6.2.1.4 T-Girders

Eight pretensioned T-girders with a depth of 24 in. were fabricated in the laboratory. Each specimen contained six 0.7-in. strands that were located on a 2-in. grid and stressed to 75 percent of their ultimate strength, consistent to the allowable jacking stress limit according to AASHTO LRFD specifications. The specimens were released at an age of 6 days and a concrete strength of 9 ksi through gradual retraction of hydraulic rams. Splitting cracks were reported within the end-regions of the specimens. However, no detailed information on the width or pattern of cracks was provided. The transfer length was measured as 19.6-28.5 in. thirty minutes after release, and 20.1 to 30.1 in. fourteen days after release.

All specimens were loaded at midspan, resulting in a shear span length of 153 in. Loading of the specimens continued until failure. All specimens exceeded their nominal flexural capacities according to AASHTO LRFD without significant strand slip. After flexural failure, four out of eight specimens were tested in shear. The supports were moved towards midspan to eliminate the damaged end portions of the girders from the test span. In three out of these four tests, the peak load exceeded nominal shear strength according to AASHTO LRFD. However, one specimen could not reach its nominal capacity in this test, likely due to the significant damage from flexural failure.

#### 2.6.2.1.5 NU 1100 Girders

Three NU 1100 girders were fabricated at a precasting plant using 0.7-in. diameter strands that were located on a 2-in. grid. The specimens were released at a concrete strength of 8 ksi. Twenty-five percent of strands were debonded at one end of all three specimens. The main difference among the specimens was the confinement reinforcement within the bottom flange. Each specimen was tested twice: first for development length, using a 14 ft test span, and then for shear strength, at a relatively low shear span that was 1.77 times the height of the specimen. The specimen had noticeable damage, including diagonal cracks, due to the first test before being tested in the second loading configuration. Premature slippage of strands was measured at the free end of the specimen in the shear test. However, the specimens failed at a load that was at least 16 percent greater than their nominal capacities according to AASHTO LRFD. No information regarding the performance of the girders at the time of prestress transfer was provided.

From the specimens listed in Sections 2.6.2.1.1 through 2.6.2.1.4, Tadros and Morcous (2011) concluded that transfer length for 0.7-in. strands was smaller than those estimated on the basis of code provisions. Given a 2-in. by 2-in. strand spacing, adequate concrete strength ( $f'_c$  greater than 10 ksi), and proper end-region reinforcement as per the AASHTO LRFD requirements, it was also found that 0.7-in. diameter strands can be fully developed within the length estimated by AASHTO LRFD.

#### 2.6.2.2 *Morcous et al. (2012)*

Morcous et al. (2012) studied the mechanical and bond properties of Grade 270, low-relaxation, 0.7-in. diameter strands. More than a hundred strand specimens were obtained from two strand producers and were tested to evaluate the mechanical properties in accordance with the procedures of ASTM A370-05. Additionally, 58 strand specimens were tested to evaluate their bond performances in mortar and concrete according to the North America Strand Producers (NASP) pull-out test method. The results showed that the strands met the strength and elongation requirements of ASTM A416. However, some strands were found to yield at strengths lower than 90 percent of the ultimate strength and thus, did not conform to minimum yield strength requirements. It was also found that the power formula provides an appropriate estimate of the

measured stress-strain response of 0.7-in. diameter strands. The NASP bond test method was found to be successful for the 0.7-in. strand diameter, and the bond was found to be exponentially proportional to the concrete strength. Lastly, it was reported that at an end slip of 0.01 in., the average NASP bond test values were 40 percent greater for strands that had a rusty surface as compared to clean strands.

#### *2.6.2.3 Morcous et al. (2013, 2014)*

Morcous et al. (2013, 2014) evaluated the application of 0.7-in. diameter strands on a 2-in. by 2-in. grid in the Oxford South Bridge in Oxford, Nebraska. The bridge, which was completed in fall 2013, consisted of twenty NU1350 prestressed girders fabricated using self-consolidating concrete and thirty-four 0.7-in. strands that were located on a 2- by 2-in. grid. The measured compressive strength of concrete at release ranged approximately between 6,000 to 10,000 psi. The 95percent AMS method was used to determine transfer lengths in two girders at release and after 14 days. Measurements from two girders showed that the transfer length for 0.7-in. diameter strands was approximately 32 in. immediately after release and 36 in. fourteen days after release, which are consistent with the values estimated using ACI 318-11, and are conservatively estimated using AASHTO LRFD Specification. The end-zone cracking was also evaluated through visual examination for a few days after release. No end-region cracking visible by naked eye was reported, indicating satisfactory performance of AASHTO LRFD provisions for bursting and confinement reinforcement in the girders using 0.7-in. diameter strands.

#### **2.6.3 University of Arkansas**

Dang et al. (2016, 2016) conducted a series of experimental studies on 24 small-scale specimens to measure the transfer and development lengths of 0.7-in diameter strands. The specimens had cross-sectional dimensions of 6.5 in. by 12 in. and a length of 18 ft, and were reinforced with one strand or two strands spaced at 2 in. The strands were released at a concrete strength that ranged between 5.9 and 9.8 ksi. DEMEC measurements and free end-slip were used to determine the transfer length whereas the development lengths were determined through bending tests on specimens with different embedment lengths.

The transfer length was reported between 23 and 28 in. one day after release, and between 26 and 31 in. twenty-eight days after release. The development length was reported between 3.5 and 4 ft. The researchers concluded that ACI 318-14 and AASHTO LRFD specifications are applicable for predicting the transfer length of 0.7 in. (17.8 mm) strands at release and at 28 days, but both specifications overestimate the development lengths.

## **2.7 Summary and Conclusions**

This chapter provided an overview of the concepts related to transfer of prestress, development of prestressing strands, and atypical failure modes in pretensioned concrete girders. Moreover, a review of the previous studies on the use of 0.7-in. diameter strands in pretensioned concrete elements was presented in this chapter.

Transfer and development lengths are critical parameters that affect the behavior of pretensioned concrete elements. Current design provisions contain equations that estimate these parameters primarily as a function of strand diameter. However, such provisions have been developed based on experimental results from specimens that were reinforced with 0.6-in. or smaller-diameter strands, and the applicability of those results to members employing 0.7-in. strands has yet to be verified. In recent years, several studies have been conducted on the transfer

and development lengths of specimens that were fabricated with 0.7-in. diameter strands. All of these studies reported that the current provisions underestimate the transfer and development lengths for 0.7-in. strands. However, further research is needed to obtain a realistic assessment of the performance of the current provisions for these larger-diameter strands.

Some of the previously reported studies on the behavior of members employing 0.7-in. strands have been conducted on small-scale specimens that were reinforced with one or two strand. The boundary conditions and the interaction between adjacent strands are not realistically represented in such specimens. As a result, the applicability of results from these studies to full-scale girders might be questionable. Few studies have employed full-scale specimens that were fabricated using 0.7-in. diameter strands. In most of these studies, the strands were released at a concrete strength considerably greater than what is commonly used in practice. Therefore, the observed behavior of the specimens and parameters of interest may not represent the performance of actual pretensioned girders in the field. Moreover, the information reported from these studies regarding the patterns or widths of cracks developed within the end-regions of the specimens has been very limited. Furthermore, no measurements of end-region stresses have been made in any of these studies, resulting in little insight into the efficacy of end-region detailing in girders employing 0.7-in. diameter strands.

The existing shear tests data from full-scale I- or bulb-tee girders with 0.7-in. strands have also been very limited. Previously reported shear tests on NU girders were conducted on specimens that had sustained damage prior to starting the test. Moreover, the specimens were tested at a relatively low span-to-depth ratio, and were not sufficiently instrumented to evaluate the mechanisms contributing to the shear strength of the girder.

Based on the background provided in this chapter, there is a critical need to further research on the behavior of pretensioned concrete elements employing 0.7-in. diameter prestressing strands to ensure the desired serviceability and strength for such girders before they are used in bridge applications. The remainder of this report presents how the researchers from UT have tried to fill in some of the gaps in the knowledge regarding the behavior of pretensioned concrete elements fabricated with these larger-diameter strands.



# CHAPTER 3

## Manufacturer Survey

### 3.1 Overview

The research team at UT conducted two surveys to obtain the information on design and construction practices related to using 0.7-in. diameter strands in pretensioned girders. The surveys were created for distribution to in-state precast fabricators and to all 50 state transportation departments, respectively. This chapter provides an overview of the efforts to develop and distribute the surveys and a summary of the results. The background section describes goals that guided the development of the surveys as well as a brief overview of survey questions. The results and analysis sections summarize and analyze the responses that were collected. The final versions of both surveys are provided in Appendix A.

### 3.2 Background

The original objective of the survey was to identify practical considerations for using 0.7-in. diameter strands through obtaining precast concrete manufacturers' feedback regarding: 1) current capabilities, 2) necessary equipment upgrades, and 3) manufacturer's perception of value for the use of 0.7-in. diameter strands. During the course of the project, the research team realized that expanding the scope of the survey to other states could provide valuable information for developing a research program with the greatest possible likelihood of producing results useful to both the design and fabrication communities. Therefore, separate surveys were developed for in-state fabricators and all state transportation departments. Both surveys were distributed by the TxDOT Bridge Division. The specific goals of each survey are outlined below.

#### 3.2.1 Texas Precast Fabricators Survey

Since the focus of the project was on the implementation of 0.7-in. diameter strands in Tx-girders, the team was most interested in evaluating the capabilities and construction practices of Texas precast fabricators. Their responses were of particular interest for the development of the experimental program, as the team was interested in considering the precast fabricators' limitations when designing the test specimens to ensure that the specimen fabrication was representative of common practice and the recommended end-region modifications were constructible.

The survey for Texas precast fabricators included 27 questions, which were organized into the following three categories.

- General Information: These questions were aimed at the fabricator's common products and contact information.
- Construction Practices for Precast, Pretensioned Girders: These questions were generally focused on: a) fabrication details, such as typical concrete release strength and strand tensioning and release methods, b) capabilities and limitations of the prestressing facility, and c) observed problems in I- and bulb-T girders with 0.6-in. diameter strands. The responses to these questions were very valuable to obtain an understanding of typical construction practices for Tx-girders so that the experimental program is consistent with common practice. Furthermore, knowledge of fabrication limitations was essential in recommending end-region reinforcing details that are constructible.

- Implementation of 0.7-in. Strands in Pretensioned Girders: Questions in this section addressed the goals of identifying required equipment upgrades and evaluating the manufacturer's perception of value. The recipients were asked to express their potential concerns, list all necessary equipment upgrades, and describe any previous experiences involving 0.7-in. diameter prestressing strands.

### **3.2.2 State Transportation Departments Survey**

While 0.7-in. diameter strands have not been implemented in Texas, the literature review conducted as the first task of this research revealed that two bridges had been constructed with pretensioned girders implementing 0.7-in. strands in Nebraska. The implementation of these larger diameter strands was supported by the research conducted at the University of Nebraska- Lincoln. Moreover, research involving transfer length and end-region behavior of bulb-T girders with 0.7-in. prestressing strands has recently been conducted at the University of Tennessee-Knoxville. Therefore, a separate survey was developed to obtain information from successful past experience in other states. The primary targets of the survey were state transportation departments, especially those that had implemented the 0.7-in. strands in practice or performed research on the use of larger-diameter strands.

This survey included 17 questions, which were organized into two broad categories as follows:

- General Information: The first few questions in this section explored the recipient's existing experience with and interest in 0.7-in. strands. If these strands have not been used in the recipient's state, questions were asked to find out the reason. The recipients were asked to proceed with answering other questions only if they had experience with 0.7-in. strands. The remaining questions in the General Information section addressed general implications of using 0.7-in. strands, including necessary equipment modifications and challenges faced by the fabricators while using larger-diameter strands.
- Design and Construction Practices for Prestressed I-Girders with 0.7-in. Strands: The majority of questions in this section were designed to find the extent of use, practical considerations, and limitations of using 0.7-in. diameter strands in pretensioned I-girders. Consequently, this section contained technical questions regarding material properties, strand patterns, and fabrication procedures that have been successfully implemented for girders with 0.7-in. strands. Moreover, the recipients were asked to provide details regarding observed crack patterns in I-girders with 0.7-in. strands. The section also contained an open-ended question on the perceived value of incorporating the larger-diameter strand from the perspective gained after project completion. The survey culminated in a request for additional materials (i.e. drawings or specifications) that had been developed to implement larger-diameter prestressing strands.

## **3.3 Survey Results**

### **3.3.1 Texas Precast Fabricator Survey**

In lieu of responses to the survey developed for individual precast fabricators in Texas, the team received a letter from the Precast Concrete Manufacturer's Association (PCMA) of Texas explaining their reservations toward implementing larger-diameter strands. The letter expressed a number of reasons the industry might be negatively affected by the introduction of 0.7-in. strands, as follows:

- Diminished Production Efficiency: The letter stated that an increase in strand diameter would diminish the efficiency of prestressed girder production because of necessary equipment modifications, increased difficulty in handling the strands, and safety considerations.
- Shipping Restrictions: The letter accepted that the use of larger-diameter strands would allow spans to increase. However, it stated that using longer precast girders than those currently available is not practical due to transportation complications.
- Material Availability: The Texas PCMA expressed economic concerns with the change in strand size by citing “a thirty to forty two percent per pound cost increase” due to the strand’s limited availability. The letter recognizes that the scale of the Texas precast market could eliminate this issue but insinuates that costs associated with equipment modifications and safety concerns would negate the benefits it could provide.

### **3.3.2 State Transportation Departments Survey**

The team collected responses from 27 state Departments of Transportation (DOTs). Figure 3-1 provides an overview of the responses. All but two states expressed a complete lack of experience with 0.7-in. strands. However, of the majority of DOTs that have not yet used large-diameter prestressing strands, six departments expressed interest in the new strand size, among which the Georgian and Alaskan DOTs stated previous consideration of implementing 0.7-in. strands. Common reasons for not considering the use of 0.7-in. diameter strands use or for choosing to continue using smaller-diameter strands included the current lack of published research on the behavior of girders with larger diameter strands, limited material availability, and required facility upgrades at local precast fabrication plants.

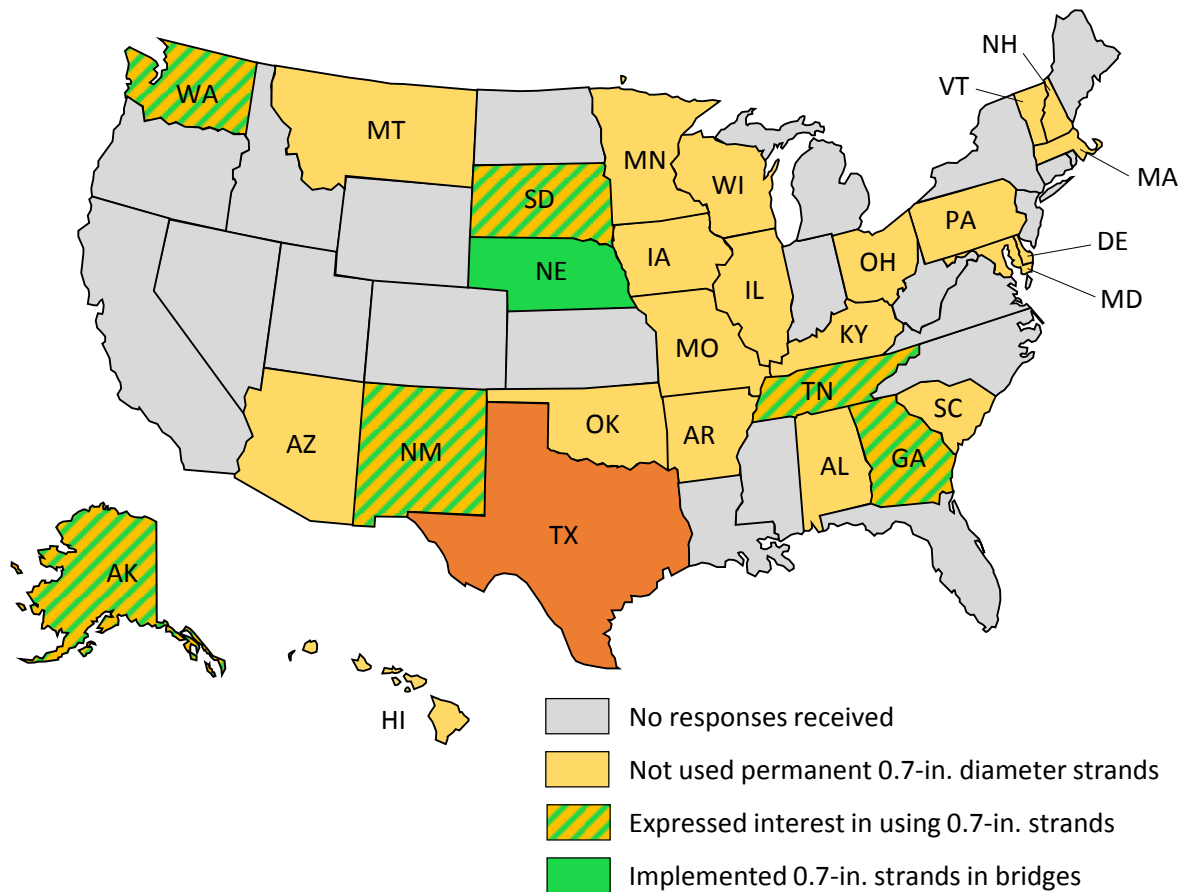


**Figure 3-1- Responses to the nationwide survey of state transportation departments**

The two state transportation departments that reported previous experience with 0.7-in. diameter prestressing strands were the Washington State Department of Transportation (WSDOT) and Nebraska Department of Roads (NDOR). WSDOT expressed that their experience with 0.7-in. strands was limited to temporary strands for shipping and handling of long-span girders. Therefore, their responses to the survey did not contain details concerning the implementation of 0.7-in. strands that are particularly advantageous to this research project. WSDOT expressed a lack of support from the local industry to incorporate 0.7-in. strands and cited strand handling difficulties, safety considerations, and availability of accessories as the primary challenges.

The Nebraska Department of Roads (NDOR) confirmed that they had sponsored research at the University of Nebraska-Lincoln on the behavior of pretensioned girders employing 0.7-in. diameter strands and had successfully constructed bridges using NU-girders with 0.7-in. diameter strands. The research team at UT was already aware of the research at the University of Nebraska (Tadros & Morcouc, 2011) as well as the implementation of the 0.7-in. diameter strands is two bridges in Nebraska, as described in detail in Chapter 2. According to the responses received from NDOR, 0.7-in. diameter strands were used on a 2- by 2-in. grid for the fabrication of NU-girders that were 165 ft long. The concrete release strength was reported as 10 ksi, which was typically achieved 24 to 36 hours after casting.

As described in Chapter 2, a research project was also conducted at the University of Tennessee-Knoxville on AASHTO I-girders with 0.7-in. strands (Vadivelu, 2009). The responses received from the Tennessee Department of Transportation (TDOT) referred to that study and

mentioned the potential implementation of 0.7-in. diameter strands following the recommendations of that study.

## **3.4 Analysis of Survey Results**

### **3.4.1 Texas Precast Fabricator Survey**

The opinions expressed in the letter received from Texas PCMA came as no surprise to the research team. The transition from 0.5-in. to 0.6-in. diameter strands and the introduction of Tx-girders raised similar concerns. However, these initial concerns have been addressed and overcome, greatly through research findings. In fact, the implementation of modern designs, materials, and fabrication practices has been a major contributor to Texas' position as a leader in economy and efficiency of prestressed concrete construction. The continued success of the precast industry in Texas is possible through embracing new technologies and materials, which will be economically beneficial to the precast manufacturers. Recent development of Tx-girders and widespread use of 0.6-in. strands constitute two examples where progressive approach taken by TxDOT and the precast industry in Texas has led to a more competitive market place, reduced construction costs, and helped Texas maintain its leadership position in precasting in the country. To alleviate the concerns brought up by the Texas PCMA, the research team considered practical issues such as handling difficulties and required equipment modifications in the full-scale experimental research that is presented in Chapter 4.

### **3.4.2 State Transportation Department Survey**

The collected responses from the state transportation department survey confirmed the findings of the literature review presented in Chapter 2 concerning the general lack of experience with 0.7-in. diameter prestressing strands in the United States. The response from NDOR confirmed that the current state-of-the-art concerning the use of 0.7-in. strands in the U.S. stands as reported in the published research reports from the University of Nebraska-Lincoln. These reports were analyzed by the research team during the literature review effort (Task 1). The received responses also revealed encouraging levels of interest from several state transportation departments, which support the significance of this research in filling the gaps in knowledge regarding the use of larger-diameter strands.

## **3.5 Summary**

The received responses confirmed the general gap in knowledge concerning larger-diameter strands. The overwhelming theme in the responses was a general apprehension toward using larger diameter strands based mostly on unknown behavior of the girder and material availability or handling concerns. The only reported cases of using 0.7-in. strands in bridges were in Nebraska and had been previously investigated by the research team during the literature review effort.

In the analytical and experimental programs presented in this report, the research team has tried to address the full breadth of logistical and behavioral concerns regarding 0.7-in. strands to curb the concerns expressed by the Texas PCMA and interested state transportation departments to pave the way for new pretensioned girder solutions. The full-scale experimental research at FSEL involved practical considerations related to the use of 0.7-in. strands in a realistic setting, including all necessary equipment upgrades and potential handling problems. Therefore, the

outcome of this research provides valuable insight into the design and fabrication of girders with 0.7-in. strands considering all practical limitations.

# CHAPTER 4

## Parametric Investigation

### 4.1 Overview

As part of TxDOT Project 0-6831, the research team at UT completed a series of parametric investigations to evaluate the benefits and limitations of using 0.7-in. diameter strands in pretensioned bridge girders and assess the potential impacts of transitioning to these larger-diameter strands from a design perspective. This chapter presents a summary of the activities performed to complete the parametric studies along with some of the major findings of these investigations. Note that most of the contents of this chapter have been previously published in a paper by Salazar et al. (2017), submission of which was coordinated with TxDOT PMC.

### 4.2 Background

Since greater forces are applied to 0.7-in. diameter strands, widespread implementation of these larger-diameter strands might require a considerable initial investment by the precast manufacturers to upgrade the hydraulic equipment, anchorage and hold-down devices, and foundations. Such upgrades are feasible only if the benefits obtained from using 0.7-in. strands outweigh the initial investment. Therefore, it is essential to quantitatively assess the potential benefits and limitations of using 0.7-in. diameter strands before making decisions regarding potential use of these larger-diameter strands in the precast industry.

Quantifying the potential benefits of using 0.7-in. diameter strands has been the subject of a limited number of studies. In an investigation by Vadivelu (Vadivelu, 2009), the effects of using 0.7-in. diameter strands on the span capabilities and required number of strands within NU I-girders and AASHTO bulb-tee girders were evaluated. The sections investigated included NU1350, NU1800, and AASHTO Type V and Type VI. Three compressive release strengths of 10, 15, and 28 ksi were considered. It was reported that the use of 0.7-in. diameter strands compared to 0.6-in. diameter strands resulted in an increase in the span capability of AASHTO Type V girders by 17 percent. The same maximum span of 140 feet could be achieved with AASHTO Type VI with 0.6-in. diameter strands and AASHTO Type V with 0.7-in. diameter strands, which emphasizes a possible reduction in the section size when employing 0.7-in. diameter strands. Increasing the compressive release strength of concrete from 10 to 15 ksi resulted in an increase in the span capability of girders employing 0.7-in. diameter strands by 8.5 percent. However, no further increase was observed in the span capability of the girders when the compressive release strength was increased from 15 to 28 ksi.

Hanna, Morcous, and Tadros (2010) conducted parametric designs of NU girders with 0.6- and 0.7-in. diameter strands. The spacing between girders varied between 6 and 12 ft, and the compressive strength of concrete ranged between 6 and 11 ksi for girders with 0.6 in. strands and between 9 and 11 ksi for girders with 0.7 in. strands. The use of 0.7-in. strands was reported to result in a general increase in the span capability of NU girder and a decrease in the number of required strands. The design of girders employing 0.7-in. strands was found to be governed by stresses at the time of release, whereas AASHTO LRFD Service III load combination controlled the design of girders employing 0.6-in. strands. In a separate publication, Morcous, Hanna, and Tadros (2011) reported the number of required strands and the span capability of the NU900 cross section when employing 0.6- and 0.7-in. strands. The compressive strength of concrete at release

varied between 6 and 11 ksi, and spacing between the girders ranged between 6 and 12 ft. The use of 0.7-in. strands was reported to require a minimum concrete release strength of 11 ksi, as opposed to 0.5- and 0.6-in. strands requiring 6 to 8.5 ksi. The number of 0.7-in. strands needed was approximately 40 and 60 percent less than that of 0.6- and 0.5-in. strands, respectively. For a given girder spacing, an increase in span length of 15 to 20 ft was reported when the girder employed the same number of 0.7-in. strands instead of 0.6-in. strands.

The aforementioned studies provide valuable insight into the potential benefits of using 0.7-in. diameter strands. However, several critical aspects of this problem have not been sufficiently investigated. Most importantly, all previous studies have been limited to a few types of NU girders and AASHTO bulb-tee sections. The benefits and limitations of 0.7-in. diameter strands need to be studied in a much wider variety of precast, pretensioned cross sections. Moreover, in none of the previous studies has the entire set of design parameters, including stresses at the time of release, service-level stresses, ultimate strengths in flexure and shear, deflection limits, harping requirements, and shipping restrictions, been considered holistically. Considering these gaps in the literature, the work conducted as part of Task 3 in this research project involved a comprehensive parametric study on the benefits and limitations of using 0.7-in. diameter strands in pretensioned bridge girders, with a primary focus on the precast sections used in Texas.

### **4.3 Methodology of Investigation**

A simple bridge configuration consisting of straight pretensioned girders was considered. The girders were designed using 0.5-, 0.6-, and 0.7-in. diameter prestressing strands, assuming a variety of combinations for the girder cross sections, span lengths, concrete release strengths, girder spacings, and the use of harped versus straight strands.

The precast cross sections investigated in this study are shown in Figure 4-1. Twenty cross-section types were investigated, which included AASHTO I-beams, Tx-girders, Texas spread box beams (X-beams), and Texas U-beams. Three concrete release strengths of 5.5, 7.5, and 10 ksi were considered. As can be seen in Figure 4-1, the majority of cross sections considered were Texas precast sections. In Texas, due to durability concerns, the compressive strength of concrete at release is generally limited to 5.5 ksi. However, to evaluate the potential benefits of increasing the release strength, values of 7.5 and 10 ksi were also studied. The effect of using a transverse girder spacing of 6 ft through 16 ft was considered within the bridge configuration. To evaluate the role of harping in the ability to benefit from 0.7-in. diameter strands and therefore assess the need for upgrading the hold-down devices, I- and bulb-tee girders were designed both in straight and harped strand configurations. The combination of selected designed parameters resulted in 10,320 cases, which required a versatile parametric study tool that could quickly generate thousands of designs and provide flexibility on input and output parameters.

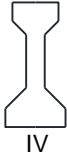
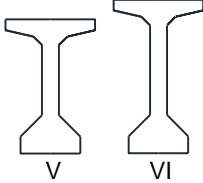
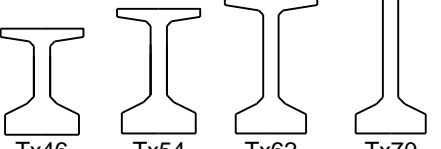
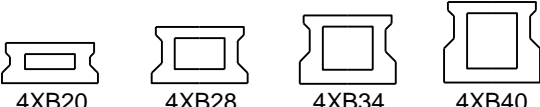
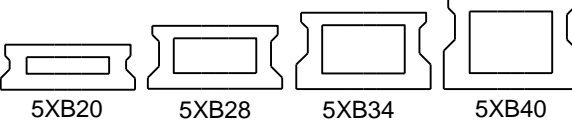
	AASHTO precast concrete sections	Texas precast concrete sections
I-beams	 IV	
Bulb tees	 V VI	 Tx28 Tx34 Tx40  Tx46 Tx54 Tx62 Tx70
Spread box beams (X beams)		 4XB20 4XB28 4XB34 4XB40  5XB20 5XB28 5XB34 5XB40
U beams		 U40  U54

Figure 4-1- Cross sections evaluated in the parametric investigation

#### 4.3.1 The Parametric Study Tool

A parametric study tool was used for performing the designs, which employs a combination of spreadsheet formulas and Visual Basic macros in Microsoft Excel. The tool was originally developed as part of TxDOT Project 0-6374 by Garber et al. (2013, 2016) to investigate the effects of different prestress loss equations on the design of pretensioned girders. To meet the requirements of the current study, this tool was modified to incorporate 0.7-in. diameter strands and reflect the most recent changes in design codes, including the 2016 interim revisions to AASHTO LRFD 2014 Bridge Design Specifications (AASHTO, 2016). Compared to the bridge design software currently available, such as PGSuper (Bridgesight Inc., 2014), this parametric study tool provides a much greater control on input and output parameters, allows for procedures to be customized, and quickly generates numerous bridge designs in order to accelerate analyses.

Figure 4-2 provides an overview of the design procedure employed within the parametric study tool. In the flowchart presented, relevant articles from AASHTO LRFD Bridge Design Specifications are provided. The design process starts with gathering the input parameters that

define the design case. These input parameters, which are summarized in Table 4-1, include the general layout and geometry of the bridge, site conditions, cross-sectional properties of the precast section, and assumptions for mechanical properties of the materials. These parameters are manually inserted in the input sheets of the tool and updated as needed.

**Table 4-1- Input variables used within the parametric study tool**

Bridge configuration	Site conditions	Section properties	Material properties	
<ul style="list-style-type: none"> <li>• Length</li> <li>• Girder spacing</li> <li>• Number of girders</li> <li>• Interior/exterior girder</li> <li>• Barrier base width</li> <li>• Additional sustained dead load</li> <li>• Future overlay load</li> </ul>	<ul style="list-style-type: none"> <li>• Relative humidity</li> </ul>	<ul style="list-style-type: none"> <li>• Girder cross section type</li> <li>• Haunch thickness</li> <li>• Slab thickness</li> </ul>	<ul style="list-style-type: none"> <li>Girder concrete</li> <li>Slab concrete</li> <li>Prestressing strand</li> <li>Mild steel</li> </ul>	<ul style="list-style-type: none"> <li>• Release compressive strength (<math>f'_{ci}</math>)</li> <li>• 28-Day compressive strength (<math>f'_c</math>)</li> <li>• Modulus of elasticity (<math>E_c</math>)</li> <li>• Concrete weight (<math>w_c</math>)</li> <li>• 28-Day compressive strength (<math>f'_c</math>)</li> <li>• Modulus of elasticity (<math>E_c</math>)</li> <li>• Concrete weight (<math>w_c</math>)</li> <li>• Ultimate strength (<math>f_{pu}</math>)</li> <li>• Stress limit (<math>f_{pi}</math>)</li> <li>• Yield strength (<math>f_{py}</math>)</li> <li>• Modulus of elasticity (<math>E_p</math>)</li> <li>• Strand diameter (<math>d_b</math>)</li> <li>• Yield strength (<math>f_y</math>)</li> <li>• Modulus of elasticity (<math>E_s</math>)</li> <li>• Steel Area</li> </ul>

Using these input parameters, flexural demands on the girder in the final bridge configuration are determined based on dead and live loads that are applied to the bridge and the Strength I load combination from AASHTO LRFD Bridge Specifications. The number of strands needed at the mid-span of the girder to satisfy this flexural demand is then determined. Next, the minimum reinforcement requirements as well as tensile and compressive stress requirements for AASHTO Service I and Service III limit states are checked, and the quantity of prestressing strands is increased as needed. Once a satisfactory design that meets the flexural demands at ultimate and service conditions is achieved, the stresses at the time of release are calculated. The strands are then harped (deflected) as needed to satisfy the stress requirements at the time of prestress transfer. Finally, the girder is checked for shear strength at a section that is located  $d_v$  away from the support, where  $d_v$  is the effective shear depth.

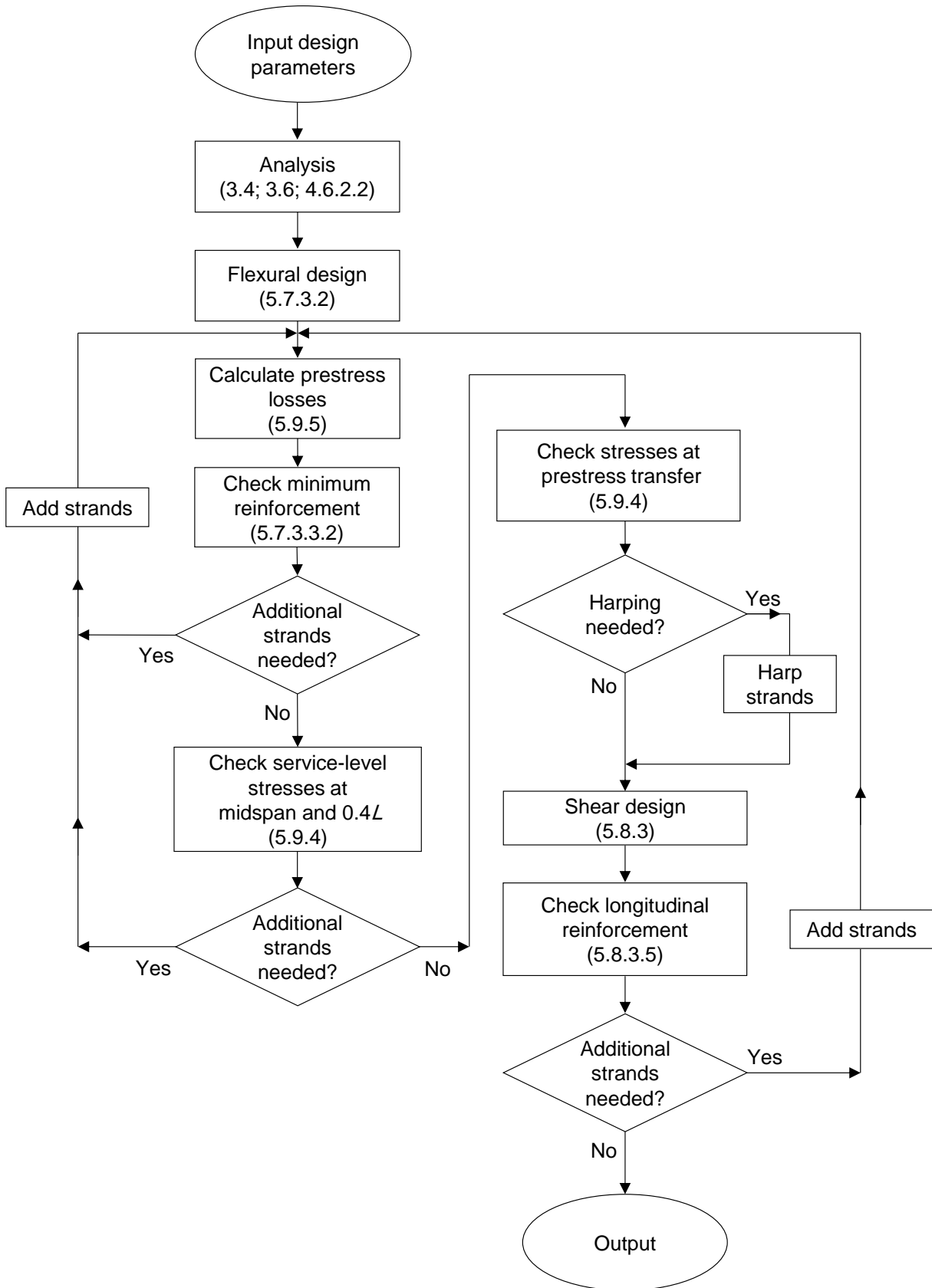


Figure 4-2- Design procedure for the parametric study tool

The design procedure in the parametric study tool includes iterations to recalculate the relevant design parameters, such as section properties and prestress losses, whenever the number of strands is altered. Once a design is finalized, a full set of output parameters is generated. If a design meeting all requirements is not possible for a set of assumptions, the analysis tool outputs an error message, which describes the requirement that cannot be satisfied.

A set of comparative studies was carried out using PGSuper (Bridgesight Inc., 2014) to validate the parametric study tool. A variety of Tx-girders, Texas U- and X-, and AASHTO I- and bulb-tee girders at different lengths and concrete compressive strengths were designed using the tool. The validation procedure included a comprehensive comparison between the design outputs as well as intermediate design parameters, such as stresses at the times of prestress transfer and deck placement, prestress losses, live load distribution factors, service-level stresses, ultimate bending moment, nominal flexural capacity, and minimum reinforcement requirements. The difference in the design parameters between the analysis tool and PGSuper was generally less than 5 percent in all validation cases. Details of this validation effort are reported by Salazar (2016).

#### **4.3.2 Parametric Investigation**

The parametric study tool was used to provide an inventory of design cases, which were then filtered as necessary to provide insight into the effects of using larger-diameter strands on different aspects of pretensioned girder designs. The design cases were generated by changing the input parameters, most importantly the diameter of strands (0.5-, 0.6-, and 0.7-in.), girder spacing, and span length, which was varied between 30 and 210 ft at 5 ft intervals.

All design cases were generated based on the assumption that 0.7-in. diameter strands can be used on a standard 2- by 2-in. grid without negatively impacting the serviceability or shear strength of the girders, and the end-region transverse reinforcement was assumed to sufficiently control the width of end-region cracks. This assumption is extensively investigated in the experimental investigation conducted as part of Tasks 4 and 6 of this research project.

A summary of the input parameters that were used for generating the design cases is provided in Table 4-2. As can be seen in this table, an interior girder of a slab-on-girder bridge that contained six girders was considered. The 28-day compressive strengths of 10 ksi and 4 ksi were assumed for the concretes used in the girders and the slab, respectively. The compressive strength of concrete at the time of prestress transfer varied between 5.5 ksi and 10 ksi. Release strengths greater than 10 ksi were not investigated because they do not represent a practical solution for the fabrication of precast girders. For simplicity, the modulus of elasticity of concrete was assumed to be constant at the time of prestress transfer, equal to what is estimated for a compressive strength of 5.5 ksi from Equation C5.4.2.4-1 in AASHTO LRFD (2016). For analysis purposes, the span length was assumed 1.5 ft shorter than the girder length. No haunch thickness was taken into account for this parametric investigation. The prestress losses were calculated according to the refined method (Section 5.9.5.4) in AASHTO LRFD specifications, assuming that the girders were subjected to prestress at an age of 0.8 days and the deck was constructed when the girder had an age of 120 days. The prestress level at the final conditions of the girders was calculated assuming a girder age of 100 years. The effects of deck shrinkage on prestress losses were neglected in the analysis.

**Table 4-2- Properties used in the parametric study**

Bridge configuration	Length of girder ( $L_{girder}$ )		30-210 ft
	Girder spacing		6, 8, 10, and 12 ft
	Number of girders		6
	Interior/ exterior girder		Interior
	Additional sustained dead load		0.191 kip/ft
Site conditions	Relative humidity		60 %
Section properties	Girder cross section type		Based on Figure 4-1
	Slab thickness		8.0 in.
Material properties	Girder concrete	$f'_{ci}$	5.5, 7.5, and 10.0 ksi
		$f'_c$	10.0 ksi
		$E_{ci}$	4,270 ksi
		$E_c$	5,760 ksi
		$w_c$	150 lb/ft <sup>3</sup>
	Slab concrete	$f'_c$	4.0 ksi
		$E_c$	3,640 ksi
		$w_c$	150 lb/ft <sup>3</sup>
	Prestressing strand	$f_{pu}$	270.0 ksi
		$f_{pi}$	202.5 ksi
		$E_p$	29,000 ksi
		$d_b$	0.5, 0.6, and 0.7 in.
	Mild steel	$f_y$	60.0 ksi

All relevant loading combinations and stress limits according to AASHTO LRFD (2016) were considered in design. In addition to the flexural design of the girders in ultimate conditions considering the live loads, the stresses were calculated at three stages: 1) at the time of prestress transfer, 2) at the time of deck placement, and 3) under live loads in the final bridge configuration. These stresses were checked at three sections along the girder that were located at the transfer length ( $60d_b$ ), at 40 percent of the girder length ( $0.4L_{girder}$ ), and at mid-span. Moreover, the deflection of the girders under live loads was compared with the allowable limit of  $L_{girder}/800$ , according to Section 2.5.2.6.2 in AASHTO LRFD (2016).

Deflecting (harping) of the strands was assumed as the only method for controlling the stresses within the end region of the girders, which was applied as necessary to I- and bulb-tee girders. U- and X-girders were designed only with straight strands. No straight strands were assumed in the top flange of the girders.

## 4.4 Results and Discussion

Within the following sections, the results of the parametric investigation are provided and discussed. These results are categorized to provide insight into the effects of using 0.7-in. diameter strands on: 1) steel quantity, 2) maximum span capability, 3) maximum attainable slenderness ratio for the superstructure, and 4) maximum allowable spacing between the girders. Under each category, benefits obtained from using 0.7-in. diameter strands are discussed and quantified in light of comparisons with results obtained for girders employing 0.6-in. diameter strands.

### 4.4.1 Steel Quantity

Figure 4-3 and Figure 4-4 present the number of required strands versus span length for 0.5-, 0.6-, and 0.7-in. diameter strands in a variety of precast, pretensioned cross sections. A transverse spacing of 8 ft between the girders was assumed for generating the plots in these figures. The data points are located in one of the three zones (5.5 ksi, 7.5 ksi, or 10 ksi), based on the compressive release strength required to reach each span length. The maximum span length before the live load deflection exceeds the  $L_{girder}/800$  limit is also shown in each plot as the “deflection limit.” As visible in the figures, the deflection limit did not govern any of the design cases.

A considerable reduction in the number of strands due to the use of larger-diameter strands is evident in all plots in Figure 4-3 and Figure 4-4. This observation comes as no surprise, since fewer large-diameter strands would be needed to provide the same area of prestressing steel. As can be seen in Figure 4-3, up to 34 fewer strands could be used in AASHTO Type V girders when 0.7-in. diameter strands are used instead of 0.6-in. diameter strands. This change, which corresponds to a 35 percent reduction, was the greatest saving in the number of strands in the entire set of design cases investigated. At the maximum span length that can be achieved with all strand diameters for each cross section ( $L_{common}$ ), the use of 0.7-in. diameter strands results in a need for 10 to 16 fewer strands in Tx-girders, and 12 to 16 fewer strands in AASHTO sections when compared to 0.6-in. diameter strands. Similar observations regarding the saving in the number of strands can be made for U- and X-girders. As can be seen in Figure 4-4, when 0.7-in. diameter strands are used instead of 0.6-in. diameter strands, at the maximum attainable span, 10 to 12 fewer strands will be needed in U-girders, and 8 to 14 fewer strands will be needed in X-girders.

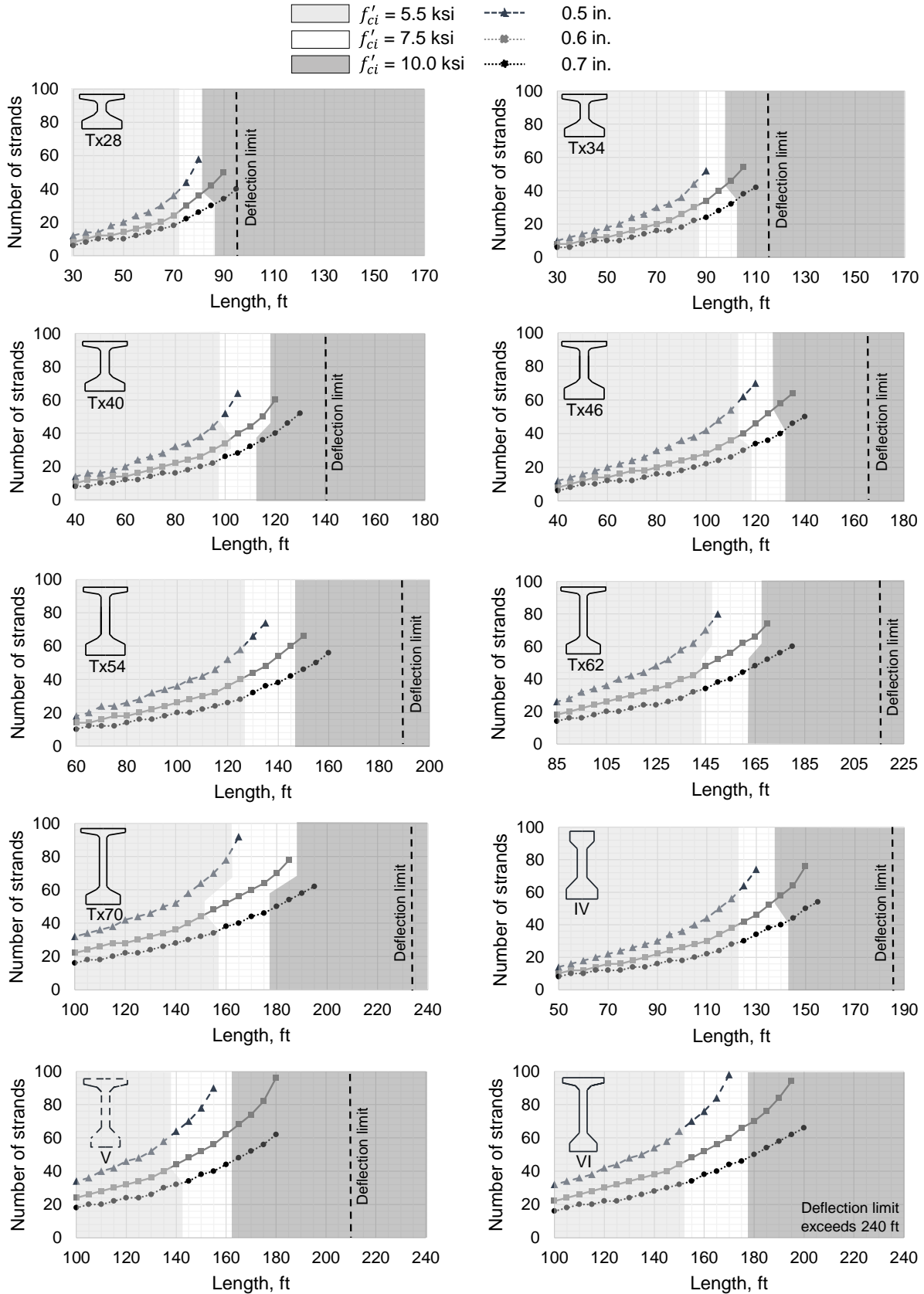


Figure 4-3- Number of strands vs. span length for I- and bulb-tee girders with different strand diameters

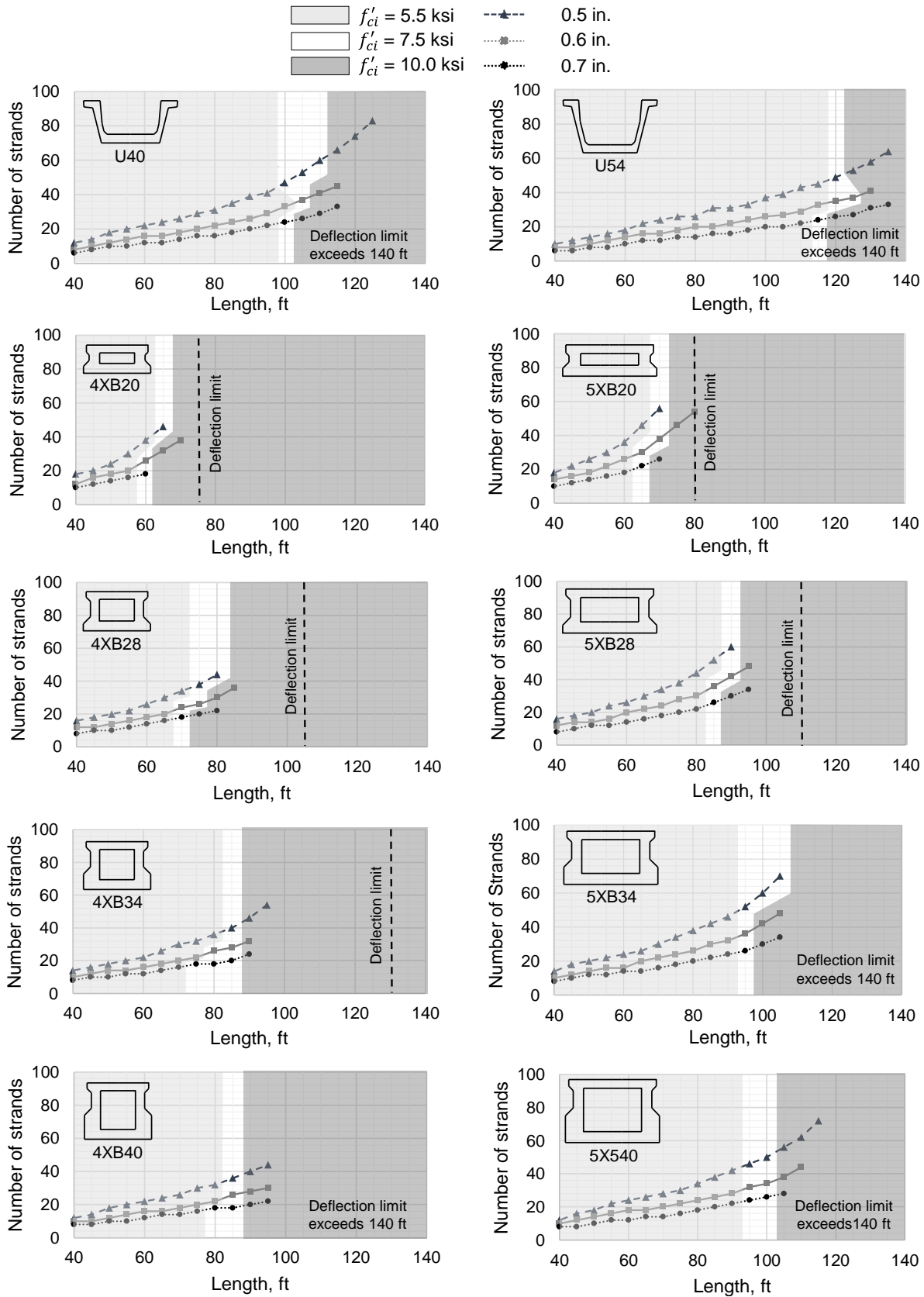


Figure 4-4- Number of strands vs. span length for U- and X-girders with different strand diameters

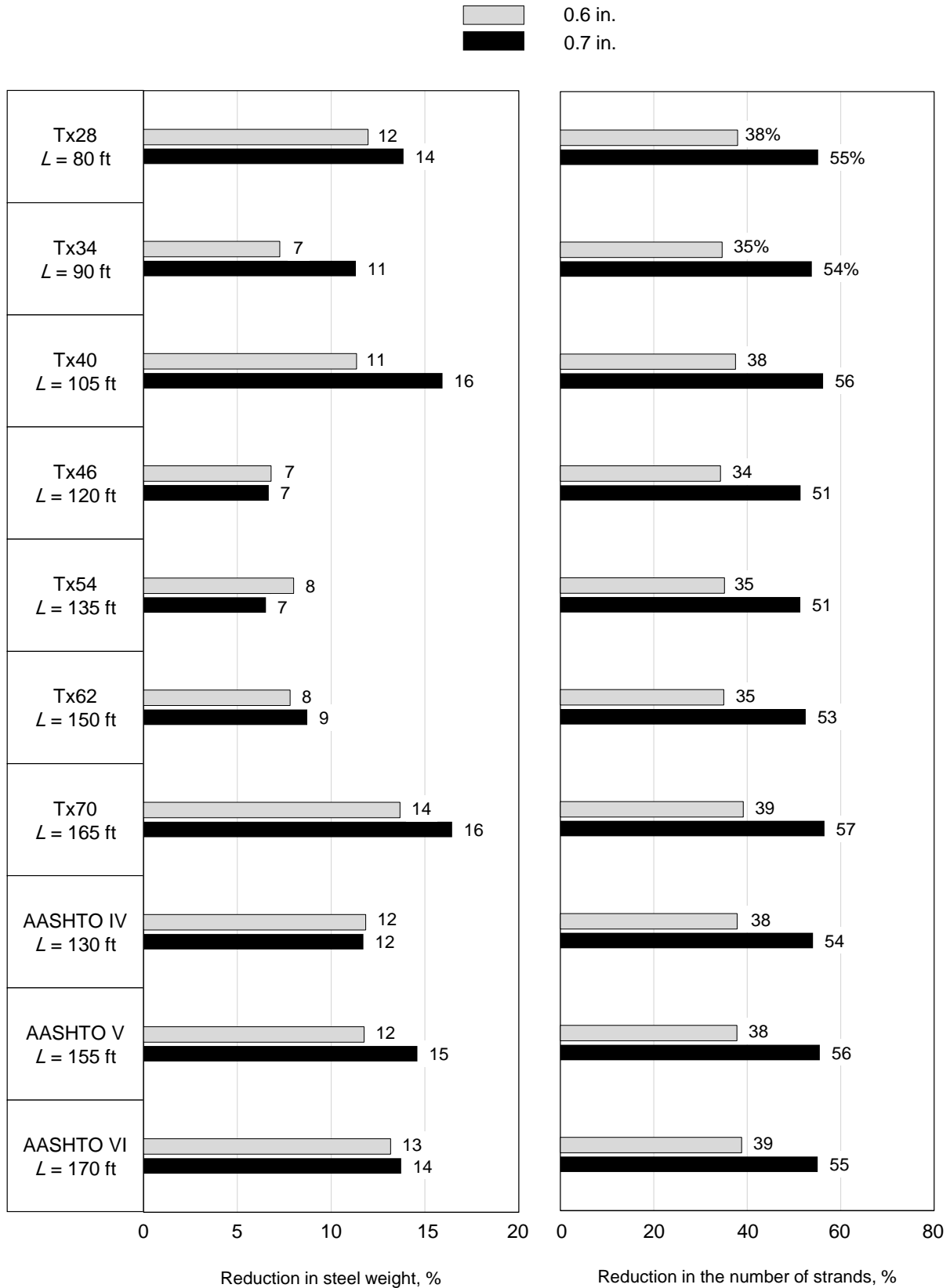
The reduction in steel quantity when 0.6- and 0.7-in. diameter strands are used instead of 0.5-in. diameter strands is shown in Figure 4-5 (for I- and bulb-tee girders) and Figure 4-6 (for U- and X-girders). The comparisons presented in these figures are based on designs that were made at a transverse spacing of 8 ft and a length of  $L_{common}$  for each cross section. The reduction in steel quantity in the figures is presented in two categories: total weight of prestressing steel (shown on the left), and number of strands (shown on the right). The weight of steel is the primary indicator of material efficiency. However, the number of strands has a more noticeable effect on the physical demands of the fabrication process. Therefore, any reduction in the number of strands, regardless of the total weight of prestressing steel, will provide significant benefits to the cost-effectiveness of the construction.

Figure 4-5 and Figure 4-6 show that the use of 0.6-in. diameter strands results in up to 16 percent reduction in the weight of prestressing steel compared to 0.5-in. diameter strands. Such a reduction is primarily due to the possibility of greater concentration of steel near the bottom fiber and increased internal moment lever arm. However, using 0.7-in. diameter strands provides no significant benefit in terms of steel weight compared to 0.6-in. diameter strands. The maximum additional benefit from 0.7-in. diameter strands compared to 0.6-in. diameter strands was 5 percent (for Tx40) among I- and bulb-tee girders, and 7 percent (for 5XB20) among U- and X-girders. An opposite trend was observed for U54, in which the weight of 0.6- and 0.7-in. diameter strands exceeded that of 0.5-in. diameter strands.

As can be seen in Figure 4-5 and Figure 4-6, a relatively uniform reduction in the number of strands was observed within each category of cross sections. In I- and bulb-tee girders, the use of 0.6-in. diameter strands instead of 0.5-in. diameter strands results in an average reduction of 34 to 39 percent in the number of strands. For 0.7-in. diameter strands compared to 0.5-in. diameter strands, this reduction is 51 to 57 percent. For U- and X-girders, the reduction is 29 to 32 percent for 0.6-in. diameter strands, and 47 to 54 percent for 0.7-in. diameter strands.

The cross-sectional area of a 0.5-in. diameter strand is 29 and 48 percent less than those of 0.6- and 0.7-in. diameter strands, respectively. Therefore, the additional savings in the number of strands is associated with the improved flexural efficiency of the cross sections and reduction in the required steel area.

For U- and X-girders, the reduction in the weight of steel and number of strands due to using larger-diameter strands was slightly smaller because the strand layout in these cross sections restricts how far the center of gravity of prestressing steel can be moved by concentrating greater steel area near the bottom fiber. The maximum benefit from the use of 0.7-in. diameter strands was in 5XB20 (11 percent reduction compared to 0.5-in. diameter strands). Among I- and bulb-tee girders, Tx-girders with a height between 46 and 62 in. benefitted the least from the use of larger-diameter strands. The use of 0.7-in. diameter strands instead of 0.5-in. diameter strands benefitted Tx70 the most, both in terms of number of strands and weight of steel.



**Figure 4-5- Percent reduction in steel weight and number of strands for 0.6- and 0.7-in. diameter strands compared to 0.5-in. diameter strands within I- and bulb-tee girders**

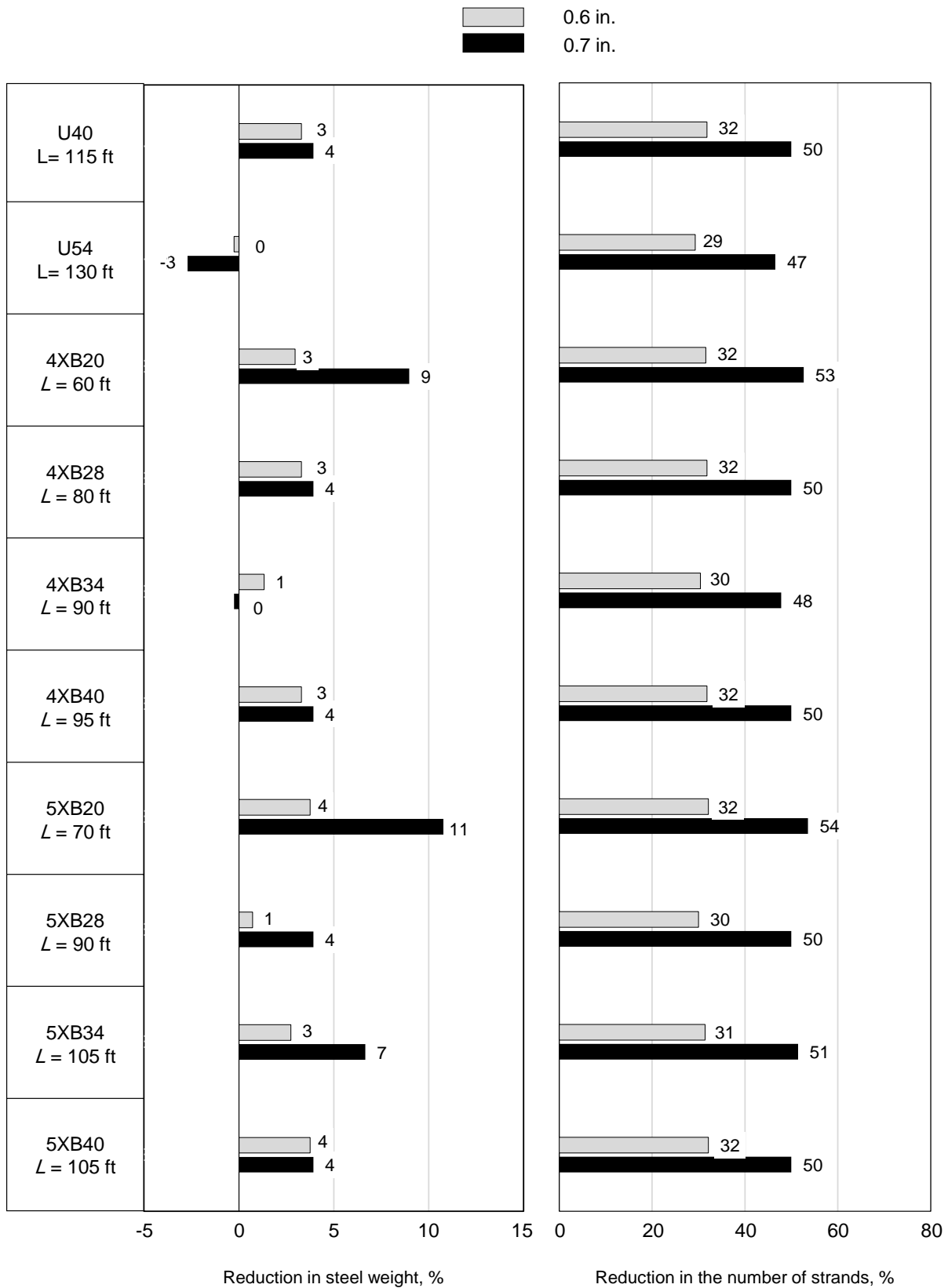


**Figure 4-6- Percent reduction in steel weight and number of strands for 0.6- and 0.7-in. diameter strands compared to 0.5-in. diameter strands within U- and X-girders**

#### 4.4.2 Maximum Span Capability

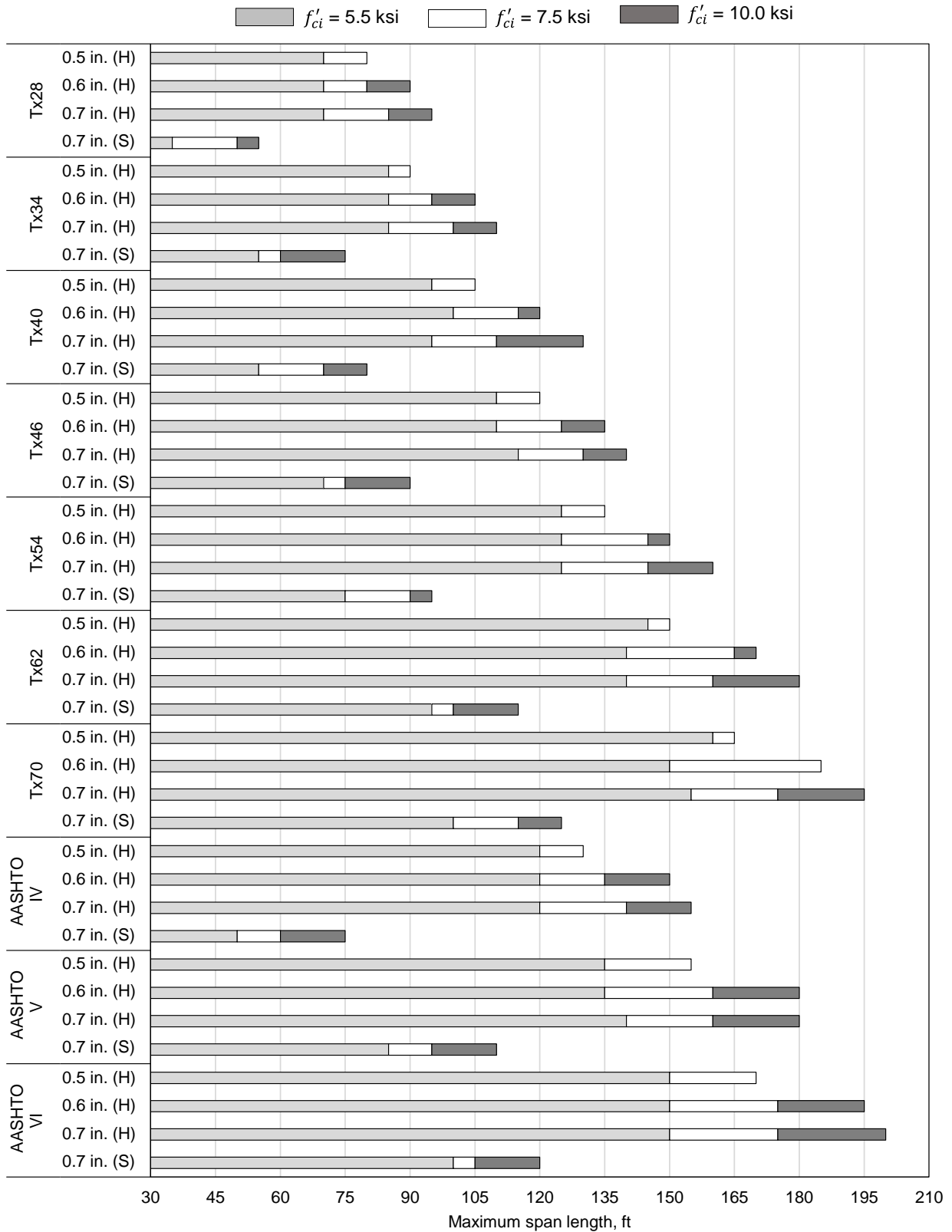
The maximum span lengths for girders with 0.5-, 0.6-, and 0.7-in. diameter strands fabricated with different concrete release strengths are shown in Figure 4-7 and Figure 4-8. The span lengths in these figures are primarily extracted from Figure 4-3 and Figure 4-4, in which a spacing of 8 ft was assumed between the girders. Additionally, Figure 4-7 includes information on I- and bulb-tee girders with straight 0.7-in. diameter strands to illustrate the importance of harping the strands in achieving greater span lengths. For U- and X-girders, only straight strands were considered. All span lengths reported in the figures have a resolution of 5 ft.

Figure 4-7 and Figure 4-8 show that for each section, different span lengths could be achieved with different strand sizes. The two limits that governed the maximum span lengths were 1) the maximum number of strands that could be accommodated in each girder cross section, and 2) maximum stresses, either in final bridge configurations under live loads or at the time of prestress transfer. With 0.5-in. diameter strands, the maximum span lengths for all I-, bulb-tee, U-, and X-girders were governed by the number of strands that could be used within the girder cross section. The same situation applied to AASHTO bulb-tee girders and smaller Tx-girders with 0.6-in. diameter strands. Concrete release strength was the governing factor for all girders with 0.7-in. diameter strands, as well as midsize to large Tx-girders and U- and X-girders with 0.6-in. diameter strands

None of the combinations of strand size and cross-section type could reach the maximum span capability with a compressive release strength of 5.5 ksi. A release strength of 7.5 ksi is needed to eliminate the release stresses from factors that governed the design of I-, bulb-tee, and small and midsize X-girders with 0.5-in. diameter strands, Tx70 girders with 0.6-in. diameter strands, and 4XB20 girders with 0.7-in. diameter strands. All other design cases, including almost all girders with 0.7-in. diameter strands, require compressive release strengths greater than 7.5 ksi to be used efficiently.

As illustrated in in Figure 4-7, a compressive release strength of 5.5 ksi limits the span capability of almost all girders with 0.7-in. diameter strands to the same or smaller lengths as those with 0.5- or 0.6-in. diameter strands. The only exceptions are Tx46 and AASHTO Type V, for which a 5 ft increase in the span length could be achieved by replacing 0.6- with 0.7-in. diameter strands.

If the release strength is increased to 7.5 ksi, the span capability of I- and bulb-tee girders will increase for all design cases. The effects of such an increase in release strength are most visible in larger cross sections and larger-diameter strands, e.g. up to 35 ft for Tx70 with 0.6-in. diameter strands. However, even with this release strength, the maximum span length of girders with 0.7-in. diameter strands is only 5 ft greater than that of girders with 0.6-in. diameter strands.



**Figure 4-7- Maximum span lengths achieved for I- and bulb-tee girders with different strand diameters.**  
**Note: H= strands harped as needed; S= Straight strands only**

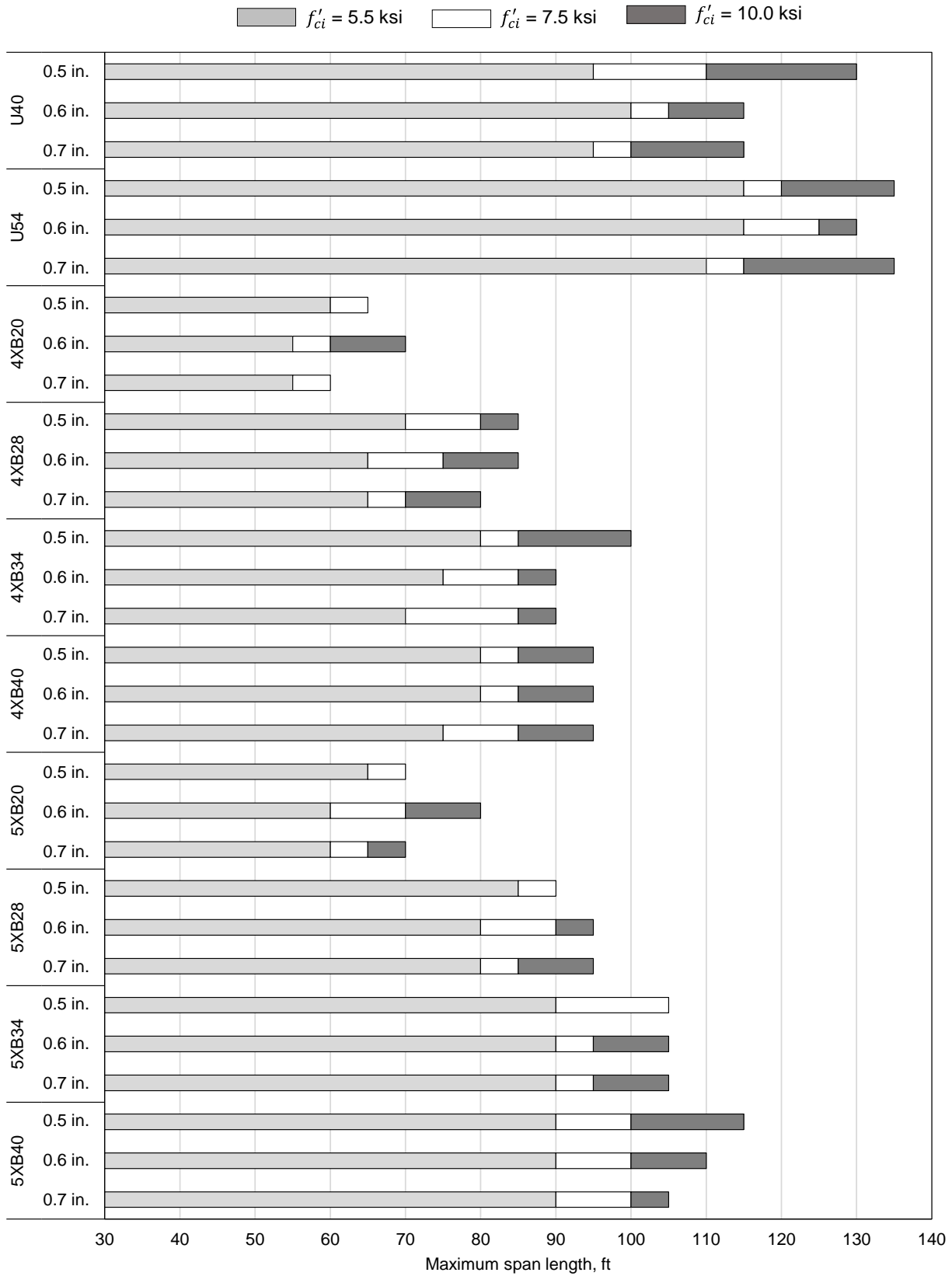


Figure 4-8- Maximum span lengths achieved for U- and X-girders with different strand diameters

A further increase in the release strength to 10 ksi results in an increase in the span capability of most design cases, especially those with 0.7-in. diameter strands. As previously mentioned, if the release strength of 7.5 ksi is provided, I- and bulb-tee girders with 0.5-in. diameter strands will not be governed by release stresses. Therefore, increasing the release strength beyond 7.5 ksi does not improve the span capability of girders with 0.5-in. diameter strands. For 0.6- and 0.7-in. diameter strands, however, increasing the release strength from 7.5 to 10 ksi increases the span capability by up to 25 ft in some cases (e.g., AASHTO Type VI).

If the release strength is increased to 10 ksi, I- and bulb-tee girders can benefit considerably from an increase in their span capability when 0.6- or 0.7-in. diameter strands are used instead of 0.5-in. diameter strands. For example, Tx70 benefits from a 30-ft increase in its span capability with the use of 0.7-in. instead of 0.5-in. diameter strands. Moreover, the use of 0.7-in. diameter strands instead of 0.6-in. diameter strands can result in an increase of up to 10 ft in the span capability of I- and bulb-tee girders. This increase can be observed in Tx40, Tx54, Tx62 and Tx70. However, since shipping limitations need to be considered for precast elements in most applications, Tx54, Tx62, and Tx70 are unlikely to benefit from the 10 ft increase in their span capability. For other cross sections, a gain of 5 ft can be observed in the span length when 0.7-in. diameter strands are used instead of 0.6-in. diameter strands.

Figure 4-7 also shows that controlling the end-region stresses through harping of the strands or other methods plays a major role in utilizing the larger-diameter strands. The span lengths of girders with straight 0.7-in. diameter strands are much more limited, especially for AASHTO precast cross sections. For a similar reason, with release strengths up to 10 ksi, 0.7-in. diameter strands do not provide any benefit to the span capability of U- and X-girders, as shown in Figure 4-8.

Since the design for a majority of U- and X-girders is governed by stresses at the time of prestress transfer, increasing the release strength can significantly improve the span capability of these sections. For example, for U40, an increase in the release strength from 7.5 to 10 ksi results in a 35-ft increase in the maximum span. However, the maximum span length of U- and X-girders with 0.7- in. diameter strands is not greater than those with 0.5-in. diameter strands for any of the release strengths considered. In cross sections such as 5XB20 and 5XB34, girders with 0.7-in. diameter strands and a release strength of 10 ksi could reach the same span capability as those with 0.5-in. diameter strands that are released at 7.5 ksi. Similar observations can be made for girders with 0.6-in. diameter strands, with the exception of 4XB20 and 5XB20, which respectively gain 5 and 10 ft compared to those with 0.5- in. diameter strands.

#### 4.4.3 Slenderness of the Superstructure

Figure 4-9 shows the effects of using different diameters of strands on the slenderness of the superstructure. To summarize the results, the Maximum Attainable Slenderness Ratio (*MASR*), which is defined as the maximum span length over the depth of the girder cross section, was obtained for different strand diameters and concrete release strengths. The spacing between girders was varied between 6, 8, 10 and 12 ft. For ease of discussion, only Tx-girders are presented.

A comparison between the three plots in Figure 4-9 shows that regardless of the strand diameter, *MASR* can be significantly increased with an increase in the concrete release strength. However, the transition from 5.5 to 7.5 ksi results in a greater gain in *MASR* compared to that from 7.5 to 10 ksi. When the release strength is increased from 5.5 ksi to 7.5 and 10 ksi, the maximum increase in *MASR* was approximately 20 and 30 percent, respectively.

With a release strength of 5.5 ksi, the *MASR* of most girders with larger-diameter strands does not exceed that of girders with 0.5-in. diameter strands, due to restrictive release conditions. However, girders with 0.7-in. diameter strands achieve equal or greater slenderness ratios than girders with 0.6-in. diameter strands.

By increasing the release strength to 7.5 ksi, the use of larger-diameter strands positively influence the *MASR* for all Tx-girders. At a spacing of 6 ft, the use of 0.6-in. diameter strands increases the *MASR* between 6 (for Tx34) and 14 percent (for Tx70). Similar improvements are found for the use of 0.7-in. diameter strands, which increase the *MASR* between 6 (for Tx62) and 12 percent (for Tx28) compared to 0.5-in. diameter strands. At this release strength, the use of 0.7-in. diameter strands result in a slight improvement in the slenderness ratio for Tx28, Tx34, and Tx54 compared to 0.6-in. diameter strands. However, such an improvement cannot be observed for other Tx-girders. The *MASR* for Tx70 girders with 0.7-in. diameter strands is less than that of girders with 0.6-in. diameter strands.

A further increase in release strength to 10 ksi positively influences the *MASR* for all Tx-girders. At this release strength, Tx28 girders benefit the most from using larger-diameter strands, with an improvement of 18 and 24 percent in *MASR* when 0.6- and 0.7-in. diameter strands, respectively, are used instead of 0.5-in. diameter strands. The use of 0.7-in. diameter strands instead of 0.6-in. diameter strands resulted in an increase in *MASR* for all Tx-girders except Tx54. However, increasing the diameter of strands from 0.5- to 0.6-in. results in noticeably greater improvement in *MASR* compared to changing from 0.6- to 0.7- in. diameter strands. Among the design cases investigated, the ratio of *MASR* for 0.7-in. diameter strands to that for 0.6-in. diameter strands was the greatest for Tx62 girders that were spaced at 6 ft. For this cross section, the use of 0.7-in. diameter strands instead of 0.5-in. diameter strands increases *MASR* by 15 percent, while the increase associated with the use of 0.6-in. diameter strands was only 6 percent. If a more practical spacing of 8 ft is considered, Tx40 girders represent the greatest improvement in *MASR* (by 8 percent) when 0.7-in. diameter strands are used instead of 0.6-in. diameter strands.

Another important observation from Figure 4-9 is how *MASR* was dependent on the girder size. For each release strength investigated, a declining trend was detected in *MASR* as the girder depth increased. In other words, the use of larger Tx-girders generally results in less slender superstructures. Moreover, the *MASR* of smaller Tx-girders benefitted the most from the use of 0.7-in. diameter strands.

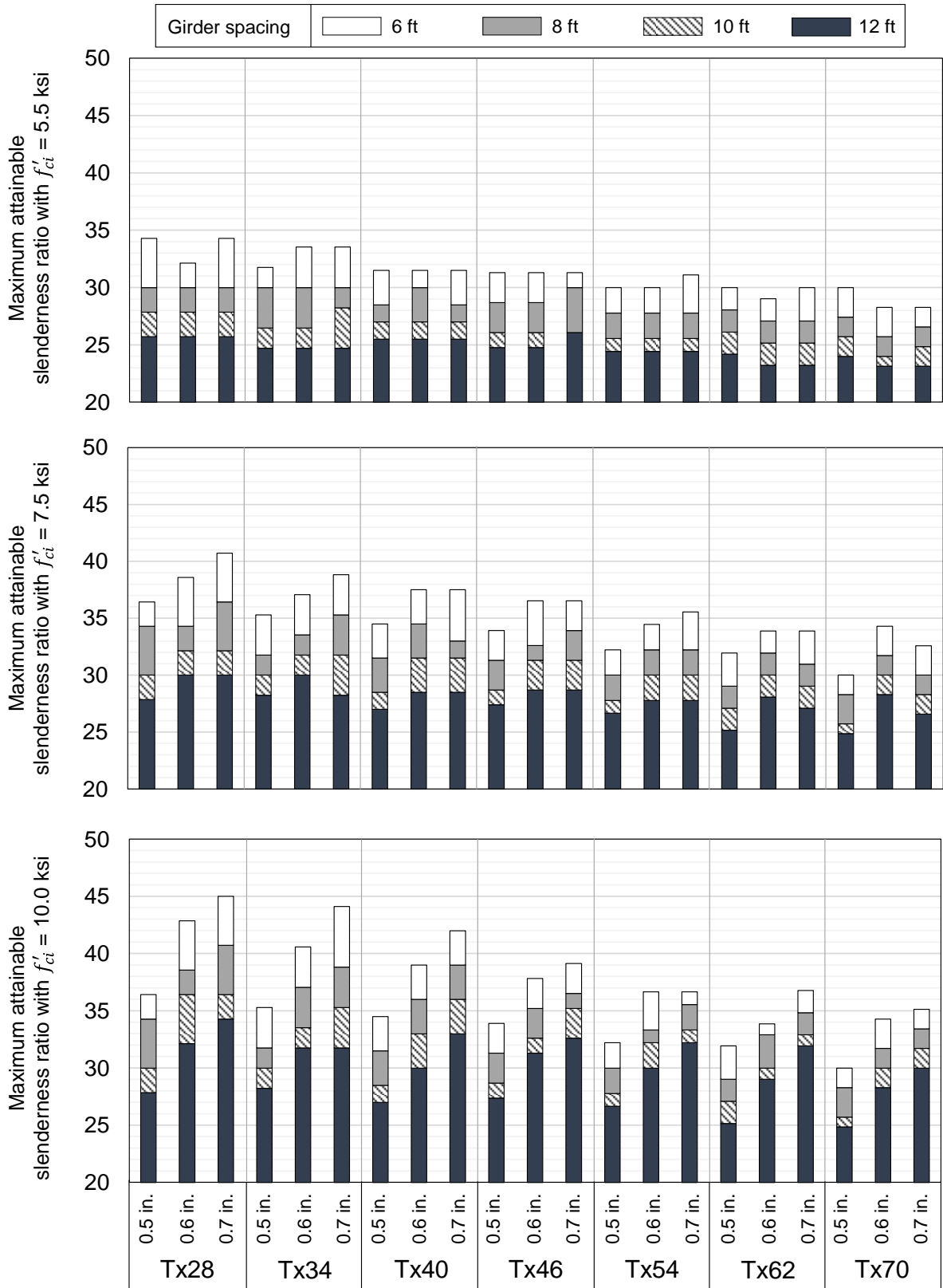


Figure 4-9- Maximum attainable slenderness ratio (MASR) for 0.5-, 0.6-, and 0.7-in. diameter strands in Tx-girders

#### 4.4.4 Girder Spacing

Figure 4-10 shows the effects of using different strand diameters on the maximum allowable transverse spacing between I- and bulb-tee girders that are fabricated using different release strengths. To generate this figure, the girder spacing was varied between 6 and 16 ft at 1 ft increments, and the maximum spacing at which the design requirements could be satisfied was identified. To simplify the discussion, the investigation was made at a selected span for each cross section. The selected span, which is referred to as “maximum practical span,” is chosen as 85 percent of  $L_{common}$  from Figure 4-3, regardless of the release strength. Recall that in determining  $L_{common}$ , the girders were assumed to be used at a spacing of 8 ft. The live load deflection limit was also considered but was not found to govern any of the design cases presented herein.

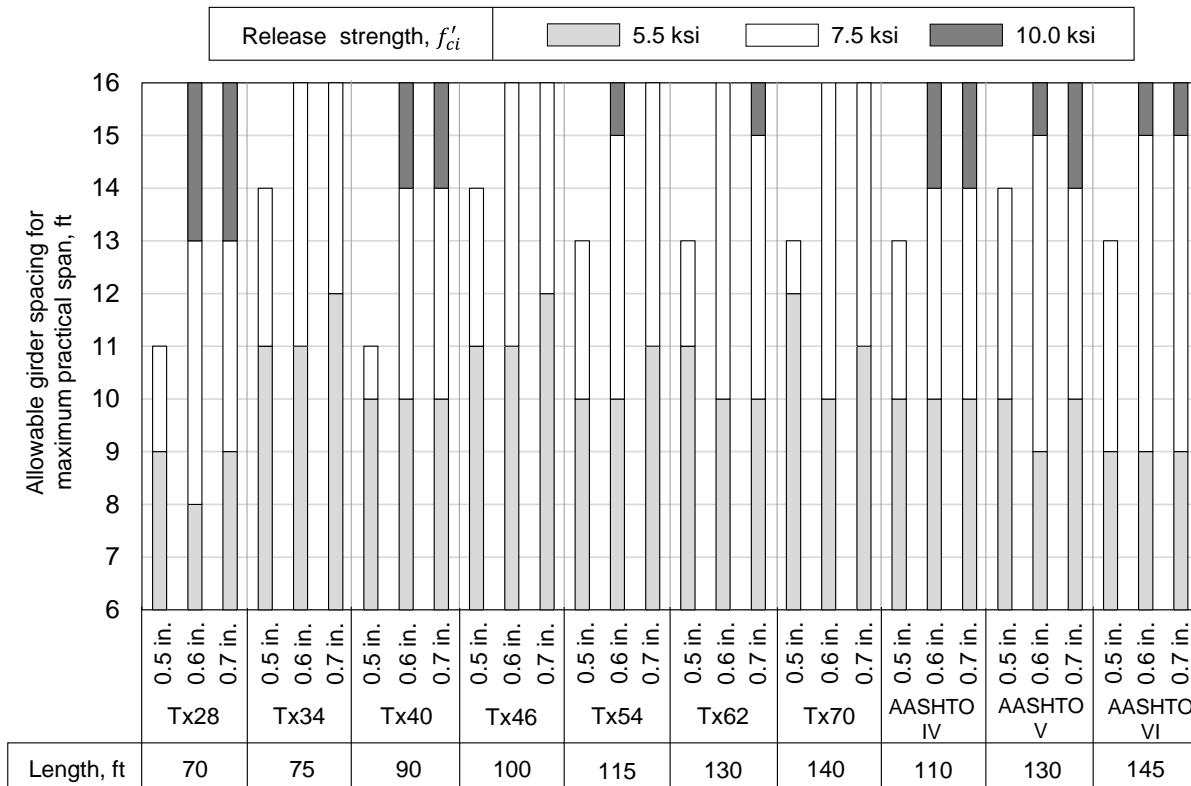


Figure 4-10- Allowable girder spacing at maximum practical spans for I- and bulb-tee girders employing 0.5-, 0.6-, and 0.7-in. diameter strands

With a release strength of 5.5 ksi, most cross sections (except Tx28, and AASHTO Types V and VI) could be used at a girder spacing of 10 ft at their maximum practical spans with all three strand diameters. In practice, the maximum girder spacing is usually limited to 10 ft due to costs associated with the slab that spans between girders. However, greater spacings were evaluated to gain insight into the potential benefits offered by larger-diameter strands.

Increasing the release strength from 5.5 to 7.5 ksi results in a considerable increase in the allowable spacing for all girders, especially those with larger-diameter strands. With this release strength, all girders with 0.6- and 0.7-in. diameter strands could be used at a girder spacing of 13 ft at their maximum practical spans. A maximum gain of 6 ft in girder spacing takes place for Tx54, Tx62, Tx70, and AASHTO Types V and VI girders that used 0.6-in. diameter strands. A

transverse spacing of up to 16 ft is made possible for Tx34, Tx46, and Tx70 for both 0.6- and 0.7-in. diameter strands.

For girders that employ 0.5-in. diameter strands, increasing the release strength beyond 7.5 ksi provides no additional benefit to the allowable transverse spacing. However, if the release strength is increased to 10 ksi, all girders with larger-diameter strands could potentially be used at greater transverse spacings, up to 16 ft. The increase is most noticeable for Tx28.

Figure 4-10 shows that the use of larger-diameter strands results in a noticeable increase in the allowable spacing between girders, especially when a release strength of 7.5 ksi or greater is used. However, for girder spacings up to 16 ft, which were investigated herein, 0.7-in. diameter strands offered very limited additional benefits compared to 0.6-in. diameter strands. The few cases in which 0.7-in. diameter strands outperformed 0.6-in. diameter strands by 1 ft in terms of allowable spacing were Tx34, Tx46, Tx54, and Tx62 with a release strength of 5.5 ksi, and Tx54 with a release strength of 7.5 ksi.

With a release strength of 7.5 ksi, all girders can be used at a transverse spacing of 11 ft, regardless of the strand diameter. Therefore, the use of 0.7-in. diameter strands offers benefits to girder spacing that are well beyond the practical limits and are therefore of limited real-world application.

## 4.5 Summary and Conclusions

A comprehensive parametric investigation was conducted to quantify the potential benefits obtained from using 0.7-in. diameter strands. This objective was achieved through the use of a validated parametric study tool that is capable of designing a variety of precast, pretensioned sections employing 0.5-, 0.6-, and 0.7-in. diameter strands. Thousands of design cases were generated to determine the benefits of using 0.7-in. diameter strands and the requirements for the efficient use of these larger-diameter strands.

The primary conclusions of the parametric study, which are categorized based on the perceived benefits attributed to the use of 0.7-in. diameter strands, are as follows:

- **Steel quantity:** The use of 0.7-in. diameter strands results in a considerable reduction in the number of strands. To achieve any particular span, the number of 0.7-in. diameter strands needed is less than half the number of 0.5-in. diameter strands. The increased internal moment lever arm also results in a reduction of up to 16 percent in the weight of prestressing steel compared to 0.5-in. diameter strands. However, the weight of 0.7-in. diameter strands would be comparable to that of 0.6-in. diameter strands. Benefits of 0.7-in. diameter strands are most significant in larger I- and bulb-tee girders, where up to 16 fewer strands will be needed compared to 0.6-in. diameter strands at practical span lengths. In U- and X- girders, the strand layout restricts how far the center of gravity of the strands can be moved. Therefore, the reduction in the number of strands does not correspond to a noticeable reduction in the total weight of prestressing steel in these sections.
- **Span capability:** I- and bulb-tee girders might benefit from a maximum gain of 10 ft in span capability when 0.7-in. diameter strands are used instead of 0.6-in. diameter strands. However, this increase in span length requires the release strength of 10 ksi or greater. In addition, harping or other methods for controlling end-region stresses will be needed. Unlike I- and bulb-tee girders, U- and X- girders that employ 0.7-in. diameter strands do not reach greater span lengths compared to those with 0.5-in. diameter strands.

- **Slenderness of superstructure:** benefits to the slenderness ratio with the use of 0.7-in. diameter strands were found to be highly dependent on the allowable release strength. For a release strength of 10 ksi, the use of 0.7-in. diameter strands instead of 0.6-in. diameter strands resulted in an increase in the allowable slenderness ratio for the majority of Tx-girders. However, increasing the diameter of strands from 0.5- to 0.6-in. results in noticeably greater improvement in the slenderness ratio compared to changing from 0.6- to 0.7-in. diameter strands. Of the Tx-girders considered, the smaller girder cross sections benefited the most from 0.7-in. diameter strands.
- **Allowable girder spacing:** the majority of I- and bulb-tee girders investigated herein could be used at a girder spacing of up to 10 ft with 0.5-in. diameter strands. The use of larger-diameter strands results in a noticeable increase in the allowable spacing between girders. However, for girder spacings up to 16 ft, 0.7-in. diameter strands offer very limited additional benefits compared to 0.6-in. diameter strands, and those benefits are observed at a spacing considerably greater than the practical limits associated with the slab construction.

Other than reducing the number of strands, realizing the benefits associated with 0.7-in. diameter strands require greater release strengths compared to what is currently used in practice. A release strength of 7.5 ksi provides the opportunity to observe some benefits in terms of span length, girder spacing, and slenderness of superstructure from 0.7-in. diameter strands compared to 0.6-in. diameter strands. A further increase in release strength to 10 ksi results in noticeable advantages for 0.7-in. diameter strands over 0.6- in. diameter strands in terms of span capability (by 10 ft) and slenderness of superstructure (by 8 percent at a transverse spacing of 8 ft). Evaluating the practicality of such a release strength is beyond the scope of the current study. It is important to note that unlike 0.6- and 0.7-in. diameter strands, girders with 0.5-in. diameter strands do not benefit from release strengths greater than 7.5 ksi because their design will be governed by the maximum number of strands that can physically exist in the girder strand layout.

All of the conclusions mentioned above are based on the assumption that 0.7-in. diameter strands can be used on a standard 2- by 2-in. grid without negatively impacting the serviceability or strength of pretensioned girders. The validity of this assumption was extensively investigated in the full-scale experimental program conducted as part of Tasks 4 and 6 of this research project, as discussed in the next few chapters of this report.

# CHAPTER 5

## Experimental Program

### 5.1 Overview

As part of TxDOT Project 0-6831, the research team at UT designed, fabricated, and tested seven full-scale pretensioned Tx-girders in which 0.7-in. diameter strands located on a 2- by 2-in. grid were used as the prestressing steel. The specimens were fabricated using typical industry practices to provide a realistic representation of the conditions of girders in the field. On the other hand, fabrication of the specimens was performed in the controlled laboratory environment, which made it possible to enforce careful quality-control measures and obtain unlimited access to the specimens for extensive instrumentation. Each specimen was monitored for transfer length, end-region cracking, and transverse end-region stresses at the time of prestress transfer as well as load-deflection behavior, strains in the mild-steel reinforcement, strand slip, and patterns of cracking and damage under applied loads until failure. This chapter provides an overview of activities to complete the experimental program involving the aforementioned efforts, which helped accomplish the objectives of Task 4 (End-Region Serviceability) and Task 6 (Ultimate Shear Strength).

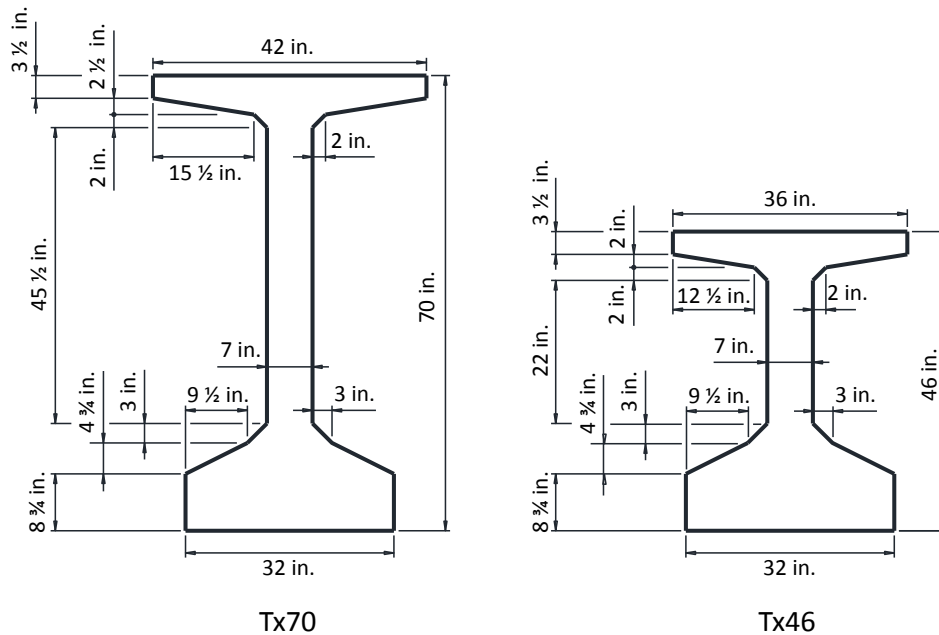
### 5.2 Specimen Design

Seven pretensioned Tx-girders were designed to employ 0.7-in. diameter strands on a 2- by 2-in. grid. These girders included five Tx46 girders (Tx46-I through Tx46-V) and two Tx70 girders (Tx70-I and Tx70-II), with the cross-sectional properties shown in Figure 5-1. The Tx46 specimens were selected to represent the mid-sized bulb-tee cross sections that are used on a frequent basis in Texas. The Tx70 specimens, on the other hand, are the deepest girders among this family of precast sections, which are likely to benefit the most from using larger-diameter strands based on the results of the parametric study discussed in Chapter 4.

Table 5-1 shows a summary of specimen design parameters. All specimens were designed according to the 7<sup>th</sup> edition of AASHTO LRFD Bridge Design Specifications, considering 2016 interim revisions (AASHTO, 2016). For the purposes of designing the specimens in this test program, these specifications were in agreement with the provisions of TxDOT LRFD Bridge Design Manual (2015). According to these specifications, at the time of prestress transfer, the stresses are limited to  $0.65f'_{ci}$  in compression and  $0.24\sqrt{f'_{ci}}$  in tension, where  $f'_{ci}$  is the compressive release strength of concrete in ksi. To generate the most critical conditions for end-region stresses, all specimens were designed to reach the maximum allowable stresses at the top, bottom, or both extreme fibers of the cross section.

Each specimen was assumed to be 30 ft long to fit in the prestressing facility at FSEL. Therefore, the specimens were considerably shorter than their typical lengths in bridge applications. However, this length was sufficient for investigating the end-region behavior and shear strength of the specimens in realistic conditions.

Property	Tx46	Tx70
Gross cross-sectional area, in. <sup>2</sup>	761	966
Distance from the bottom fiber to the center of gravity of the girder, in.	20.1	31.91
Moment of inertia around the x-axis, in. <sup>4</sup>	198,089	628,747
Moment of inertia around the y-axis, in. <sup>4</sup>	46,478	57,579
Weight, lb/ft	819	1,040

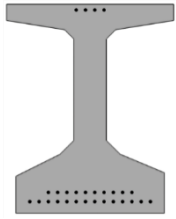
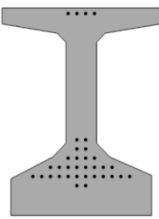
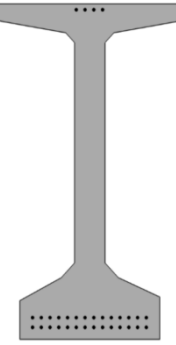
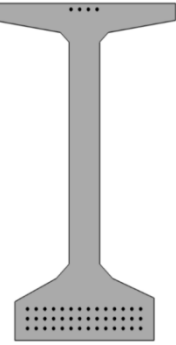
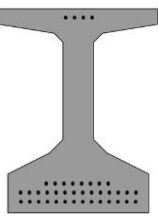


**Figure 5-1- Cross-sectional properties of Tx46 ad Tx70 girders**

Straight 0.7-in. strands were used as the prestressing reinforcement within the specimens. The strands in Tx46-II were concentrated near the centroid of the cross section to allow for the greatest prestressing force and therefore, generate the greatest bursting stresses. In all other specimens, the strands were placed conventionally, i.e. at the greatest possible eccentricity within the specimen cross section, to generate the maximum spalling stresses. To control the stresses within the cross section at the time of prestress transfer, all specimens included four 0.7-in. diameter strands within the top flange in addition to those within the bottom flange. The stress level in these top-flange strands was variable among the specimens to optimize the capacity of the specimens and maximize the number of strands that could be accommodated in the specimens.

Specimens Tx46-I, Tx46-II, and Tx70-I were designed assuming concrete release strengths that are typically used for prestressed concrete superstructures in Texas. However, based on the results of the parametric study described in Chapter 4, a greater concrete release strength, in the order of 8 ksi, was considered for the design of other specimens to investigate the behavior of girders fabricated with a greater number of 0.7-in. diameter strands.

**Table 5-1- Specimen design parameters**

Specimen ID		Tx46-I	Tx46-II	Tx70-I	Tx70-II	Tx46-III Tx46-IV Tx46-V
Strand layout						
Design objective		Max. $e$	Max. $P_i$	Max. $e$	Max. $e$	Max. $e$
End-region detailing		Standard	Standard	Standard	Standard	Modified
Design $f'_{ci}$ , ksi		5.5	5.2	5.5	7.8	8.0
No. of strands	Top flange	4	4	4	4	4
	Bottom flange	24	30	28	42	36
$y_p$ , in.	Top strands	44.03	44.03	68.03	68.03	44.03
	Bottom strands	3.3	10.4	3.5	4.5	4.2
$f_{pi}$ , ksi	Top strands	157.5	202.5	110.0	202.5	170.0
	Bottom strands	202.5	202.5	202.5	202.5	202.5
$\sigma_{predicted}$ , ksi	Top fiber	0.23 (T)	1.13 (C)	0.55 (T)	0.55 (T)	0.48 (T)
	Bottom fiber	3.57 (C)	3.40 (C)	3.53 (C)	5.04 (C)	5.19 (C)

Note:  $e$  = eccentricity;  $P_i$  = initial prestressing force;  $y_p$  = distance from the bottom fiber of girder to centroid of strands;  $f_{pi}$  = jacking stress;  $\sigma_{predicted}$  = predicted concrete stress after prestress transfer; (C) = Compression; (T) = Tension.

The end-region and shear reinforcement detailing in the first four specimens (Tx46-I, Tx46-II, Tx70-I, and Tx70-II) followed the standard TxDOT drawings for girders with 0.5- and 0.6-in. diameter strands (Texas Department of Transportation, 2015), which is primarily based on studies by O'Callaghan (2007). Figure 5-2 shows the details of mild-steel reinforcement in the first four specimens along with a 3D rendering that shows the arrangement of end-region reinforcement in these specimens. The end-region reinforcement in this standard detailing consists of:

- 1) Thirteen No. 4 bars (R-bars) that are spaced at 3 in.;
- 2) Thirteen pairs of No. 6 bars (S-bars) that are tied to the closely spaced R-bars within the end-region;
- 3) Pairs of No. 4 bars (C-bars) that are spaced at 6 in. and continue for a distance of 1.5 times the depth of the precast girder; and
- 4) Two No. 5 bars (U-bars).

Following the fabrication of these four specimens, the research team decided to fabricate the next specimen with modified end-region detailing to reduce the width of spalling cracks. In Tx46-III, No. 8 S-bars were used at one end instead of No. 6 bars. Due to issues related to the compressive release strength of this specimen, which are discussed later in this chapter, the research team decided to repeat Tx46-III. Therefore, the design and detailing of Tx46-IV were identical to those of Tx46-III.

For Tx46-V, the research team made two changes to the end-region reinforcement, as shown in Figure 5-3. First, a series of horizontal No. 4 hairpin bars spaced at 3 in. (W-bars and WT-bars) were added to one end-region to evaluate the effectiveness of horizontal reinforcement in controlling the width of end-region cracks. Second, No. 4 bars (cap bars) were added to all pairs of C-bars within the bottom flange at both ends of the specimen to improve the effectiveness of bottom flange confinement and control strand slip. The S-bars in this specimen remained as No. 6 bars.

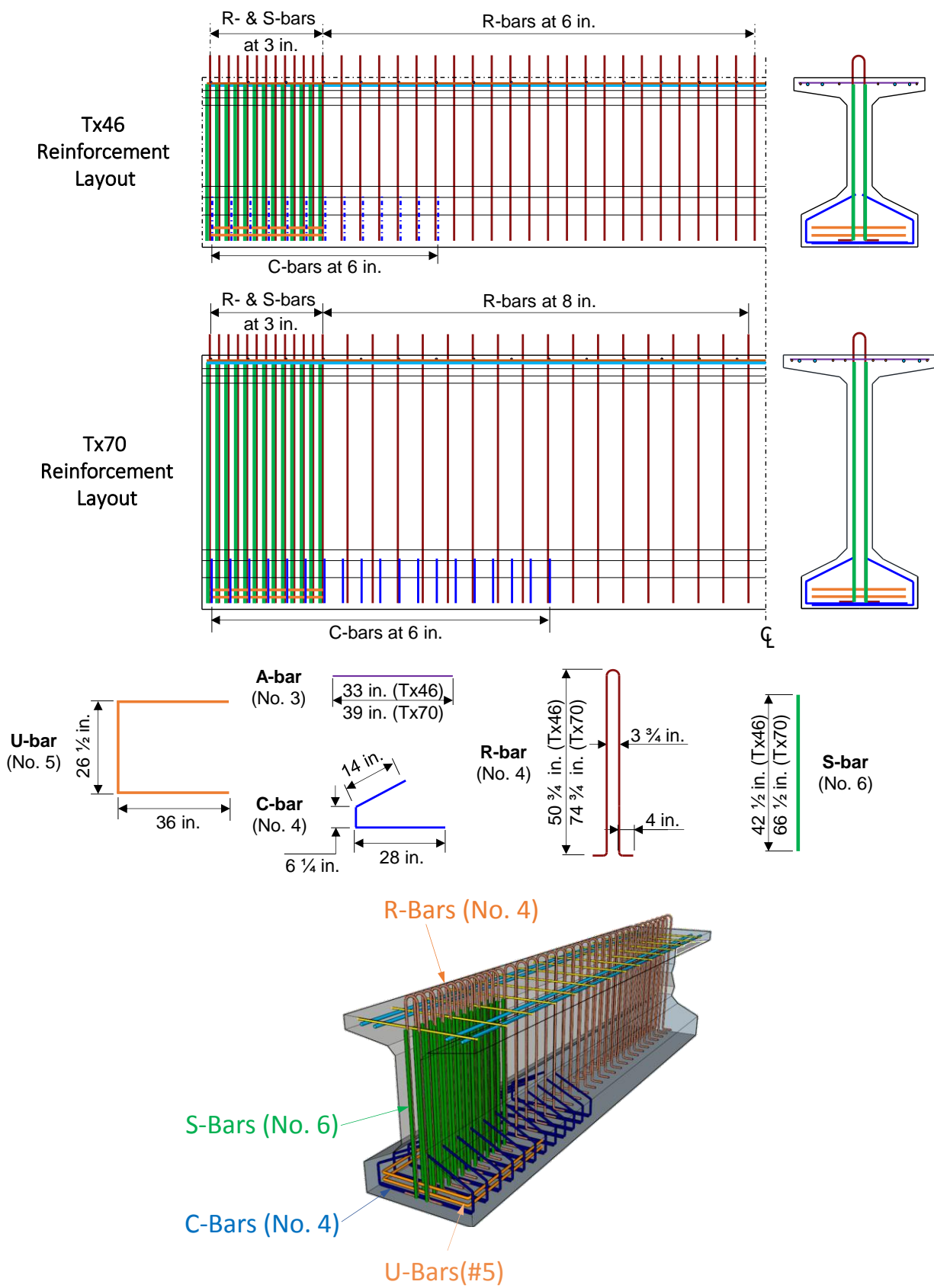
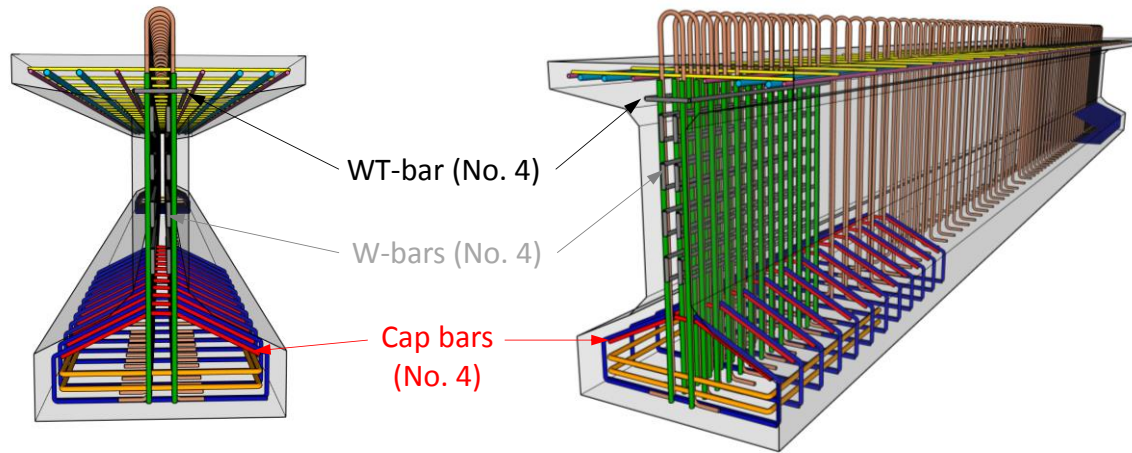


Figure 5-2- End-region and shear reinforcement in the first four specimens



**Figure 5-3- Additional bars added to the end-region reinforcement in Tx46-V**

### 5.3 Specimen Fabrication

The specimens were fabricated using the prestressing facility at FSEL (Figure 5-4), which is designed to accommodate prestressing forces up to 2,500 kips. Steel bulkheads measuring 12 in. thick are used at each end of the prestressing facility to anchor the strands. The bulkhead at one end is fixed, while the bulkhead at the other end is supported by four 800-kip hydraulic rams, which are extended for stressing the strands and retracted at the time of release. These two ends are herein referred to as the dead and live ends, respectively. Two adjustable cross beams are also used within the prestressing facility, making it possible to apply prestressing forces of up to 300 kips to top strands in different types of cross sections. To accommodate 0.7-in. strands, modifications were made to the prestressing facility, including drilling larger holes in stressing plates and fabricating a new frame for prestressing the top strands.

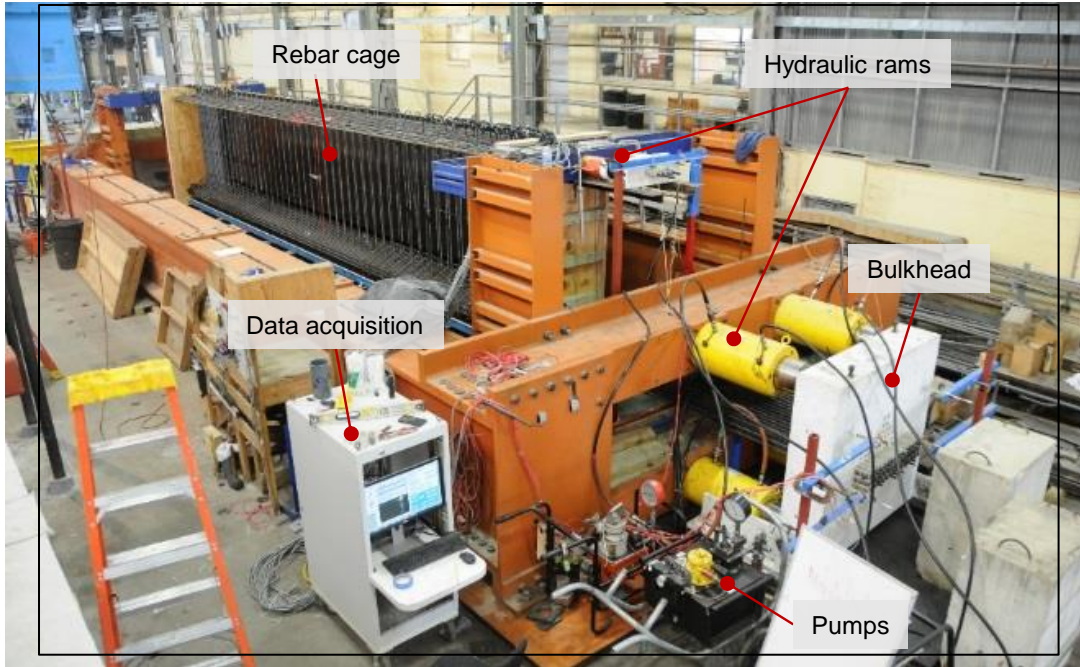


**Figure 5-4- Prestressing facility at FSEL**

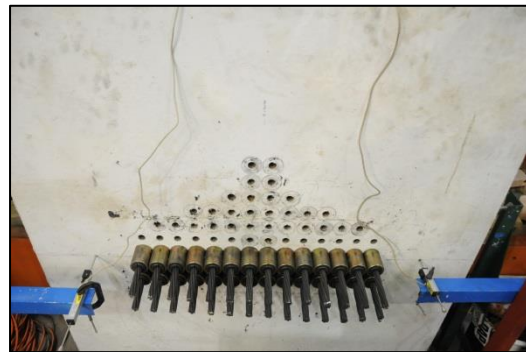
Fabrication of each specimen began by placing the 0.7-in. diameter strands in the prestressing facility and installing the anchorage devices, as shown in Figure 5-5. Reusable strand chucks were used for anchoring the 0.7-in. diameter strands at each end, which had an external diameter of 2 in. Therefore, the strands could be used on the standard 2- by 2-in. grid without any constructability issues.



(a) Installing the strands



(b) Live-end chucks



(c) Dead-end chucks

**Figure 5-5- Strand installation**

To remove the slack and ensure uniform stressing of the strands, each strand was individually stressed to 2 kips, as shown in Figure 5-6(a), after which the strands were “gang-stressed” using the main hydraulic rams [Figure 5-6(b)]. Gang-stressing of the strands was carried out in a minimum of 10 increments. The prestress level was controlled through measurements of hydraulic pressure in the rams using pressure transducers. The elongation of the strands was measured using a series of linear potentiometers at each end of the prestressing facility and verified to be within 5 percent of the calculated value after each increment. Once the strands were stressed to the desired level, the mild-steel reinforcement was tied to the prestressing strands [Figure 5-6(c)] with a tolerance of 1/4 in. Photos illustrating modified end-region reinforcement in Tx46-IV and Tx46-V are provided in Figure 5-7.



(a) Removing the slack from individual strands



(b) Gang-stressing the strands



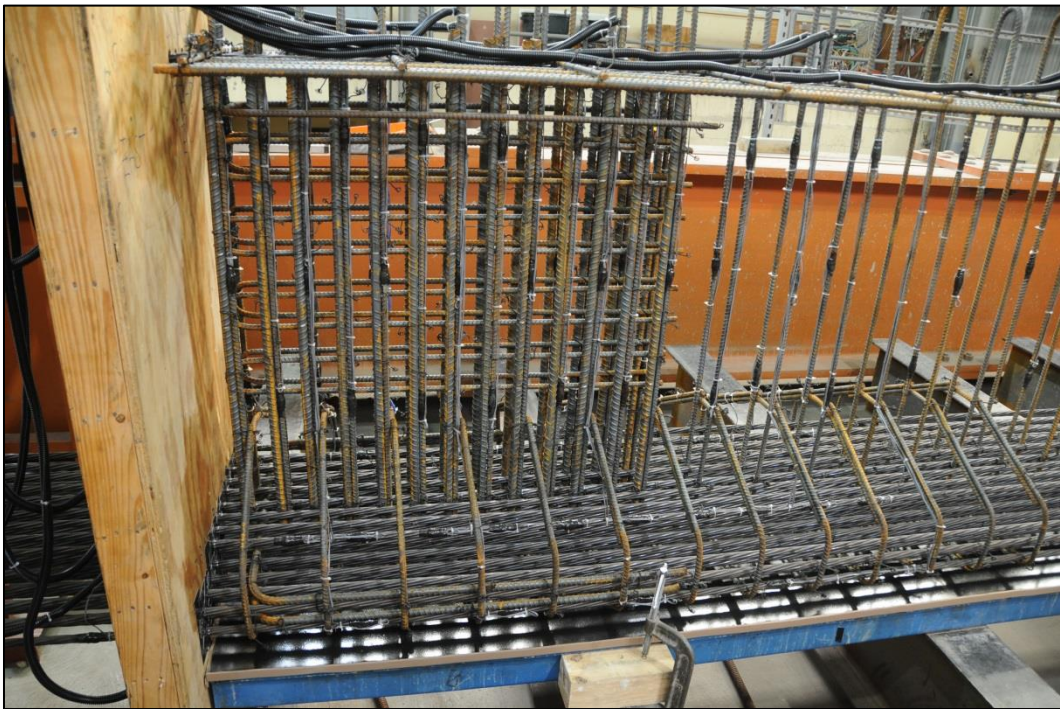
(c) Tying the mild-steel reinforcement

**Figure 5-6- Specimen fabrication steps**

Typically, each specimen contained 90 electrical resistance strain gauges on the strands to measure the transfer length. At each end of the specimen, four strands were instrumented, as shown in Figure 5-8. Among the instrumented strands, the strain gauges were installed at two intervals of 12.0 in. and 6.0 in., to examine any potential changes in transfer length due to the presence of strain gauges. These gauges were continued up to a distance of 60 in. from the end face of the specimens. One strain gauge was also installed outside the specimen on each of the instrumented strands to serve as a reference measurement representing the stress-free strain condition of the strand after prestress transfer. All strand strain gauges were installed on the helical wires. An example of strain gauge application on a strand is shown in Figure 5-9(a).



(a) Tx46-IV



(b) Tx46-V

**Figure 5-7- Modified end-region reinforcement in Tx46-IV**

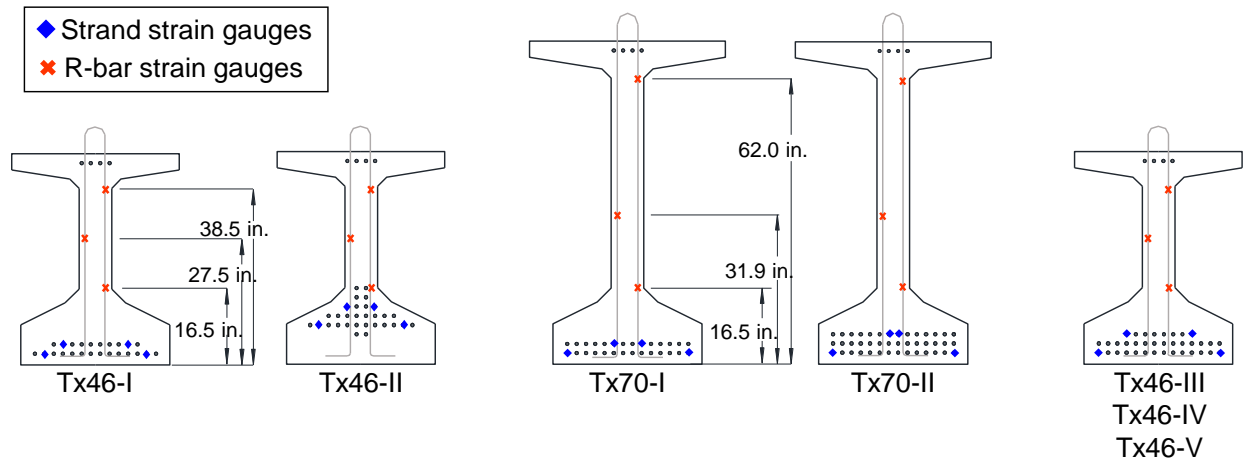


**Figure 5-8- Strain gauge locations for monitoring transfer length and transverse reinforcement stresses**

Each specimen also contained a considerable number of strain gauges on the transverse reinforcement to determine strains due to bursting and spalling stresses as well as strains at the time of future structural tests. At a minimum, the first fifteen stirrups (R-bars) from each end of the specimen were instrumented. Three strain gauges were installed on each instrumented stirrup, as shown in Figure 5-8. The stirrup leg that contained two strain gauges was alternated from one stirrup to the next. The initial installation of a strain gauge on one of the stirrups, prior to applying protective layers, is shown in Figure 5-9(b). Figure 5-9(c and d) show the completed end-region instrumentation, after applying the protective materials.

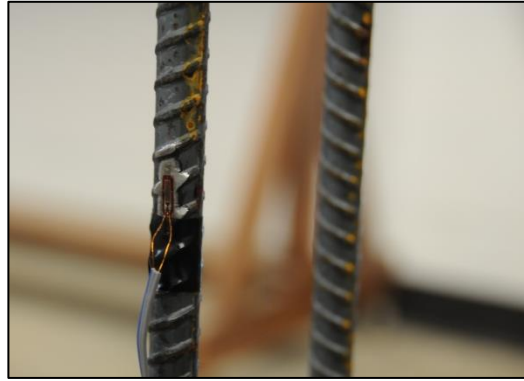
The specimens were also instrumented using three Vibrating Wire Strain Gauges (VWGs) that were embedded at the midspan of the specimen [Figure 5-10 (a)]. Measurements from VWGs were used to develop a strain profile at the midspan section and to estimate prestress losses due to elastic shortening, shrinkage, and creep over the life of the specimen. To measure the hydration temperatures in the concrete, six thermocouples were placed in a section located within 2 ft from the end face of the specimens. As shown in Figure 5-10 (b), these thermocouples were distributed within the cross section to capture the variability of concrete curing temperatures within the end-region of the girders.

Strain gauges on strands



(a)

Strain gauges on R-bars

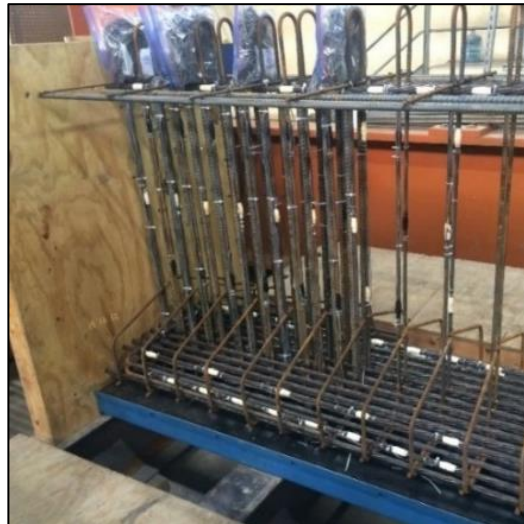


(b)

Before applying the protective materials



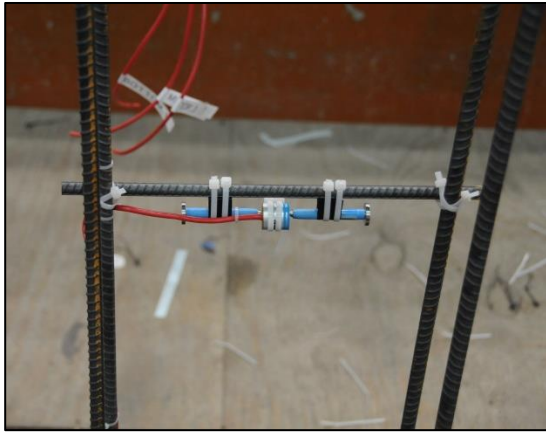
(c)



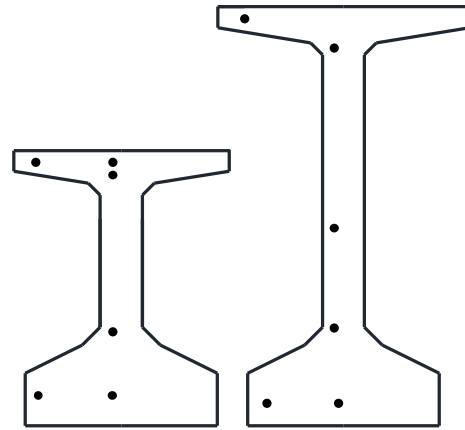
(d)

After applying the protective materials

**Figure 5-9- Instrumentation embedded in the specimens**



(a) Vibrating wire gauge



(b) Locations of thermocouples

**Figure 5-10- Additional embedded instrumentation**

Once the reinforcement and the instrumentation were installed, the formwork was assembled, and the concrete was cast. The properties of concrete mixtures used within the test program are provided in Table 5-2. Type III portland cement was used in all mixtures to represent the realistic conditions of pretensioned girders in the field. Crushed limestone was the coarse aggregate used within the mixtures, which had a maximum nominal aggregate size of 1/2 in. in the mixture used for Tx46-III and 3/8 in. in all other mixtures. The mixtures used for Tx46-I and Tx46-II were batched and mixed at FSEL. The concrete comprising the other specimens was batched and mixed by Coreslab Structures in Cedar Park, Texas and transported to FSEL. Note that the mixture used within Tx46-III did not match that requested by the research team. The higher-than-desired water-to-cement ratio used within this mixture resulted in a significantly lower compressive strength than desired.



(a) Casting the specimen



(b) Casting match-curing cylinders

**Figure 5-11- Concrete placement**

In all cases, a combination of internal and external vibration was used to ensure satisfactory consolidation of concrete [Figure 5-11(a)]. Forty-eight 4- by 8-in. match-curing concrete cylinders were cast using the concrete comprising each specimen [Figure 5-11(b)]. These cylinders were connected to a relay system that maintained the same temperatures within the cylinders as those

measured from the embedded thermocouples (Figure 5-12). Therefore, eight cylinders were match-cured based on each of the six thermocouples shown in Figure 5-10(d), which made it possible to capture the variability of concrete strength within the specimen cross section.

**Table 5-2- Concrete mixture properties**

	Tx46-I	Tx46-II	Tx70-I	Tx70-II	Tx46-III*	Tx46-IV	Tx46-V	
Mixture components	Type III portland cement, lb/yd <sup>3</sup>	725	725	600	801	600	800	800
	Fly ash, lb/yd <sup>3</sup>	0	0	200	196	200	200	200
	Coarse aggregate, lb/yd <sup>3</sup>	1951	1956	1400	1345	1400	1345	1345
	Fine aggregate, lb/yd <sup>3</sup>	1072	1082	1400	1117	1400	1117	1117
	Water, lb/yd <sup>3</sup>	285	274	191.9	282	268	284	284
	Super plasticizer, oz/yd <sup>3</sup>	29	14.5	45	81	28	81	81
	Retarder, oz/yd <sup>3</sup>	29	29	30	40	22	40	40
	Air entraining agent, oz/yd <sup>3</sup>	0	0	4	0	4	0	0
	Water-cementitious ratio	0.39	0.38	0.24	0.28	0.34	0.28	0.28
	Ambient temperature at time of casting, °F	85	77	78	75	87	66	78
Maximum hydration temperature, °F	154	138	129	152	145	146	157	

\* Note: The mixture used within Tx46-III did not match the mixture requested by the research team.



**Figure 5-12- Match-curing system**

In the hours following the concrete placement, match-cured specimens were periodically tested to identify the appropriate timing for formwork removal and subsequent prestress transfer (Figure 5-13). The team started the steps to remove the side forms after confirming a compressive strength of 3 ksi from the cylinders cured based on all six thermocouples. Prestress transfer commenced as soon as the compressive strength of match-cured cylinders based on all thermocouple measurements exceeded the desired release strength, an example of which is shown in Figure 5-14. The prestressing strands were released through gradual retraction of hydraulic rams in 20 steps, which typically took 1 hour. As the strands were being released, the compressive strength and modulus of elasticity of match-cured concrete specimens were measured to obtain the mechanical properties at prestress transfer.



(a) Tested match-cured specimens



(b) Match-cured cylinder being tested

Figure 5-13- Testing of match-cured cylinders

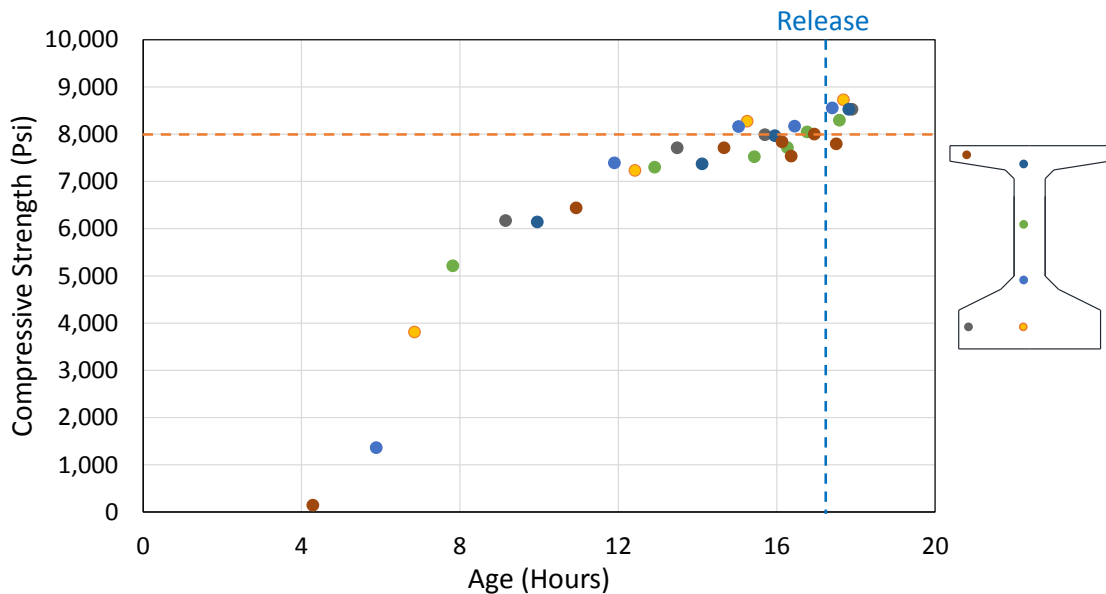


Figure 5-14- Determining the time of release for a typical specimen based on match-cured specimens

Since the concrete comprising Tx46-III showed a very slow rate of strength gain, the prestressing strands in this specimen were released at a considerably lower concrete compressive strength than desired. As a result, compressive stresses at the bottom of this girder at release exceeded the  $0.65f'_c$  allowed by AASHTO LRFD specifications and TxDOT Bridge Design Manual. Therefore, the results obtained from this specimen were not deemed representative of the conditions of pretensioned girders in the field, and the research team repeated this specimen as Tx46-IV.

In addition to the match-cured cylinders, additional cylinders were prepared to measure mechanical properties of concrete at 28-days and at the time of shear test. Moreover, the mechanical properties of the prestressing strands and the mild-steel reinforcing bars used in the construction of the girders were determined by performing ASTM-compliant tests.

Data acquisition from the instrumentation commenced immediately prior to prestress transfer and was continued for 24 hours after the end of the release operation. After the release operation was completed, the specimens were carefully examined for end-region cracking.

Within three weeks after the release of the prestressing force, a cast-in-place reinforced concrete deck with a thickness of 8 in. was cast on the top flange of each specimen to increase the flexural capacity of the specimens and simulate the composite deck in a bridge system. The deck had a width of 34 in. for the Tx46 specimens and 40 in. for the Tx70 specimens. High-strength concrete was used for the construction of the deck to ensure a faster strength gain. Once the concrete in the precast girder and the deck had cured sufficiently, the specimens were moved to the test setup and loaded in a shear-critical loading configuration until failure. The girders had a minimum age of 28 days at the time of shear testing.



(a) Deck reinforcement and formwork



(b) Casting the deck concrete

Figure 5-15- Construction of the cast-in-place deck

## 5.4 Shear Testing

All specimens were tested as simply supported members under shear-critical loading conditions. To evaluate potential differences between the behavior of the live and dead ends and to ensure a consistent shear span-to-depth ratio regardless of the failed span, all specimens were subjected to symmetric loading configurations in which both ends of the specimen were subjected to equal shear forces.

Figure 5-16 shows the test configurations used for the specimens. The Tx46 specimens were subjected to two symmetrically located concentrated loads that were applied using a steel spreader beam. Steel rollers were used to transfer the load from the spreader beam to the test specimens, providing a shear span-to-depth ratio of 3.0. The Tx70 specimens were subjected to a single point load at the midspan to obtain the longest possible shear span. This configuration resulted in two shear spans with equal lengths, each with a span-to-depth ratio of approximately 2.3.

The Tx46 and Tx70 specimens were supported on 8- by 21-in. and 9- by 21-in. steel plates, respectively. As shown in Figure 5-16, the centroids of these plates were located at a distance of 9 in. from the end face of the girder. These plates were supported by a roller support fixture at one end and a pin support fixture at the other end. Both support fixtures were carefully designed and fabricated using machined steel components to provide controlled, idealized boundary conditions, as shown in Figure 5-17. The roller support included a 3-in. diameter roller that permitted free rotation and translation while the pin support included a tilt-saddle that permitted only free rotation.

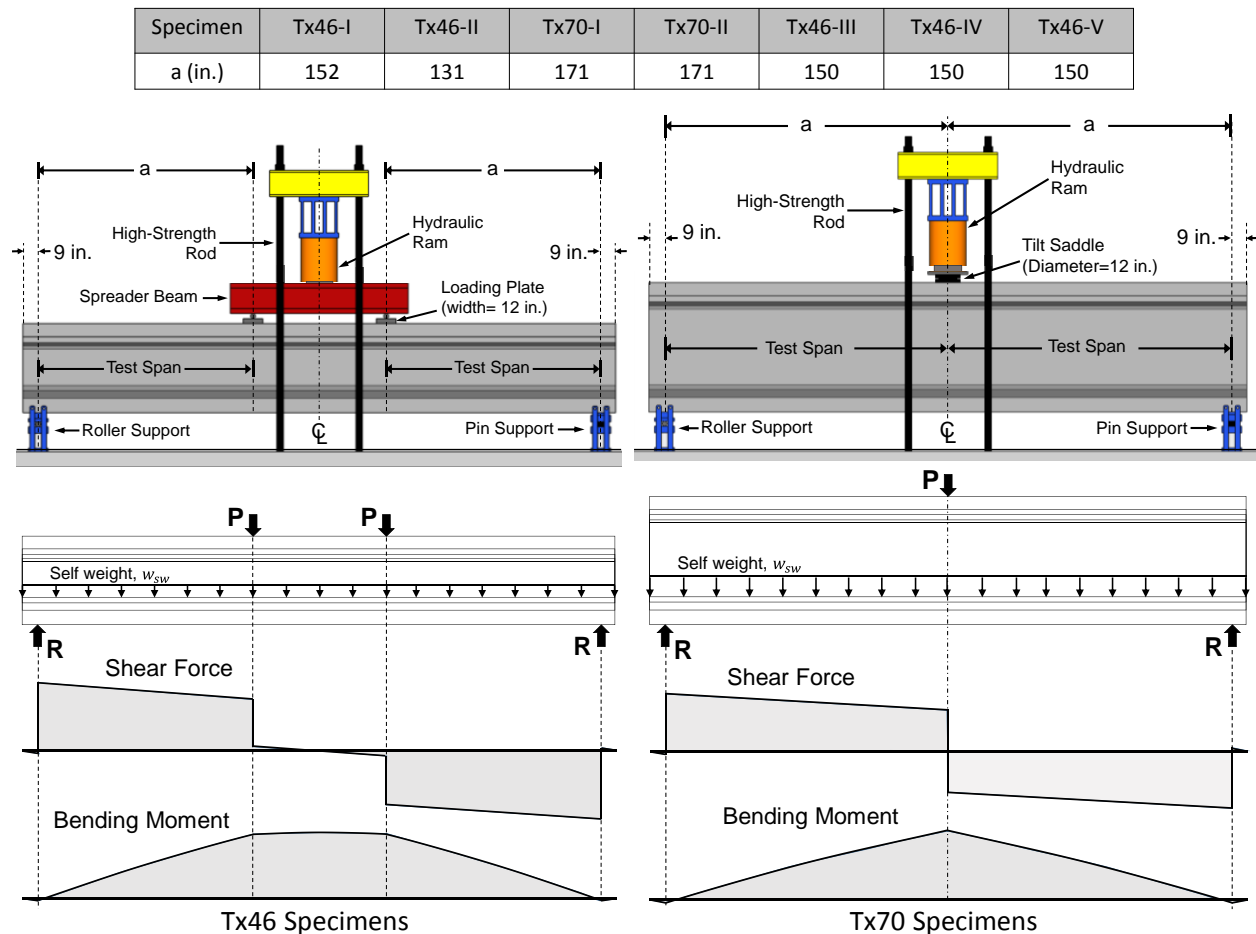


Figure 5-16- Testing configuration



(a) Roller Support



(b) Tilt Support

**Figure 5-17-Supports for the shear test**

Load was applied to the specimens using a hydraulic ram that was pressurized by means of a pneumatically controlled hydraulic pump. The ram reacted against a stiff loading frame that was connected to the strong floor by way of high-strength steel rods. Photos of the test setup for the Tx46 and Tx70 specimens are shown in Figure 5-18.



(a) Tx46



(b) Tx70

**Figure 5-18- Photos of the shear test setup**

The schematic shear force and bending moment diagrams for the Tx46 and Tx70 specimens are also shown in Figure 5-16. In the Tx46 specimens, the applied loads resulted in a constant bending moment between the two test spans. However, the specimens were designed to fail in shear well before reaching the flexural capacity. Therefore, this region was not expected to undergo any distress that could potentially affect the performance of the specimen until shear failure in any of the test spans. The bending moments and shear force diagrams presented in Figure 5-16 represent the conditions that occur under small externally applied forces. At ultimate conditions,

the large concentrated forces dominate the shear force and bending moment diagrams, and the effects of self-weight are hardly visible.

The girders were extensively instrumented to monitor loads, displacements, strains, and strand slip over the course of testing. The load for each test was monitored using four 500-kip load cells that were placed in the support fixtures (Figure 5-17). These load cells were also used during the initial placement of the specimens and the test frame components to measure self-weight and frame weight. Linear potentiometers were placed on both sides of the specimen at the supports and directly under the load points to measure the vertical displacements under the load points and at the supports. Stress development in the transverse reinforcement was monitored via strain gauges installed on the stirrups during specimen fabrication. For Tx46-I and Tx46-II, 15 stirrups were monitored on each end, over a distance of 50.5 in. from the end faces of the specimens. The number of stirrups instrumented within each end-region of Tx46-III, Tx46-IV, and Tx46-V was increased to 20, increasing the monitored region of the specimens to a distance of 104.5 in. from the end faces. For the Tx70 specimens, 21 stirrups were monitored on each end, over a distance of 102.5 in. from each end face. Displacement transducers were installed at the ends of the specimens to measure the free strand slip, as shown in Figure 5-19. Three strands were monitored for end slip at both ends of Tx46-I and Tx46-II. In subsequent specimens, these measurements were made on five or six strands at each girder end.



**Figure 5-19- Displacement transducers used for measuring strand slip**

Loading was applied in a series of predefined stages, each corresponding to an increase in the load level that was smaller than one-tenth of the nominal capacity of the specimen, as estimated using the AASHTO LRFD Bridge Design Specifications (AASHTO, 2016). As a result, typical load-stage increments of 100 kips or smaller were used. Each stage of loading was applied in a continuous, quasi-static manner, at a rate of 500 lb per second or less. Upon reaching each of the predefined load levels, the condition of the specimen was visually inspected and documented. Once the specimen sustained significant damage, visual inspection efforts were suspended, and the specimen was subsequently loaded to failure while simultaneously recording data from instrumentation and video.

## **5.5 Summary**

Seven full-scale Tx-girder specimens employing 0.7-in. diameter strands on a 2- by 2-in. grid were designed, fabricated, and tested to investigate their end-region behavior at the time of prestress transfer and their failure mechanisms and load-carrying capacities under shear-critical loading. The specimens were extensively instrumented to provide a detailed picture of transfer length, stresses within reinforcement, prestress losses, strand slip, and load-deflection behavior. Moreover, each specimen was carefully examined for cracking after prestress transfer and under applied loads. The results of the experimental procedures described in this chapter are presented and discussed in Chapter 6.



# CHAPTER 6

## Experimental Results and Discussion

### 6.1 Overview

As described in Chapter 5, seven full-scale Tx-girders were fabricated and tested to determine their end-region behavior at the time of prestress transfer and their failure mechanisms and load-carrying capacities under shear-critical loading. Therefore, the experimental program consisted of 14 end-region tests and seven shear tests. Among the specimens, Tx46-III was released at an undesirably low concrete compressive strength. As a result, this specimen was not deemed representative of the conditions of pretensioned girders in the field. Observations and measurements from all specimens except Tx46-III are presented and discussed in this chapter.

### 6.2 Measured Mechanical Properties

Table 6-1 and Table 6-2 present a summary of the measured mechanical properties of the specimens over the course of the experimental program. The properties reported in these tables were all measured at FSEL from a minimum of three samples through ASTM-compliant testing procedures. As can be seen in Table 6-1, the measured compressive strength of concrete at the time of prestress transfer was slightly greater than that assumed in design for most specimens.

**Table 6-1- Measured mechanical properties of concrete**

Property	Girder concrete							Deck concrete	
	$f'_{ci}$ , ksi	$f_{cim}$ , ksi	$f_{cm}$ , ksi	$E_{cim}$ , ksi	$E_{cm}$ , ksi	$f_{tm}$ , ksi	$f_{rm}$ , ksi	$f_{cm}$ , ksi	$E_{cm}$ , ksi
Test method	N/A	ASTM C39 (2014)		ASTM C469 (2014)		ASTM C496 (2011)	ASTM C78 (2015)	ASTM C39 (2014)	ASTM C469 (2014)
Tx46-I	5.5	5.7	7.6	N/M	4,910	0.63	0.83	10.7	6,930
Tx46-II	5.2	5.2	6.9	4,940	5,420	0.56	0.89	7.9	5,910
Tx70-I	5.5	6.5	10.7	4,490	6,100	0.86	1.07	7.9	5,970
Tx70-II	7.8	8.3	12.7	4,900	6,020	0.97	N/M	9.2	5,890
Tx46-IV	8.0	8.4	13.9	5,660	6,040	0.86	N/M	9.4	6,080
Tx46-V	8.0	8.3	14.5	5,820	7,520	0.90	1.54	7.9	6,000

Note: N/M = Not measured; N/A = Not applicable.

$f'_{ci}$  = Compressive release strength assumed in design;  $f_{cim}$  = Measured compressive release strength based on match-cured specimens;  $E_{cim}$  = Measured modulus of elasticity of concrete at the time of release, based on match-cured specimens;  $f_{cm}$  = Measured compressive strength on the day of shear testing, based on wet-cured specimens;  $E_{cm}$  = Measured modulus of elasticity of concrete on the day of shear test, based on wet-cured specimens;  $f_{tm}$  = Measured splitting tensile strength of concrete on the day of shear test, based on wet-cured specimens;  $f_{rm}$  = Measured modulus of rupture on the day of shear test, based on wet-cured specimens.

The mechanical properties of the 0.7-in. diameter strands used within the specimens were also measured according to ASTM A1061 (2016). As a result, yield strength, ultimate strength,

and modulus of elasticity of the prestressing steel were determined as 232.0 ksi, 276.1 ksi, and 27,810 ksi, respectively.

**Table 6-2- Measured mechanical properties of the mild steel used for the fabrication of the specimens**

Property	R-bars		S-bars (Live end) and P-bars		S-bars (Dead end)		C-, T-, and Deck bars		U-bars	
	$f_{ym}$ , ksi	$f_{um}$ , ksi	$f_{ym}$ , ksi	$f_{um}$ , ksi	$f_{ym}$ , ksi	$f_{um}$ , ksi	$f_{ym}$ , ksi	$f_{um}$ , ksi	$f_{ym}$ , ksi	$f_{um}$ , ksi
Test method	ASTM A370 (2016)									
Tx46-I	60.7	99.3	71.8	115.5	71.8	115.5	60.7	99.3	74.0	114.7
Tx46-II										
Tx70-I	72.2	111.6	69.6	108.8	69.6	108.8	72.2	111.6	67.7	106.4
Tx70-II										
Tx46-IV	63.1	100.5	64.7	105.4	75.5	108.5	62.0	101.9	62.9	100.8
Tx46-V	64.1	103.9	67.4	111.0	67.4	111.0	62.0	103.0	62.2	101.5

Note:  $f_{ym}$ ,  $f_{um}$  = Measured yield and ultimate strengths of mild-steel reinforcement.

### 6.3 End-Region Behavior

The following subsections present the observations and measurements obtained from the end-regions of the specimens at the time of prestress transfer and over time, before the specimens were subjected to shear-critical loading.

#### 6.3.1 Transfer Length

The transfer length was determined by comparing the data obtained from the strain gauges before the release operation with those obtained immediately after release and 24 hours after release. To determine the transfer lengths, a modified version of the 95 percent average maximum strain (AMS) method introduced by Russell and Burns (1993) was used. With the increase in distance from the end face, the strains gradually increased from zero until reaching a plateau. For each end of each specimen, the strains in the plateaued region were averaged to determine the average maximum strain. The transfer length is defined as the distance at which the strain-versus-distance plot intersects the 95 percent of AMS. An example of determining the transfer length through this method is shown in Figure 6-1.

The strains used in this procedure were obtained from strain gauges that were installed on helical wires, which are linearly correlated to the average axial strain in the strand (O'Callaghan, 2007). Therefore, using these strains as opposed to the average axial strain in the strand is not expected to affect the transfer lengths.

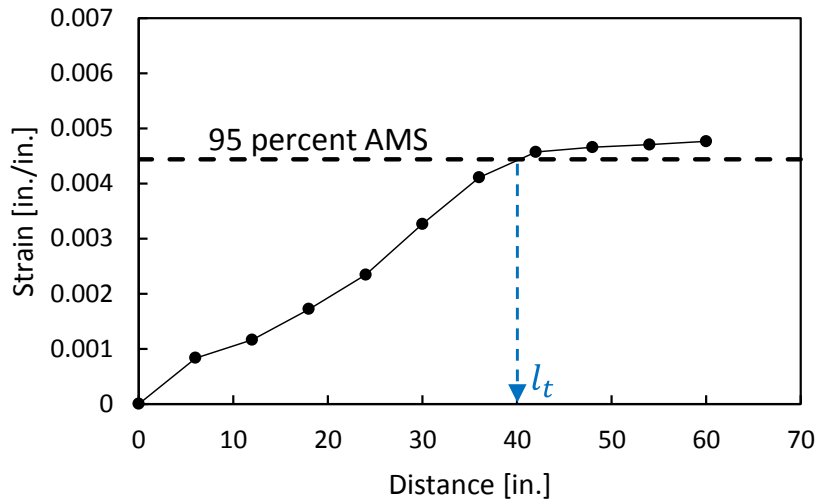


**Figure 6-1- Determining the transfer length based on strain gauge data**

Table 6-3 provides a summary of the distances corresponding to the start of the plateau region and to the 95 percent AMS at dead and live ends of each specimen. Since some of the strain gauges did not function properly, determining the transfer length was not possible for all instrumented strands. For each end-region, the number of strands from which a reliable transfer length could be determined is shown in the table. In this table,  $l_{plateau}$  values represent the distances at which the strains reached the plateau whereas  $l_t$  values are the transfer lengths determined based on the 95 percent AMS method.

In general, the transfer lengths obtained from live and dead ends of each specimen were similar. This observation comes as no surprise because the gradual release of strands by hydraulic rams is expected to result in little difference between the live and dead ends of the specimens. Immediately after release, the shortest transfer length was 29 in., which was observed in Tx46-II and Tx70-I. The longest transfer length at this time was 47 in., which was found at the dead end of Tx46-I.

**Table 6-3- Transfer lengths determined for the specimens based on strain gauge data**

			Live End			Dead End		
			$l_{plateau}$ , in.	$l_t$ , in.	n	$l_{plateau}$ , in.	$l_t$ , in.	n
Tx46-I	At release	Max.	42	40	1	48	47	4
		Min.	42	40		42	40	
	24-Hour	Max.	48	45	1	48	46	3
		Min.	48	45		42	41	
Tx46-II	At release	Max.	42	35	4	48	41	4
		Min.	36	29		36	29	
	24-Hour	Max.	54	52	3	54	48	3
		Min.	48	44		48	45	
Tx70-I	At release	Max.	42	39	4	42	41	3
		Min.	36	29		36	34	
	24-Hour	Max.	48	46	3	54	51	2
		Min.	36	31		36	35	
Tx70-II	At release	Max.	48	43	4	42	40	3
		Min.	36	34		36	34	
	24-Hour	Max.	48	45	2	48	45	3
		Min.	48	45		48	41	
Tx46-IV	At release	Max.	42	37	4	42	40	4
		Min.	36	33		36	33	
	24-Hour	Max.	54	47	4	54	51	4
		Min.	48	36		36	35	
Tx46-V	At release	Max.	42	39	4	48	43	4
		Min.	36	34		36	34	
	24-Hour	Max.	48	46	4	54	48	4
		Min.	36	34		48	40	
Summary*	At release	Max.	48	43	21	48	47	22
		Min.	36	29		36	29	
	24-Hour	Max.	54	52	17	54	51	19
		Min.	36	31		36	35	

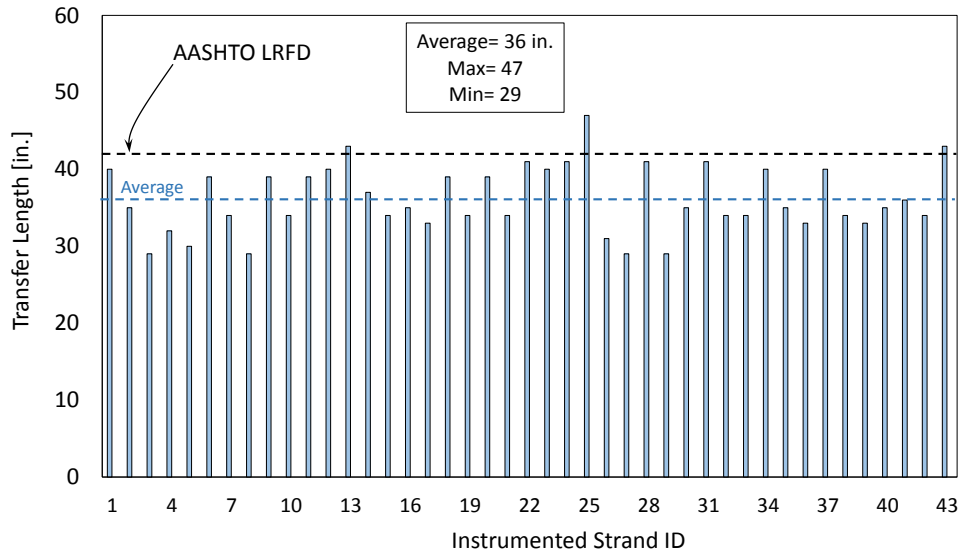
Note: n = number of strands used for determining the transfer length.

\* Due to the low release strength of Specimen Tx46-III, the data from this specimen are not included.

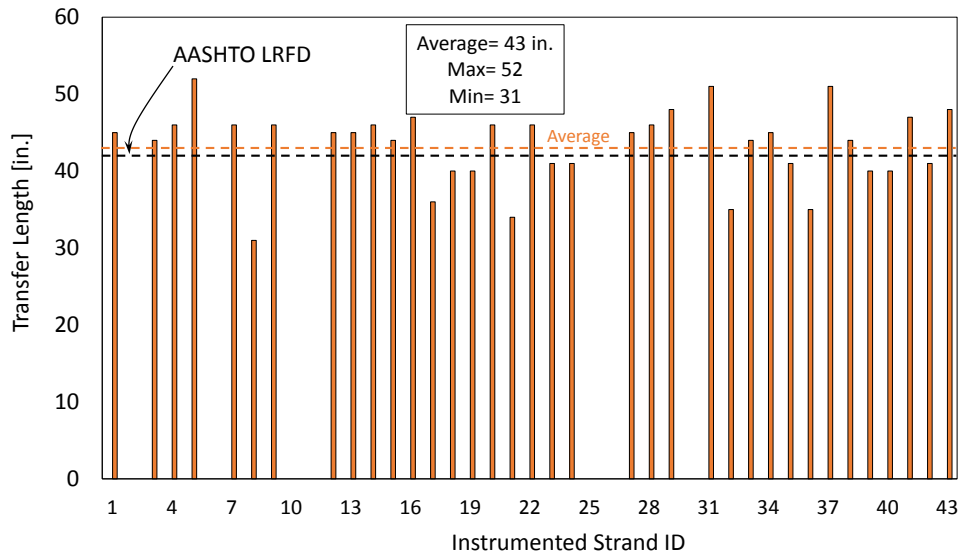
Table 6-3 also shows a noticeable increase in the transfer lengths measured within the first 24 hours after release, which is consistent with the known effect of time-dependent deformations of concrete on transfer length (Barnes et al., 2003). At 24 hours after release, the shortest and longest transfer lengths were recorded as 31 in. and 52 in., obtained from the live end of Tx70-I and the live end of Tx46-II, respectively.

Figure 6-2 provides a comparison between the transfer lengths determined for instrumented strands and the estimate obtained from AASHTO LRFD. In developing this figure, the data obtained from dead and live ends of the specimens were combined. According to AASHTO LRFD specifications (2016), the transfer length is estimated as 60 times the diameter of the strands, which

yields 42 in. for 0.7-in. diameter strands. It can be seen that the transfer lengths immediately after release were generally shorter than that predicted by AASHTO LRFD provisions. However, after 24 hours, the average transfer length slightly exceeded 42 in., and several instrumented strands showed transfer lengths greater than the estimate by AASHTO LRFD. A greater increase in the transfer lengths is anticipated for all specimens over time. However, monitoring the growth in transfer length after 24 hours was not considered in this study.



(a) Transfer lengths immediately after release



(b) Transfer lengths 24 hours after release

**Figure 6-2- Transfer lengths from individual strands in comparison with the value estimated by AASHTO LRFD**

The use of strain gauges in this study is believed to provide a more precise picture of stress changes in the strands compared to the mechanical measurements of surface strains. However, the presence of strain gauges could also potentially have a negative effect on the prestress transfer

within the instrumented strands. Thus, the transfer lengths from strands instrumented at 6-in. and 12-in. intervals were compared. The results showed that the transfer lengths from strands with 6-in. spacing were consistently greater than those with gauges placed at 12-in. spacing. However, the difference was generally limited to 6 in., which is the resolution of the estimated transfer lengths.

### 6.3.2 End-Region Cracking

All specimens were carefully inspected for cracks immediately after prestress transfer. Moreover, a final survey of the specimens for cracks was conducted at least 28 days after the specimen was cast. For Tx70-II, Tx46-IV, and Tx46-V, in addition to the initial and final measurements, cracks were also measured and documented every week after prestress transfer until the age of 28 days. The following paragraphs provide a description of the observed cracking patterns within the specimens, which is divided into two categories: specimens with standard end-region detailing (Tx46-I through Tx70-II), and specimens with modified end-region detailing (Tx46-IV and Tx46-V).

In the figures presented in this section, a series of small circles is used to present the measured width of the cracks at each location at the time of final crack measurements. In the regions where no circles are shown, the crack width was less than or equal to 0.004 in. The widths of the cracks in the first three specimens (Tx46-I, Tx46-II, and Tx70-I) were measured using a crack comparator with a resolution of 0.002 in. [Figure 6-3(a)]. For other specimens, a 7x magnifying loupe was used with reticles that provided a crack measurement resolution of 0.0004 in. [Figure 6-3(b)]. However, for brevity and simplicity, crack widths shown for these specimens are also categorized in a manner similar to that used for the first three specimens.



(a) Magnifying loupe



(b) Crack-comparator gauge

Figure 6-3- Crack-measurement tools

#### 6.3.2.1 Specimens with Standard End-Region Detailing

The measured cracking patterns of the first four specimens, which were fabricated using standard TxDOT details (Texas Department of Transportation, 2015) for end-region reinforcement, are presented in Figure 6-4 through Figure 6-7. As visible these figures, the specimens constructed with a conventional strand pattern revealed spalling cracks in their end-regions. As the prestressing force increased near the bottom fiber of these specimens, the spalling cracks extended further into the beam. Tx46-II, which was designed to accommodate the greatest prestressing force with low concrete release strength, showed bursting cracks that were primarily limited to the bottom flange.

<b>Crack width</b>	<ul style="list-style-type: none"> <li>○ 0.004 in.</li> <li>● 0.006 in.</li> <li>● 0.008 in.</li> </ul>
<b>Time crack was measured</b>	<ul style="list-style-type: none"> <li>— At release</li> <li>— 131 days</li> </ul>

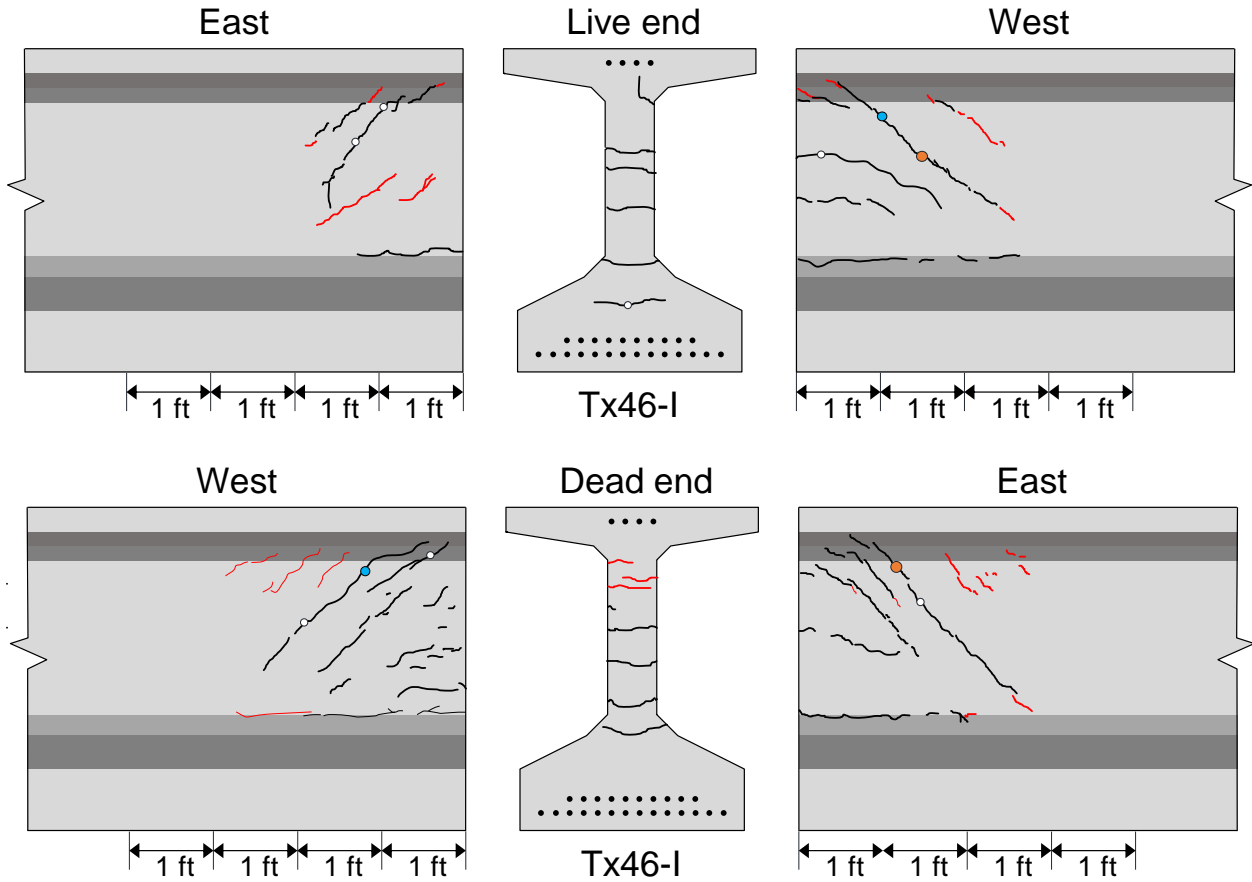


Figure 6-4- Observed cracking patterns in Tx46-I

<b>Crack width</b>	<ul style="list-style-type: none"> <li>○ 0.004 in.</li> <li>● 0.006 in.</li> <li>● 0.008 in.</li> </ul>
<b>Time crack was measured</b>	<ul style="list-style-type: none"> <li>— At release</li> <li>— 40 days</li> </ul>

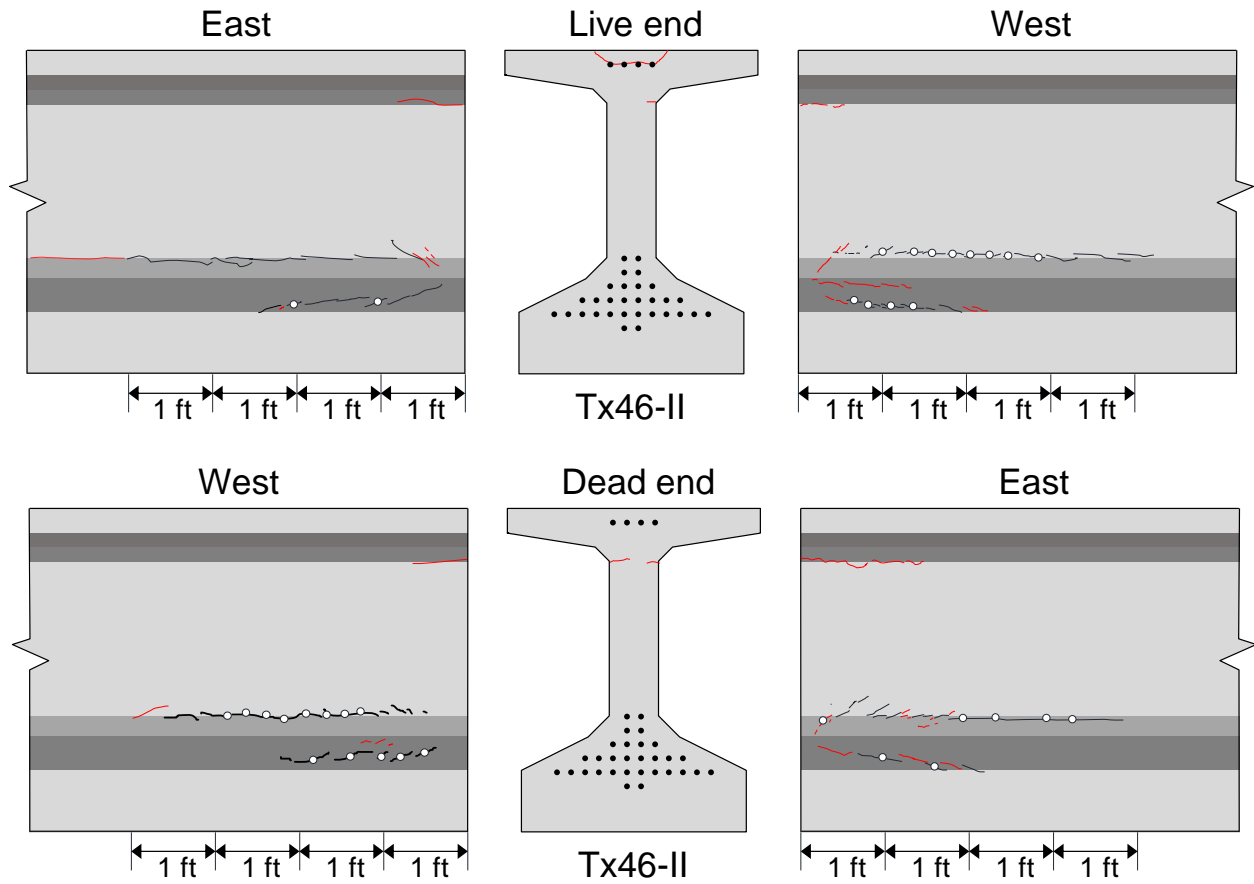


Figure 6-5- Observed cracking patterns in Tx46-II

<b>Crack width</b>	○ 0.004 in.	<b>Time crack was measured</b>	— At release
	● 0.006 in.		— 41 days
	● 0.008 in.		

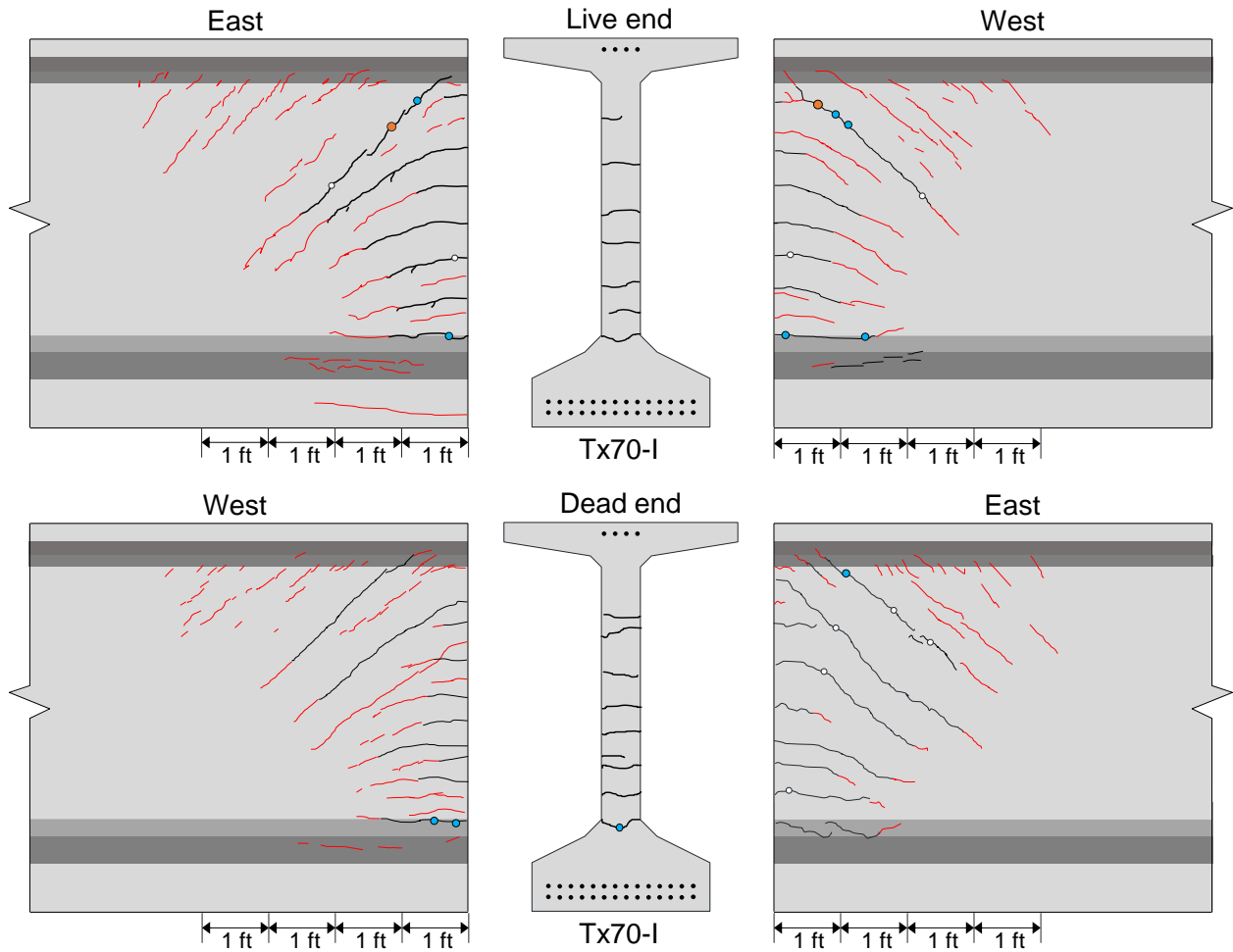
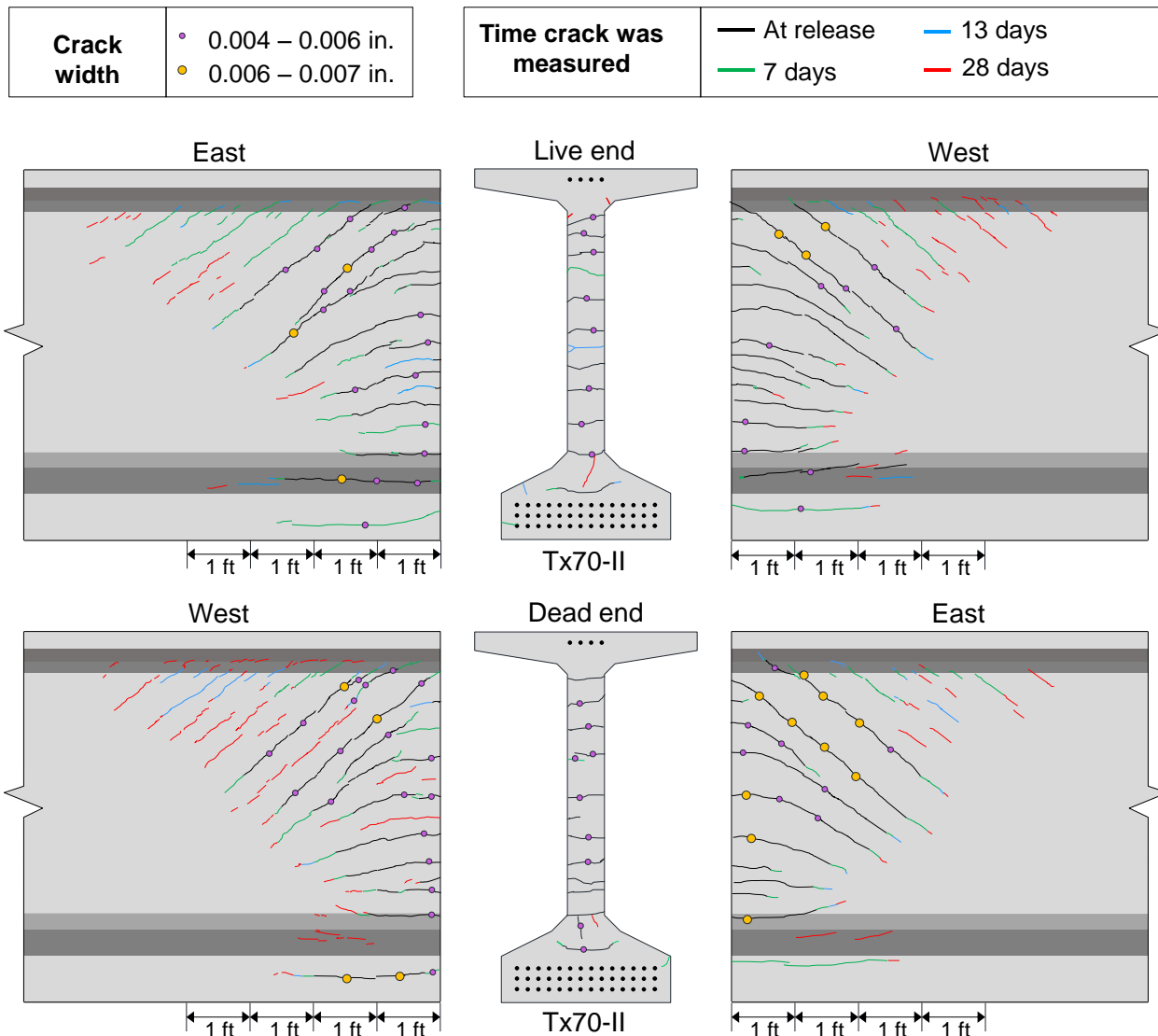


Figure 6-6- Observed cracking patterns in Tx70-I



**Figure 6-7- Observed cracking patterns in Tx70-II**

All specimens showed near-continuous cracking at the interface between the web and the bottom flange within the end-region. In all specimens except Tx46-II, such cracking was also observed through the width of the web at the end faces. In Tx70-II, cracks parallel to the outermost strands, which are indicative of bond-related damage, were also observed.

The maximum crack width recorded within the first four specimens was 0.008 in. This crack width was observed immediately after prestress transfer in an isolated length of a few spalling cracks within the web of Tx46-I and Tx70-I. Note that the crack widths in both of these specimens were recorded with a resolution of 0.002 in. The maximum crack width in Tx46-II and Tx70-II were recorded as 0.004 in. and 0.007 in., respectively. Note that in Tx70-II, crack widths between 0.006 and 0.007 in. were measured at several locations. The greatest crack width was observed in the dead end of all specimens except Tx70-I. However, the overall difference in patterns or widths of cracks between the two ends was not significant.

All specimens demonstrated noticeable changes in their cracking conditions over time. These changes included growth in the length and width of cracks that were detected immediately

after prestress transfer, as well as the development of new cracks, especially in the Tx70 specimens. However, in most end-regions, the widest crack did not demonstrate noticeable growth between the time of release and the time of final measurement. A summary of the maximum crack widths in the specimens is shown in Figure 6-8.

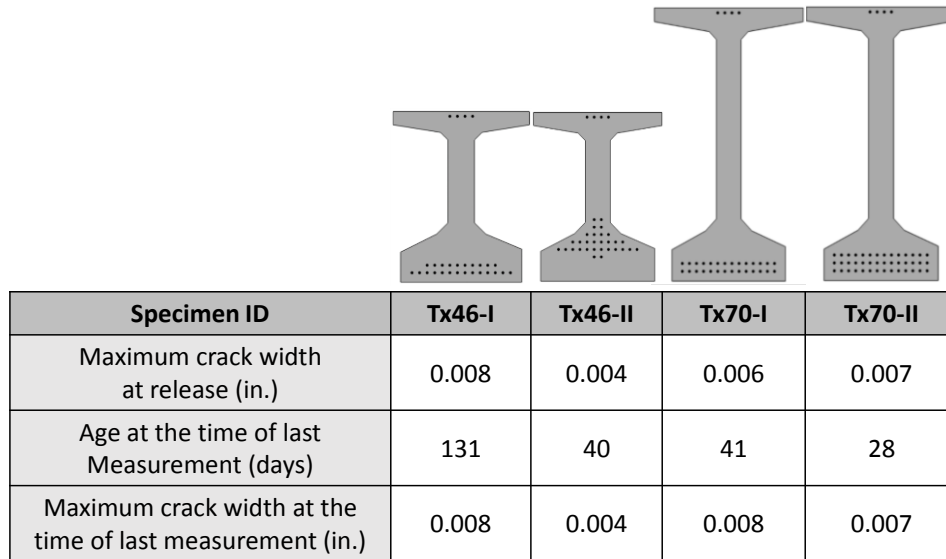


**Figure 6-8- Maximum crack widths in specimens with standard detailing for end-region reinforcement**

The research team assessed the observed cracking patterns in the first four specimens to evaluate the need to modifying the end-region detailing in Tx-girders to incorporate the larger-diameter 0.7-in. diameter strands on the 2- by 2-in. grid. The observed cracking within the end-regions of the specimens did not reveal patterns that were noticeably different from those observed in Tx-girders fabricated using smaller-diameter strands. Therefore, the use of 0.7-in. prestressing strands on a 2- by 2-in. grid does not seem to trigger unusual end-region damage in Tx-girders. However, the widths of some of the spalling cracks in the specimens appeared to be slightly greater than that commonly observed in girders employing smaller-diameter strands.

There is no globally accepted limit for the permissible crack width within the end-regions of pretensioned concrete elements. To evaluate the performance of the first four specimens in this test program, three references were used, as follows:

- 1) ACI 224R-01 (2001), a report by the ACI committee on concrete cracking, provides general guidelines on acceptable crack widths in reinforced concrete flexural elements under service loads. According to these guidelines, the “reasonable” crack width is 0.007 in. for elements exposed to deicing chemicals and 0.012 in. for elements exposed to humidity, moist air, and soil. Table 4.1 in these guidelines notes that a portion of the cracks in the structure might have widths that exceed these limits. As presented above, no cracks within the end-regions of the girders exceeded the limit recognized by ACI 224R as tolerable for humidity and soil exposure. In Tx46-I and Tx70-I, isolated cracks in excess of 0.007 in. were observed. However, as noted above, a few cracks with widths greater than the listed limits are considered acceptable. Therefore, according to ACI 224R, all girders comprising this test program met the conditions for use in exposure to deicing chemicals.

2) NCHRP Report 654 (2010), a comprehensive study on the acceptance criteria for the width of end-region cracks by Tadros, Badie, and Tuan, recommends that no action be taken for any end-region cracks that are 0.012 in. in width or less. The observed crack widths in this study did not exceed the recommended limit. Therefore, no repair is required according to these guidelines.

3) TxDOT specifications for construction and maintenance of highways, streets, and bridges (2014), require corrective action if cracks in excess of 0.005 in. form within the end-regions of I-girders. The specimens except Tx46-II did not satisfy this strict requirement.

After evaluating a few alternatives using validated FE models, which is discussed in Chapter 7, the designs for Tx46-IV and Tx46-V were developed with the objective of reducing the width of end-region cracks, preferably below the 0.005-in. limit mentioned above.

#### *6.3.2.1 Specimens with Modified End-Region Detailing*

As described in Chapter 5, the only modification made to the end-region detailing in Tx46-IV was changing the S-bars at one end from No. 6 bars to No. 8 bars. This change was made to the dead end of this specimen, and the detailing in the live end remained identical to that in standard drawings. In Tx46-V, a series of horizontal No. 4 bars (W-bars and WT-bars) were added to the web and the top flange at the dead end. Moreover, cap bars were added to the bottom flange confinement at both ends of this specimen.

The measured cracking patterns in Tx46-IV and Tx46-V are shown in Figure 6-9 and Figure 6-10, respectively. In general, the end-region cracking was not noticeably affected by the modifications to end-region detailing in any of the specimens. Immediately after prestress transfer, a maximum crack width of 0.005 in. was observed at both dead and live ends of Tx46-IV. At an age of 63 days, when the last measurements were taken from this specimen prior to shear testing, the maximum crack width at both ends was 0.007 in. Therefore, the crack patterns and widths showed no benefits from the use of No. 8 S-bars instead of No. 6 bars in this specimen. Observations from Tx46-V showed that horizontal bars were not effective in controlling the end-region cracks either. Despite the significant number of horizontal bars that were added to the dead end of this specimen, the widths of end-region cracks were similar at both ends, 0.005 in. immediately after release and 0.006 in. at an age of 29 days.

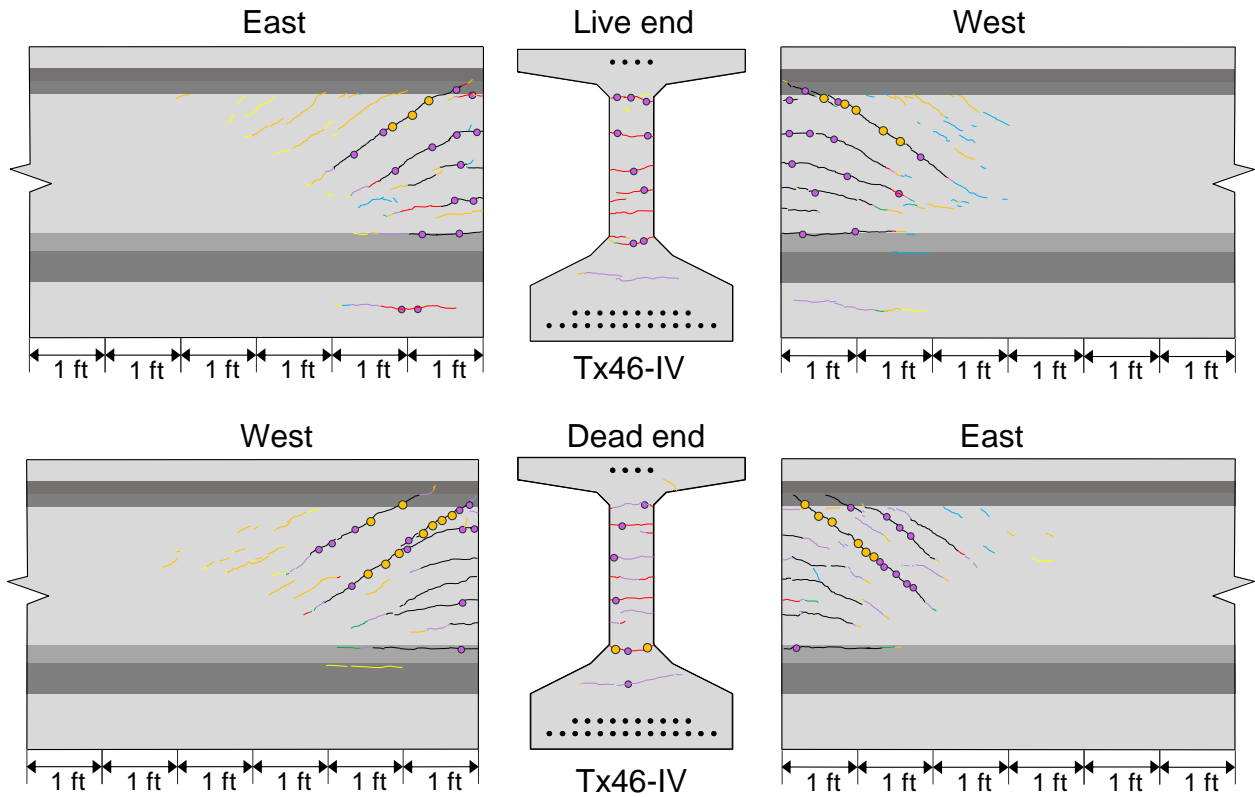
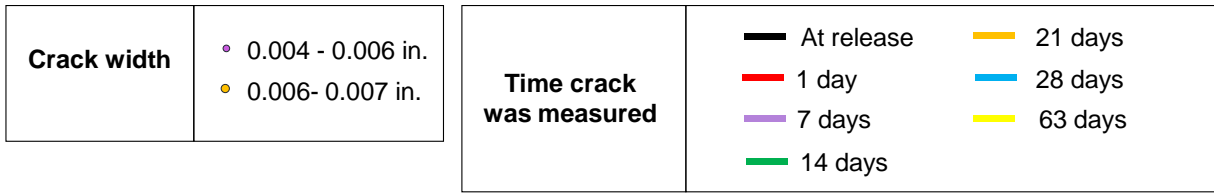


Figure 6-9- Observed cracking patterns in Tx46-IV

<b>Crack width</b>	• 0.004 – 0.006 in.
	• 0.006 – 0.007 in.

<b>Time crack was measured</b>	
— At release	— 21 days
— 1 day	— 29 days
— 7 days	
— 14 days	

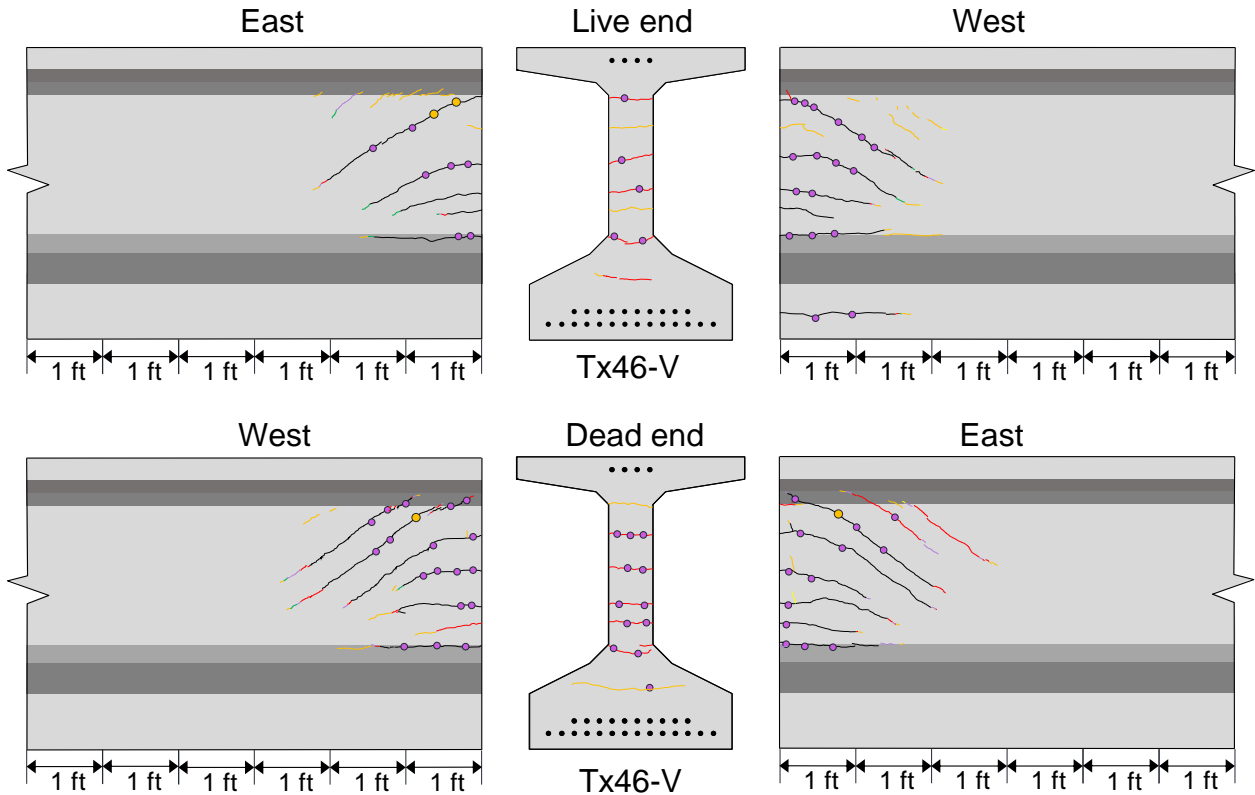


Figure 6-10- Observed cracking patterns in Tx46-V

### 6.3.3 End-Region Stresses

Figure 6-11 provides a graphical presentation of the stresses inferred from strain measurements in the transverse reinforcement of the first four specimens. As can be seen in this figure, among the specimens with conventional strand patterns, the increase in the transverse reinforcement stress levels is correlated with the increase in the total prestress force. The maximum stress level in the specimens was 26 ksi, which was observed in Tx70-II. The greatest stresses in all specimens were observed at the interface between the web and the bottom flange, mostly due to the change in geometry and the flow of the stresses from the bottom flange into the web. However, the stresses also remained large at the centroids of the specimens with conventional strand patterns. In Tx46 II, which was designed in an effort to represent critical bursting conditions, smaller stresses were detected compared to Tx46-I despite a greater prestressing force. Large stresses were observed only at the interface between the web and the bottom flange in this specimen.

In the specimens constructed with conventional strand patterns, the stresses in transverse reinforcement were found to diminish very quickly with distance from the end face of the specimen. Stresses greater than 15 ksi were observed only in the first three stirrups, which were located within a distance of 8.5 in. from the end face of the girder. In any bridge application, this distance is normally in the overhang segment, i.e. outside the main span. Therefore, these stresses are not expected to affect the performance of the girder under in-service loading conditions. Typical detailing used for Tx-girders includes a 9-in. overhang segment, and an 8-in. support width for Tx46 and a 9-in. support width for Tx70 girders. Using this detailing, the first four stirrups in the girders are not expected to be mobilized under external loads. The stresses in other stirrups were generally less than 10 ksi.

Tx46-II exhibited transverse stresses that extended over a distance of 3 ft into the beam. This distance was considerably greater than that in the other specimens. The stresses were primarily concentrated along the web-bottom flange interface, and only small stresses were detected at the centroid depth and at the interface between the web and the top flange. The maximum stresses were not observed in the first few stirrups, but in the stirrups that were farther away from the end face of the girder. Large stresses within this region are known to increase the likelihood of horizontal shear distress (Hovell et al., 2011). However, the magnitudes of these stresses were generally limited to 10 ksi, which was small compared to stresses observed in the other three specimens. These observations are consistent with the results obtained by O'Callaghan (2007) from Tx-girders that employed 0.6-in. diameter strands on a layout resembling that of Tx46-II.

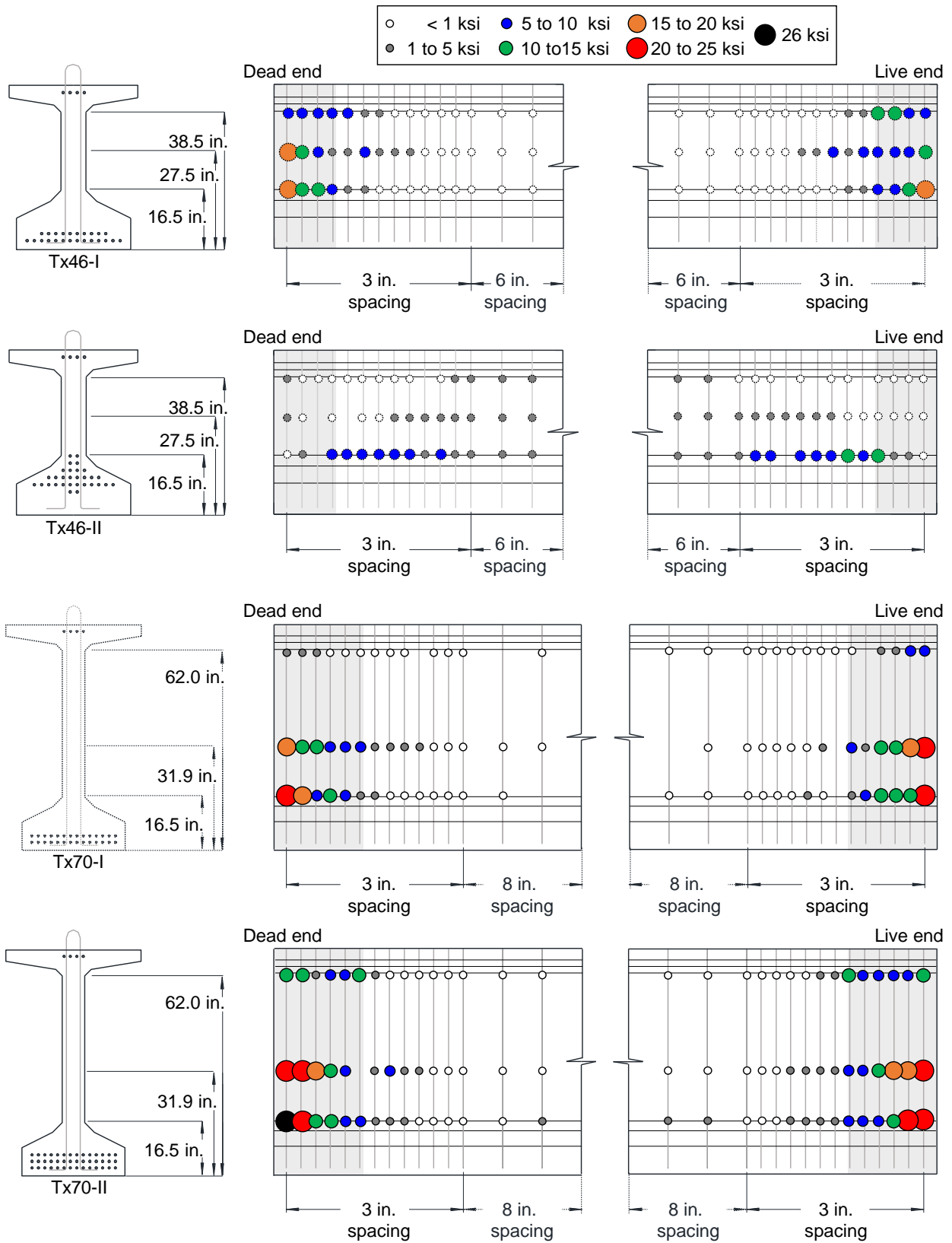


Figure 6-11- End-region stresses in the first four specimens

Figure 6-12 shows the end-region stresses in specimens with modified end-region detailing. As can be seen in this figure, patterns for the distribution of end-region stresses in these two specimens were generally similar to those in the other specimens with conventional strand patterns. Stresses detected in the dead end of Tx46-IV were smaller than those in the live end. This was expected because of the greater area of the No. 8 S-bars used at the dead end.

In Tx46-V, the strain gauge closest to the live end of the girder at the web-flange interface malfunctioned, due to which the maximum stress at the live end could not be estimated. However, it is evident from other strain gauges that horizontal end-region reinforcement does not help reduce the magnitude of end-region stresses in this specimen.

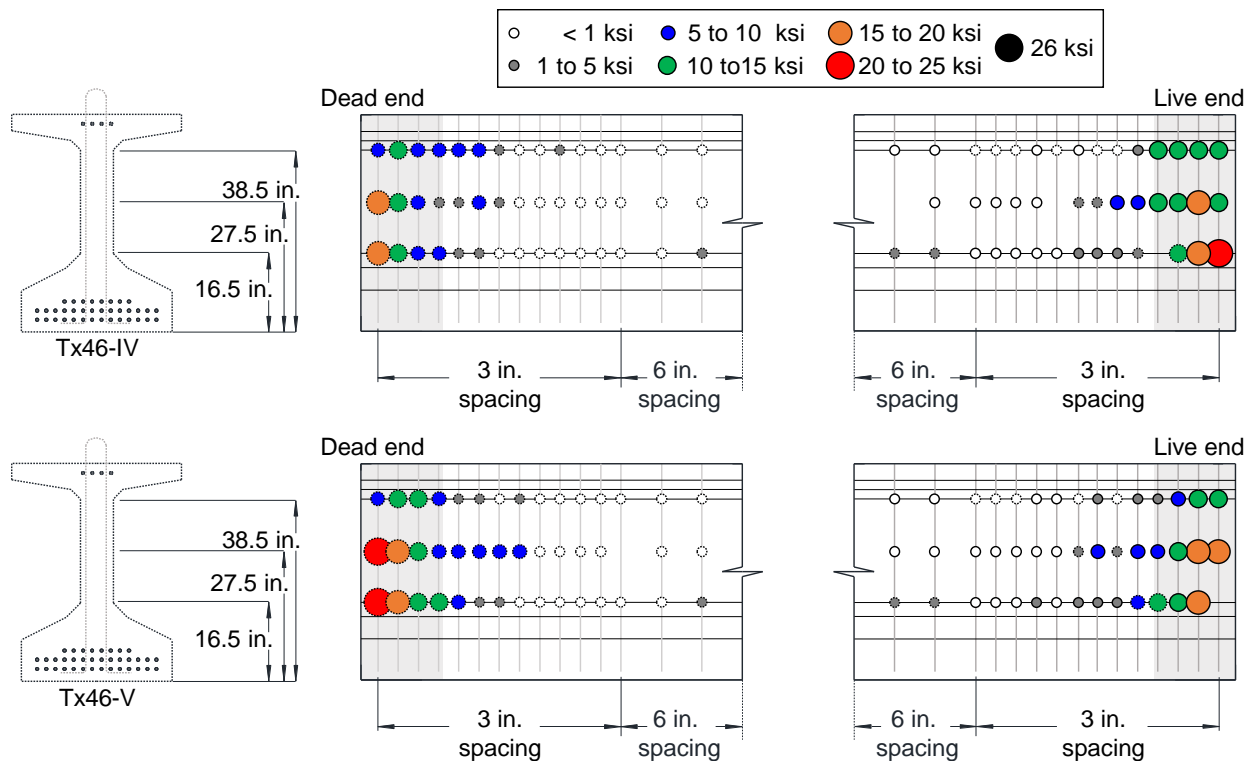


Figure 6-12- End-region stresses in specimens with modified end-region detailing

According to section 5.10.10 in AASHTO LRFD provisions, the splitting resistance of end-regions in pretensioned concrete girders,  $P_r$ , is equal to  $f_s A_{s,h/4}$ , where  $f_s$  is the stress in steel, not to exceed 20 ksi;  $A_{s,h/4}$  is the total area of reinforcement within a distance of  $h/4$  from the end of the girder; and  $h$  is the height of the girder. AASHTO LRFD provisions require the splitting resistance to be greater than 4 percent of the total prestressing force at transfer.

In this testing program, the  $h/4$  distance is equal to 11.5 in. and 17.5 in. for the Tx46 and the Tx70 specimens, respectively. On the basis of the standard details for Tx-girders, the steel required to provide the splitting resistance is limited to the first four pairs of R- and S-bars in the Tx46 specimens and the first six pairs of R- and S-bars in the Tx70 specimens. Observations from Figure 6-11 and Figure 6-12 support this selection. In specimens with conventional strand patterns, noticeable stresses were observed in the reinforcement located within the  $h/4$  region.

Figure 6-11 and Figure 6-12 show that maximum detected stresses in the Tx70 specimens, Tx46-IV, and Tx46-V exceeded 20 ksi. However, since the stresses diminished very quickly with distance from the end face, the average stresses within the bars located in the first  $h/4$  distance from the end face was less than 20 ksi, and therefore, all girders comprising this test program effectively met the stress limit defined in AASHTO LRFD. As shown in Table 6-4, the use of closely spaced R- and S-bars within the end-region of Tx-girders results in a splitting resistance that ranges between 4.3 and 8.6 percent of the initial prestressing force in each specimen.

**Table 6-4- Splitting resistance in the specimens according to AASHTO LRFD (2016) compared to initial prestressing force**

Specimen	$A_{s,h/4}$ , in. <sup>2</sup>	$P_r = f_s A_{s,h/4}$ , kips	$P_i$ , kips	$P_r/P_i$ , %
Tx46-I	5.12	102.4	1,614	6.3
Tx46-II	5.12	102.4	2,024	5.1
Tx70-I	7.68	153.6	1,796	8.6
Tx70-II	7.68	153.6	2,738	5.6
Tx46-IV (D)	7.92	158.4	2,343	6.7
Tx46-IV (L)	5.12	102.4	2,343	4.3
Tx46-V	5.12	102.4	2,343	4.3

Note:  $f_s$  is taken as 20 ksi.

Figure 6-13 includes the transverse forces developed within the distance of  $h/4$  from the end face of the girders investigated in the current study and those from a database of bursting and spalling stresses developed by Dunkman (2009). This database includes the results from eight inverted-tee specimens, four U-girders, and 53 I-girders fabricated with 0.5- or 0.6-in. diameter strands. Note that the live end of Tx46-V is not included in the figure due to the malfunctioning strain gauge. As can be seen in the figure, the transverse force developed over the distance of  $h/4$  of all previous points in the database was less than or equal to  $0.04 P_i$ , where  $P_i$  is the initial prestress force in the specimen before elastic shortening losses. However, in this study, noticeably greater bursting and spalling forces were observed in all specimens except Tx46-II, which had a nonconventional strand pattern. In both end-regions of Tx70-I, the magnitude of bursting and spalling forces reached up to 5.7 percent of the initial prestressing force.

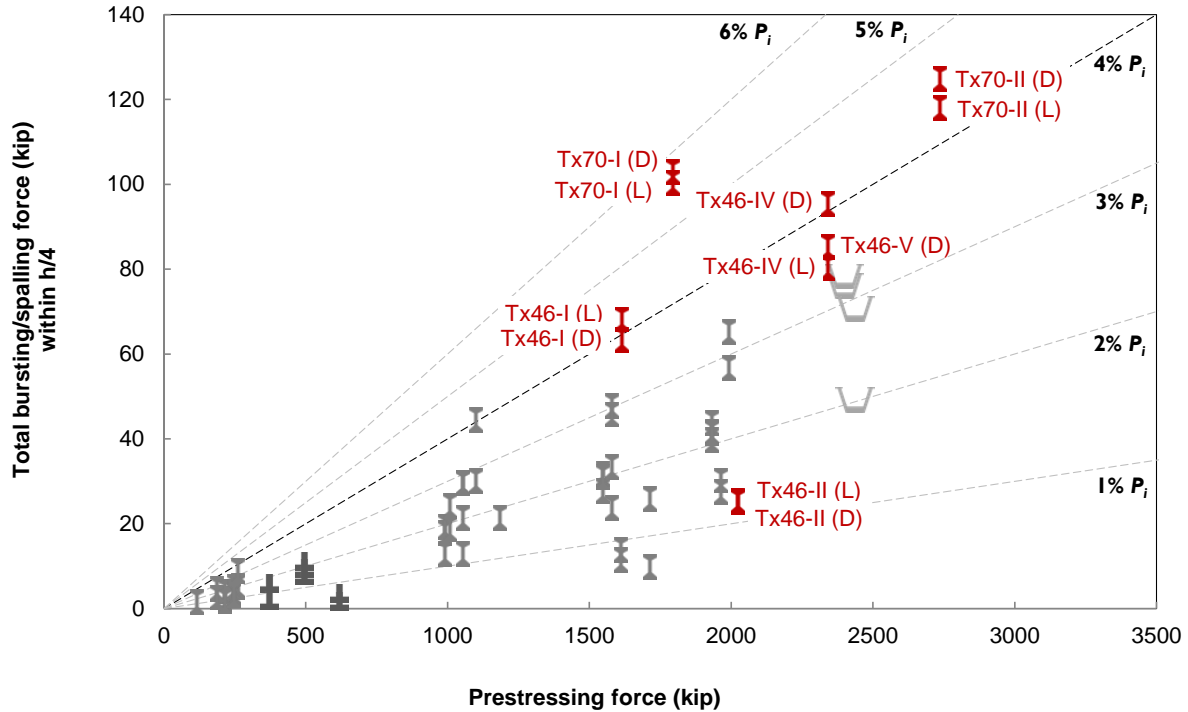


Figure 6-13- Comparison between transverse forces determined in this study and those in the database of bursting and spalling stresses developed by Dunkman (2009). Note: D= Dead end; L=Live end.

## 6.4 Shear-Resisting Performance

Table 6-5 presents a summary of the observations from the shear tests on the specimens. The shear forces reported in this table are calculated at the centerline of the support and include the effect of the applied load as well as self-weight of the specimen and the loading frame. The crack inclination angles reported in this table are obtained by averaging the inclination angle of all visible cracks at the mid-height of the specimen immediately prior to failure. Detailed results of the shear test program are discussed in the following sub-sections. Note that results from Tx46-III are excluded from the discussion due to the low compressive strength of concrete at release.

Table 6-5- Summary of test results

	Tx46-I	Tx46-II	Tx70-I	Tx70-II	Tx46-IV	Tx46-V
Specimen age at the time of shear test, days	131	42	41	28	63	29
Max. crack width before the test, in.	0.008	0.004	0.008	0.007	0.007	0.006
V at diagonal cracking, kips	228	154	304	384	271	295
V at first detected stirrup yielding, kips	455	430	573	688	420	509
$V_{Max}$ , kips	544	467	749	839	656	747
Deflection at load point at $V_{Max}$ , in.	1.58	0.76	0.85	0.66	1.08	1.65
Max. strand slip at $V_{Max}$ , in.	0.108	0.091	0.075	0.119	0.059	0.034
Average inclination angle of cracks, degrees	28	30	29	29	29	27
Failed span	Dead end	Dead end	Dead end	Live end	Dead end	Dead end

Note: The reported  $V$  values are calculated at the centroid of the support.

#### **6.4.1 Conditions of Specimens Prior to Shear Tests**

As discussed previously, all specimens had noticeable cracking within their end-regions due to prestress transfer. Among all specimens except Tx46-III, the maximum width of these cracks prior to subsequent shear testing was approximately 0.008 in. In general, the extent of damage (i.e., the length and width of cracks) was slightly greater at the dead ends of the specimens than at the live ends. The direction of inclined cracks due to prestress transfer was almost perpendicular to that of cracks due to applied load, and therefore, those cracks did not appear to negatively impact the shear-resisting performance of the girder. However, the interface between the web and the bottom flange, which is critical for the transfer of horizontal shear stresses, was found to exhibit nearly continuous longitudinal cracking within the end-regions of the girders.

Stresses as large as 26 ksi were inferred from strain gauge measurements in the stirrups immediately after prestress transfer. However, detected stresses in the stirrups that were located within the clear spans of the specimens were generally limited to approximately 10 ksi. Therefore, the transverse stresses developed due to prestress transfer were not expected to have a significant influence on the contribution of the stirrups to the load-carrying capacity, especially in sections that were critical in resisting shear. Moreover, gradual changes were expected in the transverse stresses within the girder end-regions due to time-dependent effects. However, monitoring such time-dependent effects was not considered. Thus, the stresses reported in the stirrups in this document are based on measurements of strains that were zeroed immediately prior to shear testing.

#### **6.4.2 Load-Deflection and Load-Strand Slip Behavior**

Figure 6-14 and Figure 6-15 show the plots of shear force versus deflection and shear force versus strand slip for the specimens. Similar to Table 6-5, the shear force presented in this figure is calculated at the centerline of the support and includes the self-weight of the specimen and the weight of the loading frame. The deflections shown in the figure are obtained by subtracting the measured rigid-body displacement of the specimen due to support deformations from the measured displacement at the load point. First diagonal cracking and detected yielding of each instrumented stirrup are denoted by purple circles and red diamonds on the load-deflection plot, respectively. In Tx46-I and Tx46-II, instrumented stirrups were all located within a distance of 50.5 in. from the end face. Therefore, the first yielding of the stirrups may have occurred outside of this region, under load levels smaller than those reported for first detected stirrup yielding.

The initial stages of loading on all specimens resulted in minor extension of end-region cracks that were caused by prestress transfer. However, most end-region cracks started to close with further increase in the applied load. In Tx46-I, Tx70-I, and Tx46-IV, horizontal cracks at the interfaces between the web and the top and bottom flanges formed under relatively small loading and continued to grow throughout the test. Diagonal cracking was accompanied by a considerable change in the stiffness of all specimens except Tx46-II, which showed a gradual loss of stiffness throughout the test. After the first diagonal cracking in all specimens, the diagonal cracks grew in length, width, and number until failure. However, the development of new diagonal cracks did not correspond to a sudden change in the stiffness of the specimens. Tx46-I and Tx70-II showed the most and the least softening before failure, respectively. Note that no sign of flexural distress (e.g. flexural cracking near midspan or crushing of the compression block) was observed in any of the specimens prior to failure. Therefore, the observed softening in the specimens might not be related to flexural mechanisms.

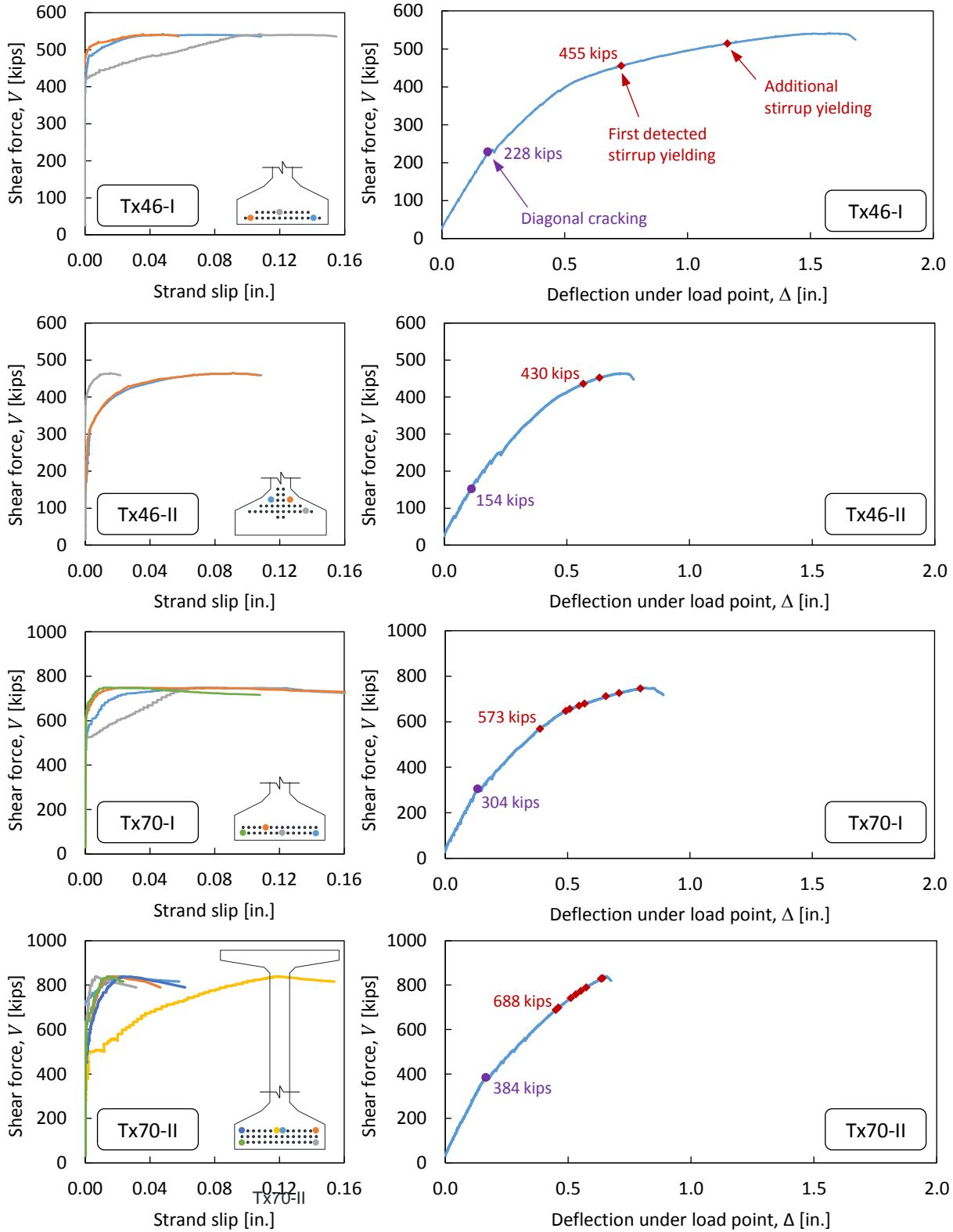
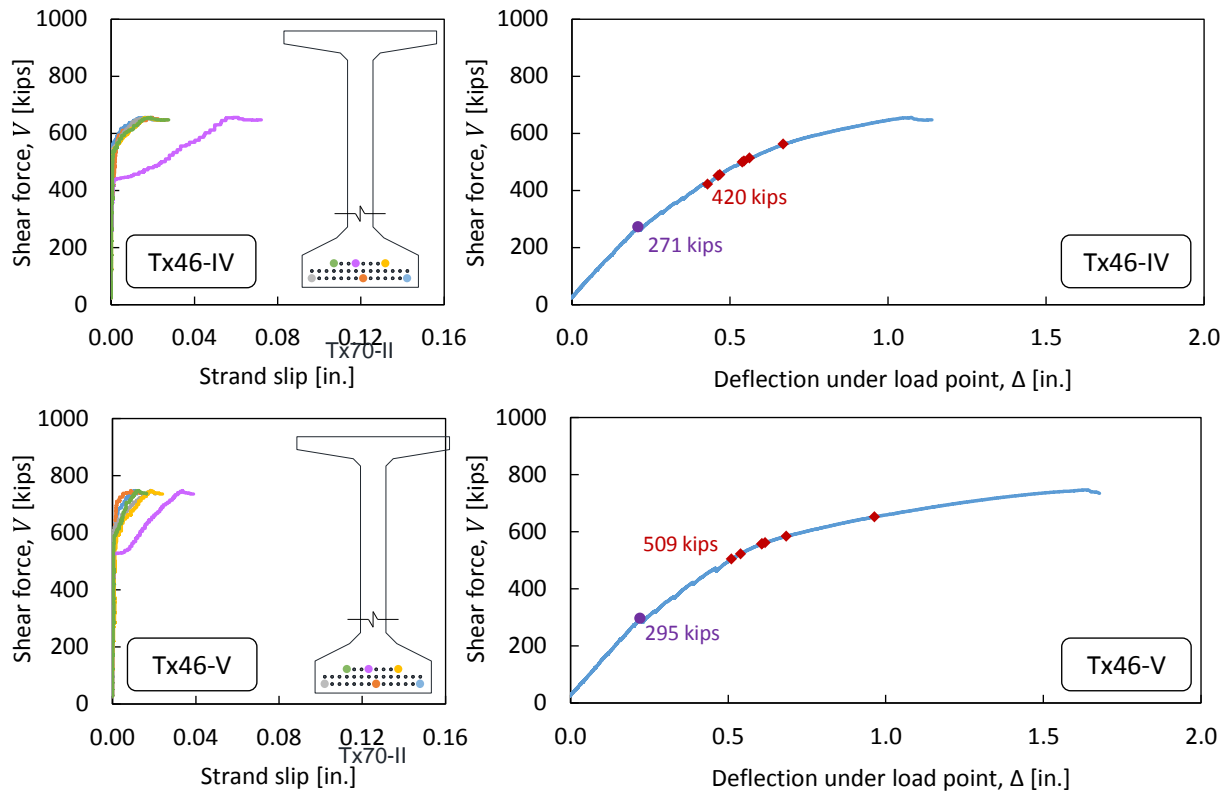


Figure 6-14- Plots of shear force versus deflection and shear force versus strand slip (first four specimens)



**Figure 6-15- Plots of shear force versus deflection and shear force versus strand slip for Tx46-IV and Tx46-V**

Figure 6-14 shows that strand slip in the first four specimens began before the first detected yielding in the stirrups. In Tx46-I, the start of noticeable strand slip coincided with a considerable reduction in the stiffness of the specimen. However, due to the limited number of stirrups that were instrumented in the critical region of this specimen, it is not clear whether strand slip or yielding in the non-instrumented stirrups was the major contributor to the loss of stiffness. In Tx46-IV, the strand slip started at approximately the load that corresponded with the first detected yielding in the stirrups whereas first yielding in Tx46-V was detected before the initiation of strand slip.

Tx70-I, Tx70-II, Tx46-IV, and Tx46-V, which were more extensively instrumented, showed considerable yielding in the stirrups prior to the peak load. In Tx46-II and Tx70-I, the final softening of the specimen appears to be due to a combination of yielding in the stirrups and loss of anchorage for the strands. At the final stages of the test on all specimens, the plots of load versus strand slip show slippage of the monitored strands without any increase in load, indicating strand bond failure.

### 6.4.3 Stirrup Stresses at Peak Load

Figure 6-16 shows tensile stresses inferred from strain measurements in the failed shear span of each specimen, at peak shear force. As can be seen in the figure, the strain gauges show extensive yielding of the stirrups in all specimens, with some stirrups entering the strain hardening range. In the Tx70 specimens, Tx46-IV, and Tx46-V, which had more extensive stirrup instrumentation, nearly all of the stirrups that were located outside the heavily reinforced end-region yielded prior to peak load. Although only two stirrups outside the end-region were instrumented in Tx46-I and Tx46-II, yielding of these stirrups was confirmed before reaching the

peak load. Thus, all specimens were found to be governed by tension-controlled shear failure conditions. Similar yielding of the stirrups prior to peak load was also confirmed in the other test span, i.e. the test span that did not fail, in all specimens.

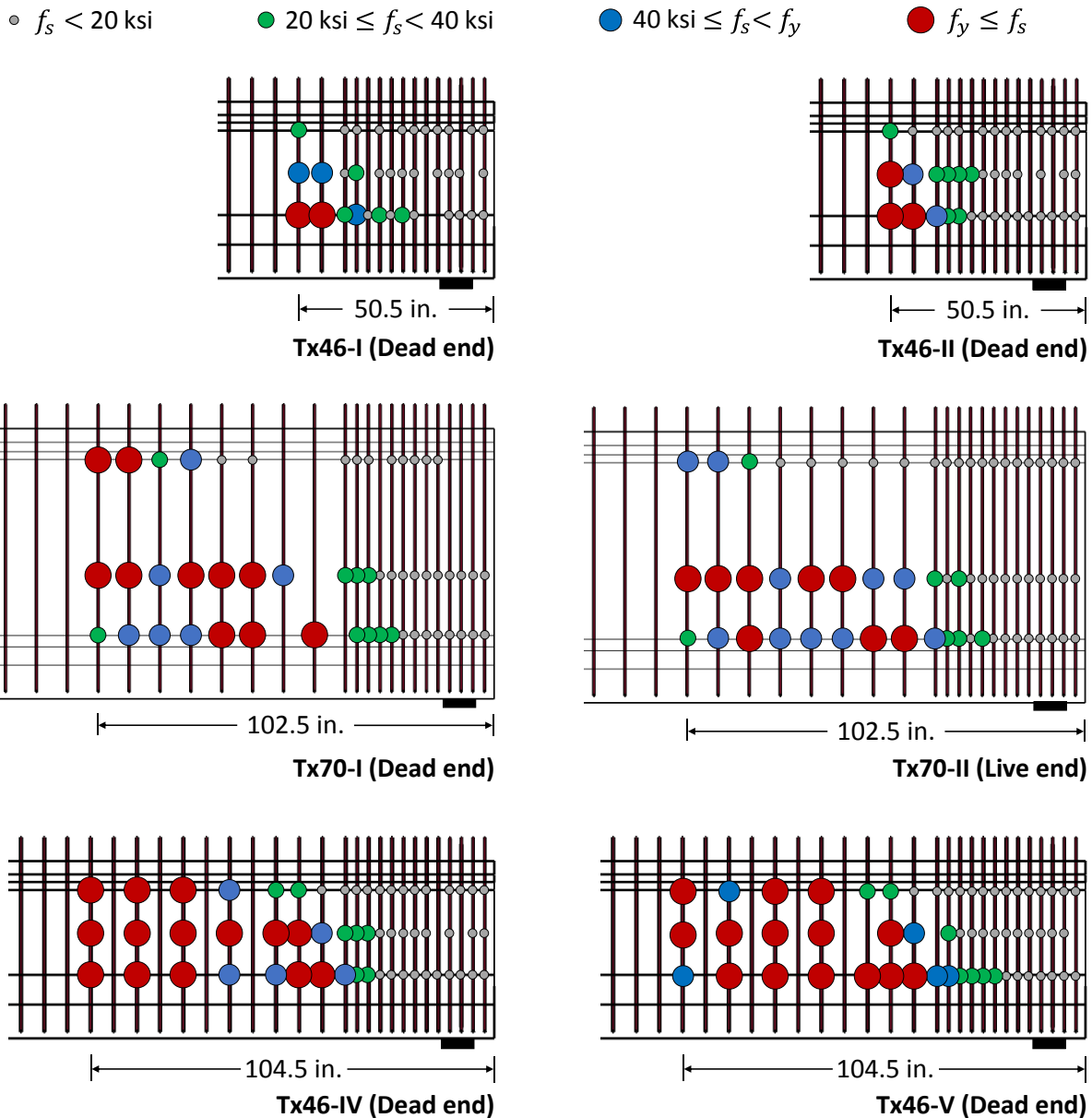


Figure 6-16- Stresses in the transverse reinforcement at peak shear force

#### 6.4.4 Cracking Patterns

Under applied loads, all specimens demonstrated considerable diagonal cracking in the region between the load application point and the support. As previously noted, no sign of flexural cracking near midspan or crushing of the compression block was observed in any of the specimens prior to failure. In Tx46-I, Tx70-I, Tx46-IV, and Tx46-V, the diagonal cracks extended beyond the web until they almost reached the bottom fiber of the beam near the supports. Inclined cracks that formed directly over the support were observed in Tx46-II. Moreover, Tx46-I, Tx70-II, and

Tx46-IV showed noticeable horizontal cracks at the interfaces between the web and top and bottom flanges. Longitudinal side-splitting cracks at the elevation of strands were observed in the Tx70 specimens, indicating bond-related damage. In Tx70-I, face-splitting cracks, i.e. vertical cracks between the bottommost strands and the bottom fiber of the specimen, were observed on the end face. Horizontal cracks also appeared between the strands in Tx46-IV in the early stages of loading. Moreover, horizontal end-face cracks at elevations far from the strands were observed in both Tx70 specimens. These cracks formed at relatively early stages of the test and extended through the thickness of the specimens. No horizontal cracking was detected between the strands on the end faces of Tx46-V. Cracking patterns on one side of each specimen are presented in Figure 6-17.

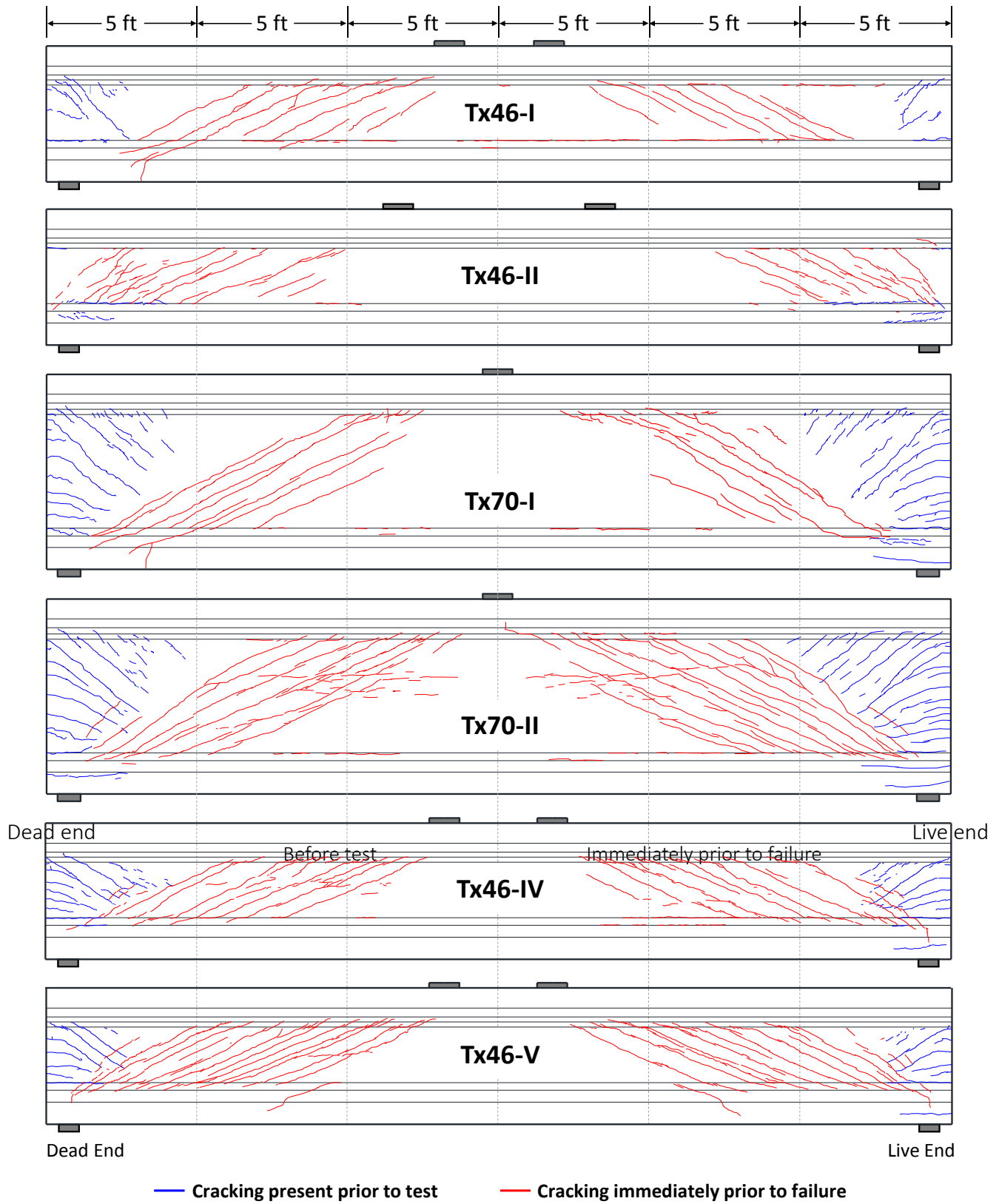


Figure 6-17- Cracking conditions in the specimens immediately prior to failure

#### 6.4.5 Post-Failure Conditions

Figure 6-18 through Figure 6-23 show the post-failure conditions of the failed test spans for each specimen. With the exception of Tx70-II, all specimens failed in the shear span near the dead-end of the specimen. Due to the gradual release operation that was used during fabrication, the difference in stress conditions and damage due to prestress transfer between the two ends of the specimens was small and is not believed to be a contributing factor in determining the failed span.

Large cracks between the strands, typical of bond failure, were observed on the failed end face of all specimens except Tx46-V. These cracks propagated in both vertical and horizontal directions, and were most noticeable in Tx70-II, where the vertical cracks initiated from the bottom flange and extended over the entire depth of the web. In Tx46-V, no cracks were detected between the strands on the end face.

Tx46-I, Tx46-II, and Tx70-II showed distinct horizontal cracking at the web-bottom flange interface that started from the intersection of the interface region and one of the diagonal cracks. The horizontal crack extended from the end face over distances of approximately 8 ft in Tx46-I and Tx46-II, and 6 ft in Tx70-II. In these three specimens, the interfacial sliding measured between the web and the bottom flange was greater than 1 in. at the girder end face. In Tx70-I, cracking at the web-bottom flange interface occurred between 1 ft and 6 ft from the end face but did not result in relative sliding of the web and the bottom flange.

In Tx46-II and Tx46-IV, failure did not induce noticeable damage on the sides of the bottom flange except within the region directly over the support within the last 1 ft distance from the end face. The bottom flange in all other specimens experienced noticeable damage due to failure. Spalling of the cover concrete occurred on one side of Tx46-I and Tx70-I. The spalled concrete extended between 6 and 10 ft from the end face of Tx46-I, and between 4 and 10 ft from the end face of Tx70-I. In Tx70-II, a large portion of the concrete cover, which extended over a distance between 2 ft and 10 ft from the end face was completely split off the specimen on one side whereas the other side showed spalling of the cover concrete up to a distance of 12 ft from the end face.

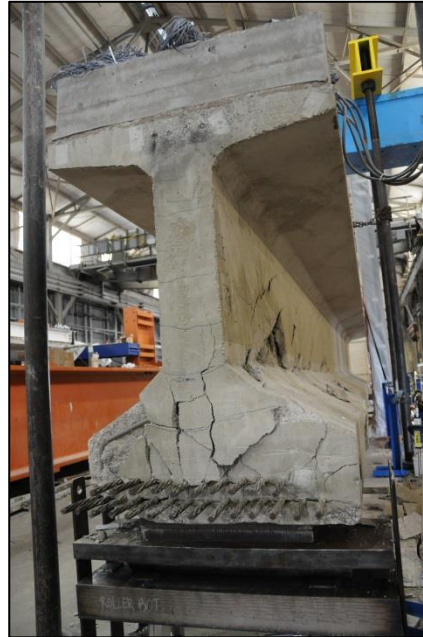
Noticeable horizontal side cracks were also observed on the bottom flange of Tx46-I, Tx70-I, and Tx70-II. In Tx46-I these cracks started at a distance of approximately 3 ft from the end face at the elevation of strands, and extended up to a distance of 7 ft. In Tx70-I, a similar crack extended from the end face over a distance of approximately 4 ft. Wide side cracks were most noticeable in Tx70-II, where they started on the end-face, and continued until they joined the spalled concrete region. These cracks were the major contributor to the splitting of the side cover on one side of this specimen.



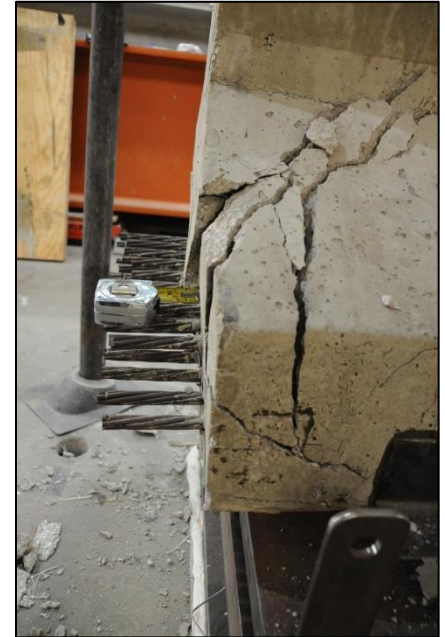
Tx46-I (East side)



Tx46-I (West side)



Tx46-I (End face)



Tx46-I (End-face details)

**Figure 6-18- Post-failure conditions of Tx46-I (Dead end)**



Tx46-II (East side)



Tx46-II (West side)



Tx46-II (End face)



Tx46-II (End-face details)

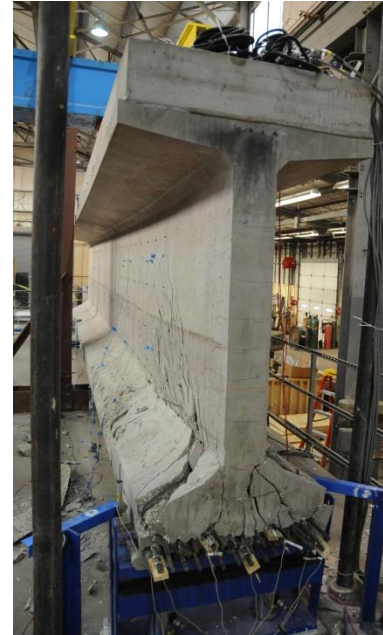
**Figure 6-19- Post-failure conditions of Tx46-II (Dead end)**



Tx70-I (East side)



Tx70-I (West side)



Tx70-I (End face)



Tx70-I (End-face details)

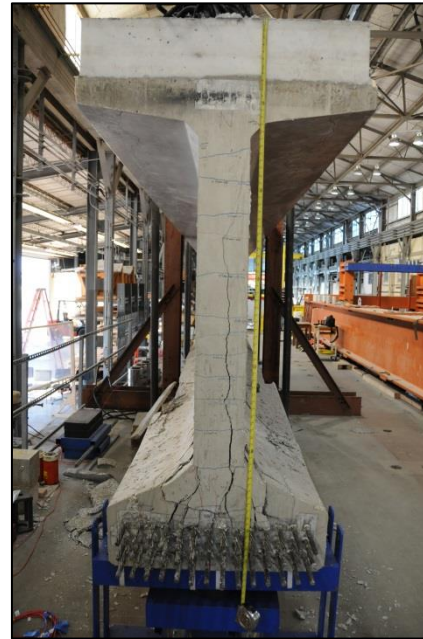
Figure 6-20- Post-failure conditions of Tx70-I (Dead end)



Tx70-II (East side)



Tx70-II (West side)



Tx70-II (End face)



Tx70-II (End-face details)

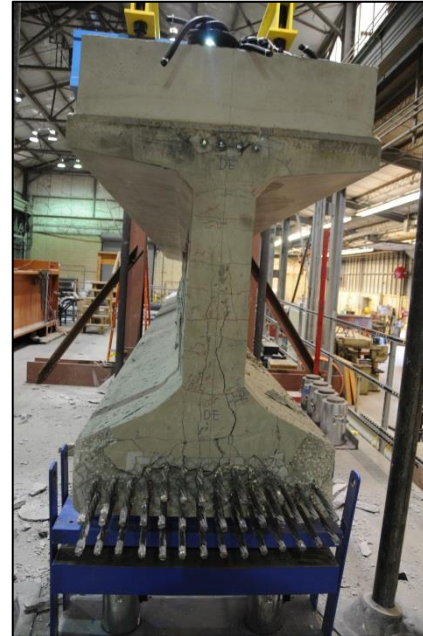
**Figure 6-21- Post-failure conditions of Tx70-II (Live end)**



Tx46-IV (East side)



Tx46-IV (West side)



Tx46-IV (End face)



Tx46-IV (End-face details)

**Figure 6-22- Post-failure conditions of Tx46-IV (Dead end)**



Tx46-V (East side)



Tx46-V (West side)



Tx46-V (End face)



Tx46-V (End-face details)

Figure 6-23- Post-failure conditions of Tx46-V (Dead end)

As can be seen in Figure 6-18 through Figure 6-23, failure of Tx46-V resulted in the most severe damage among the specimens. This specimen failed after sustaining significant diagonal cracking, which corresponded with considerable yielding detected in the stirrups (R-bars), as well as a notable deflection. After failure, the bottom flange remained intact within the last 3 ft distance from the end face, and only minor damage was observed between 3 ft and 5 ft from the end face of this specimen, suggesting a very effective role for the bottom-flange confinement reinforcement. However, as visible in Figure 6-24, failure resulted in substantial damage to the bottom flange within the distance of 5 ft to 9 ft from the end face, making all of the bottom-layer strands exposed. This specimen also showed considerable damage within the top flange in the vicinity of the loading plate. Based on the cracking patterns through the course of testing and the observed sequence of failure, the top-flange damage is only a byproduct of the dramatic failure that occurred in this specimen and the substantial energy that was released.



(a) Bottom flange



(b) Top flange

Figure 6-24- Details of the damage observed in Tx46-V after failure

All other specimens except Tx46-IV experienced damage on the bottom face near the end regions. In Tx46-I, a large longitudinal crack on the bottom face of the specimen originated at a distance of approximately 4 ft from the dead-end face and extended along the beam to midspan. The bottom face of Tx46-II developed relatively small transverse cracks at distances between 6 and 9 ft from the end face. In Tx70-I, the bottom face of the specimen developed extensive transverse cracking and damage at a distance of approximately 3 ft from the end face, resulting in significant spalling of bottom cover concrete. In Tx70-II, longitudinal cracking along the strands and transverse cracking were observed on the bottom face of the beam near the support. These cracks started at the edge of the support and continued over a distance of approximately 6 ft from the end face.

#### **6.4.6 Discussion of Shear Test Results**

The results presented above demonstrate evidence of atypical shear failure mechanisms in all specimens with standard detailing, i.e. Tx46-I, Tx46-II, Tx70-I, and Tx70-II. All of these specimens showed clear signs of anchorage-zone distress. A strand slip exceeding 0.01 in., which has been used by some researchers as an indicator of bond failure, was observed in at least one strand in each specimen prior to the first detected yielding of the stirrups. At peak load, the maximum measured strand slip in these specimens was greater than 0.05 in. Moreover, the final stages of load-versus-slip plots for all specimens were found to be nearly horizontal, which shows a total loss of resistance against strand slip. The specimens also experienced considerable cracking in the vicinity of the supports. Further, the end faces of the failed span in each specimen showed patterns of cracking between strand rows and columns, indicating bond failure.

Specimen Tx46-IV had a modified end-region detailing, i.e. larger-size S-bars at the dead end. However, this end-region modification was not expected to change the performance of this specimen with respect to anchorage-zone distress. The bottom flange of this specimen remained intact within the test span, and the strand slip was less than that measured in the first four specimens. However, the start of strand slip in this specimen occurred almost simultaneously with the first detected yielding of the stirrups, and horizontal cracks between the strands were observed on the bottom face of this specimen.

Horizontal cracking along the web-flange interfaces was also observed as a prominent feature in Tx46-I, Tx46-II, and Tx70-II after failure. In these three specimens, failure resulted in distinctive interfacial sliding of the web and the bottom flange. Moreover, in Tx46-I, Tx70-II, the development and growth of horizontal cracks were observed well before diagonal cracking in the web. These features are indicative of potential horizontal shear distress in the specimens.

In all specimens in the current test program, significant diagonal cracking occurred, and yielding of the stirrups was confirmed. In Tx46-I and Tx46-II, yielding was confirmed in at least two stirrups in each test span, although it is believed that several of the non-instrumented stirrups had likely experienced yielding prior to the first detected stirrup yielding. In other specimens, which were more extensively instrumented in the shear span, widespread yielding of the stirrups was observed outside the closely spaced end-region reinforcement.

The load-carrying capacities of all specimens in the test program were calculated according to AASHTO LRFD specifications. The calculations for nominal shear strength of the specimens are provided in Table 6-6 and Table 6-7 whereas Table 6-8 provides a summary of the results of the nominal strength calculations.

Articles 5.8.3.3 and 5.8.3.4.2 from AASHTO LRFD (2016) were used to calculate  $V_{\text{AASHTO-MCFT}}$  in Table 6-6, which is the nominal shear strength of the specimens according to

AASHTO general procedure. In Table 6-7,  $V_{\text{Anchorage}}$ , i.e. the shear force that causes the prestressing steel to reach its tensile capacity, was calculated based on the longitudinal reinforcement requirements of Article 5.8.3.5 in AASHTO LRFD, and rearranging Equation 5.8.3.5-1 in AASHTO LRFD specifications (2016) as Equation 6-1.

$$V_{\text{Anchorage}} = \frac{V_u}{\phi_v} \quad \text{Equation 6-1}$$

$$= \left( A_{ps} f_{px} + A_s f_y - \frac{|M_u|}{\phi_f d_v} + 0.5 \frac{N_u}{\phi_c} \right) \tan(\theta) + V_p + 0.5 V_s$$

In Equation 6-1,  $f_{px}$  is the available stress in the strands at the section under consideration, which is dependent on the distance from the end face of the specimen and the transfer and development lengths, as illustrated in Figure 2-9. Therefore, the shear corresponding to anchorage failure was calculated at several sections along each specimen, and the minimum value was reported as  $V_{\text{Anchorage}}$ . The transfer and development lengths used for this calculation were taken as  $60d_b$  and the  $l_d$  estimated from Equation 6-2, respectively, both according to AASHTO LRFD specifications.

$$l_d = \kappa \left( f_{ps} - \frac{2}{3} f_{pe} \right) d_b \quad \text{Equation 6-2}$$

In this equation,  $f_{ps}$  is taken as the yield strength of the prestressing steel in ksi,  $f_{pe}$  is the effective stress in the prestressing strands after losses in ksi,  $d_b$  is the diameter of the strands in in., and  $\kappa$  is a factor taken equal to 1.6 for members with a depth greater than 24 in.

The final capacity estimate from AASHTO LRFD specifications,  $V_{\text{AASHTO}}$ , is the lesser of  $V_{\text{AASHTO-MCFT}}$  and  $V_{\text{Anchorage}}$ . For each procedure, the shear strength was calculated at the critical section specific to that procedure. However, for consistency and to allow for more direct comparisons between results stemming from different procedures, the final output of each procedure is presented as the total support reaction (including the self-weight of the specimen and the weight of the loading frame) corresponding to shear failure. All load and resistance factors were taken equal to 1. Moreover, since straight strands were used in the specimens, the vertical component of the prestressing force,  $V_p$ , was taken equal to zero in the calculations.

The variables in Table 6-6 and Table 6-7 are defined as follows:

$A_{ps}$  = Area of prestressing steel.

$A_v$  = Area of transverse reinforcement within distance  $s$ .

$b_w$  = Width of member's web.

$d_e$  = Effective depth from extreme compression fiber to the centroid of the tensile force.  $d_e$  is equal to  $d_p$  in this study.

- $d_p$  = Distance from extreme compression fiber to the centroid of the prestressing steel.
- $d_v$  = Effective shear depth, equal to the distance between the resultants of the tensile and compressive forces due to flexure but not less than  $0.9d_e$  or  $0.72h$ .
- $f_{cm}$  = Measured compressive strength of concrete at the time of testing.
- $f_{pe}$  = Effective stress in the prestressing steel after losses, determined based on initial jacking stress and measurements from vibrating wire strain gages.
- $f_{po}$  = A parameter taken as modulus of elasticity of prestressing tendons multiplied by the locked-in difference in strain between the prestressing tendons and the surrounding concrete. In this study,  $f_{po}$  is taken equal to jacking stress.
- $f_{px}$  = Available stress in the prestressing strand at the section under consideration.
- $f_{pym}$  = Measured yield strength of prestressing steel.
- $f_{ym}$  = Measured yield strength of transverse reinforcement.
- $l_d$  = Development length, determined using Equation 6-2.
- $l_{px}$  = Length available for development of the strands for resisting the longitudinal demand due to combined flexure and shear. In Table 6-7, if the edge of the support is the critical section,  $l_{px}$  is taken as the distance between the end face of the member and the location at which the centroidal axis of the strands intersects the inclined crack due to shear. In other cases,  $l_{px}$  is taken equal to  $x$ .
- $l_t$  = Transfer length, taken equal to 60 times the diameter of the strands in Table 6-7.
- $M_n$  = Nominal flexural strength of the member, found using moment-curvature analysis software.
- $M_u$  = Bending moment at the critical section due to the combined effects of applied loads, self-weight of the specimen, and weight of the loading frame.
- $s$  = Spacing of transverse reinforcement.
- $V_{AASHTO-MCFT,n}$  = Nominal shear resistance at the critical section according to the general method in AASHTO LRFD (Articles 5.8.3.3 and 5.8.3.4.2).
- $V_{AASHTO-MCFT,R}$  = Reaction force at the support corresponding to  $V_{AASHTO-MCFT,n}$  at the critical section.  $V_{AASHTO-MCFT,R}$  is shown as  $V_{AASHTO-MCFT}$  in Table 6-8.
- $V_{Anchorage,n}$  = Shear force that causes the prestressing steel to reach its tensile capacity based on the longitudinal reinforcement requirements of Article 5.8.3.5 in AASHTO LRFD.

$V_{Anchorage,R}$  = Reaction force at the support corresponding to  $V_{Anchorage,n}$  at the critical section.  $V_{Anchorage,R}$  is shown as  $V_{Anchorage}$  in Table 6-8.

$V_c$  = Nominal shear strength provided by concrete.

$V_s$  = Shear strength provided by shear reinforcement.

$V_u$  = Shear force at the critical section due to externally applied loads, self-weight of the specimen, and weight of the loading frame.

$x$  = Distance between the critical section and end face of the member. In Table 6-7, if the edge of the support is the critical section,  $x$  is taken as the distance between the end face of the member and the section located  $d_v$  away from the face of the support.

$\beta$  = Factor relating effect of longitudinal strain on the shear capacity of concrete.

$\epsilon_s$  = Net longitudinal tensile strain at the centroid of the tension reinforcement.

$\theta$  = Angle of inclination of diagonal compressive stresses.

**Table 6-6- Shear strength calculations according to the general procedure in AASHTO LRFD**

Specimen	$f_{cm}$ (ksi)	$f_{ym}$ (ksi)	$f_{po}$ (ksi)	$d_v$ (in.)	$b_w$ (in.)	$M_n$ (kip-in.)	$x^*$ (in.)	$V_u$ (kips)	$M_u$ (kip-in.)
Tx46-I	7.6	60.7	202.5	45.6	7.0	91,840	108.5	452	45,459
Tx46-II	6.9	60.7	202.5	39.3	7.0	91,340	94.5	417	36,042
Tx70-I	10.7	72.2	202.5	67.1	7.0	157,530	106.9	671	66,212
Tx70-II	12.7	72.2	202.5	66.2	7.0	228,810	107.9	730	72,785
Tx46-IV	13.9	63.1	202.5	44.8	7.0	126,420	107.7	542	53,919
Tx46-V	14.5	64.1	202.5	44.8	7.0	124,200	107.7	546	54,349
Specimen	$A_{ps}$ (in. <sup>2</sup> )	$\epsilon_s$ (in./in.)	$\theta$ (degrees)	$\beta$	$A_v/s$ (in. <sup>2</sup> /in.)	$V_s$ (kips)	$V_c$ (kips)	$V_{AASHTO-MCFT,n}$ (kips)	$V_{AASHTO-MCFT,R}$ (kips)
Tx46-I	7.06	0.0001	29.36	4.46	0.067	328	124	452	463
Tx46-II	8.82	-0.0002	28.46	5.43	0.067	293	124	417	426
Tx70-I	8.23	0.0000	28.99	4.81	0.050	437	234	671	683
Tx70-II	12.35	-0.0002	28.38	5.53	0.050	442	288	730	743
Tx46-IV	10.58	-0.0001	28.57	5.29	0.067	346	196	542	552
Tx46-V	10.58	-0.0001	28.66	5.18	0.067	351	196	546	557

\* The section located at the distance  $d_v$  from the face of the loading plate was critical in all specimens.

**Table 6-7- Shear strength calculations according to the longitudinal reinforcement requirement in AASHTO LRFD**

Specimen	Critical location for anchorage	$x$ (in.)	$f_{pe}$ (ksi)	$f_{pym}$ (ksi)	$A_{ps}$ (in. <sup>2</sup> )	$l_t$ (in.)	$l_d$ (in.)	$V_u$ (kips)
Tx46-I	$d_v$ from the face of the loading plate*	108.5	157.4	232.0	7.06	42.0	142.3	439
Tx46-II	$d_v$ from the face of the loading plate*	94.5	166.9	232.0	8.82	42.0	135.2	513
Tx70-I	Edge of the support**	80.6	163.8	232.0	8.23	42.0	137.5	571
Tx70-II	Edge of the support**	79.7	156.6	232.0	12.35	42.0	142.9	763
Tx46-IV	Edge of the support**	57.8	152.7	232.0	10.58	42.0	145.8	604
Tx46-V	$d_v$ from the face of the loading plate*	107.7	158.6	232.0	10.58	42.0	141.5	622
Specimen	$M_u$ (kip-in.)	$\epsilon_s$ (in./in.)	$\theta$ (degrees)	$l_{px}$ (in.)	$f_{px}$ (ksi)	$V_s$ (kips)	$V_{Anchorage,n}$ (kips)	$V_{Anchorage,R}$ (kips)
Tx46-I	44,148	0.0000	28.97	108.5	206.9	333	439	449
Tx46-II	44,205	-0.0001	28.82	94.5	203.6	289	513	522
Tx70-I	41,153	-0.0001	28.55	19.9	77.8	445	571	580
Tx70-II	54,188	-0.0002	28.15	21.9	81.7	446	763	772
Tx46-IV	29,599	-0.0003	28.05	20.8	75.7	354	604	609
Tx46-V	61,836	0.0000	28.87	107.7	207.0	348	622	630

Note:

\* Equation 5.8.3.5-1 from AASHTO LRFD is used.

\*\* Equation 5.8.3.5-2 from AASHTO LRFD is used. The values of  $x$ ,  $V_u$ ,  $M_u$ ,  $V_s$ ,  $\epsilon_s$ , and  $\theta$  are calculated at the section that is  $d_v$  away from the face of the support. The  $M_u$  values in this case are used only for determining  $\epsilon_s$  and  $\theta$ .

**Table 6-8- Nominal shear strength calculations**

	Tx46-I	Tx46-II	Tx70-I	Tx70-II	Tx46-IV	Tx46-V
$f_{pe}$ , ksi	157.4	166.9	163.8	156.6	152.7	158.6
$l_d$ , in.	142.3	135.2	137.5	142.9	145.8	141.5
$V_{Test}$ , kips	544	467	749	839	656	747
$V_{Flexure}$ , kips	613	705	929	1,350	853	853
$V_{Flexure}/V_{Test}$	1.13	1.51	1.24	1.61	1.30	1.14
$V_{AASHTO-MCFT}$ , kips	463	426	683	743	552	557
$V_{Anchorage}$ , kips	449	522	580	772	609	630
$V_{AASHTO}$ , kips	449	426	580	743	552	557
$V_{Test}/V_{AASHTO-MCFT}$	1.17	1.09	1.10	1.13	1.19	1.34
$V_{Test}/V_{AASHTO}$	1.21	1.09	1.29	1.13	1.19	1.34

Note: The reported  $V$  values are calculated at the support and represent reaction forces.

Table 6-8 also contains the shear force corresponding to the computed flexural failure of the specimens,  $V_{Flexure}$ . Since the specimens were carefully designed to fail in shear rather than flexure,  $V_{Flexure}$  was noticeably greater than the maximum shear force recorded for each specimen. Moreover, the estimated development length and the effective prestress at the midspan of the specimen after losses,  $f_{pe}$ , which was obtained from VWG measurements, are presented in this table. Note that the critical section used in the design calculations was procedure-dependent. For consistency, all reported shear forces in Table 6-8 represent the reaction forces corresponding to failure. All resistance factors were taken equal to 1.0.

As can be seen in Table 6-8, despite the atypical failure modes observed in the test program, the AASHTO LRFD specification provided conservative estimates for the load-carrying capacities of all specimens. Table 6-8 also shows that the capacities of all specimens exceeded  $V_{AASHTO-MCFT}$  values and therefore, neglecting the  $V_{Anchorage}$  limit resulted in capacity estimates that were closer to experimental results. Although almost all specimens showed clear signs of anchorage-zone distress,  $V_{Anchorage}$  was the governing parameter for the load-carrying capacity of only Tx46-I and Tx70-I. Therefore, using  $V_{Anchorage}$  from Equation 6-1 does not appear to be a reliable indicator of the failure mode in the specimens. This observation is potentially due to the assumptions used in estimating  $f_{px}$ , which are based on the simplified bilinear approximation of strand stresses shown in Figure 2-9.

The conservativeness of AASHTO LRFD in estimating the shear capacity of the specimens in this test program may be explained by the traditional shear failure mechanisms that were also observed. In all specimens, yielding of the stirrups was confirmed prior to the development of the peak load resistance. In the specimens that were more extensively instrumented for strains in the shear reinforcement, softening of the load-deflection response was much better correlated with detected yielding of the stirrups than with the observed strand slip. Therefore, the presence of

anchorage-zone distress did not prevent the specimens from developing the tension-controlled shear failures inherently assumed in the formulation of the shear design provisions employed.

An important set of observations from the shear test program was related to the differences between the performances of Tx46-IV and Tx46-V. These two specimens had identical designs with respect to shear reinforcement. The differences stemming from using larger-diameter S-bars in one end of Tx46-IV or the horizontal W-bars and WT-bars in one end of Tx46-V were believed to be negligible. Therefore, differences in the behavior of the two specimens were attributed primarily to the use of cap bars in Tx46-V.

Figure 6-25 provides a comparison between the shear force-deflection and shear force-strand slip plots obtained from Tx46-IV and Tx46-V. As can be seen in this figure, both specimens exceeded the load-carrying capacity predicted by AASHTO LRFD. While the specimens showed identical load-deflection behavior prior to diagonal cracking, Tx46-V showed a noticeably greater ultimate strength and also a greater deformation capacity prior to failure. The shear force-strand slip plot also shows that considerably smaller strand slip was recorded from Tx46-V. Most strands in this specimen did not show noticeable strand slip until the capacity predicted by AASHTO LRFD was exceeded. The maximum strand slip in Tx46-V when reaching the nominal load-carrying capacity was just below 0.01 in. Therefore, according to the criterion used by Morcous et al. (2011), none of the strands reached bond failure in this specimen prior to reaching their nominal load-carrying capacity. These observations and the observed damage conditions in Tx46-V suggest that the use of cap bars is effective in controlling the strand slip in Tx-girders employing 0.7-in. strands.

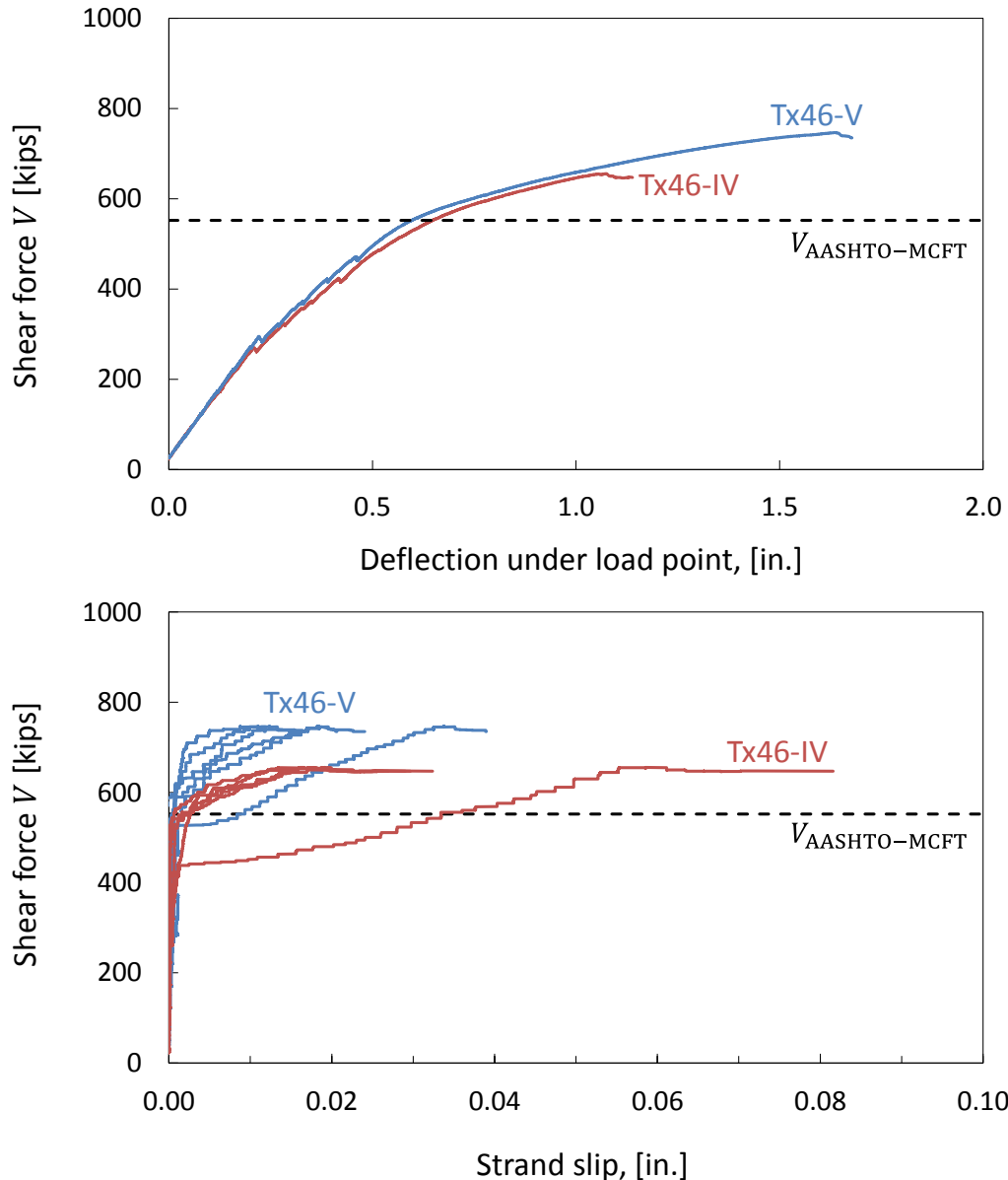
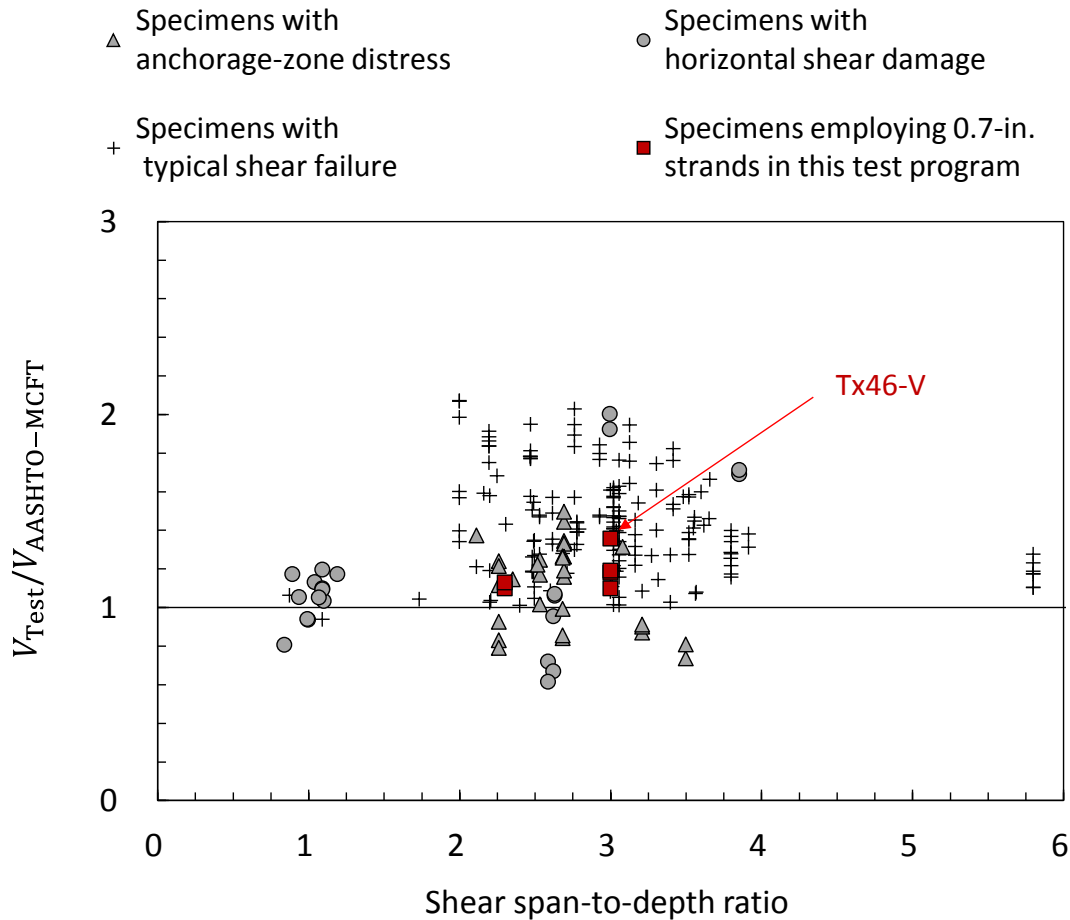


Figure 6-25- Comparison between load-deflection and load-slip behavior of Tx46-IV and Tx46-V

To shed light on the impacts of using 0.7-in. diameter strands in the context of the performance of AASHTO LRFD provisions, the results of the shear test program were compared with the experimental database developed by Nakamura et al. (2013). Figure 6-26 shows a comparison of the data obtained from this study with those comprising the database, as a function of the shear span-to-depth ratios of the specimens. In this figure, data points from Nakamura et al. are presented in three categories of typical shear failure; horizontal shear damage, i.e. failure with observed sliding of the interface between the web and the bottom flange; and anchorage-zone distress, i.e. failure with damage in anchorage regions in the forms of strand slip and breakdown of bond between strands and concrete. For consistency with other points in the database, the  $V_{Test}/V_{Calc}$  ratios in the figure are calculated at a distance equal to effective depth of the member from the face of the supports. Moreover, the longitudinal capacity requirement, i.e.  $V_{Anchorage}$ , is

not considered. As can be seen in this figure, the girders investigated in this test program demonstrated  $V_{Test}/V_{Calc}$  ratios that were conservative but generally less conservative than the majority of data points representing traditional shear failures, especially when AASHTO LRFD provisions are considered. As shown in the figure, Tx46-V, which had modified confinement reinforcement, demonstrated a  $V_{Test}/V_{Calc}$  ratio that was noticeably greater than the other specimens in this test program and more consistent with data points reflecting typical shear failures.



**Figure 6-26- Comparison of results from the current test program with the database of shear tests on prestressed concrete members**

The Tx46 and Tx70 specimens investigated in this test program had relatively large shear reinforcement ratios of 1.0 percent and 0.7 percent, respectively. However, all specimens achieved yielding in the stirrups before the peak load. It is evident that stirrup yielding would occur earlier in Tx-girders with smaller shear reinforcement ratios. Therefore, no concerns are currently identified regarding the conservativeness of AASHTO LRFD specifications in estimating the shear capacity of Tx-girders employing 0.7-in. diameter strands.

## 6.5 Summary and Conclusions

Six full-scale Tx-girder specimens employing 0.7-in. diameter strands on a 2- by 2-in. grid were designed and fabricated to investigate their end-region behavior at the time of prestress transfer and their shear-resisting performance under applied loads. The specimens were extensively instrumented to provide a detailed picture of transverse stresses within reinforcement, transfer length, prestress losses, strand slip, and load-deflection behavior. The cracking conditions within the specimens were also carefully examined throughout the life of the specimens. Moreover, extensive ASTM-compliant testing was performed to measure the mechanical properties of the materials comprising each specimen.

The transfer length was determined using the data obtained from the strain gauges. Immediately after prestress transfer, the transfer length of 0.7-in. strands in this test program was found to be generally shorter than  $60d_b$ , which is used in AASHTO LRFD to estimate the transfer length. However, 24 hours after prestress transfer, the average transfer length measured from the specimens slightly exceeded this estimate, and in some instrumented strands, transfer lengths on the order of 52 in. were detected.

In general, cracking patterns observed in the specimens in this test program due to prestress transfer were similar to those in Tx-girders fabricated using smaller-diameter strands. The crack widths during the monitoring period were generally limited to 0.007 in. but crack widths up to 0.008 in. were also observed in isolated lengths of some cracks in two specimens. These crack widths are slightly greater than those in girders fabricated using 0.6-in. diameter strands. However, all specimens are considered acceptable for exposure to de-icing chemicals according to ACI 224R guidelines. To reduce the crack widths within the end-regions of the specimens, two modifications, 1) increasing the diameter of the S-bars and 2) using horizontal bars were examined. Based on observations from specimens fabricated using these modified details, neither of the strategies was deemed effective in controlling the widths of end-region cracks.

Stresses as large as 26 ksi were detected in the transverse steel at the web-bottom flange interface in some specimens. However, the stress level was observed to diminish rapidly with the increase in distance from the end face of the girder, and large stresses were limited to the transverse steel that was used in the overhang region or directly over the supports. As a result, the stresses induced in the transverse steel due to prestress transfer did not appear to have a noticeable influence on the load-carrying capacities of the specimens.

Almost all specimens revealed signs of atypical failure mechanisms under shear-critical loading. These signs included the occurrence of significant strand slip prior to reaching the peak load, as well as the appearance of horizontal and vertical cracks between the strands on the end face after failure. Therefore, the specimens revealed the likelihood of anchorage zone distress due to using 0.7-in. strands. On the other hand, significant diagonal cracking also occurred in all specimens, and yielding was confirmed in all specimens prior to reaching the peak load, suggesting the occurrence of tension-controlled failure. The nominal shear strengths of the specimens were calculated according to AASHTO LRFD specifications and compared with the measured ultimate strengths. Despite the atypical failure modes observed, all specimens exceeded their nominal load-carrying capacities. However, the ratio of measured to predicted load-carrying capacity for the specimens in this test program was found to be generally smaller than the majority of data points in a database of shear tests on prestressed concrete elements developed by Nakamura.

The last specimen in the test program incorporated modifications to its bottom-flange reinforcement within the end-region. In this specimen, a series of No. 4 bars were added to the bottom-flange confinement steel as cap bars. Observations from the shear test program showed

that this modification was effective in controlling the strand slip under applied loads, resulting in noticeable increases in the ultimate strength and deformation capacity of this specimen.



# CHAPTER 7

## Finite Element Studies

### 7.1 Overview

In accordance with the scope of Task 3 in this research project, a series of finite element (FE) analyses was performed to study the behavior of end-regions in girders fabricated using 0.7-in. diameter strands and examine potential modifications to the detailing of mild-steel reinforcement in such girders. These analyses supplemented the experimental program and helped the research team select the end-region detailing for incorporation in the last few specimens in the research program. This chapter presents a summary of the activities performed to conduct the FE analyses, along with some of the major findings of this computational effort.

### 7.2 Background

Conducting experimental studies on full-scale specimens is the most reliable method for evaluating the performance of pretensioned members in terms of end-region behavior and shear strength, especially when new detailing for prestressing or mild-steel reinforcement is to be assessed for potential implementation. However, it is impractical to use such studies on a frequent basis for investigating the wide variety of parameters that may affect the behavior of pretensioned concrete members.

Alternatively, effective investigation of the effects of changes in detailing on the performance of pretensioned concrete members is possible through the use of computational models that are validated based on experimental data. Such validated models can help broaden the impacts of the experimental studies through examining the set of parameters that have not been directly tested in the experimental program. Moreover, these computational models may be used to obtain insights into the load-transfer or failure mechanisms using parameters that are impractical to measure in any experimental studies.

Computational assessment of the end-region behavior of pretensioned girders has been the focus of a few previous studies, such as Okumus et al. (2012), Okumus et al. (2013), and Okumus et al. (2016). However, these studies were conducted on girders that were fabricated using 0.5- or 0.6-in. diameter prestressing strands, and the findings of such studies might not be directly applicable to Tx-girders employing 0.7-in. diameter strands.

As part of Task 3 in this research project, a series of FE models were developed to examine the end-region behavior, distribution of stresses within the end-region reinforcement, and end-region cracking in pretensioned girders that employ 0.7-in. diameter strands. The same models were also used to evaluate the load-deflection behavior, failure mechanisms, and ultimate strengths of the girders under shear-critical loading. These models were not directly used for drawing conclusions regarding the performance of girders at the time of prestress transfer or under shear-critical loading. However, results from the models helped the research team gain insights into the behavior of the specimens and develop modifications to end-region reinforcement that were used in the last few specimens in the test program.

## 7.3 Methodology of Investigation

All computational modeling in this research project was performed using ATENA 3D (2015), which is a nonlinear FE analysis program specifically developed for reinforced concrete structures. This program is able to provide information related to cracking and crushing of concrete and yielding of reinforcement through a graphical interface. An important capability of ATENA 3D that was critical for the purposes of this research project was that the same FE model can be used in this program to evaluate the effects of prestress loss and the behavior of the member under applied loads. Therefore, the interaction between stresses and damage due to prestress transfer and those due to applied loads can be effectively considered.

The validation of modeling assumptions in ATENA 3D was conducted in two stages. In the first stage, experimental data from previous experimental programs available in the literature were used to develop FE models and initially validate the modeling assumptions for simulating the behavior of pretensioned concrete elements from the time of prestress transfer until failure under applied loads. Once the modeling methodology was validated, the specimens fabricated and tested as part of Tasks 4 and 6 in this research project were modeled in the second stage and validated using the results presented in Chapter 6.

### 7.3.1 Experimental Data Used for the First Stage of Validation

Two experimental studies from the literature were used in the first stage of validation. One of these studies was conducted on Tx-girders employing 0.6-in. diameter strands (the 6-Tx Series) whereas the other study was conducted on NU-girders employing 0.7-in. diameter strands (the 7-NU Series). These studies are briefly introduced in this section. Note that the experimental study conducted as part of Tasks 4 and 6 in this research project is referred to as the 7-Tx series in this chapter.

#### 7.3.1.1 Specimens in 6-Tx Series

As introduced in Chapter 2, O'Callaghan (2007) fabricated and tested four full-scale Tx-girder specimens (two Tx28, one Tx46, and one Tx70 girders) using 0.6-in. diameter strands to evaluate end-region stresses and develop end-region detailing for the then-new family of Tx-girders. This test series is referred to as the 6-Tx series in this report. The specimens fabricated in this test program were later tested by Avendaño (2008) in shear-critical loading conditions until failure. Reliable test data were not available for the Tx70 specimen. The other three specimens were used for the validation effort, and are denoted as 6-Tx28-I, 6-Tx28-II, and 6-Tx46-I. The first numeral of the names represents the diameter of the prestressing strands used within the specimens (in tenths of an inch), and the second numeral represents the overall height of the precast girders (in in. and not including the depth of the composite deck).

The cross section and the reinforcement details used within this test program are shown in Figure 7-1. Each specimen had a length of 30 ft. The strands were released at a concrete compressive strength between 6.5 and 10.0 ksi through gradual retraction of hydraulic rams. A reinforced concrete deck, which had a thickness of 8 in., was later constructed on each specimen, after which the specimens were tested in the shear-critical loading configuration shown in Figure 7-2. The shear span-depth ratio,  $a/d_p$ , ranged between 2.7 and 3.9. Reported data from this test program included the load-deflection response, cracking patterns, and failure modes, as well as the mechanical properties of the materials comprising the specimens.

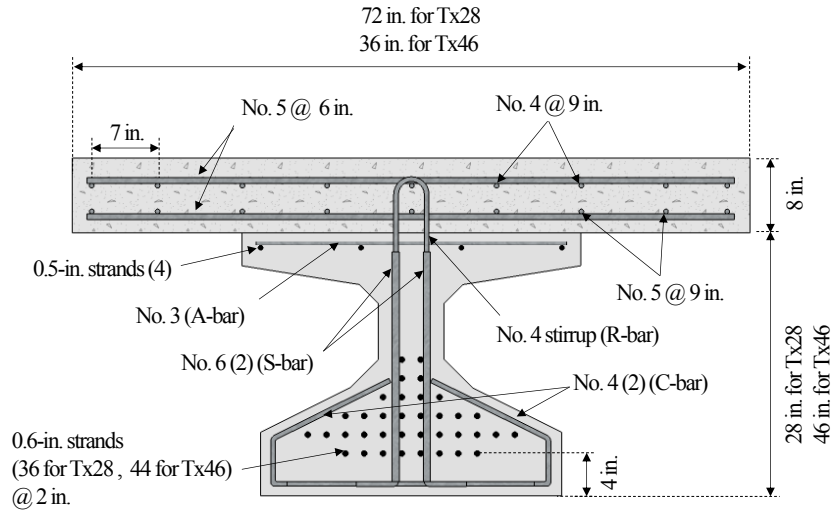


**Figure 7-1- Cross-section and reinforcement details in the 6-Tx series**

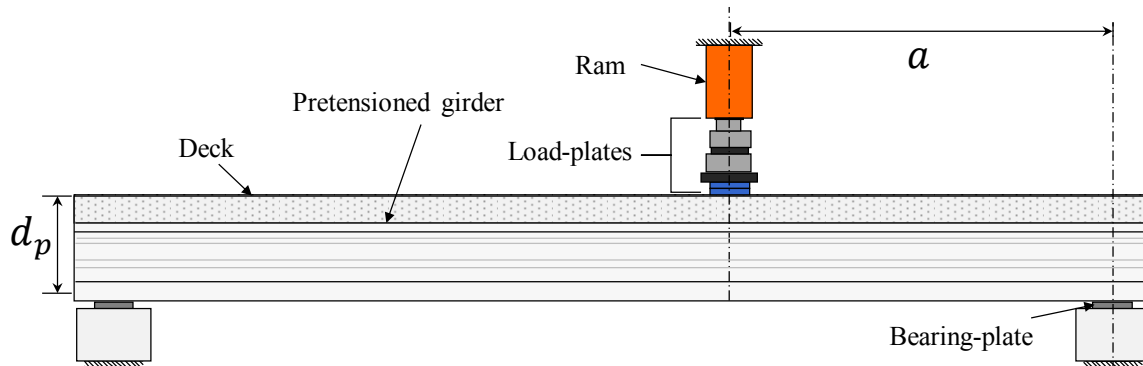


**Figure 7-2- Shear test setup used for the 6-Tx series**

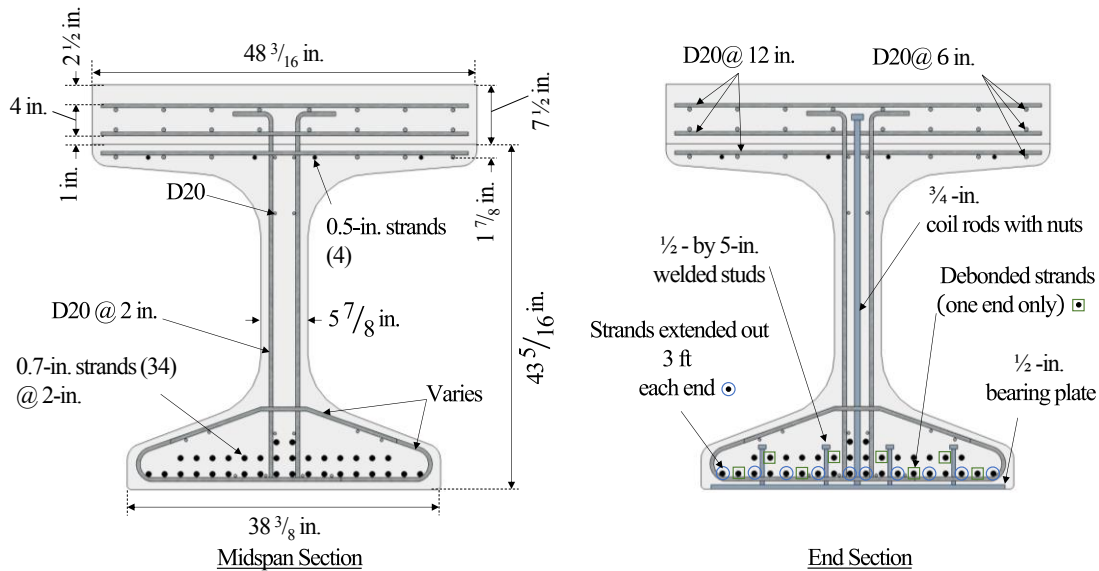
### 7.3.1.1 Specimens in 7-NU Series

Tadros and Morcos (2011) fabricated and tested three full-scale NU1100 girders, i.e. bulb-Nebraska bulb-tee girders that had a depth of 1,100 mm (43 in.). The specimens were reinforced using 0.7-in. diameter prestressing strands, which were released at a concrete compressive strength of 7.8 ksi. This test series is referred to as the 7-NU series in this report, and the specimens are identified as 7-NU1100-I, 7-NU1100-II, and 7-NU1100-III.

The cross section and the reinforcement details used within the 7-NU test series are shown in Figure 7-3. Each specimen had a length of 40 ft. The specimens contained similar details for prestressing strands and mild-steel reinforcement except for the confinement in the bottom flange. Twenty-five percent of the strands at one end of each specimen were debonded. A reinforced concrete deck, which had a thickness of 7.5 in., was later constructed on each specimen, after which the specimens were tested.

Each specimen was tested twice. First, the specimen was loaded to its nominal flexural capacity to assess the efficacy of the development length. After this test, the specimen was unloaded. The second test on the specimen was conducted on the opposite end, with a shear-span-to-height ratio of 1.77.

The reported data from the 7-NU series included the load-deflection response, cracking patterns, and failure modes under applied loads. However, no information was reported regarding the response of the specimens at the time of prestress transfer. Moreover, several critical parameters, such as the dimensions of the loading plates and actual mechanical properties of the reinforcement, were not reported. As a result, precise models were not expected for this test series. However, this study was one of the few experimental studies available on the use of 0.7-in. strands in I- or bulb-tee girders. Therefore, the 7-NU series was considered as part of the validation effort. The missing parameters were estimated based on information available from similar test programs by the same researchers who conducted the 7-NU test series.



*Note: Ten strands at each end were extended outside the end face. At the debonded end, these strands were bent into an end diaphragm.*

**Figure 7-3- Cross section and reinforcement details for the 7-NU series**

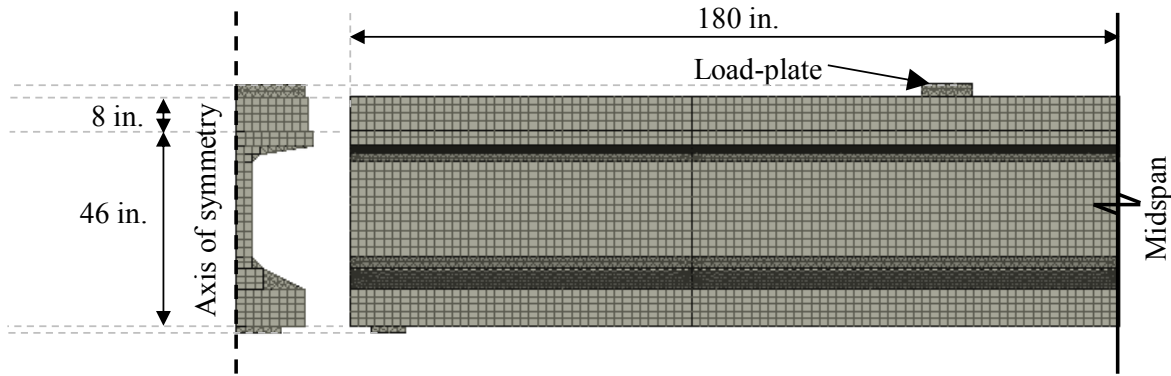
Calculations of nominal shear and flexural strengths of the 7-NU series showed that the load required to reach the reported nominal flexural capacities exceeded the nominal sectional shear capacities computed in accordance with the General Method in the provisions of AASHTO LRFD specifications. Therefore, the loading configuration in the first test was also shear-critical.

The FE models of the 7-NU test specimens also showed noticeable shear damage as a result of the first test, due to which unloading and reloading the girders to model the second experiment was not possible in the FE simulations. Therefore, only the first tests performed on these specimens were considered in the current study.

### 7.3.2 Finite Element Model

Figure 7-4 shows the FE mesh developed for one of the Tx46 girders comprising the 7-Tx series. First-order hexahedral (brick) elements were used as the primary elements for modeling concrete. In regions where geometric conditions did not permit the use of rectangular brick elements, tetrahedral elements were used. The reinforcement was modeled using truss bar elements. To reduce the size of the model and hence the time of analyses, only half of the width of each specimen was modeled.

A mesh sensitivity analysis was conducted on 6-Tx28-I and 6-Tx28-II, through which the results of the models in terms of transfer lengths of the prestressing strands, cracking patterns, and maximum crack widths at prestress transfer were compared with those experimentally obtained. Based on the results of this sensitivity analysis, a typical element size of 2.0 in. was used to model all regions of the specimens.



Note : Only half of the length of the FE model is shown.

**Figure 7-4- FE mesh created for a typical Tx46 girder**

The evolution of the models over the course of the analyses from the time of prestress transfer until member failure under applied loads is shown in Figure 7-5. The deck, bearing-plates, and load-plates were added in a series of subsequent stages using the “construction” feature in ATENA 3D. Note that no interfacial slip was permitted between the precast section and the deck.

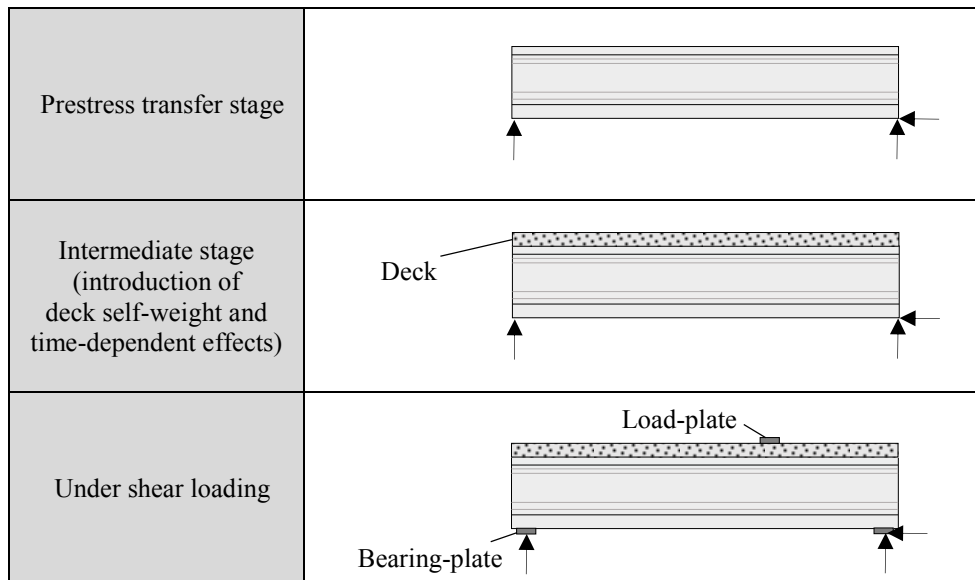


**Figure 7-5- Boundary conditions for different stages of analysis**

### 7.3.3 Loading Conditions

During the shear tests, load was applied as a prescribed displacement with 0.01-in. increments. The conditions of the specimens before the shear tests were simulated using the following load cases in the order of application: 1) a body load was used to apply the entire self-weight of the girder one load step; 2) prestressing was incrementally applied as reinforcement prestrains in steps equal to 5 percent of the total prestrain; 3) the entire self-weight of the deck was applied as one load step; and 4) a volumetric strain that was applied in one load step was used to simulate the time-dependent strains associated with creep and shrinkage.

To incorporate losses in the prestressing force over time, a uniform volumetric strain was applied to the concrete comprising each girder. No data were available for the time-dependent strain changes for the 6-Tx and 7-NU series specimens. A volumetric strain of  $-0.20 \times 10^{-3}$  in./in. was found to reasonably capture the response of these specimens. In the 7-Tx series specimens, time-dependent strains were recorded using a series of embedded vibrating wire strain gauges. For these specimens, the volumetric strain was taken as  $-0.35 \times 10^{-3}$  in./in.

### 7.3.4 Behavioral Models and Analysis Parameters

Six material types were defined in the modeling of the girders: girder concrete, deck concrete, mild-steel reinforcement, prestressing steel, and welded wire reinforcement. In cases where measured material properties were available, they were used to define the material models; in all other cases, the default material properties or those proposed by the ATENA Program Documentation (2016) were used.

The concrete material model in ATENA 3D combines concrete tensile (fracture) behavior and compressive (plastic) behavior models through a fracture-plastic model (Červenka et al., 2016). The only modeling parameter requiring specification by the user is the concrete cubic compressive strength. All other concrete material model parameters were automatically defined.

The “NonLinearVariableCementitious” material type was chosen for the girder concrete. This model makes it possible to define changing concrete material properties over the course of the analysis. A constant residual tension-stiffening, equal to 5 percent of the cracking stress, was assigned to the cracked concrete in the girder, solely for the purpose of improving numerical stability in the late stages (i.e., near failure) of the analyses. Since the deck concrete only contributes to member response during shear testing, there was no need to capture the variation of its compressive strength; therefore, the “NonLinearCementitious” material was used for the deck.

All non-prestressed steel reinforcing bars were modeled as discrete truss bar finite elements with perfect bond. In cases where measured mechanical properties of the steel were not available, property estimates obtained from ASTM A615 (2015) were used. Prestressing strands were modeled as discrete reinforcement elements with the prestressing force specified by way of an additional load case. To define the cross-sectional area of the strands, an equivalent circle diameter was specified so that the area of the modeled strand matched the actual area of the seven-wire strand. The bond model proposed by Bigaj (1999) with “very good” bond quality was found to successfully capture the transfer length and the observed concrete damage at prestress transfer. The bond model properties are, by default, held constant over the course of the analysis. However, there is often considerable compressive strength gain from the time of the prestress transfer to the time of ultimate load test, which is believed to affect bond strength. To account for the concrete strength variation, the bond modeling employed for the prestress transfer stage analysis was based on the concrete release strength. However, for the analysis of specimens under ultimate load tests,

the prestress transfer analysis was repeated from the initial step, this time with bond modeling based on the test day concrete strength.

This approximation may have altered the concrete damage computed prior to the start of the shear test. However, it was assumed that the computed shear capacities were not noticeably influenced by what were found to be marginal differences in the computed end-region damage stemming from the use of a constant concrete strength.

The Newton-Raphson method was used for the solution algorithm, with the elastic (secant) stiffness updated at each step. A total of 80 iterations were permitted per analysis step, with an absolute residual error tolerance of 10 percent.

## 7.4 Results and Discussion

The following section presents numerical modeling results for the girders comprising all three test series (6-Tx, 7-NU, and 7-Tx) at the time of prestress transfer and under shear-critical loading. Note that the experimental response of the 7-NU series girders was not reported for prestress transfer and is therefore not discussed in this section.

### 7.4.1 Prestress Transfer

The parameters used to assess the suitability of the models for prestress transfer were the transfer length, cracking patterns and widths, and stresses in the mild-steel reinforcement. Figure 7-5 presents the variation of the strand forces throughout the end-regions of a sample girder, 6-Tx28-I. While there is noticeable scatter in the reported experimental data, it can be seen that the numerically estimated trends for transfer of prestress between the strand and concrete were consistent with the data obtained from measurements.

Table 7-1 presents a comparison of the analytical and experimental results obtained from the prestress transfer stage for the specimens, whereas Figure 7-7 through Figure 7-13 graphically present the computed versus reported end-region damage at the live end of the girders, immediately following prestress transfer.

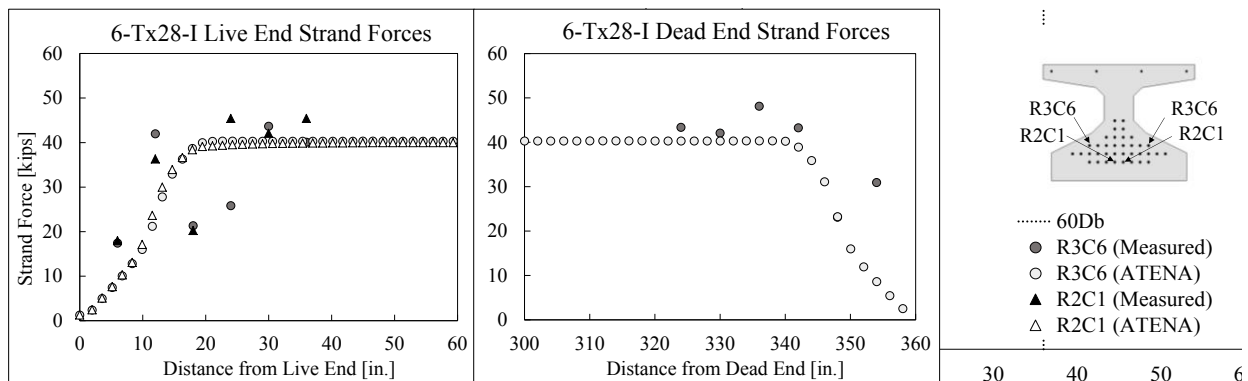


Figure 7-6- Comparison of computed and measured strand forces after transfer of prestress for 6-Tx28-I

Table 7-1 shows that the crack widths developed in specimens with 0.7-in. diameter strands were generally greater than those in specimens with 0.6-in. diameter strands. These crack widths were also more conservatively estimated by the models for specimens with 0.7-in. diameter strands.

**Table 7-1- Prestress transfer results for 6-Tx and 7-Tx series specimens**

Parameter	Max. crack width immediately after release [in.]		Transfer length <sup>1</sup> [in.]		Max. stress in transverse steel <sup>2</sup> [ksi]	
	Measured	Computed	Measured	Computed	Measured	Computed
6-Tx28-I	0.005	0.005	36	20	22	21
6-Tx28-II	0.009	0.005		32	32	16
6-Tx46-I	0.007	0.007		30	22	24
7-Tx46-I	0.008	0.009	41	31	19	22
7-Tx46-II	0.004	0.004	32	33	14	9
7-Tx70-I	0.006	0.007	35	31	25	25
7-Tx70-II	0.007	0.008	38	27	26	32
7-Tx46-IV	0.005	0.008	33	24	23	24
7-Tx46-V	0.005	0.008	35	24	23	27

<sup>1</sup>The average transfer length for the strands from both dead and live ends.

<sup>2</sup>The measured stirrup strains were converted to stresses assuming a modulus of elasticity of 29,000 ksi for the reinforcing bars.

Reinforcement stresses provide an indirect measure of the level of damage in the end-region of the specimens. Since only a few points on each end-region reinforcing bar were monitored, it would be difficult to capture the maximum stress using strain gauges. As a result, in the majority of investigated end-regions, the maximum stress obtained from the numerical model was greater than the maximum stress detected from strain gauges. However, the computed results were generally within 20 percent of stresses determined from strain gauge measurements. From the results presented above, it can be seen that the FE models of the girders captured the responses at release reasonably well.

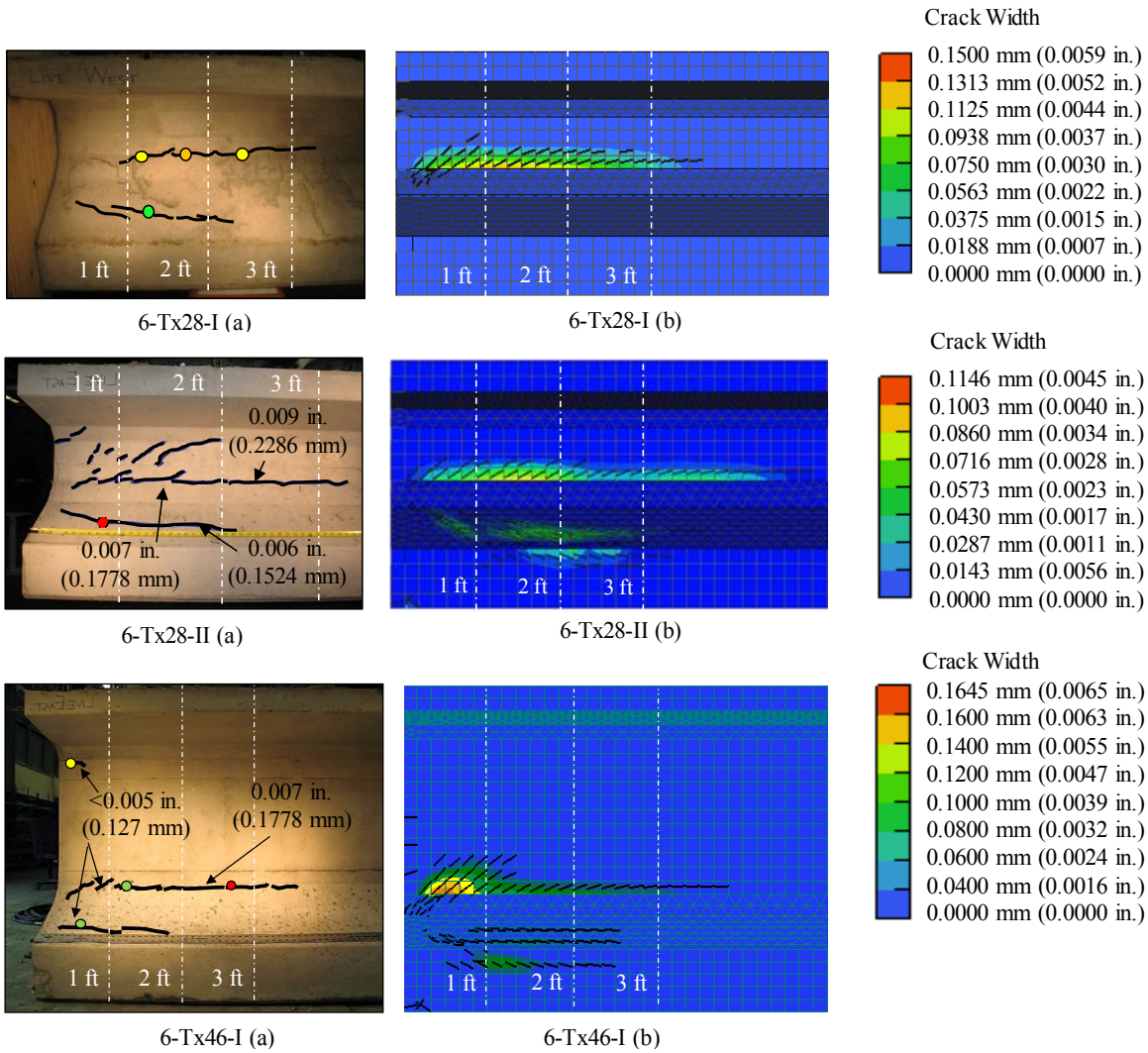
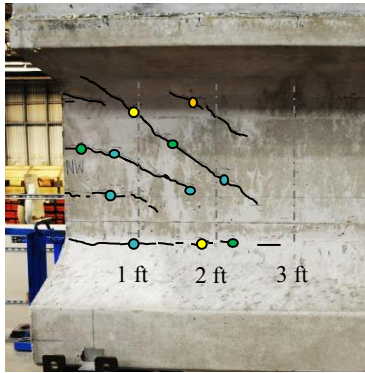
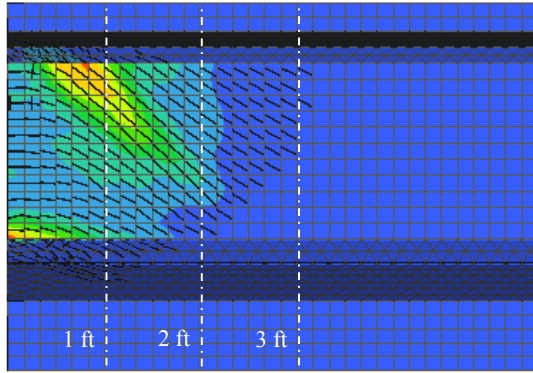


**Figure 7-7- Comparison of live-end cracking in 6-Tx series specimens. Notations (a) and (b) refer to measured and computed results for each specimen, respectively. Photos from O'Callaghan (2007).**

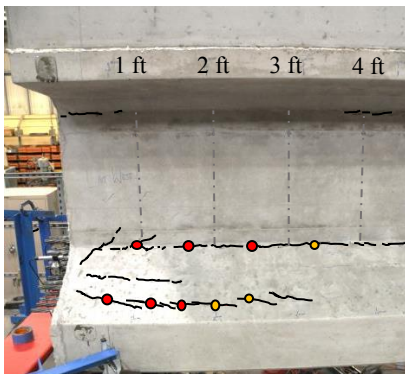


(a) Measured

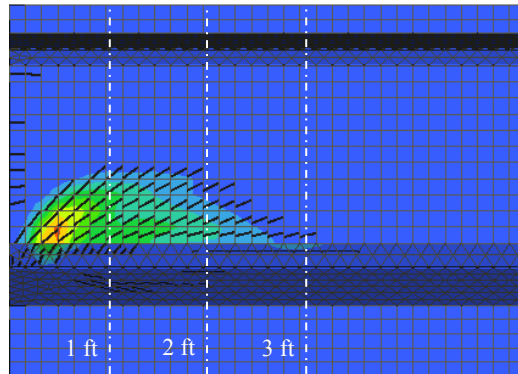


(b) Computed

**Figure 7-8-7-Tx46-I release cracks (live end)**

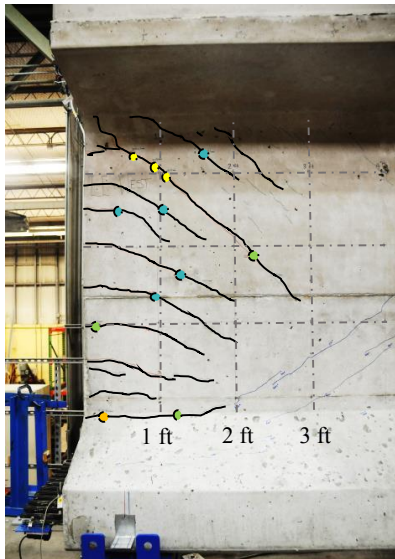


(a) Measured

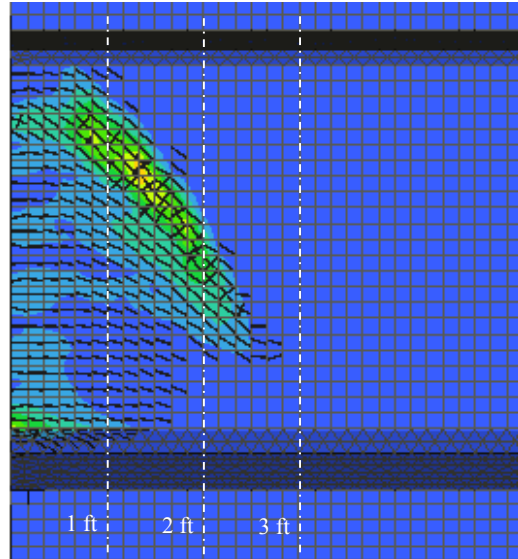


(b) Computed

**Figure 7-9-7-Tx46-II release cracks (live end)**



(a) Measured



(b) Computed

**Figure 7-10-7-Tx70-I release cracks (live end)**

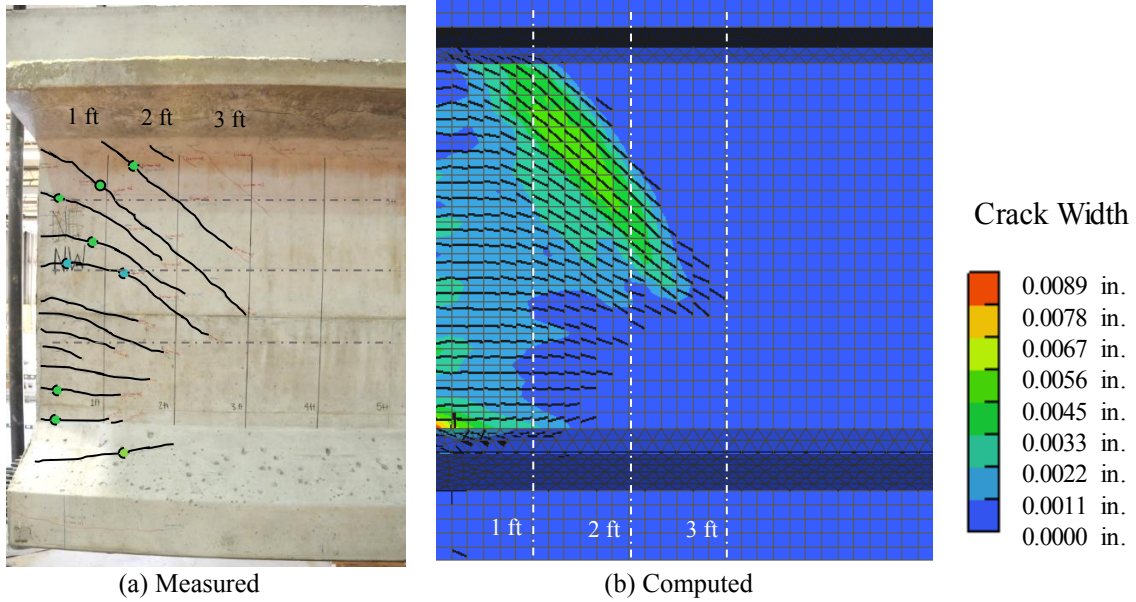


**Figure 7-11-7-Tx70-II release cracks (live end)**

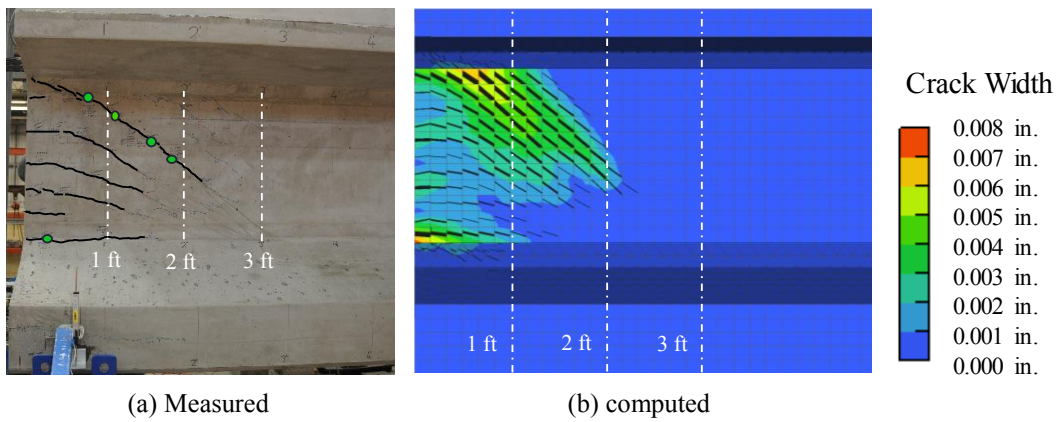


**Figure 7-12-7-Tx46-IV release cracks (live end)**

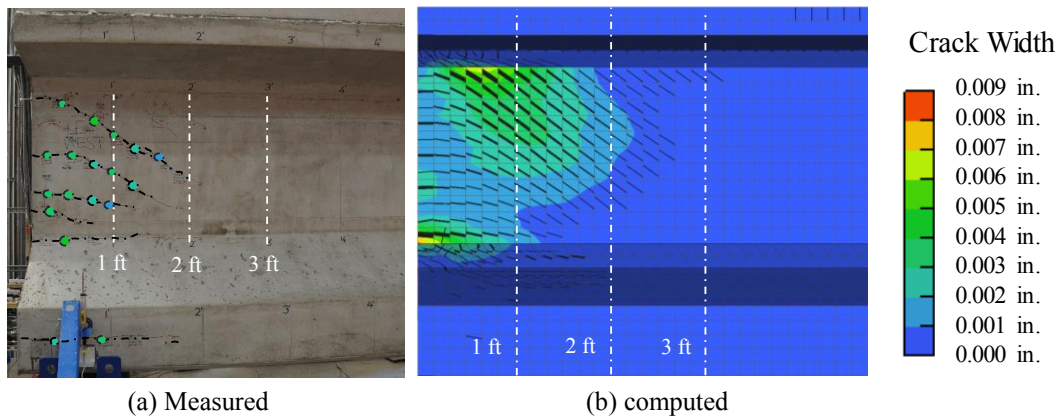


**Figure 7-13-7-Tx46-V release cracks (live end)**

### 7.4.2 End-Region Modification

As discussed in Chapter 6, the first four specimens that were fabricated as part of Task 4 in this research project using standard TxDOT detailing were assessed as having adequate crack control performance immediately following release. However, the TxDOT specifications for Construction and Maintenance of Highways, Streets, and Bridges (2014) require corrective action if cracks greater than 0.005 in. in width are detected within the end-regions of pretensioned girders immediately after release. Moreover, deck placement may take place six months to one year after prestress transfer, during which the crack widths might grow to exceed the aforementioned limits. Therefore, it became of interest to reduce the crack widths to ensure that all crack widths remain tolerable throughout the life of the member.

Using the modeling approach validated above, ATENA 3D was used to investigate alternative end-region mild-steel reinforcement details, with the objective of identifying modifications that could lead to improved serviceability and durability of prestressed Tx-girders containing 0.7-in. diameter strands. The findings of this computational study formed the basis for selecting the end-region detailing in 7-Tx46-IV and 7-Tx46-V, which were investigated experimentally as part of Tasks 4 and 6.

Three reinforcement detailing alternatives were investigated as potential modifications to the standard end-region detailing in Tx-girders. Figure 7-14 illustrates schematics of the alternatives considered, together with the additional weight of steel required for each detail. The considered modifications are described as follows:

- Detail 1: Adding four vertical No.6 bars at each end of the specimen;
- Detail 2: Replacing the first four pairs of No.6 S-bars with No.8 bars at each end; and
- Detail 3: Adding horizontal No.4 bars along the height of the web up to 3ft into the beam and at 5-in. spacing.

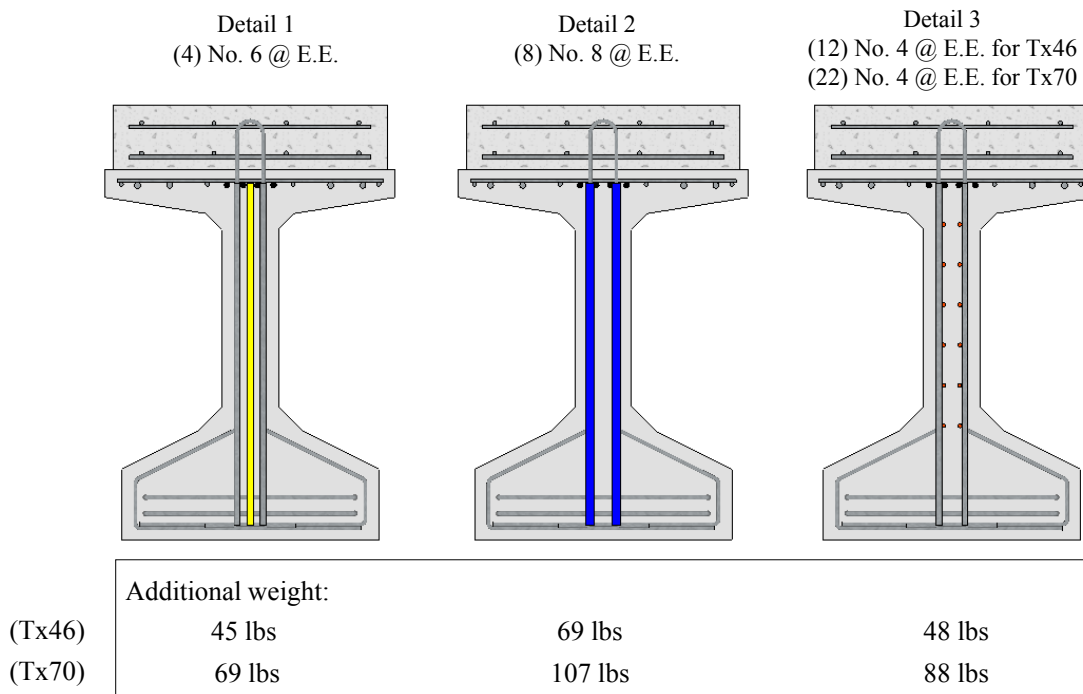


Figure 7-14- Alternative details to control end-region cracking in Tx-girders fabricated with 0.7-in. diameter strands. (Note: E.E.= Each end)

The three alternative reinforcement details were implemented in the FE models of the first four girders comprising the 7-Tx girder series, resulting in a total of twelve models. The behavior of the girders under prestressing force was investigated immediately after prestress transfer, followed by consideration of time effects that were applied through volumetric strains representative of a 28-day period. The maximum crack widths after the application of volumetric strains were 8 to 20 percent greater than those immediately after prestress transfer. Note that the results discussed herein pertain to effects of end-region reinforcement after the application of time effects.

Figure 7-15 shows a summary of the results from this investigation. The performance of each detail is presented as the percent reduction in crack width and stresses in the end-region transverse reinforcement. To eliminate the influence of member depth, the results are presented separately for Tx46 and Tx70 series. In the bottom two plots in this figure, the effectiveness of the details is compared after normalizing the results by the weight of additional steel required for each of the alternative reinforcement details.

Computed results from girders with standard detailing had shown concentrated cracking near the end face at the interface between the web and the bottom flange. The concentration of the greatest crack width within one or two elements in the web-bottom flange interface was deemed an artifact of the numerical solution. The next greatest crack widths were found near the top of the web, referred to as web cracks in Figure 7-15. These cracks showed a wider spread and better matched the experimental observations. Therefore, their widths were used as one of the primary indicators of efficiency of end-region detailing.

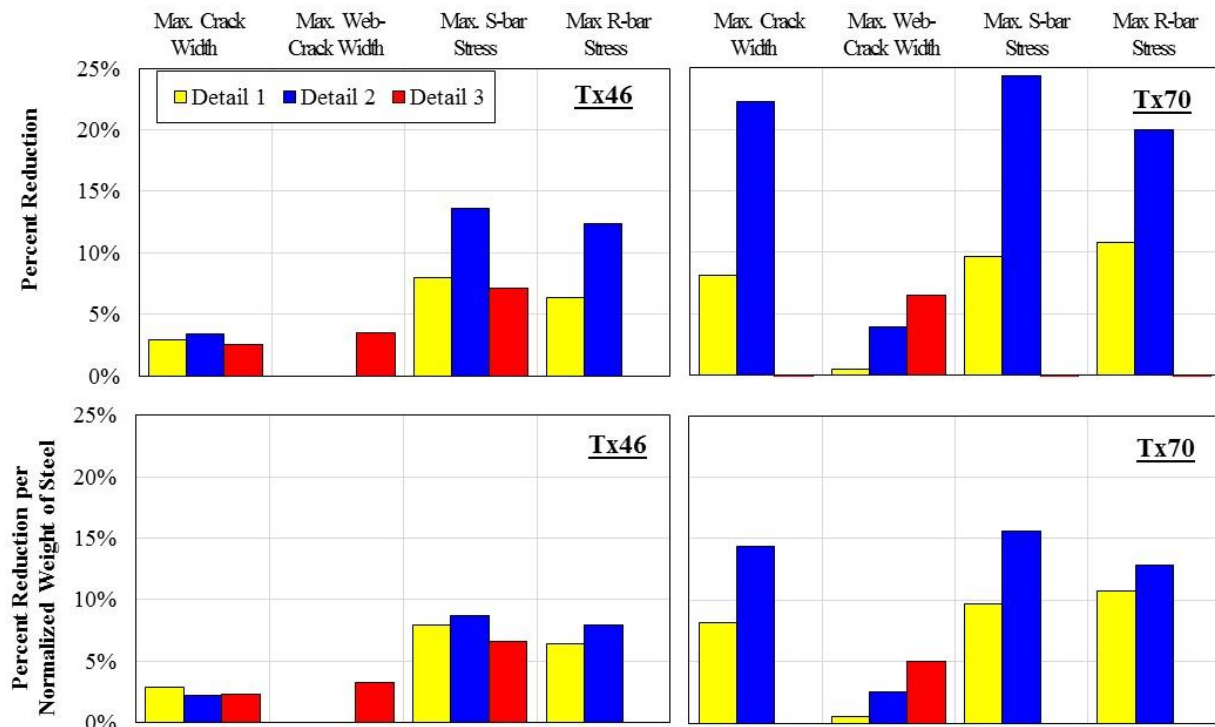


Figure 7-15- Efficiency of recommended end-region detailing

Details 1 and 2 both provide vertical reinforcement along the section; however, Detail 2 was consistently more effective in reducing the absolute maximum crack widths at the web-bottom

flange interface and stresses in end-region reinforcement. Horizontal reinforcement (Detail 3) was designed to resist spalling cracks. The results prove the reinforcement's effectiveness in reducing the maximum web-crack widths. Apart from variable effects in reducing the web cracks versus web-flange cracks, no significant changes in the cracking pattern were observed.

The vertical web reinforcement used in Detail 2 spans approximately the entire height of the cross section and therefore passes through the critical web-flange interfaces. As a result, the interface cracks were effectively restrained when using this detailing. Detail 3, however, is more effective in reducing web cracks, which are not as critical as the interface cracks in terms of potential implications on the load-carrying capacity or failure modes. Observations from the experimental studies conducted by the research team, as well as studies by Tadros et al. (2010) have shown that the majority of web cracks undergo a reduction in their width when the girder is subjected to service-level loads.

The combined use of Details 2 and 3 was also studied and appeared more effective than Detail 2 alone. However, detailed results from this case are not discussed herein because of concerns regarding the constructability of girders fabricated using this combined detailing.

It is important to note that the findings reported herein were used as the primary basis for designing the last two specimens in the experimental program for TxDOT Project 0-6831. However, the results of the experimental program in terms of the efficiency of end-region modifications did not necessarily match the observations from this computational investigation. For example, observations from 7-Tx46-V, which employed horizontal web bars within the end-region, did not show evidence of reduced crack widths in the web. This situation is not surprising, as there are simplifying assumptions in the modeling procedure. While the findings of the FE analyses provided valuable insights into the behavior of the girder end regions and guided the selection of the modified reinforcement detailing, the research team based their final conclusions and recommendations only on the observations from the full-scale specimens that were experimentally investigated.

### **7.4.3 Shear-Resisting Performance**

The end-region damage developed due to prestress transfer was considered in the subsequent analyses of the prestressed members under ultimate loading conditions. The suitability of the FE models was assessed by way of load-deflection responses and governing failure modes. The experimental and numerically predicted load-deflection plots are presented and discussed in this section. To provide context, nominal shear capacities computed using the provisions of AASHTO LRFD (2016) are also shown in the figures. Note that the AASHTO-calculated capacities presented in this section are the minimum of: 1) the strength predicted using the General Procedure, which is based on the modified compression field theory (Article 5.8.3.3), and 2) the longitudinal demand requirements (Article 5.8.3.5). For brevity, illustrations of failure modes and damage at shear failure are provided only for the 7-Tx series specimens.

#### *7.4.3.1 Results from 6-Tx Series*

Figure 7-16 presents the load-deflection behavior of the 6-Tx series specimens, as compared with the computed results. The figure shows the initial stiffness and the capacity of the specimens were predicted particularly well. The ultimate capacities for these three specimens were conservatively estimated, and were within 14 percent of the measured capacities.

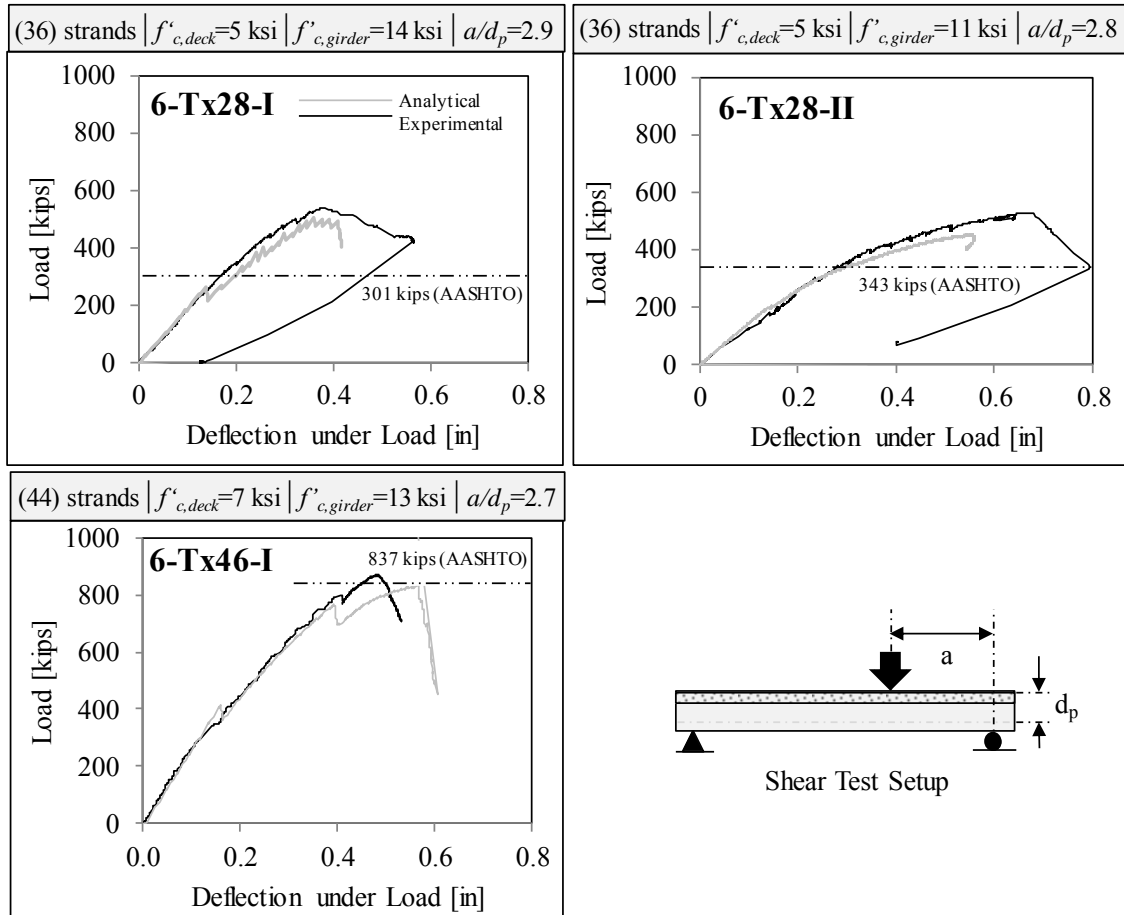


Figure 7-16- Load-deflection response of the 6-Tx series specimens

#### 7.4.3.2 Results from 7-NU Series

As previously noted, each 7-NU series specimen was tested twice, once for development length, and once for shear strength. Calculations based on nominal sectional shear capacities according to AASHTO LRFD provisions (2016) showed that the loading configuration in the first test was also shear-critical. In agreement with the nominal shear capacities, the results from the numerical models estimated extensive shear damage in the girders as a result of the first experiment.

The load-deflection results for the 7-NU series specimens are presented in Figure 7-17. In the experiments, the specimens were loaded to their nominal flexural capacities and then unloaded. However, the computational models showed that the specimens could not reach their nominal flexural capacities due to significant shear damage. Given the absence of several critical experimental details (e.g., load-plate dimensions and actual mechanical properties of the reinforcement), the initial stiffness of the load-deflection plots was predicted particularly well. The average computed capacity was also within 17 percent of the experimentally measured capacity. Similar to the 6-Tx series, the numerical results provided conservative estimates of the capacity for this series of specimens.

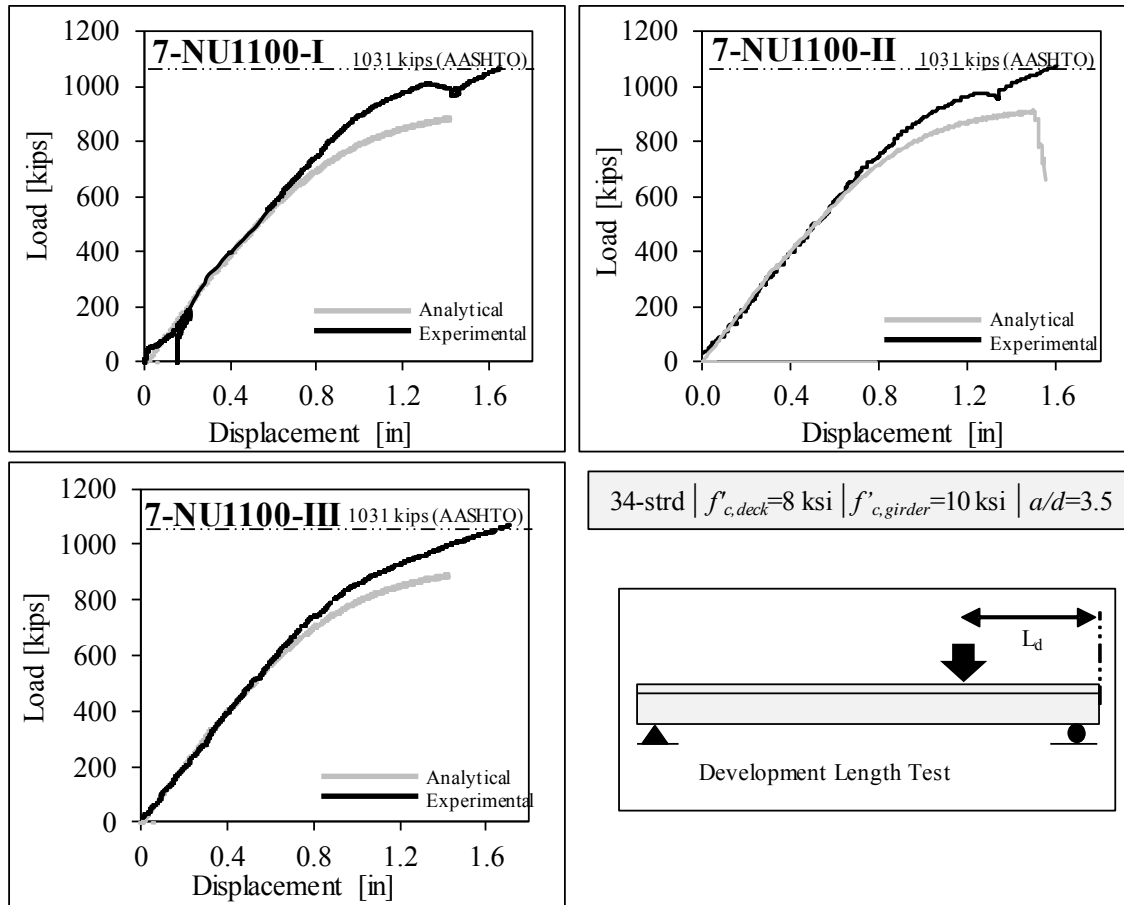


Figure 7-17- Comparison of load test results for the 7-NU series specimens

#### 7.4.3.3 Results from 7-Tx Series

Figure 7-18 presents a comparison of the load-displacement plots for the 7-Tx series specimens. As can be seen in this figure, with the exception of 7-Tx46-II, the FE models of the specimens were successful in predicting the load-deflection behavior and the ultimate capacities of the girders were predicted within approximately 7 percent of the measured capacities.

For Tx46-II, the computed capacity was 37 percent less than the measured failure load. The poor estimate may have resulted from excessive numerical bond slip for this specimen. The numerical strand slip for 7-Tx46-II was 0.08 in. at 60 percent of the peak experiment load, whereas the measured maximum slip was limited to 0.07 in. at peak experiment load. Overestimation of strand slip is likely a result of the relatively large bursting force applied to this specimen in combination with a relatively low concrete compressive strength. The mesh size used for all specimens was 2 in., which was equal to the spacing between the strands. It is believed that the model poorly captured the post-cracking bond response of the highly prestressed end-regions. Mesh refinement at the level of strands may help improve the numerical stability of the analysis.

Models of the 7-Tx series specimens were also successful in estimating the stiffness of the specimens, as well as governing failure modes. Generally, signs of anchorage and horizontal shear distress were observed in all 7-Tx series specimens. Horizontal cracks along the web-flange interface were clearly visible in both the numerical and experimental results. Figure 7-19 through Figure 7-24 illustrate the computed and observed failure modes. Note that the cracking at the

midspan is an artifact of loading the specimen beyond peak load. The computed width of such cracks at peak loads is less than 0.002 in.

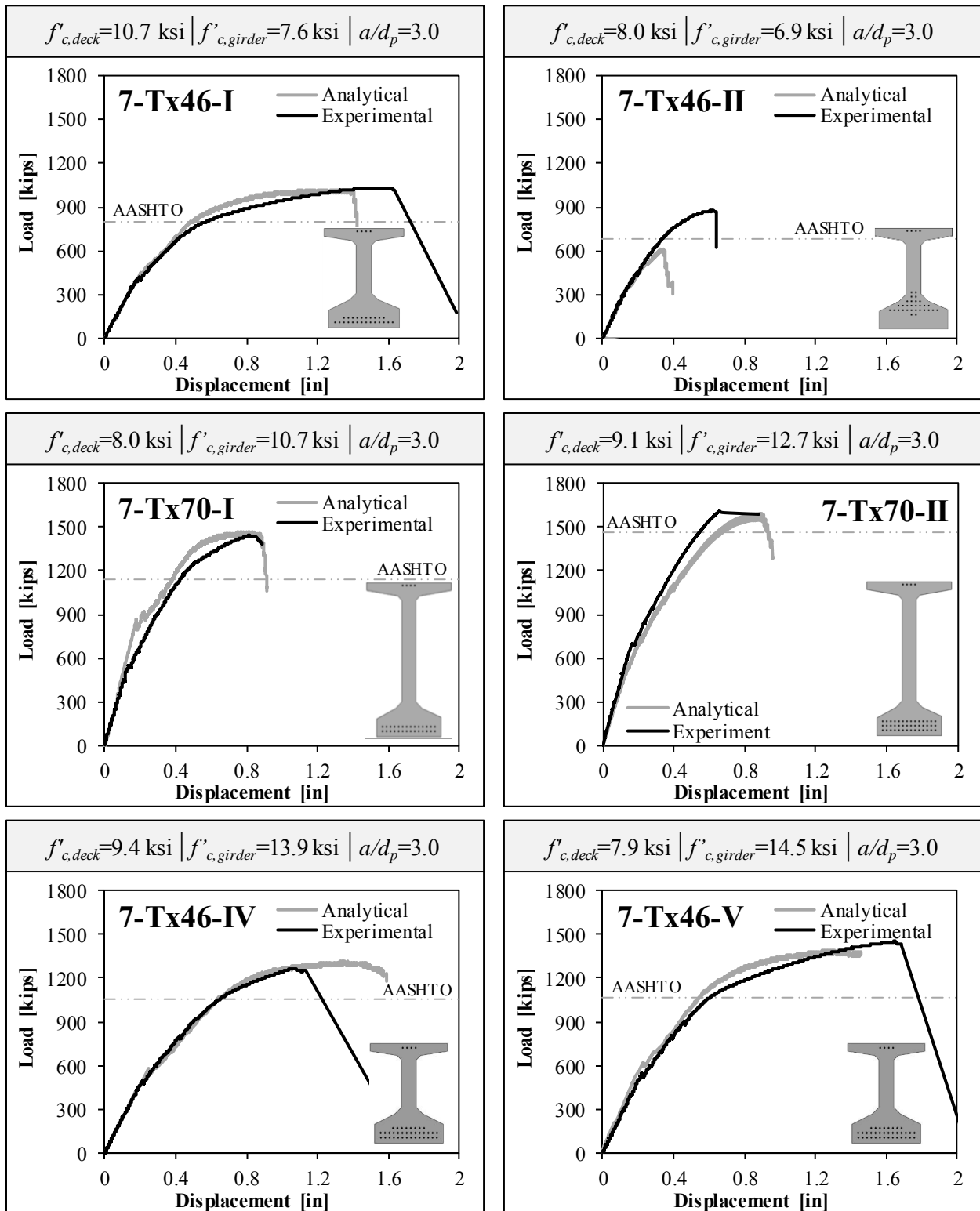


Figure 7-18- Comparison of load test results in for 7-Tx series

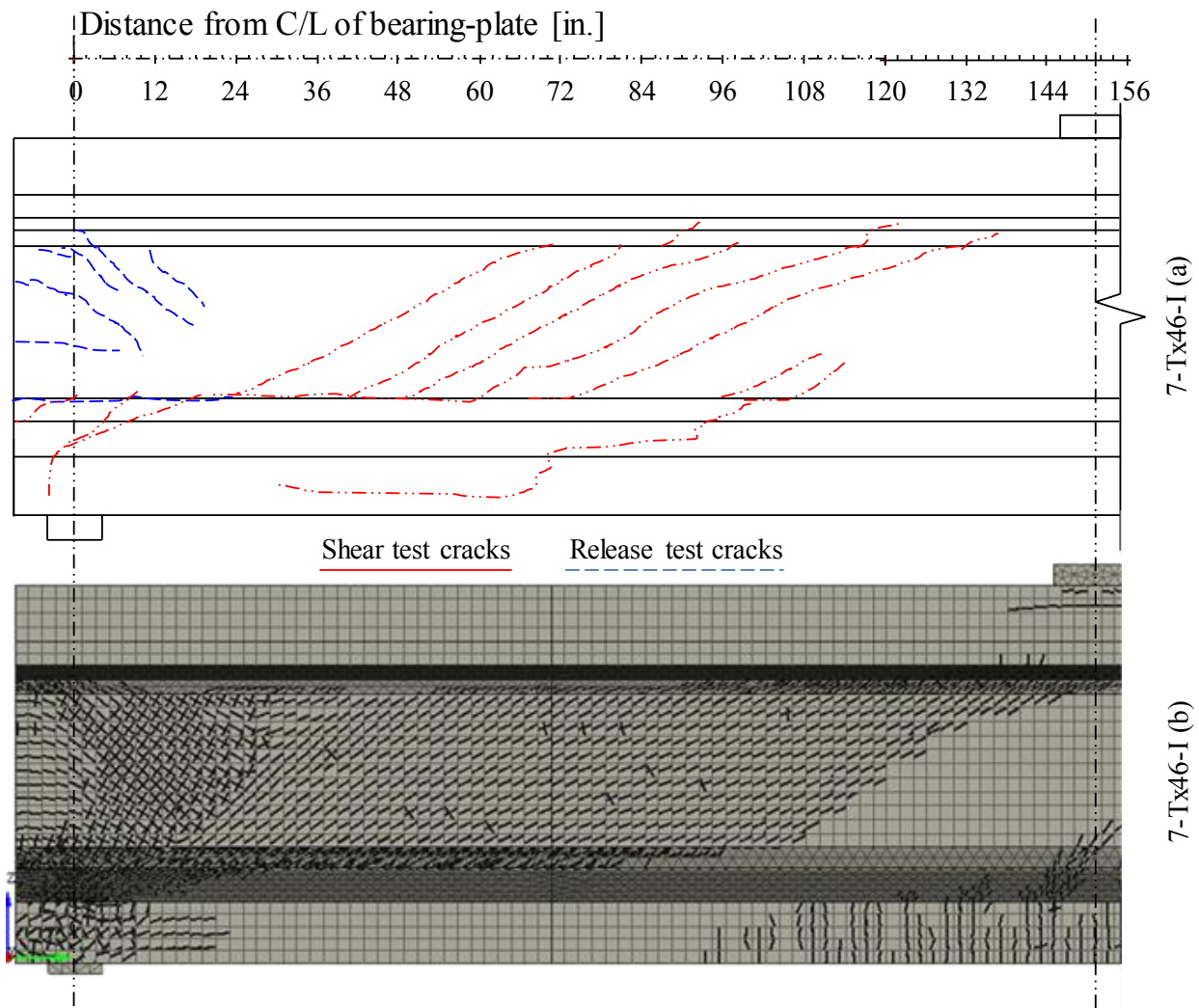


Figure 7-19- Shear test damage in 7-Tx46-I (a) measured (b) computed

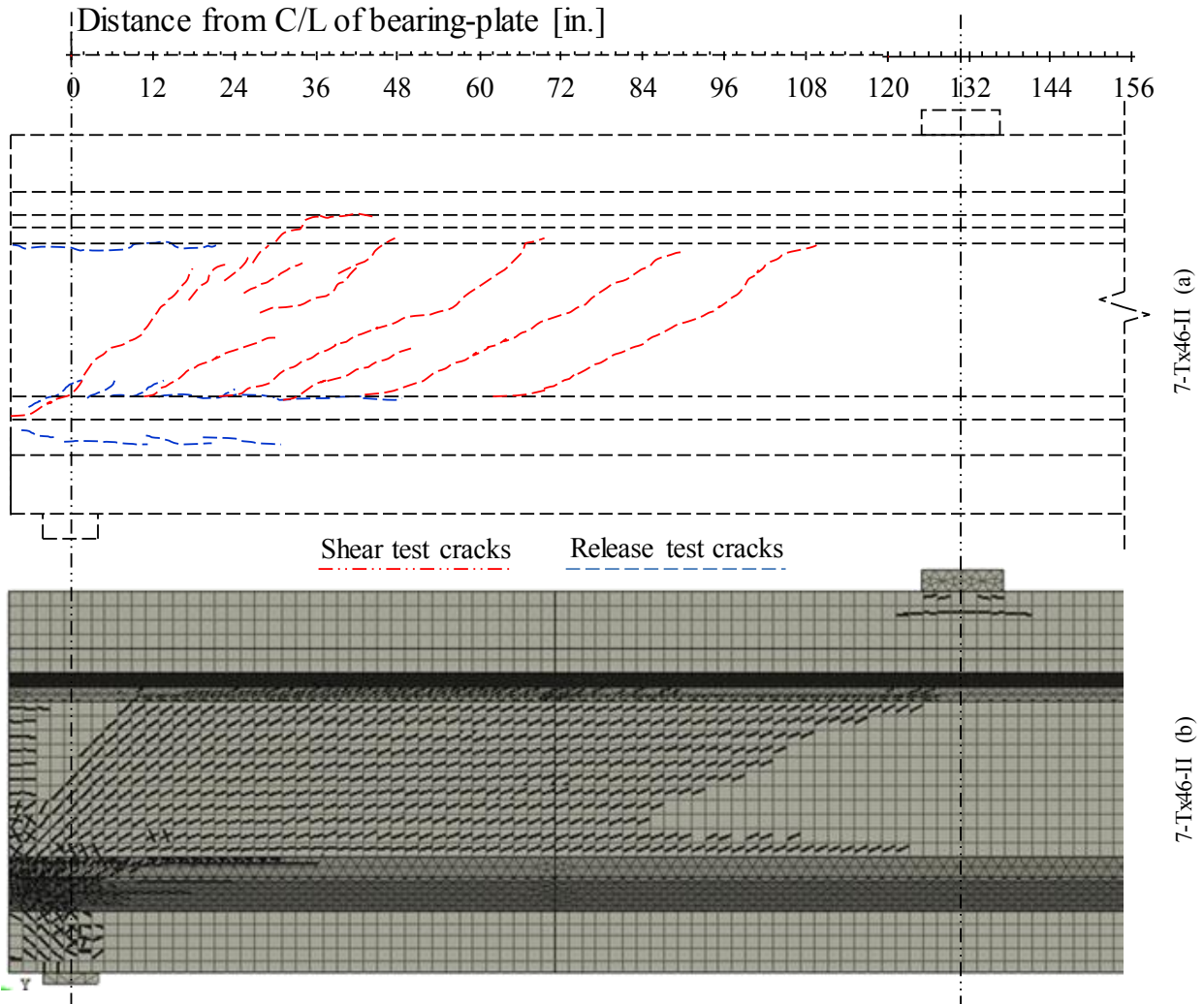


Figure 7-20- Shear test damage in 7-Tx46-II (a) measured (b) computed

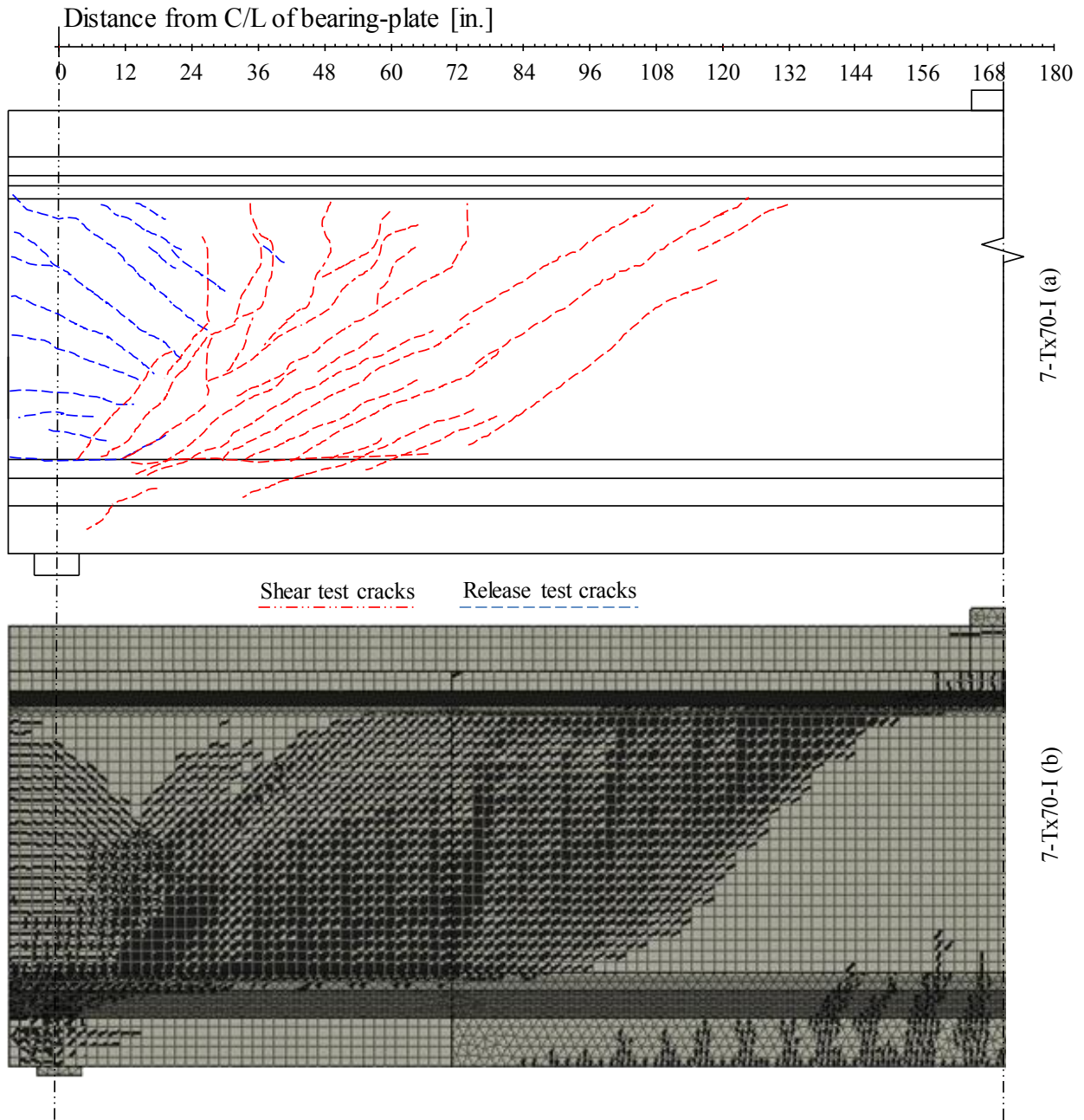


Figure 7-21- Shear test damage in 7-Tx70-I (a) measured (b) computed

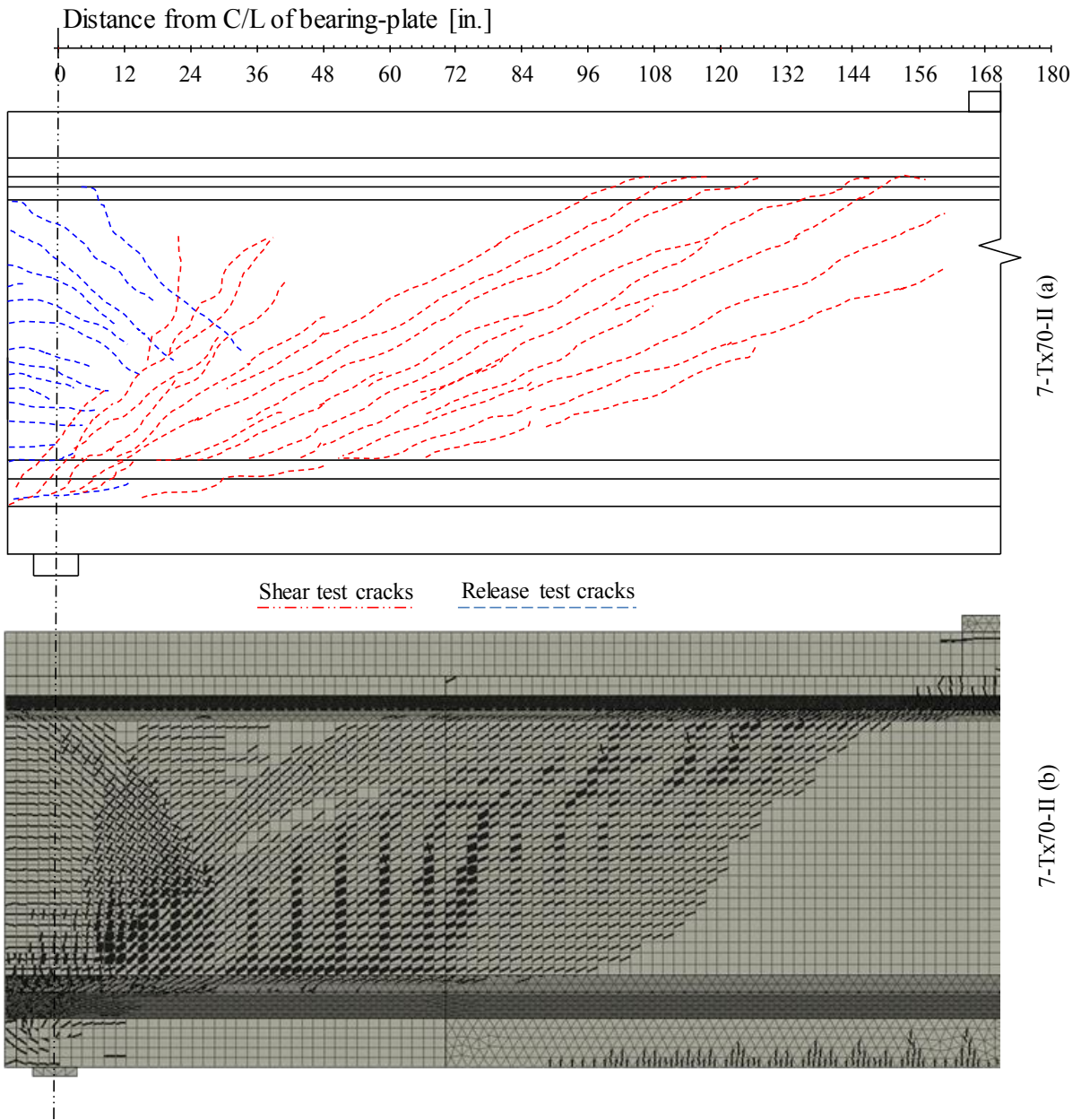


Figure 7-22- Shear test damage in 7-Tx70-II (a) measured (b) computed

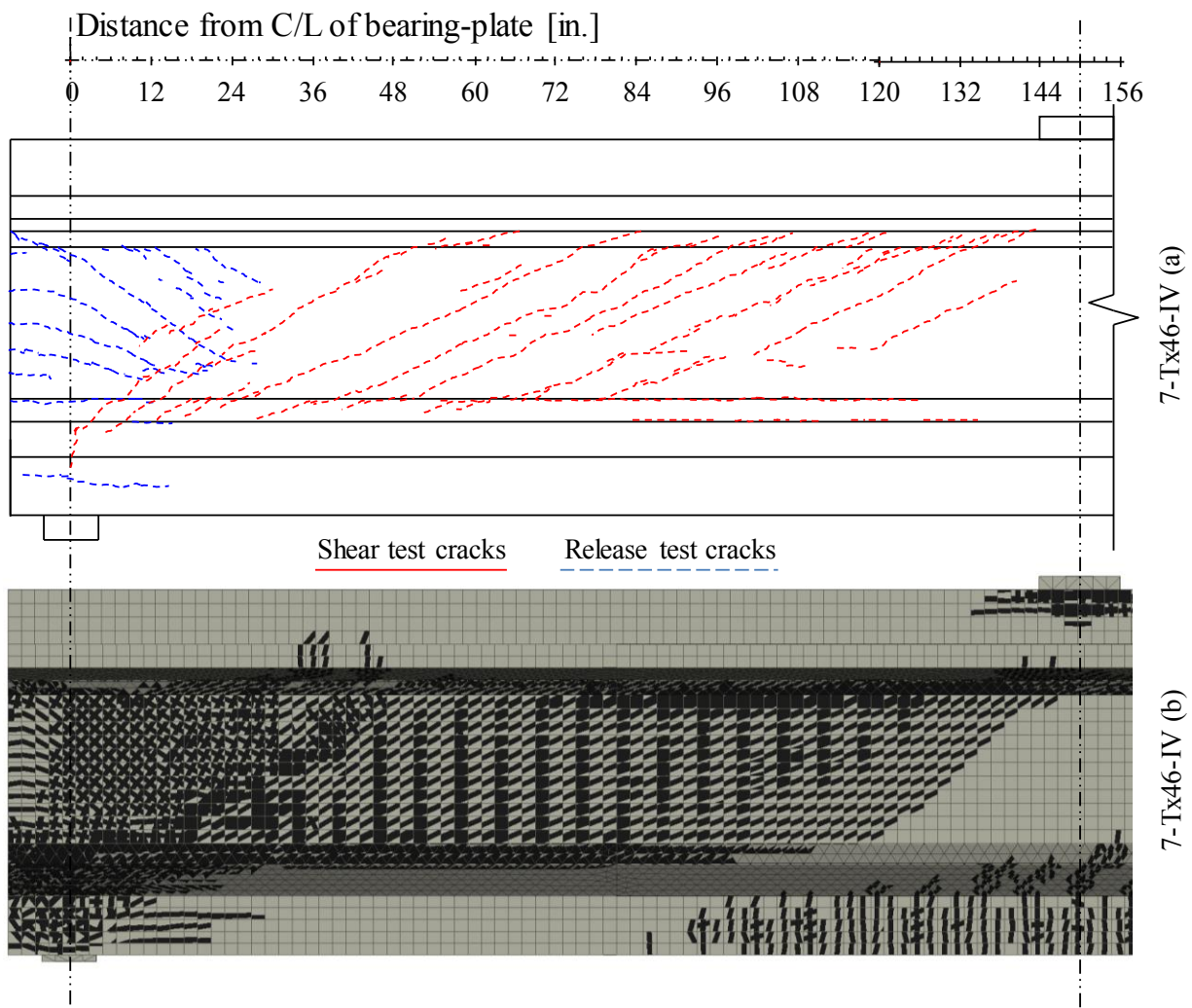
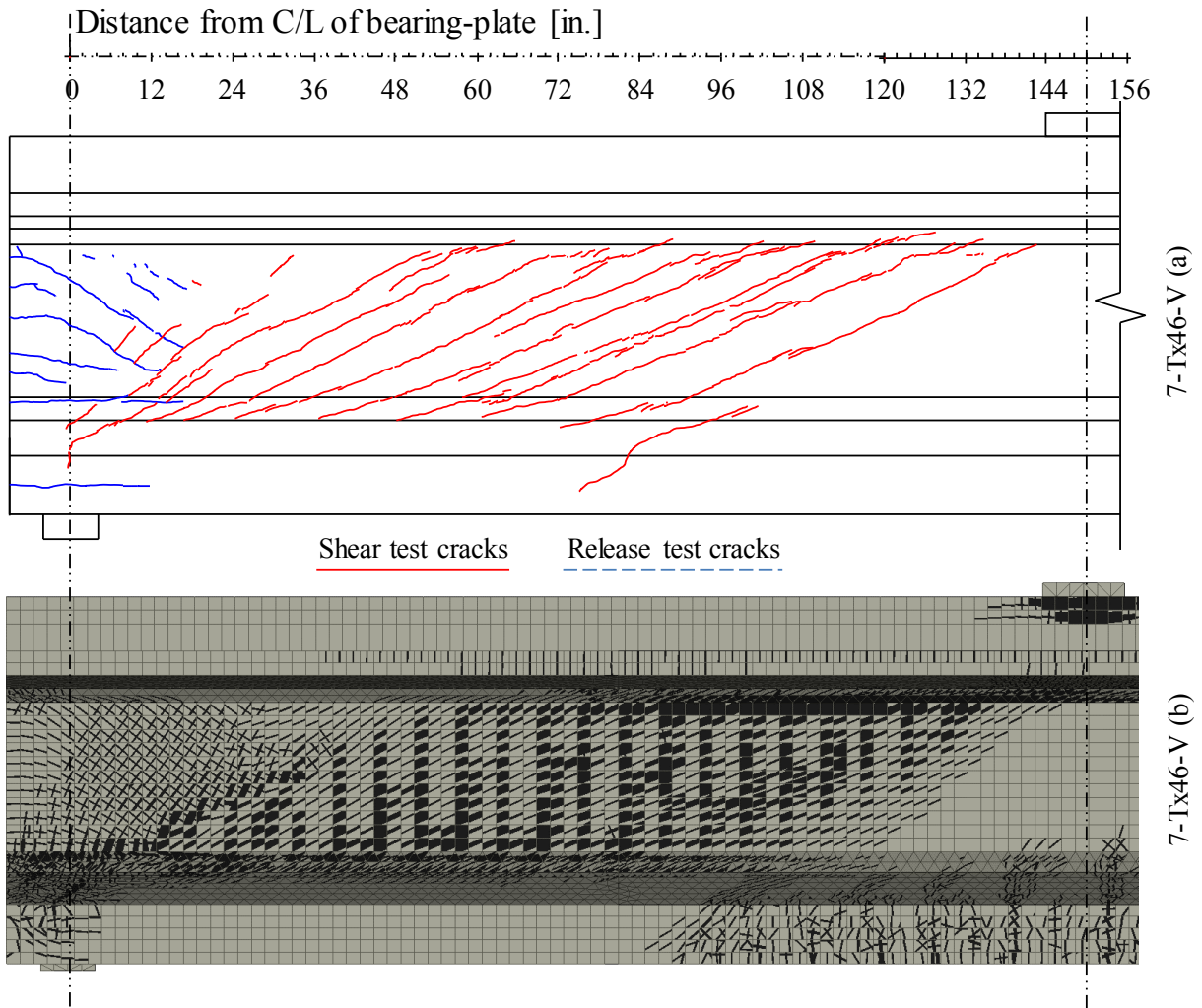


Figure 7-23- Shear test damage in 7-Tx46-IV (a) measured (b) computed



**Figure 7-24- Shear test damage in 7-Tx46-V (a) measured (b) computed**

Table 7-2 summarizes the computed and measured ultimate capacities for all three test series. As can be seen in the table, the numerical results were found to provide reasonable estimates of the response. The ratio of measured to calculated ultimate capacities of the specimens was on average 1.130, with a standard deviation of 0.19.

**Table 7-2- Summary of measured and computed ultimate capacities**

Specimen	Measured	Computed	Absolute Difference	Measured/Computed Ratio	Average Ratio per Series
	[kips]				
6-Tx28-I	417	390	6%	1.07	1.09
6-Tx28-II	371	318	14%	1.17	
6-Tx46-I	575	551	4%	1.04	
7-NU1100-I	1,075	890 <sup>1</sup>	17%	1.21	1.21
7-NU1100-II					
7-NU1100-III					
7-Tx46-I	1,029	982	5%	1.05	1.08
7-Tx46-II	873	550	37%	1.59	
7-Tx70-I	1,436	1,538	7%	0.93	
7-Tx70-II	1,609	1,621	1%	0.99	
7-Tx46-IV	1,265	1,311	4%	0.96	
7-Tx46-V	1,451	1,484	2%	0.98	
Average Measured/Computed Ratio				1.10	
Standard Deviation				0.19	

<sup>1</sup>In the computational models of the 7-NU series, the nominal flexural capacity could not be reached due to significant shear damage. The maximum load achieved in the computational models is reported.

## 7.5 Summary and Conclusions

This chapter presented an overview of the computational efforts conducted as part of Task 3 to supplement the experimental program that was the main focus of Project 0-6831. Finite element models of pretensioned girders were developed in ATENA 3D using a uniform approach to simulate the behavior of pretensioned girders at the time of prestress transfer. After incorporation of time effects, the same models were used to simulate the behavior of the specimens under load until failure. This modelling approach was validated using the experimental data from the prestress transfer of nine full-scale specimens and load testing of 12 full-scale specimens.

The models were successful in capturing the response of specimens at the time of prestress transfer and under applied loads. Computed end-region cracking, transfer length, reinforcement stresses, load-deflection response, and patterns of cracking and damage due to applied loads were compared with the experimentally obtained parameters, which showed a satisfactory performance for the FE models. All models except the one representing 7-Tx46-II were also successful in predicting the ultimate strengths of the specimens. The relatively large error observed in predicting the capacity of 7-Tx46-II was believed to be due to numerical instabilities that stemmed from the application of high prestress levels coupled with relatively low concrete compressive resistance, and potentially from the inadequate resolution of the FE mesh at the locations of the strands.

Three alternative modifications to standard end-region detailing were developed to control the end-region damage in Tx-girders that are fabricated using 0.7-in. diameter strands. These alternatives were investigated using the validated modeling procedure. The models showed that

replacing the first eight No.6 S-bars with No. 8 bars at each end resulted in the greatest reductions in computed crack widths and steel stresses. As discussed in Chapter 6, the experimental results from the specimens did not match these FE results, and increasing the diameter of S-bars, or using horizontal bars were found to be ineffective in controlling the widths of end-region cracks. This discrepancy is believed to be due to the simplifying assumptions used for developing the models, most importantly, the assumption of perfect bond between the bars and the concrete.



## **CHAPTER 8**

### **Summary and Conclusions**

#### **8.1 Summary**

This report has provided an overview of a comprehensive research program at The University of Texas at Austin on the end-region behavior and shear strength of pretensioned Texas bulb-tee girders (Tx-girders) in which 0.7-in. diameter strands are used as the prestressing steel. The work conducted in this research project primarily consisted of an experimental program on a series of full-scale specimens as well as a parametric investigation and a series of finite element studies.

The parametric investigation in this project aimed to examine the benefits and limitations of using 0.7-in. prestressing strands in pretensioned concrete girders. More than 10,000 bridge configurations were designed using a parametric study tool that enabled changes in design parameters in a convenient manner. The main parameters of interest in this investigation were strand diameter, girder cross section type, compressive release strength, span length, and spacing between the girders. The design cases were evaluated to determine the potential benefits of using 0.7-in. diameter strands on the quantity of prestressing steel, maximum span capability, allowable spacing between girders, and allowable slenderness of the superstructure.

The experimental program was the main focus of this research project. Seven full-scale Tx-girder specimens (two Tx70 and five Tx46 girders) were fabricated at Ferguson Structural Engineering Laboratory using typical industry practices. The specimens employed 0.7-in. diameter strands on the standard 2- by 2-in. grid that is commonly used for pretensioned girders with smaller-diameter strands. The compressive release strength of concrete varied between 5.2 and 8.4 ksi. Each specimen was designed to reach the maximum allowable stresses at the time of prestress transfer based on the latest edition of AASHTO LRFD bridge design specifications. In all specimens except one, conventional patterns were used for strands, i.e. the strands were placed at the greatest possible eccentricity from the centroid of the cross section. In the other specimen, the strands were concentrated near the centroid of the cross section to enable the application of the greatest possible prestressing force.

The first four specimens in the test program contained identical detailing for their end-region reinforcement to that used in Tx-girders currently fabricated using 0.6-in. diameter strands. After evaluating the performance of these specimens, a few modifications were made to the end-region reinforcement in later specimens in the test program to reduce the crack widths within the end-regions and help reduce the strand slip under applied loads.

The concrete mixture delivered for one of the Tx46 specimens in the experimental program did not match that requested by the research team. As a result, this specimen did not reach the design concrete release strength. Since the specimen had to be released at an undesirably low compressive strength, the results from this specimen were not deemed representative of the conditions of pretensioned concrete girders in the field. Therefore, the research team repeated the specimen to meet the objectives of the research program. Results from the specimen with the lower-than-desired release strength have been omitted from the discussions of this report.

All specimens were extensively instrumented to determine the transfer length, end-region stresses, and prestress losses. Moreover, the specimens were carefully examined for their end-region cracking immediately after prestress transfer and for a minimum of 28 days after prestress

transfer. Within three weeks after prestress transfer, a reinforced concrete deck was constructed on each specimen, and the specimen was prepared for shear testing.

The specimens were tested as simply supported elements under shear-critical loading. A symmetric loading configuration was used for testing the specimens, with shear span-depth ratios of 3 and 2.3 for Tx46 and Tx70 specimens, respectively. During the shear tests, the specimens were monitored for load-deflection response, stresses within transverse reinforcement, strand slip, and patterns of cracking and damage. The nominal load-carrying capacities of the specimens were calculated using AASHTO LRFD specifications and compared with the measured ultimate strengths of the specimens to assess the performance of these specifications in predicting the capacities of the specimens.

The experimental program was supplemented by a series of finite element simulations in ATENA 3D. Data from specimens tested in previous experimental studies on pretensioned girders and those tested in the current research project were used to validate the modeling assumptions in the finite element simulations. The validated models were used to help examine the end-region stresses and damage, as well as failure mechanisms in pretensioned girders employing 0.7-in. diameter strands. Moreover, the models were used to evaluate potential modifications to end-region reinforcement before fabricating specimens in the experimental program that employed such modifications.

## **8.2 Conclusions**

The primary conclusions of this research project are provided in the following subsections. Note that these findings are based on parametric studies on precast sections that are primarily used in Texas and experimental studies on full-scale Tx-girder specimens. The behavior of pretensioned girders employing large-diameter strands is sensitive to a variety of parameters, including those related to the geometry of the precast cross section, detailing of the mild-steel reinforcement within the end-regions, and the interaction between stresses and damage due to prestress transfer and those due to applied loads. Therefore, the conclusions presented in this section should not be generalized to a wider variety of cross sections or girders employing different reinforcement details without careful consideration of the array of variables that might affect the behavior of pretensioned girders.

### **8.2.1 Benefits of Using 0.7-in. Strands**

The use of 0.7-in. diameter strands was found to result in a considerable reduction in the number of strands required compared to smaller-diameter strands, which may lead to notable savings in the time and cost of precast fabrication. This benefit is primarily due to the greater cross-sectional area of 0.7-in. diameter strands than those of 0.5- and 0.6-in. diameter strands. The possibility of concentrating a greater steel area near the bottom fiber also results in up to 16 percent reduction in the total weight of prestressing steel when 0.7-in. strands are used instead of 0.5-in. strands. However, the use of 0.7-in. strands instead of 0.6-in. strands did not provide noticeable benefits in terms of total steel weight. The 0.7-in. strands were found to be most beneficial to larger I- and bulb-tee girders, where up to 16 fewer strands would be needed compared to 0.6-in. strands at practical span lengths.

Benefits other than the reduction in the number of strands are highly dependent on increasing the compressive release strength of concrete above the currently used values. An increase in the release strength up to 7.5 ksi was needed among the investigated cases before

improvements could be observed in the span length or slenderness of superstructure from the use of 0.7-in. strands instead of 0.6-in. strands. Further increase of release strength to 10 ksi was found to enable more noticeable advantages for 0.7-in. strands over 0.6-in. strands in terms of span capability (by up to 10 ft) and slenderness of superstructure (by up to 8 percent at a transverse spacing of 8 ft). These benefits are also dependent on the possibility of using harping or other methods for controlling end-region stresses at the time of prestress transfer. In terms of maximum allowable spacing between the girders, 0.7-in. strands were found to offer limited additional benefits compared to smaller-diameter strands for the range considered practical for slab construction.

### **8.2.2 Transfer Length**

The transfer length for 0.7-in. diameter prestressing strands was found to be between 29 and 47 in. immediately after prestress transfer, and between 31 and 52 in. based on strain measurements that were obtained 24 hours after prestress transfer. In general, the transfer lengths immediately after prestress transfer were shorter than the  $60d_b$  estimate, i.e. 42 in., used in AASHTO LRFD but slightly exceeded this estimate after 24 hours. It is expected that the transfer lengths continue to grow over time, although the growth in this parameter after 24 hours is not discussed in this report. Therefore, the obtained data suggest that AASHTO LRFD specifications might underestimate the transfer length for 0.7-in. diameter strands in bridge girders. A longer transfer length results in a more gradual transfer of prestressing force, hence reducing the end-region damage, but results in diminished shear strength near the ends of the girders. However, observations from the shear test program indicate that nominal shear strength calculations assuming a transfer length of 42 in. resulted in conservative estimates for the load-carrying capacities of the specimens. Therefore, the findings of this research project do not reveal any concerns regarding the use of 42 in. as the transfer length for 0.7-in. diameter strands in the calculations for Tx-girders. Further research, using a wider variety of full-scale specimens, might be needed to evaluate the transfer length of 0.7-in. diameter strands.

### **8.2.3 End-Region Cracking**

All specimens in this research project developed cracks within their end-regions after prestress transfer, which continued to grow in length, width, and number over time. The majority of specimens, which had conventional strand patterns, demonstrated patterns of spalling cracks, with the greatest crack widths observed in the web or near the interface between the web and top flange. Noticeable cracking was also observed at the interface between the web and the bottom flange of all specimens. In general, the crack widths in this test program were limited to 0.007 in. while crack widths up to 0.008 in. were also detected in a few isolated locations in some specimens. These crack widths are slightly greater than those observed in Tx-girders fabricated using 0.6-in. diameter strands. However, the patterns of end-region cracking in this test program were similar to those observed in Tx-girders currently fabricated using 0.6-in. diameter strands. Therefore, the use of 0.7-in. diameter strands on the 2- by 2-in. grid does not seem to trigger unusual cracking or damage within the end-regions of Tx-girders.

### **8.2.4 End-Region Stresses**

In all specimens, the greatest stresses in the end-region reinforcement at the time of prestress transfer were detected at the interface between the web and the bottom flange. The maximum stress level detected in the end-region reinforcement due to prestress transfer throughout

the test program was 26 ksi. However, in specimens with conventional strand patterns, these stresses were found to diminish very quickly with the increase in distance from the end face. As a result, large stresses were generated only in the end-region reinforcement that was located within the overhang region or directly over the support. The stresses in the loaded span of the girders were generally limited to 10 ksi, and were not believed to affect the load-carrying capacities of the specimens. The specimen in which the strands were concentrated near the centroid of the cross section showed a different distribution for stresses within its end-region reinforcement. The maximum stress in this specimen was detected in stirrups that were located further away from the end face of the girder. However, the stresses in this specimen were generally smaller than those in specimens with conventional strand patterns.

The standard detailing for mild-steel reinforcement used within Tx-girders results in using greater amounts of transverse reinforcement than that required by AASHTO LRFD. While the performance of the specimens was relatively satisfactory with respect to end-region behavior, the transverse forces developed within the first  $h/4$  of the length of several end-regions in this test program were greater than 4 percent of the initial prestressing force, which is the strength required by AASHTO LRFD specifications. Therefore, further research might be needed on the efficacy of end-region reinforcement requirements in AASHTO LRFD specifications for pretensioned concrete members fabricated using 0.7-in. diameter strands.

### **8.2.5 Shear Strength**

With the exception of the specimen with modified bottom flange confinement reinforcement, all specimens in this test program showed clear signs of anchorage-zone distress. Significant strand slip was recorded in these specimens prior to developing the peak load resistance. Moreover, cracks between the strands were observed on the end face of these specimens after failure. In three specimens, failure also resulted in considerable interfacial slip between the web and bottom flange on the end face, as well as a prominent horizontal crack at the web-bottom flange interface, which indicate horizontal shear damage. These observations demonstrate that the use of 0.7-in. diameter prestressing strands increases the likelihood of atypical failure modes in Tx-girders. However, alongside these failure mechanisms, significant diagonal cracking occurred, and yielding of the transverse steel was confirmed in all specimens prior to reaching the peak load. Therefore, the atypical failure mechanisms did not prohibit the specimens from achieving the shear-tension failure, which is the basis for calculations of shear strength in AASHTO LRFD general method. As a result, all specimens in this test program could reach their nominal load-carrying capacities that were calculated according to the general method in AASHTO LRFD specifications. A comparison was made between the data points obtained from this study and those included in an existing database of shear tests on prestressed concrete members. Results revealed that the general method in AASHTO LRFD was generally less conservative in predicting the ultimate strengths of the specimens in this test program compared with the majority of those included in the database, which were reported to demonstrate typical shear failures.

The anchorage performance of the specimens was evaluated through the use of longitudinal demand requirements in AASHTO LRFD specifications. The results showed that comparing the longitudinal demand according to Article 5.8.3.5 of these specifications with the nominal available force in the strands, which is calculated assuming bilinear changes in available strand stress along the girder length, does not provide a reliable indicator of the performance of the girders with respect to anchorage-zone distress. Further research might be needed on the longitudinal demand requirements on the strands due to the combined effects of shear forces and bending moments, as

well as changes in the available capacity of strands in resisting that demand as a function of distance from the girder end.

### **8.2.6 Modifications to End-Region Detailing**

The cracking patterns in the specimens fabricated in this test program were not different from those observed in Tx-girders with smaller-diameter strands. Slightly greater crack widths were observed in the specimens compared to Tx-girders currently fabricated using 0.6-in. diameter strands. However, all specimens were deemed acceptable for exposure to deicing chemicals according to ACI 224R-01 guidelines. Therefore, the observations from the test program did not reveal a critical need to modify the end-region reinforcement in Tx-girders for incorporating 0.7-in. diameter strands. However, to reduce the widths of spalling cracks below the 0.005-in. limit currently stated in the TxDOT specifications for construction and maintenance of highways, streets, and bridges, a few alternatives for modifications to end-region reinforcement were initially developed based on finite-element studies, and were implemented in the last few specimens in the experimental program.

Results from specimens with modified end-region detailing showed that increasing the diameter of S-bars from No. 6 to No.8 or adding horizontal end-region reinforcement in the web did not reduce the widths of spalling cracks. Therefore, these end-region modifications were deemed ineffective. However, the addition of a series of “cap bars,” which result in closed bottom-flange confinement reinforcement, provided significant benefits to the behavior of the specimen under applied loads. The specimen that contained cap bars demonstrated noticeably smaller strand slip and a greater deformation capacity. Moreover, the ultimate strength of this specimen was 14 percent greater than that of a similar specimen that did not contain cap bars. These observations suggest that the addition of cap bars, while requiring negligible additional cost and minor additional effort, is effective in controlling the strand slip in Tx-girders employing 0.7-in. diameter strands. The research team also recommends that the use of these bars be incorporated in the standard drawings of Tx-girders fabricated using 0.6-in. diameter strands.



## REFERENCES

- American Association of State Highway and Transportation Officials (AASHTO). (2014). *AASHTO LRFD Bridge Design Specifications, U.S. Customary U.S. Units, 3rd Edition*. Washington, D.C.
- American Association of State Highway and Transportation Officials (AASHTO). (2016). *AASHTO LRFD Bridge Design Specifications, 7th Edition- with 2015 and 2016 Interim Revisions*. Washington, DC: AASHTO.
- ACI Committee 224. (2001). *Control of Cracking in Concrete Structures (ACI 224R-01)*. Farmington Hills, Michigan: American Concrete Institute.
- ACI Committee 318. (2014). *Building Code Requirements for Structural Concrete (ACI 318R-14)*. American Concrete Institute, Farmington Hills, Michigan.
- Alirezaei Abyaneh, R., Salaza, J., Katz, A., Kim, H., Yousefpour, H., Hrynyk, T., & Bayrak, O. (2017). Computational Modelling of Prestressed Concrete Girders Fabricated with 17.8-mm (0.7-in.) Diameter Strands. *Computers and Concrete*.
- American Society for Testing and Materials (ASTM). (2014). *ASTM C39/C39M Standard Test Method for Compressive Strength of Cylindrical Concrete Specimens*. West Conshohocken, PA: ASTM.
- American Society for Testing and Materials (ASTM). (2015). *ASTM C78/C78M Standard Test Method for Flexural Strength of Concrete (Using Simple Beam with Third-Point Loading)*. West Conshohocken, PA: ASTM.
- American Society for Testing and Materials (ASTM). (2016). *ASTM A370/A370M Standard Test Methods and Definitions for Mechanical Testing of Steel Products*. West Conshohocken, PA: ASTM.
- American Society for Testing and Materials (ASTM). (2014). *ASTM C469/C469M Standard Test Method for Static Modulus of Elasticity and Poisson's Ratio of Concrete in Compression*. West Conshohocken, PA: ASTM.
- American Society for Testing and Materials (ASTM). (2011). *ASTM C496/C496M Standard Test Method for Splitting Tensile Strength of Cylindrical Concrete Specimens*. West Conshohocken, PA: ASTM.
- American Society for Testing and Materials (ASTM). (2015). *ASTM A615/A615M Standard Specification for Deformed and Plain Carbon-Steel Bars for Concrete Reinforcement*. West Conshohocken, PA: ASTM.
- American Society for Testing and Materials (ASTM). (2016). *ASTM A1061/A1061M Standard Test Methods for Testing Multi-Wire Steel Prestressing Strand*. West Conshohocken, PA: ASTM.
- Avendaño, A., & Bayrak, O. (2008). *Shear Strength and Behavior of Prestressed Concrete Beams*. Austin, TX: Technical Report, The University of Texas at Austin.
- Barnes, R. W., Burns, N. H., & Kreger, M. E. (1999). *Development Length of 0.6-inch prestressing Strand in Standard I-Shaped Pretensioned Concrete Beams*. Austin, TX: Center for Transportation Research, The University of Texas at Austin.
- Barnes, R., Grove, J., & Burns, N. (2003). Experimental Assessment of Factors Affecting Transfer Length. *ACI Structural Journal*, 100(6), 740-748.
- Bigaj, A. J. (1999). *Structural Dependence of Rotations Capacity of Plastic Hinges in RC Beams and Slabs*. TU Delft, Netherlands: PhD Dissertation, Delft University of Technology.

- Braun, M. O. (2002). *Bond Behavior of 15.2-mm (0.6-inch) Diameter Prestressing Strands in San Angelo Bridge Research Beams*. University of Texas at Austin: Austin, TX.
- Bridgesight Inc. (2014). PGSuper: Software for design, analysis, and load rating of precast, prestressed girder bridges.
- Buckner, C. D. (1995). Review of Strand Development Length for Pretensioned Concrete Members. *PCI Journal*.
- Burkett, W. R., & Kose, M. M. (1999). *Development Length of 0.6-inch (15-mm) Diameter Prestressing Strand at 2-inch (50-mm) Grid Spacing in Standard I-Shaped Pretensioned Concrete Beams*. Lubbock, TX: Research Report 0-1388, Texas Tech University.
- Červenka, V. a. (2015). ATENA 3D, Version 5.1.1. Prague, Czech Republic.
- Červenka, V., Jendele, Libor, & Červenka, J. (2016). *ATENA Program Documentation Part 1*. Prague, Czech Republic: Červenka Consulting.
- Comité Euro-International Du Béton (CEB). (1987). Anchorage Zones of Prestressed Concrete Members. *State-of-the-Art Report, CEB Bulletin No. 181*.
- Cousins, T., Johnston, D., & Zia, P. (1990). Transfer and Development Length of Epoxy Coated Prestressing Strands. *PCI Journal*, 35(4).
- Dang, C. N., Floyd, R. W., Hale, M., & Marti-Vargas, J. R. (2016). Measured Development Lengths of 0.7 in. (17.8 mm) Strands for Pretensioned Beams. *ACI Structural Journal*, 113(3), 525-535.
- Dang, C. N., Floyd, R. W., Hale, M., & Marti-Vargas, J. R. (2016). Measured Transfer Lengths of 0.7 in. (17.8 mm) Strands for Pretensioned Beams. *ACI Structural Journal*, 113(3), 85-94.
- Dassault Systèmes Simulia Corporation. (2009). Abaqus 6.9. Providence, RI.
- Detherage, J. H., Burdette, E. G., & Chew, C. K. (1994). Development Length and Lateral Spacing Requirements of Prestressing Strand in High Performance Concrete. *PCI Journal*, 39(1).
- Dunkman, D. (2009). *Bursting and Spalling in Pretensioned U-Beams*. Thesis, The University of Texas at Austin.
- Garber, D. B., Gallardo, J. M., Deschenes, D. J., & Bayrak, M. ASCE, O. (2016). Nontraditional Shear Failures in Bulb-T Prestressed Concrete Bridge Girders. *Journal of Bridge Engineering (ASCE)*.
- Garber, D. B., Gallardo, J. M., Deschenes, D. J., & Bayrak, O. (2016). Prestress Loss Calculations: Another Perspective. *PCI Journal*, 61(3).
- Garber, D., Gallardo, J., Deschenes, D., Dunkman, D., & Bayrak, O. (2013). *Effect of New Prestress Loss Estimates on Pretensioned Concrete Bridge Girder Design*. Austin, Texas: Center for Transportation Research, The University of Texas at Austin.
- Gross, S. P., & Burns, N. H. (1995). *Transfer and Development Length of 15.2 mm (0.6 in.) Diameter Prestressing Strand in High Performance Concrete: Results of Hoblitzell-Bucnkner Beam Tests*. Research Report 580-2, The Univeristy of Texas at Austin: Center for Transportation Research.
- Hanna, K., Morcou, G., & Tadros, M. K. (2010). *Design Aids of NU I-Girder Bridges*. Lincoln, NE: Nebraska Department of Roads.
- Hanson, N., & Kaar, P. (1959). Flexural Bond Tests of Pretensioned Prestressed Beams. *ACI Structural Journal*.
- Hovell, C., Avedano, A., Moore, A., Dunkman, D., Bayrak, O., & Jirsa, J. (2011). *Structural Performance of Texas U-Beams at Prestressed Transfer and Under Shear-Critical Loads*. Research Report: Austin, TX.

- Hovell, C., Avendano, A., Moore, A., Dunkman, D., Bayrak, O., & Jirsa, J. (2012). *Structural Performance of Texas U-Beams at Prestress Transfer and Under Shear-Critical Loads*. Austin, TX: Center for Transportation Research at The University of Texas at Austin.
- Hoyer, E., & Friedrich, E. (1939). Beitrag zur Frage der Haftspannung in Eisenbetonbauteilen [Contribution to the question of bond in concrete elements]. *Beton und Eisen*, 30(6), 107-110.
- Janney, J. R. (1954). Nature of Bond in Pre-Tensioned, Prestressed Concrete. *ACI Journal*, 50(5), 717-736.
- Kaar, P. H., LaFraugh, R. W., & Mass, M. A. (1963). Influence of Concrete Strength on Strand Transfer Length. *PCI Journal*, 8(5).
- Katz, A., Yousefpour, H., Kim, H., Alirezaei Abyaneh, R., Salazar, J., Hrynyk, T., & Bayrak, O. (2017). Shear Performance of Pretensioned Concrete I-Girders Employing 0.7 in. (17.8 mm) Strands. *ACI Structural Journal*, 114(5).
- Kim, H., Katz, A., Salazar, J., Abyaneh, R., Yousefpour, H., Hrynyk, T., & Bayrak, O. (2017). End-Region Serviceability and Shear Strength of Precast, Pretensioned I-Girders Employing 0.7-in. Diameter Strands. *PCI/NBC 2017*. Cleveland, OH.
- Kose, M. K., & Burkett, W. R. (2005). Formulation of New Development Length Equation for 0.6 in. Prestressing Strand. *PCI Journal*.
- Lane, S. N. (1992). Transfer Length in regular Prestressed Concrete Concentric Beams. *Public Roads*, 56(2).
- Langefeld, D. P. (2012). *Anchorage-Controlled Shear Capacity of Prestressed Bridge Girders*. Austin, TX: The University of Texas at Austin.
- Maguire, M., Morcou, G., & Tadros, M. K. (2012). Structural Performance of Precast/Prestressed Bridge Double Tee Girders Made of High Strength Concrete, Welded Wire Reinforcement, and 18 mm Diameter Strands. *Journal of Bridge Engineering*, 18(10).
- Marti-Vargas, J. R., Arbelaez, C. A., Serna-Ros, P., Navarro-Gregorie, J., & Pallares-Rubio, L. (2007). Analytical Model for Transfer Length Prediction of 13 mm Prestressing Strands. *Structural Engineering and Mechanics*, 26(2).
- Marti-Vargas, J. R., Arbelaez, C., Serna-Ros, P., & Castro-Bugallo, C. (2007). Reliability of Transfer Length Estimation from Strand End Slip. *ACI Structural Journal*, 104(4).
- Mitchell, D., Cook, W. D., & Kahn, A. A. (1993). Influence of High Strength Concrete on Transfer and Development Length of pretensioned Strands. *PCI Journal*, 38(3).
- Morcou, G., Assad, S., & Hatami, A. (2013). *Implementation of 0.7 in. Diameter Strands in Prestressed Concrete Girders*. Lincoln, NE: Technical Report, University of Nebraska-Lincoln.
- Morcou, G., Assad, S., Hatami, A., & Tadros, M. K. (2014). Implementation of 0.7 in. diameter strands at 2.0 x 2.0 in. spacing in pretensioned bridge girders. *PCI Journal*.
- Morcou, G., Hanna, K., & Tadros, M. K. (2011). Use of 0.7-in. diameter strands in pretensioned bridge girders. *PCI Journal*.
- Morcou, G., Hatami, A., Maguire, M., Hanna, K., & Tadros, M. K. (2012). Mechanical and Bond Properties of 18-mm Diameter Prestressing Strands. *Journal of Materials in Civil Engineering*, 24(6).
- Nakamura, E., Avendaño, A. R., & Bayrak, O. (2013). Shear Database for Prestressed Concrete Members. *ACI Structural Journal*, 909-918.
- O'Callaghan, M. R. (2007). *Tensile Stresses in the End Regions of Pretensioned I-Beams at Release*. Thesis, The University of Texas at Austin.

- Okumus, P. a. (2013). Evaluation of Crack Control Methods for End Zone Cracking in Prestressed Concrete Bridge Girders. *PCI Journal*, 58(2), 91-105.
- Okumus, P., Kristam, R. P., & Arancibia, M. D. (2016). Sources of Crack Growth in Pretensioned Concrete-Bridge Girder Anchorage Zones after Detensioning. *Journal of Bridge Engineering*, 21(10).
- Okumus, P., Oliva, M. G., & Becker, S. (2012). Nonlinear Finite Element Modeling of Cracking at Ends of Pretensioned Bridge Girders. *Engineering Structures*, 40, 267-275.
- Pozolo, A., & Andrawes, B. (2011). Transfer Length in Prestressed Self-Consolidating Concrete Box and I-Girders. *ACI Structural Journal*, 108(3).
- Russel, B., & Burns, N. (1996). Measured Transfer Lengths of 0.5 and 0.6 in. Strands in Pretensioned Concrete. *PCI Journal*.
- Russell, B. W., & Burns, N. H. (1993). *Design Guidelines for Transfer, Development, and Debonding of Large-Diameter Seven Wire Strands in Pretensioned Concrete Girders*. Austin, TX: Center for Transportation Research, The University of Texas at Austin.
- Salazar, J. (2016). *End-Region Behavior of Precast, Pretensioned I-Girders Employing 0.7-inch Diameter Prestressing Strands*. Austin, Tx: Master's Thesis, The University of Texas at Austin.
- Salazar, J., Yousefpour, H., Abyaneh, R., Kim, H., Katz, A., Hrynyk, T., & Bayrak, O. (2017). End-Region Behavior of Pretensioned I-Girders Employing 0.7 in. (17.8 mm) Strands. *ACI Structural Journal*.
- Salazar, J., Yousefpour, H., Katz, A., Abyaneh, R., Kim, H., Garber, D., Hrynyk, T. & Bayrak, O. (2017). Benefits of Using 0.7-inch Strands in Precast, Pretensioned Girders: A Parametric Investigation. *PCI Journal*(November-December).
- Shahawy, M. A., Issa, M., & Batchelor, B. (1992). Strand Transfer Lengths in Full-Scale AASHTO PRestressed Concrete Girders. *PCI Journal*, 37(3).
- Tadros, M. K., & Morcou, G. (2011). *Impact of 0.7 Inch Diameter Strands on NU I-Girders. Technical Report*. Lincoln, Nebraska: Nebraska Department of Roads.
- Tadros, M. K., Al-Omaishi, N., Seguirant, S. J., & Gallt, J. G. (2003). *Prestress Losses in High-Strength Concrete Bridge Girders*. Washington, D.C.: National Cooperative Highway Research Program.
- Tadros, M. K., Badie, S. S., & Tuan, C. Y. (2010). *Evaluation and Repair Procedures for Precast/Prestressed Concrete Girders with Longitudinal Cracking in the Web*. Washington D.C.: NCHRP Report 654, Transportation Research Board.
- Texas Department of Transportation . (2015). *Concrete I-Girder Details*. Standard Drawings by the Bridge Division, Austin, Texas.
- Texas Department of Transportation (TxDOT). (2012). *Standard Specifications for Construction and Maintenance of Highways, Streets, and Bridges*. Austin: Texas Department of Transportation.
- Texas Department of Transportation. (2015). *Bridge Design Manual-LRFD*. Austin, Tx: Texas Department of Transportation.
- Vadivelu, J. (2009). *Impact of larger diameter strands on AASHTO/ PCI Bulb-Tees*. Thesis, Univeristy of Tennessee, Knoxville.
- Zia, P., & Mostafa, T. (1977). Development of Prestressing Strands. *PCI Journal*.

# **Appendix A**

## **Manufacturer Surveys**

### **A.1 Overview**

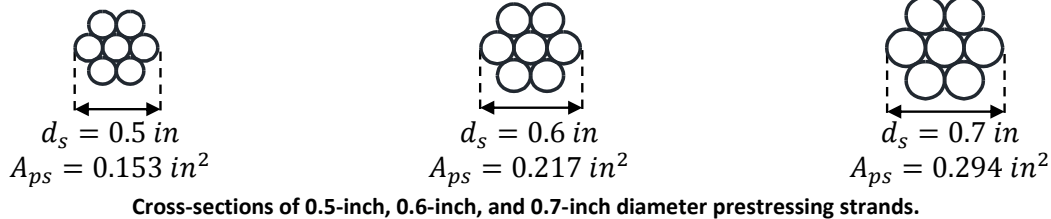
This appendix contains the two surveys that were developed as part of Task 2 in this research project. The first survey was distributed to the state transportation departments whereas the second survey was developed for distribution among the precast concrete manufacturers in Texas.



# Ferguson Structural Engineering Laboratory at The University of Texas at Austin in Collaboration with the Texas Department of Transportation (TxDOT)

## Survey of Design and Construction Practices Related to Using 0.7-inch Strands in Pretensioned I-Girders

The use of 0.7-inch strands in bridge applications is perceived to provide significant benefits, including the need for fewer prestressing strands and an increase in the working range of pretensioned girders. However, the limits on the application of these larger diameter strands have yet to be defined in order to fabricate safe, serviceable girders.



The objective of the following survey is to identify design and construction practices that have been successfully implemented within precast I-girders with 0.7-inch strands. Considering the most common practices that are identified, a full-scale testing program will be conducted in an effort to develop recommendations for end-region and shear reinforcement detailing standards for Texas I-girders with 0.7-inch strands.

Your response to the survey will be invaluable to the research team. Please answer the questions as thoroughly as possible, providing details where necessary. The research results will be summarized in a final report that will become available online. Your time is greatly appreciated.

Please return this survey **by May 29** to: Geetha Chandar, TxDOT Bridge Division  
Email: [geetha.chandar@txdot.gov](mailto:geetha.chandar@txdot.gov)

<p><b>Texas Department of Transportation Contact:</b> Geetha Chandar , PE</p> <p><b>Address:</b> Bridge Division 125 East 11th St. Austin, TX 78701</p> <p><b>Phone:</b> 512-416-2753 <b>Email:</b> <a href="mailto:geetha.chandar@txdot.gov">geetha.chandar@txdot.gov</a></p>	<p><b>The University of Texas Research Team:</b> Dr. Oguzhan Bayrak Dr. Trevor Hrynyk Dean Deschenes Hossein Yousefpour Roya Abyaneh Jessica Salazar Alex Katz: <a href="mailto:akatz@utexas.edu">akatz@utexas.edu</a></p> <p><b>Address:</b> Ferguson Structural Engineering Laboratory The University of Texas at Austin 10100 Burnet Rd., Building 177 Austin TX, 78758</p>
--	--

### Respondent Information

Name of Person Completing the Survey: \_\_\_\_\_

Title: \_\_\_\_\_

State/District: \_\_\_\_\_

Organization/Unit: \_\_\_\_\_

Address: \_\_\_\_\_

\_\_\_\_\_

Phone: \_\_\_\_\_ Fax: \_\_\_\_\_

Email: \_\_\_\_\_

May the researchers from The University of Texas at Austin contact you regarding your responses to the survey?

Yes       No

If you responded Yes to the previous question, what is the best means of communication?

Phone       E-Mail       Fax       Post

### A. General Information

1. Approximately what percentage of **pretensioned girders** in your state/district is produced with **0.6-inch** diameter prestressing strands?

0-20%       20-40%       40-60%       60-80%       80-100%

2. Has your state/district had experience with the design and/or construction of precast, pretensioned girders with **0.7-inch** diameter strands?

Yes       No

If No, has your state/district considered the use of 0.7-inch strands for future bridges?

Yes       No

If 0.7-inch strands are not currently being considered as a design option for new bridges, please explain why.

***If your state/district has had experience with 0.7-inch strands, please proceed with the remainder of the survey. If not, thank you for providing the above information.***

3. What girder types have been constructed with **0.7-inch** strands in your state/district? (Please check all that apply)

I-Beams       Bulb-Tees       U-Beams       Box Beams       Double-Tees  
 Other \_\_\_\_\_

4. Which of the following challenges did the precast plants in your state/district face when fabricating girders with 0.7-inch strand? (Please check all that apply)

Availability of strands       Availability of accessories (chucks, etc.)  
 Strand handling difficulties       Safety concerns  
 Limitations of the prestressing facility  
 Other (please explain any perceived problems associated with 0.7-inch strands that could inhibit its use)

5. What equipment needed to be modified at the plants to incorporate 0.7-inch strands? (Please check all that apply)

Hold downs       Hold down foundations       Anchor plates  
 Jacks/rams       Beds/frames  
 Other (Please elaborate)

6. Have you had any constructability issues (e.g., concrete consolidation issues, steel congestion, etc.) related to 0.7-inch strands?

Yes       No

If Yes, please briefly describe the issue(s) and any actions that have been taken to resolve the problem(s).

**B. Design and Construction Practices for Prestressed I-Girders with 0.7-inch strands**

7. How many **I-girder** bridges have been constructed in your state/district using **0.7-inch strands**?  
 None       1 to 5       6 to 10       11 to 20       Greater than 20

**If your answer to Question 7 was *None* please go to Question 16. If not, please proceed to Question 8.**

8. Please list the types of the **I-girders with 0.7-inch strands** in your state/district. (e.g. AASHTO Type IV)

9. What was the concrete strength at the time of prestress release for **I-girders with 0.7-inch strands**?  
**Minimum:** \_\_\_\_ksi      **Average:** \_\_\_\_ksi      **Maximum:** \_\_\_\_ksi

10. What was the typical age of concrete at the time of prestress transfer for **I-girders with 0.7-inch strands**?  
 0-12 hours       12-24 hours       24-36 hours       36-48 hours       More than 48 hours

11. What methods were implemented to control end region stresses at the time of release in **I-girders** with 0.7-inch strands?  
 None  
 Harping (deflecting) the strands       Partial debonding of the strands  
 Using counterweights  
 Other (please specify) \_\_\_\_\_

12. What span length(s) of pretensioned **I-girders with 0.7-inch strands** has been produced?  
**Minimum:** \_\_\_\_ft      **Average:** \_\_\_\_ft      **Maximum:** \_\_\_\_ft

13. Which crack patterns (shown on the figure below) were found specifically in the **live end regions** of I-girders with 0.7-inch strands after release? More than one answer can be selected.

(a)

(b)

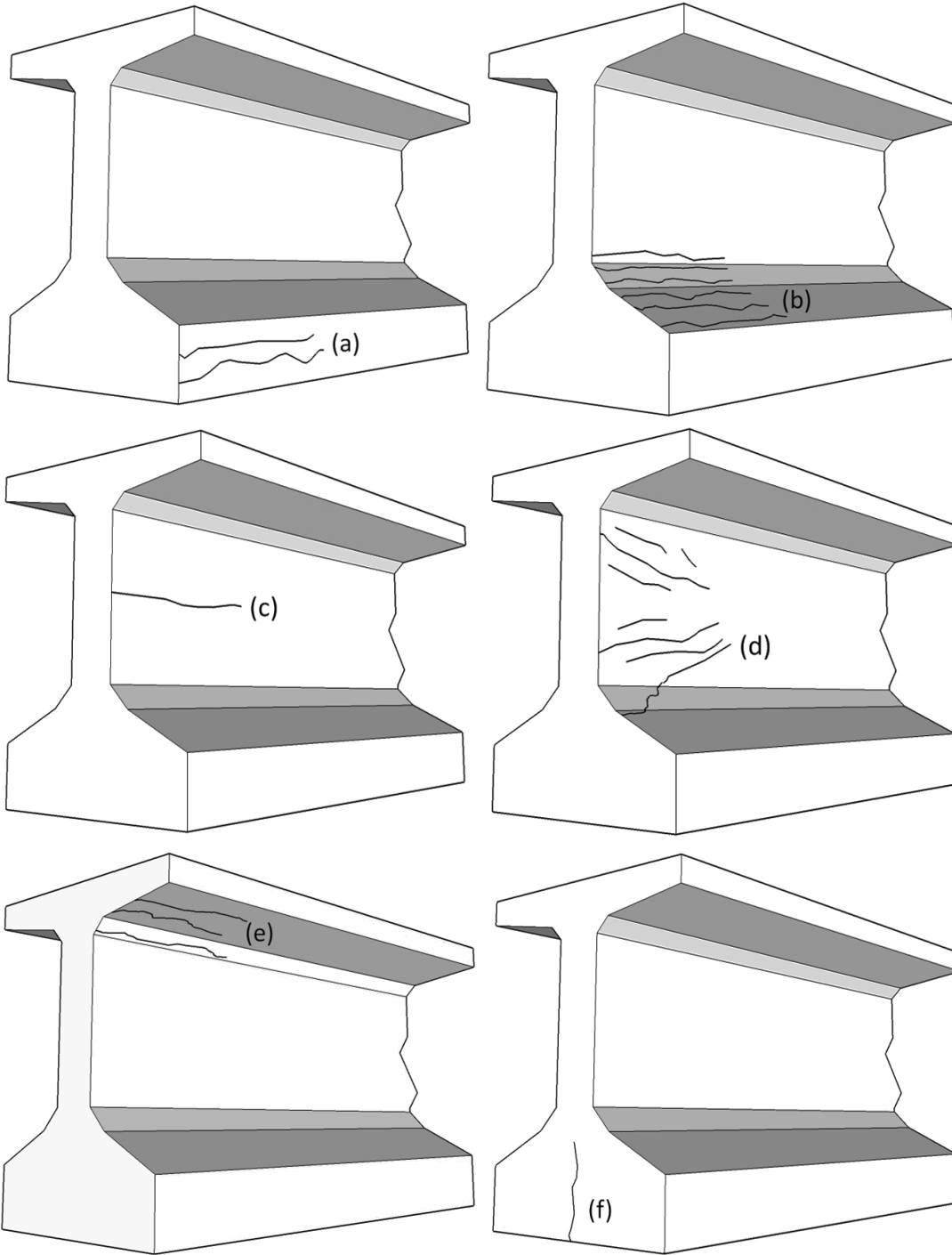
(c)

(d)

(e)

(f)

Other; please describe:



14. Which crack patterns (shown on the figure below) were found specifically in the **dead end regions** of I-girders with 0.7-inch strands after release? More than one answer can be selected.

(a)

(b)

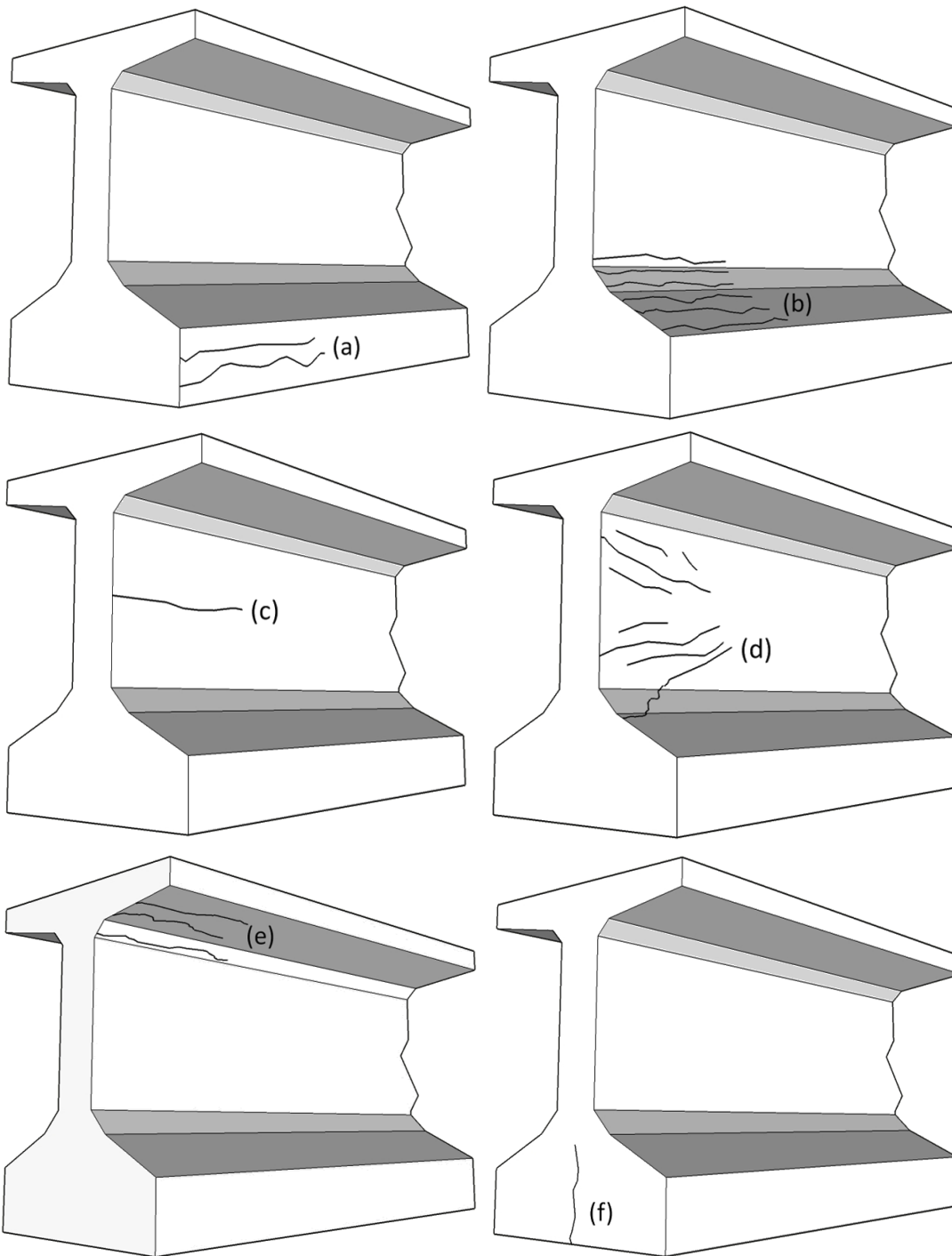
(c)

(d)

(e)

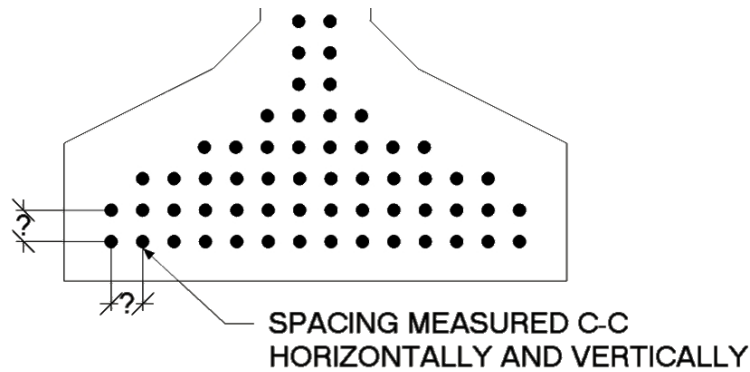
(f)

Other; please describe:



Please elaborate on the observed end region crack patterns if necessary.

15. At what spacing(s) have 0.7-inch prestressing strands been used in **I-girders** in your state/district? (Please check all that apply)



- Horizontal:  Spacing < 2 in.     Spacing = 2 in.     2 < Spacing ≤ 3 in.     Spacing > 3 in.  
Vertical:     Spacing < 2 in.     Spacing = 2 in.     2 < Spacing ≤ 3 in.     Spacing > 3 in.

16. Does your state/district use any special detailing within the end regions of the I-girders with 0.7-inch strands?

- Yes     No

If Yes, please briefly describe the special detailing used.

17. Please provide any additional information regarding your perceived value of using 0.7-inch strands or associated problems that you believe may be useful to the research team. Feel free to give specific examples regarding any aspect of the design and construction.

**C. Request for Additional Material**

If possible, please attach **drawings of existing bridges prestressed with 0.7-inch strand** in your state. If your state/district has specific **design guidelines/requirements for 0.7-inch strands**, please submit this material with the survey. Alternatively, a web link to the guidelines/requirements can be provided here:

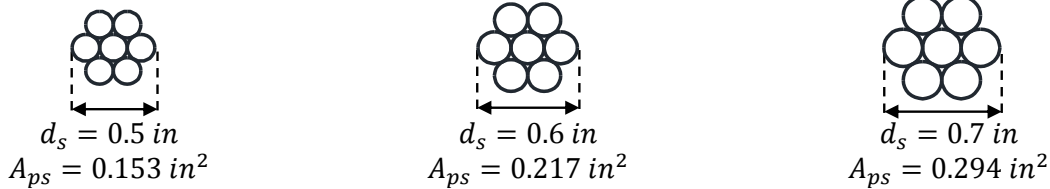
---

Any other relevant information you can offer the research team will be greatly appreciated. Please upload supplemental material to [geetha.chandar@txdot.gov](mailto:geetha.chandar@txdot.gov).

# Ferguson Structural Engineering Laboratory at The University of Texas at Austin in Collaboration with the Texas Department of Transportation (TxDOT)

## Survey of Fabrication Practices Related to Using 0.7-inch Diameter Strands in Pretensioned Girders

The use of 0.7-inch strands in bridge applications is perceived to provide significant benefits, including the need for fewer prestressing strands and an increase in the working range of pretensioned girders. However, the limits on the application of these larger diameter strands have yet to be defined in order to fabricate safe and serviceable girders.



Cross-sections of 0.5-inch, 0.6-inch, and 0.7-inch diameter prestressing strands.

The objective of the following survey is to evaluate the precast fabricators' capabilities and limitations in using larger diameter strands and obtain feedback on the potential implementation of 0.7-inch strands in Texas I-girders. Considering the identified capabilities and limitations, a full-scale testing program will be conducted in an effort to develop recommendations for end-region and shear reinforcement detailing standards for Texas I-girders with 0.7-inch strands.

Your response to the survey will be invaluable to the research team. Please answer the questions as thoroughly as possible, providing details where necessary. The research results will be summarized in a final report that will become available online. Your time is greatly appreciated.

Please return this survey **by May 29** to: Geetha Chandar, TxDOT Bridge Division  
Email: [geetha.chandar@txdot.gov](mailto:geetha.chandar@txdot.gov)

<p><b><u>Texas Department of Transportation Contact:</u></b> Geetha Chandar , PE</p> <p><b>Address:</b> Bridge Division 125 East 11th St. Austin, TX 78701</p> <p><b>Phone:</b> 512-416-2753 <b>Email:</b> <a href="mailto:geetha.chandar@txdot.gov">geetha.chandar@txdot.gov</a></p>	<p><b><u>The University of Texas Research Team:</u></b> Dr. Oguzhan Bayrak Dr. Trevor Hrynyk Dean Deschenes Hossein Yousefpour Roya Abyaneh Jessica Salazar Alex Katz: <a href="mailto:akatz@utexas.edu">akatz@utexas.edu</a></p> <p><b>Address:</b> Ferguson Structural Engineering Laboratory The University of Texas at Austin 10100 Burnet Rd., Building 177 Austin TX, 78758</p>
---	---

**Respondent Information**

Name of Person Completing the Survey: \_\_\_\_\_

Manufacturing Plant: \_\_\_\_\_

Address: \_\_\_\_\_

\_\_\_\_\_

Phone: \_\_\_\_\_

Fax: \_\_\_\_\_

Email: \_\_\_\_\_

**A. General Information**

1. Approximately, how many linear feet of pretensioned girders does your plant produce in a given year?

Up to 1,000     Up to 10,000     Up to 100,000     Over 100,000

Other \_\_\_\_\_

2. What type of pretensioned girders does your plant produce on a routine basis?

(Please check all that apply)

I-Beams     Bulb-Tees     U-Beams     Box Beams     Double-Tees

Other \_\_\_\_\_

3. Which strand diameters do you commonly use? (Please specify products.)

0.5 inch for \_\_\_\_\_

0.6 inch for \_\_\_\_\_

Other \_\_\_\_\_

4. May the researchers from The University of Texas at Austin contact you regarding your responses to the survey?

Yes     No

5. If you responded Yes to the previous question, what is the best means of communication?

Phone     E-Mail     Fax     Post

**B. Construction Practices for Precast, Pretensioned Girders**

6. What is the typical age of concrete at the time of prestress transfer?

- 0-12 hours     12-24 hours     24-36 hours     36-48 hours     More than 48 hours

7. What is the typical concrete strength at the time of prestress release?

**Minimum:** \_\_\_\_ksi                      **Average:** \_\_\_\_ksi                      **Maximum:** \_\_\_\_ksi

8. What span length(s) of pretensioned girders does your plant produce on a routine basis?

**Minimum:** \_\_\_\_ft                      **Average:** \_\_\_\_ft                      **Maximum:** \_\_\_\_ft

9. Does your plant use match curing systems?

- Yes                       No

10. What is the primary type of coarse aggregate used?

- Limestone     River gravel     Granite

11. What is the primary size of coarse aggregate used?

- Size < ½"     ½" ≤ Size < ¾"     ¾" ≤ Size < 1"     Size ≥ 1"

12. Approximately what percentage of girders at your plant is produced with **0.6-inch** strands?

- 0-20%     20-40%     40-60%     60-80%     80-100%

13. In which capacity range do your **average** prestressing beds/lines fall within?

- < 2,000 kips     2,000-3,000 k     3,000-4,000 k     4,000-5,000 k     > 5,000 kips

14. In which capacity range does your **maximum capacity** prestressing bed/line fall within?

- < 2,000 kips     2,000-3,000 k     3,000-4,000 k     4,000-5,000 k     > 5,000 kips

15. At your plant, is Welded Wire Fabric used within **I-girders'** mild steel reinforcement?

- Yes                       No

16. Which crack patterns (shown on the figure below) are typically found in the **live end regions** of I-girders after release? More than one answer can be selected.

(a)

(b)

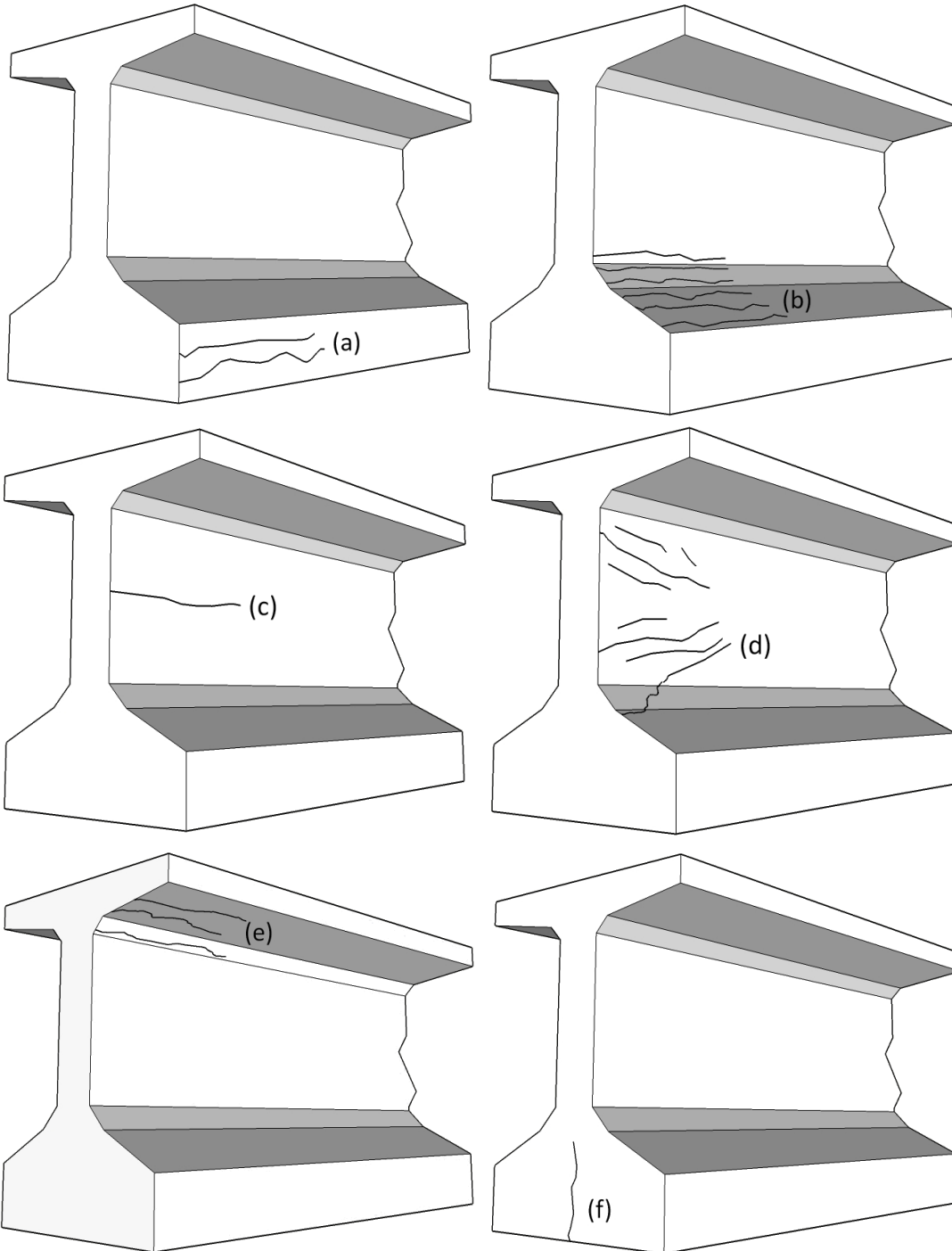
(c)

(d)

(e)

(f)

Other; please describe:



17. Which crack patterns (shown on the figure below) are typically found in the **dead end regions** of I-girders after release? More than one answer can be selected.

(a)

(b)

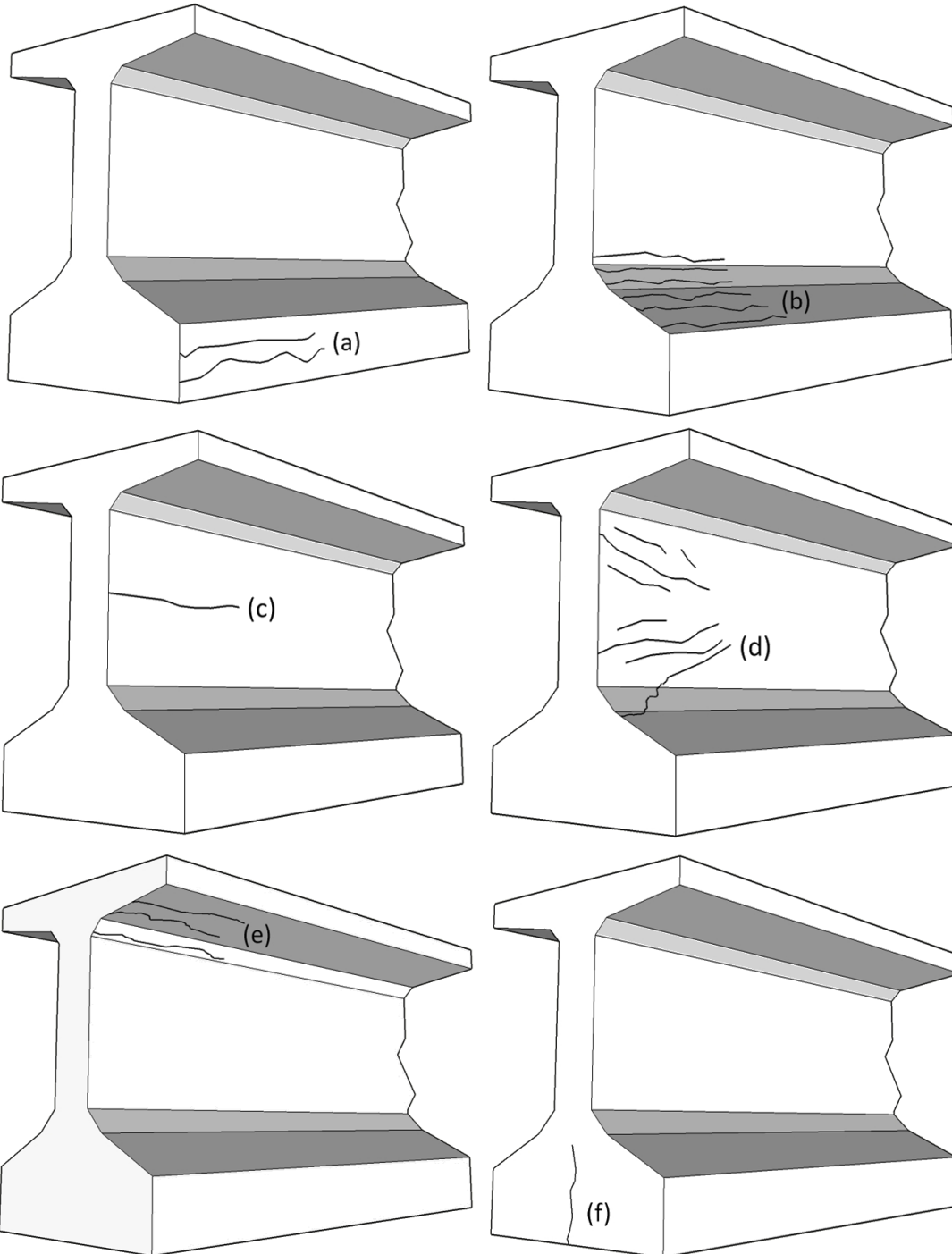
(c)

(d)

(e)

(f)

Other; please describe:



Please elaborate on the observed end region crack patterns if necessary.

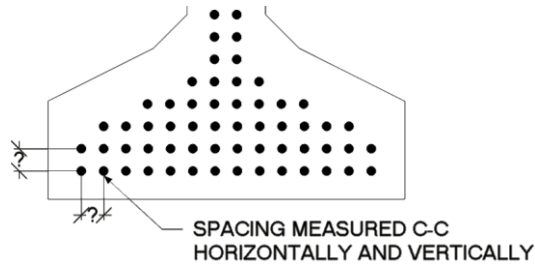
18. How are the strands typically tensioned?

- Individual Tensioning       Group Tensioning

19. Which release method do you usually use?

- Hydraulic release of all strands     Flame cutting of individual strands  
 Other (Please specify) \_\_\_\_\_

20. At what spacing(s) have prestressing strands been used in the I-girders produced at your plant?  
(Please check all that apply)



- Horizontal:  Spacing < 2 in.     Spacing = 2 in.     2 < Spacing ≤ 3 in.     Spacing > 3 in.  
Vertical:     Spacing < 2 in.     Spacing = 2 in.     2 < Spacing ≤ 3 in.     Spacing > 3 in.

21. Have you had any constructability issues (e.g., concrete consolidation problems, rebar congestion, etc.) specific to girders with 0.6-inch diameter strands?

- Yes       No

If Yes, please briefly describe the issue(s) and any actions that have been taken to resolve the problem(s).



27. Please provide any additional information regarding your perceived value of using 0.7-inch strands or associated problems that you believe may be useful to the research team. Feel free to give specific examples regarding any aspect of the design and construction.

## **Appendix B**

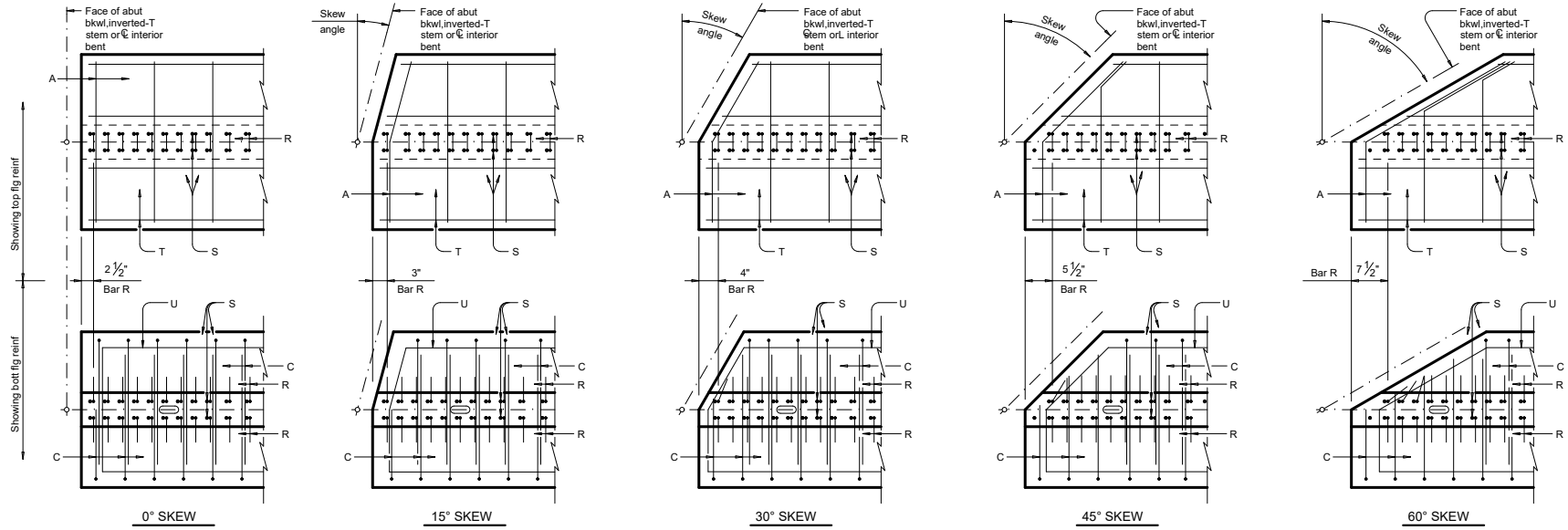
### **Summary of Design Recommendations**

#### **B.1 Summary of Design Recommendations**

1. Tx-girders may be fabricated with 0.7-in. diameter prestressing strands that are located on the standard 2- by 2-in. grid and initially stressed to 75 percent of their ultimate strength.
2. For satisfactory performance of Tx-girders that employ 0.7-in. diameter strands, the compressive release strength of such girders need not be greater than that for girders fabricated using smaller-diameter strands. However, without increasing the concrete release strength to a minimum of 7.5 ksi, the maximum span capabilities and attainable slenderness of the superstructure will not benefit from the use of 0.7-in. diameter strands instead of 0.6-in. diameter strands.
3. The allowable compressive and tensile stress limits at the time of prestress transfer for Tx-girders employing 0.7-in. diameter strands shall be taken as those stated in Section 5.9.4 of AASHTO LRFD Bridge Design Specifications (7<sup>th</sup> editions, with 2015 and 2016 interim revisions).
4. The nominal capacities of Tx-girders employing 0.7-in. diameter prestressing strands under shear-critical loading may be calculated using the current AASHTO LRFD Bridge Design specifications. In determining the nominal shear resistance, the provisions of Article 5.8.3.4.2 (General Procedure) shall be used.
5. Experimental evidence suggests that the transfer length of 0.7-in. diameter strands is likely to exceed 60 strand diameters, i.e. 42 in. However, in nominal shear strength calculations for Tx-girders employing 0.7-in. diameter strands, the transfer length may still be taken as 42 in. without concerns regarding the conservativeness of the estimated strength.
6. Figures B-1 and B-2 show the reinforcement details for Tx-girders employing 0.7-in. diameter strands. The detailing shown in this figure is identical to that currently used within Tx-girders employing 0.6-in. diameter strands, with the exception of containing CP bars. Experimental results suggest that crack widths in Tx-girders employing 0.7-in. strands on the standard 2- by 2-in. grid and the detailing shown in this figure are likely to be acceptable for exposure to de-icing chemicals according to the guidelines stated in ACI 224R-01.
7. The use of CP bars, which requires negligible additional cost and minor additional effort, is also recommended for incorporation in the standard drawing of Tx-girders employing 0.6-in. diameter strands.

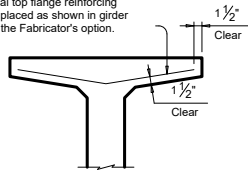




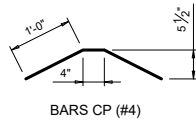


**PLAN OF GIRDER ENDS** ⑪

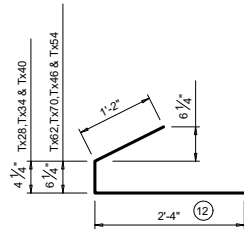
To control top flange cracking that may occur during form removal, additional top flange reinforcing may be placed as shown in girder ends at the Fabricator's option.



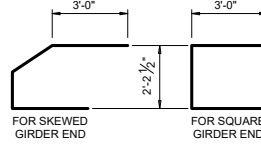
**OPTIONAL TOP FLANGE REINFORCING DETAIL**



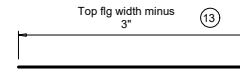
**BARS CP (#4)**



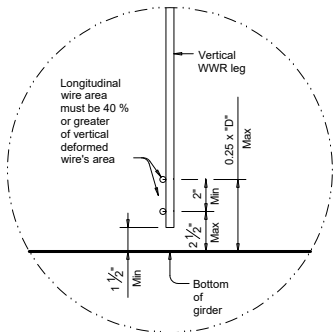
**BARS C (#4)** ⑫



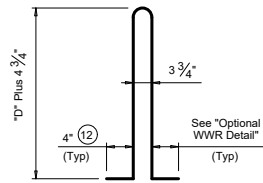
**BARS U (#5)**



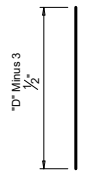
**BARS A (#3)** ⑬



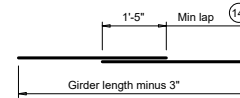
**OPTIONAL WELDED WIRE REINFORCEMENT (WWR) DETAIL**



**BARS R (#4)** ⑮



**BARS S (#6)**



**BARS T (#4)** ⑭

- ⑪ Reinforcing patterns shown are provided as guides to determine reinforcement placement in skewed ends. Place Bars S as close to girder end as cover requirements permit, which may prevent them to be bundled with Bars R.
- ⑫ Bars may be cut or bent at skewed end as required.
- ⑬ Increase as necessary for bars at skewed end.
- ⑭ No portion of bar less than 10 ft.
- ⑮ For Welded Wire Reinforcement (WWR) option, area of Bars R may be reduced in proportion to the increase in reinforcement yield strength over 60 ksi. Yield strength of WWR is limited to 75 ksi.

**Figure B-2-Reinforcement details for Tx-girders employing 0.7-in. diameter strands(continued)**